DEVELOPMENT OF SUBSTRATES FOR THE EX VIVO EXPANSION OF CONJUNCTIVAL EPITHELIUM

Thesis submitted in accordance with the requirements of the University of Liverpool for the degree of Doctor of Medicine

by

Shivani Kasbekar

January 2016

Abstract

The conjunctiva is a mucous membrane lining the ocular surface and is crucial to ocular surface homeostasis. Ocular surface diseases lead to a poor tear film, irreversible conjunctival scarring and continual corneal desiccation that may result in painful loss of vision. Conjunctival integrity and a tear film with appropriate consituents are crucial to the survival of corneal and limbal stem cell transplants. I hypothesised that two novel substrates could be developed for the ex vivo expansion of conjunctival epithelium to address a range of transplantation requirements: 1) a degradable biological substrate from the decellularisation of human conjunctiva and 2) a synthetic non-degradable substrate from expanded polytetrafluoroethylene (ePTFE).

This study demonstrated that conjunctival epithelial cells (HCjE-Gi cell line) were supported at a greater cell density on ePTFE subjected to ammonia gas plasma treatment. Flow cytometry determined the phenotype of conjunctival epithelium developed on treated ePTFE was similar to that developed on an established cell culture product; Thincert, a chemically modified polyethylene terephthalate (PET) membrane. Primary conjunctival epithelium was also expanded ex vivo on ammonia plasma treated ePTFE, however, the cell density declined after 14 days in culture. No significant differences were found in terms of intracellular marker expression between primary conjunctival epithelium developed on ammonia plasma treated ePTFE and the positive control (PET membrane). Human conjunctiva was successfully decellularised (99% DNA removal). There was no demonstrable cytotoxicity, evidence of collagen denaturation, change in tensile strength or change in the qualitative detection of extracellular matrix proteins collagen IV, laminin and fibronectin. The development of stratified conjunctival epithelium of an appropriate phenotype was also demonstrated following explant culture on a freshly decellularised conjunctival tissue substrate.

This is the first study to develop decellularised conjunctiva and plasma modified ePTFE as substrates for the ex vivo expansion of conjunctival epithelium. Novel conjunctival constructs developed from both substrates may be further developed to address a range of transplantation requirements.

Acknowledgements

I would like to thank my supervisors Professors Kaye and Williams and Dr Stewart for their direction along this journey obtaining external funding and undertaking a Doctorate in Medicine. The endless encouragement and expert guidance they have given me has been crucial to the undertaking of this work. I would like to gratefully acknowledge their hard work.

I would also like to thank the Medical Research Council, Royal College of Ophthalmologists and Novartis for the jointly funded Clinical Research Training Fellowship I was awarded to enable me to undertake this research.

I would also like to thank Dr Paul Rooney and staff at tissue services at NHS Blood and Transplant (NHSBT) for their guidance and assistance undertaking experimental work. I am also grateful to NHSBT nursing staff, eye retrieval coordinators, mortuary staff, donors and their relatives, without whom these studies would not have materialised. I am also grateful to Professor Darlene Dartt at the Harvard Medical School, Boston for hosting my visit to their laboratories, during which I received training in cell culture of primary conjunctiva that was crucial to this research. I would also like to thank Dr Gabriella Czanner for her expert advice on statistical methods, Mr Jim Buckhurst for producing materials that were used in experimental work and Dr Simon Biddolph for his advice on undertaking immunohistochemistry. I would also like to thank Dr Ilene Gipson for the gift of the HCjE-Gi cell line. I am also grateful to the research staff and students at the Department of Eye and Vision Science for their guidance and companionship.

I must also gratefully acknowledge the encouragement and support from my husband, Anand, and family through the highs and lows of the last few years. This work was possible because of their unrelenting support and wisdom.

Table of contents

List of figures

List of tables

Abbreviations

ABCG2	ATP-binding cassette sub-family G member 2
BCVA	Best corrected visual acuity
BPE	Bovine pituitary extract
BSA	Bovine serum albumin
CK	Cytokeratin
DAPI	4', 6-diamidino-2-phenylindole
DMEM	Dulbecco's Modified Eagle Medium
DMSO	Dimethyl sulphoxide
DNA	Deoxyribonucleic acid
ECM	Extracellular matrix
EDTA	Ethylenediaminetetraacetic acid
EGF	Epidermal growth factor
ePTFE	Expanded polytetrafluoroethylene
FCS	Foetal calf serum
HEPES	4-(2-hydroxyethyl)-1-piperazineethanesulfonic acid
HCjE-Gi	Human conjunctival epithelial cell line (Gipson laboratories)
HCl	Hydrochloric acid
H&E	Haematoxylin and Eosin
HPA lectin	Helix pomatia lectin
MMP	Mucous membrane pemphigoid
mRNA	Messenger ribonucleic acid

MUC1/4/7/16	Mucin 1/4/7/16
MUC5AC	Mucin 5AC
NaOH	Sodium hydroxide
PAS	Periodic acid Schiff
PBS	Phosphate buffered saline
PCNA	Proliferating cell nuclear antigen
PET	Polyethylene terephthalate
p63	Tumour protein p63
PGLA	poly(lactic-co-glycolic acid)
RFGD	Radio frequency glow discharge
RNAse	Ribonuclease
RPMI medium	Roswell Park Memorial Institute medium
SCCM	Standard cubic centimetres per minute
SDS	Sodium dodecyl sulfate
TRIS	2-Amino-2-hydroxymethyl-propane-1,3-diol
TBS	Tris buffered saline
TFF	Trefoil factor family
3T3	Murine fibroblast cell line; 3-day transfer, inoculum 3 x10^5cells
UAE-1 lectin	Ulex Europaeus lectin 1
VA	Visual acuity
ZO-1	Zonula occludens-1
Z-stack	Focus stacking/focal plane sections

1. Introduction

1.1 The ocular surface

The ocular surface comprises the cornea, conjunctiva and the tear film. The cornea and conjunctiva line the anterior surface of the globe. The cornea is a transparent convex structure and is the main refractive component of the eye. It is surrounded by and is contiguous with the conjunctiva, which covers the anterior episcleral tissue. The conjunctiva extends from the corneal limbus and covers the tarsal (inner) surface of the eyelids. It is a moist translucent membrane with redundant folds that are most prominent in the fornices which are anatomical spaces between the globe and eyelids that enable free ocular movement.[1] The tear film and conjunctiva are essential for the homeostasis of the cornea. The associated tear film is crucial to the maintenance of corneal clarity, and to the prevention of infection.[1] The ocular surface is also protected from drying, desiccation and injury by the upper and lower eyelids and its components including the eyelashes and sebaceous secretions from meibomian glands. [1]

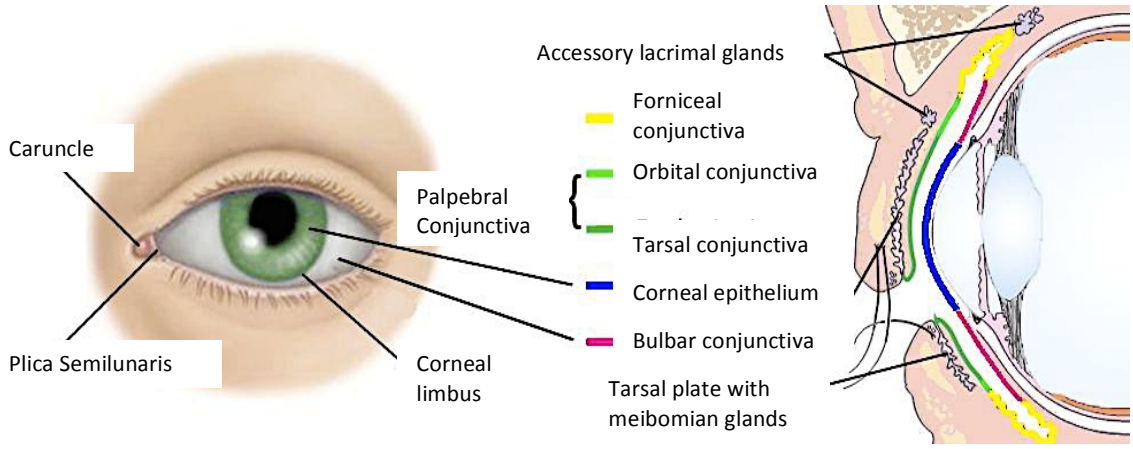

Figure 1: Schematic drawing illustrating a cross section of the globe and eyelids. Taken from Stewart RMK. (2013) Identification of progenitor rich sites in the conjunctiva. PhD Thesis. University of Liverpool; adapted in part from Paulsen and Berry (2006).[2]

1.1.1 The cornea and limbus

The cornea is a transparent structure that enables the entry of light and is the main refractive component of the eye. The average vertical and horizontal diameters in an adult are 10.6mm and 11.77mm, respectively.[1] From superficial to deep, the cornea is composed of an epithelial layer and basement membrane, an anterior limiting lamina (Bowman's layer), the substantia propria (stroma), a posterior limiting lamina (Descemet's membrane) and an endothelial layer, which is contact with the aqueous humour of the anterior chamber of the eye.

The corneal epithelium is a stratified squamous non-keratinising epithelium that is 5-6 cell layers deep. The basal epithelial cells are associated with the basal lamina via type VII and VI collagen.[3] Continuous turnover of corneal epithelial cells occurs in which transiently amplifying cells arise from the corneal stem cell niche at the basal limbus and migrate centripetally.[4] The corneal epithelium is densely innervated by sensory but also by a smaller proportion of sympathetic fibres. The sensory nerves can respond to temperature, chemical and mechanical stimuli.[5] Epithelial defects heal rapidly through the amoeboid movement of corneal epithelial cells.[6] The apical corneal epithelial cells possess a glycocalyx, microplicae and microvilli that interact with and stabilise the tear film.[7] The corneal epithelium meets the conjunctival epithelium at the limbus, a transition zone at the edge of the cornea.

Corneal and conjunctival epithelia have similar features in terms of ABGC2 and ΔNp63 expression in progenitor cell populations but differ in cytokeratin expression.[8-10] Differentiating features include the absence of goblet cells in normal corneal epithelium and differential cytokeratin expression.[11] Corneal stem cells are found in the basal crypts of limbal epithelium. Notable features of the limbus are radial papillae (termed palisades of Vogt), dense vascularisation and an epithelial layer around 10 cells deep.[1] In this transition zone, conjunctival epithelial cells end along with its blood vessels. The vascular supply of the peripheral cornea originates from the marginal

corneal arcades and that of the limbus is from an episcleral plexus derived from the anterior ciliary arteries that travel anteriorly from the rectus muscles deep to the conjunctiva.[1] The basement membrane composition of the limbus differs from the corneal basement membrane such that laminins α1, β1 and γ1 are found in greater abundance together with collagen IVα2.[12] In limbal stem cell disease conjunctival epithelialisation of the cornea occurs, resulting in a loss of corneal clarity.[1]

Bowman's layer is a modified layer of the corneal stroma containing collagens type I, III, V and VI and terminates at the limbus. The corneal basement membrane at the corneal limbus is composed mainly of collagen IV and VII, but also extracellular matrix proteins laminin (subtypes 332 and γ2), fibronectin and a number of glycoproteins: perlecan, nidogen, fibrillin, clusterin.[3] The corneal stroma consists of collagen I, III, V and VI in regularly arranged lamellae, the spacing of which, is determined by intervening glycosaminoglycans and proteoglycans.[1] The maintenance of corneal clarity is dependant upon the regular arrangement and diameter of collagen fibrils and the tight regulation of hydration. In the healthy cornea no blood vessels are found in within the corneal stroma apart from the marginal corneal arcades. Nerve fibres are present in the anterior stroma. The nerve supply of the cornea is via the long ciliary nerves that originate from the ophthalmic division of the trigeminal nerve. [1] Descemet's membrane is basement membrane of the corneal endothelium and is continuous with the trabecular meshwork peripherally. The corneal endothelium is a monolayer of continuous polygonal squamous epithelium rich in mitochondria.[1] These cells are responsible for active transport regulating the fluid and electrolyte balance of the cornea and therefore its clarity.

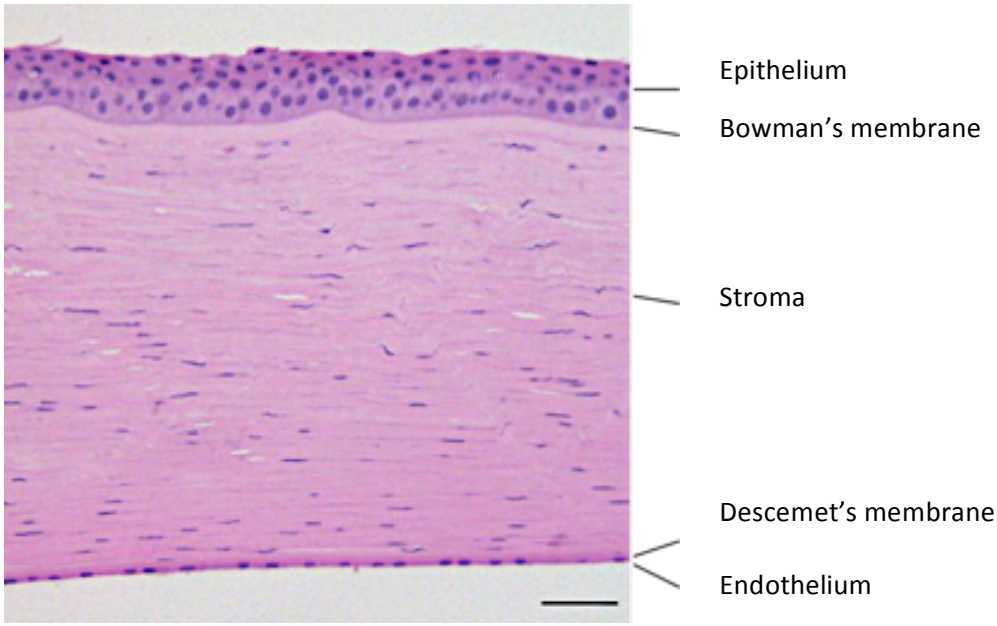

Figure 2: Photomicrograph of the normal human cornea. Paraffin embedded tissue section was subjected to staining with Haematoxylin and Eosin. Scale bar 50µm. Taken from Taken from Stewart RMK. (2013) Identification of progenitor rich sites in the conjunctiva. PhD Thesis.

1.1.2 The human conjunctiva

The conjunctival is a thin, translucent vascularised membrane that lines the sclera and the inner aspect of the upper and lower eyelids. It is a stratified epithelium supported by a basement membrane that overlies a thin layer of vascularised loose connective stromal tissue.[(1)] Between the conjunctival connective tissue and the sclera lies the tenon's capsule, which is a thin layer of fibrous tissue that forms adhesions with the underlying episclera and also serves a protective function.

The conjunctiva is a stratified non-keratinised squamous and columnar epithelium and contains goblet cells, which bear similarities to glandular epithelia. The conjunctiva varies between 3 and 9 cell layers deep and extends from the edge of the corneal limbus, to the mucocutaneous junction of the eyelid margin where the transition zone from non-keratinising to keratinising epithelium occurs.[(1)] The conjunctiva is reflected

from the anterior sclera to the tarsal (inner) surface of the eyelids to form an anatomical space between the upper and lower eyelids and the globe known as the conjunctival fornices. The excess conjunctival tissue seen as folds in these areas, allows a full range of ocular movement. The volume of this space with the eyelids closed has been estimated at approximately 7µl. [1]

The conjunctiva can be divided anatomically into three regions: the bulbar, forniceal and palpebral conjunctiva. The bulbar conjunctiva covers and is loosely adherent to the globe. In contrast, the palpebral or tarsal conjunctiva is tightly adherent to the tarsal plate on the inner aspect of the eyelids. The forniceal conjunctiva forms the blind pouch between the eyelids and globe where it is thrown into folds. The subepithelial connective tissue is sparse in the palpebral conjunctiva. The lacrimal puncti open into the lid margin medially. These are small openings of the narrow passages that connect the eyelids to the nasal cavity allowing the drainage of tears. The conjunctival epithelium is continuous with that lining the inferior meatus of the nasal cavity. The forniceal conjunctiva is also continuous with the medial and lateral canthi and contains accessory lacrimal glands (Krause's glands).

The secretions from most of the accessory lacrimal glands in addition to those from the main duct of the lacrimal gland open into the superolateral fornix. The facial sheaths of the rectus muscles in the upper and lower eyelids and levator palpebrae superioris in the upper lid are associated with the conjunctiva. The bulbar conjunctiva acts a coating for the sclera, which is also covered with episclera and Tenon's capsule and also covers the extraocular muscles. The conjunctiva is loosely adherent to episcleral tissue over the bulbar conjunctiva but is tightly adherent at the limbus. At the medial fornix the bulbar conjunctiva forms a semilunar fold (plica semilunaris) of thickened tissue that is highly vascularised, rich in immunocompetent and mucin producing goblet cells.[1] Medial to this is a nodular tissue known as the caruncle that contains densely packed sebaceous glands, accessory lacrimal glands and lymphoid cells.[1]

The conjunctival epithelial cells are mostly cuboidal or polyhedral in shape. Goblet cells can be found interspersed within layers of stratified conjunctival epithelia either in isolation or in clusters lining crypts. They are found within apical layers of epithelium and can be easily recognisable as they are often more rounded in appearance than the surrounding epithelia. [13] Goblet cells tend to be large and are characterised by an apical portion that is broad in comparison to their basal proportions. These cells are characteristically rich in intracellular organelles owing to their secretory and storage capacity for the gel forming mucin MUC5AC. [11]

Other than goblet cell secretions, the conjunctiva also contains accessory lacrimal glands known as Krause's glands in the conjunctival fornices and glands of Wolfring located in the upper border of the tarsus. These glands contribute to the baseline tear production and are innervated by sympathetic nerves.[1] The conjunctiva is also known to have lymphoid tissue known as conjunctiva associated lymphoid tissue (CALT) where MHC II dendritic cells transport internalised antigens and signals to mount an adaptive immune response.[1] In addition, intraepithelial CD3+ve lymphocytes are a recognised feature of conjunctiva and occasionally B-lymphocytes as part of the immune defence system of the conjunctiva. Scattered melanocytes can also be found.[1]

The sensory supply of the conjunctiva is derived from the ophthalmic branch of the trigeminal nerve. Parasympathetic and sympathetic nerves arise from the pterygopalatine ganglion and sympathetic plexus respectively and course along branches of the ophthalmic artery, terminating around goblet cells. The vascular supply of the conjunctiva is in the substantia propria, delivered by the anterior conjunctival branches of the anterior ciliary artery and the palpebral branches of the ophthalmic and lacrimal arteries. These vessels anastomose with the marginal corneal arcades and the limbal plexus. Venous drainage occurs into a venous plexus that leads to the superior and inferior ophthalmic veins. Lymphatic vessels are also found within a network in the bulbar and palpebral conjunctiva. [14]

Biochemical components of the conjunctival basement membrane zone have been characterised and include collagens I/IV/VII, laminins and also fibronectin.[15] Collagen IV and VII, however, are found with greatest abundance with laminins specifically of -332, α3, γ1, γ2 and 5: integrin β4, fibronectin, nidogen, perlecan, and clusterin.[3] Although these components are identical to those of the corneal and limbal basement membranes, the proportions of some of these components vary between the aforementioned tissues.[3]

There is a continual turnover of conjunctival epithelium, which has a great regenerative capacity. This applies to cells of both an epithelial and goblet phenotype.[11, 16, 17] Evidence for this was determined from cloning studies in which it was also demonstrated that goblet cells were not terminally differentiated.[18] Markers associated with progenitor cells were mostly found in basal epithelium and were found in greatest abundance at the inferior fornix and medial canthus.[19]

1.1.3 Protection of the ocular surface and the tear film

There are physical barriers to chemical, environmental and infectious insults such as the blink reflex, eyelids and eyelashes. The conjunctiva covering the majority of the ocular surface provides a barrier function and plays a role in mucosal immunity. The eyelids contain meibomian glands that are found within the fibrous tarsal plates and secrete the lipid component of the tear film (Figure 1). Blinking is a reflex action that redistributes the tear film and together eyelashes prevent trauma and the entry of foreign bodies. The meibomian gland secretions form the superficial layer of the tear film. It is a complex lipid layer comprising heterogeneous species of polar and non-polar lipids, 13-100nm in depth that stabilises the tear film and prevents evaporation from its aqueous phase. [20]

The tear film is crucial to the normal function of the ocular surface including the maintenance of corneal clarity. Several models of the tear film have been suggested. It is generally accepted however, that tear film comprises an outer meibomian lipid layer, a gel phase comprising aqueous secretion including electrolytes, antimicrobial factors and gel forming mucin, and an inner mucin layer directly in contact with the apical epithelia of both corneal and conjunctival cells.[7] The structure of the precorneal tear film has more recently been considered as mattress structure comprising three layers; an epithelial cell surface glycocalyx layer, an aqueous/mucin layer and a superficial lipid layer.[7]

The aqueous component of the tear film is produced primary by the lacrimal gland, which is located in the lacrimal fossa in the superotemporal orbit. There are also contributions from the accessory lacrimal glands. The aqueous secretions contain lactoferrin, immunoglobulin A, defensin, betalysin, lysozyme, lipocalin and the antibody-complement system of proteins that serve an antimicrobial function. [7, 21]

Mucins are a critical component of the tear film and are produced by conjunctival epithelial goblet cells. These are glycosylated complex high molecular weight glycoproteins that are hydrophilic in nature and capable of forming gels. Mucins serve to create a mucin-aqueous complex that lubricates the surface of ocular surface epithelia and prevents drying. The role of mucin also extends to a role in the primary defence against microorganisms as goblet cells also interact with antimicrobial constituents of the tear film, such as defensins and peroxidase.[17, 22] Mucins have been recognised not only to bind to bacterial cell walls but also to participate in the innate immune response through interactions with neutrophils and leucocytes via oligosaccharide epitopes found on mucins.[23] In addition to mucin, goblet cells also secrete the trefoil family peptides (TFF) TFF1 and 3.[2] These peptides together with mucin promote epithelial cell migration and have anti-apoptotic properties.[24]

The mucins on the ocular surface comprise membrane-associated mucins on the microplicae of apical conjunctival and corneal epithelium and form the glycocalyx that supports interactions at the cell-tear interface.[1] The large gel forming mucin MUC5AC is produced exclusively by conjunctival goblet cells by exocytosis. MUC5AC and a further small soluble mucin MUC7 produced by the lacrimal gland are the major mucin components of the aqueous layer of the tear film and are responsible for its lubricating and visco-elastic properties.[7] Mucins also form a protective layer within the tear film reducing evaporation of the aqueous components of the tear film, thereby maintaining moisture of the conjunctiva and cornea.

Ocular surface disease can be associated with both the overproduction and underproduction of mucin.[17] Of these conditions however, mucin depletion leads to more severe disease and goblet cell depletion is associated with most ocular surface diseases and include ocular mucous membrane pemphigoid, neurotropic keratitis and chemical injury.[25, 26] In the severe dry eye state the continual microtrauma of the cornea occurs leading to desiccation, opacity, ulceration and eventually painful blindness. In such conditions, the conjunctival epithelium also undergoes squamous metaplasia with loss of goblet cells and propensity to infection.[27]

The regulation of mucin production is complex and not fully understood. Mucins are produced by conjunctival squamous epithelial cells (MUC 1, 4, 16) and are found as transmembrane glycoproteins but have also as secreted components in the tear film.[28] The precise pathways and mechanisms by which the shedding of these mucins occurs are still under investigation. In contrast, MUC5AC secretion from goblet cells is known to occur through an apocrine mechanism mediated by growth factors, in addition to parasympathetic and sympathetic nervous stimulation. Purinergic and muscarinic agonists together with acetylcholine, carbachol and vasoactive intestinal peptide have been shown to stimulate goblet cell mucin secretion.[17] In addition, epidermal growth

factor (EGF) stimulates goblet cells and may occur following release from bacteria, platelets and nerves.[17]

1.2 Conjunctival disease in humans

Homeostasis of the ocular surface is dependent upon normal conjunctival function including mucin production. The conjunctival epithelium may become irreversibly destroyed by infective, inflammatory, neoplastic conditions and traumatic injury. This may lead to keratinisation, loss of goblet cells, cicatrisation, forniceal contraction and corneal ulceration leading to painful loss of vision.[29] These factors may result in limbal stem cell deficiency and visual deterioration.

A number of acquired and autoimmune diseases may cause these changes. Pathological change in the conjunctiva includes the formation of neoplastic lesions, both malignant and benign including the formation of pterygium, proposed to occur from ultraviolet damage. Inflammation can arise through autoimmune disease, infectious diseases including those from viral and bacterial pathogens, allergy and also induced iatrogenically from topical agents such medications used to treat glaucoma.

Trachoma is an eye disease caused by the intracellular bacteria *Chlamydia trachomitis*. It is an important infectious cause of cicatrising eye disease and is the second commonest cause of blindness in developing nations. An estimated 1.3 million people are blind worldwide from this condition.[30] The highest prevalence of trachoma is in sub-Saharan Africa, Middle East and Southeast Asia. Although easily treatable with oral tetracyclines, the global burden of this disease is significant as many do not have access to treatment and therefore a high proportion develop end stage cicatrising conjunctival disease which leads to chronic pain and corneal blindness.

Trauma may occur from a variety of injuries including thermal injury and chemical burns. Ocular burns constitute 7-18% of ocular injuries seen in emergency departments and 17.3% of battlefield injuries have been recorded in Iraq and Afghanistan.[31, 32] Visual disability occurred in 33% and blindness in 15% of patients with battlefield injury. [31]

Autoimmune diseases of the conjunctiva include mucous membrane pemphigoid, Stevens-Johnson syndrome, linear IgA disease and graft-versus-host disease. Autoimmune disease in particular, mucous membrane pemphigoid, can be one of the most challenging conditions to treat given the chronicity of the inflammation that leads to irreversible cicatricial eye disease. The incidence of mucous membrane pemphigoid has been reported between 1.13 and 1.78 per million per year in European countries with ocular involvement in 60-95% of patients.[33] The incidence of Stevens Johnson syndrome is estimated at 2-3 per million per year in Europe and the USA of which 43-81% have ocular involvement and 35% have permanent visual disability.[34] Developing countries such as India are recognised to have a significant number of Stevens-Johnson syndrome cases, thought to be the result of widespread availability and unprescribed use of antimicrobial drugs including sulphonamide containing drugs and fluoroquinolones.[35] The incidence of cicatrising conjunctivitis overall in the UK has been estimated at 1.3 per million per year, however, the authors of this surveillance study stated that this figure was likely to be an underestimation.[36] In contrast to developing nations, the burden in developed countries is largely due to autoimmune conjunctival disease, particularly ocular mucous membrane pemphigoid. Diagnosis of the latter may at times be considered at a relatively late stage in the disease process, and even in those diagnosed, under-recognised exacerbations between follow up periods despite treatment have been noted. [36]

Ocular surface disorders lead to squamous metaplasia and cicatrisation characterised by progressive fibrosis and scarring. Cicatrisation may be defined by the presence of

limbal stem cell deficiency, forniceal shortening and symblepharon.[27] The histological changes in conjunctival squamous metaplasia have been described in the following three stages by impression cytology: a) loss of goblet cells b) increase in cellular stratification and/or enlargement of the superficial cells and c) keratinisation.[37] Many ocular surface diseases lead to squamous metaplasia and cicatrising eye disease both in advanced stages of chronic inflammation and by a severe insult such a chemical injury. Ocular surface disorders are an important clinical problem as irreversible scarring and keratinisation of the conjunctiva leads to an abnormal epithelium with loss of secretory and membrane bound mucin and therefore compromised defence against infection.[38] It is also accompanied by depletion of goblet cells and secondary tear film deficiency. When severe, along with forniceal shortening, symblepharon and ankyloblepharon, lid deformities also occur such as entropion and ectropion. This results in trichiasis, exposure keratopathy and recurrent corneal desiccation. These factors in combination may lead to corneal blindness due to limbal stem cell deficiency resulting in ulceration or progressive conjunctivalisation and opacification.

Causes of cicatrising conjunctivitis	
Trauma:	Chemical, thermal, radiation, physical
Infection:	Trachoma, membranous conjunctivitis, chronic mucocutaneous candidiasis
Allergic eye disease	Atopic keratoconjunctivits
Drug induced cicatrisation	Benzalkonium chloride containing solutions
Mucocutaneous disorders:	Stevens-Johnson disease, graft versus host disease, lichen planus
Immunobullous disease:	Mucous membrane pemphigoid, linear IgA disease, bullous pemphigoid, paraneoplastic pemphigus
Neoplasia:	Sebaceous cell carcinoma, squamous cell carcinoma

Table 1: Table of potential causes of cicatrizing conjunctivitis. This list has been adapted from Saw et al. (2008) and illustrates a non-exhaustive list of the diseases processes that may lead to conjunctival cicatrisation.[39]

1.2.1 Medical strategies in cicatrising conjunctival disease

Crucial to the management of cicatrising conjunctival disease is early diagnosis and treatment to remove the inciting agent if present, reduce or terminate the inflammatory process and encourage epithelial regeneration. The treatment strategy depends upon the nature and cause of the inflammation. For example, the medical treatment of ocular burns comprises acute irrigation to remove the inciting agent, tetracyclines and citrate to reduce metalloproteinase activity, steroids to reduce inflammation, tear supplements, antimicrobials to prevent infection and ascorbate to promote healing. In trachoma, the inflammation is caused by *Chlamydia trachomitis* and therefore responds to oral tetracyclines.

Stevens-Johnson syndrome may be diagnosed through skin biopsy rather than any specific serological test together with clinical findings. The treatment of Stevens-Johnson syndrome involves cessation of the inciting agent, intravenous immunoglobulin, systemic corticosteroids and the management of the systemic sequelae of this severe illness.[40] None of the immunomodulatory treatments however have been found to influence the ocular outcomes.[41, 42] Similarly, other autoimmune conjunctival diseases including ocular mucous membrane pemphigoid may be diagnosed through their clinical features, biochemical features of autoimmune disease and the direct immunofluorescence assay of a mucous membrane biopsy which may be taken from the conjunctiva.[39] A negative biopsy, however, is not conclusive. Immunosuppressive therapy is only required when the autoimmune disease process is active. First line therapy involves the use of dapsone, sulfasalazine or methotrexate.[39] Second line agents include azathioprine, mycophenolate mofetil and cyclophosphamide.[39] Adjunctive use of corticosteroids including pulsed intravenous methylprednisolone may also be considered for the short-term control of severe inflammation. The use of biologics including anti- tumour necrosis factor agents etanercept and infliximab, and the anti-CD20 antibody rituximab have been successfully used to treat severe refractory disease.[43-45] It is recognised, however, that symblepharon formation may still progress despite the apparent control of ocular inflammation in autoimmune conjunctivitis, particularly in ocular mucous membrane pemphigoid.[36] In many cases of cicatrising conjunctivitis, irreversible and significant conjunctival damage occurs such that medical strategies alone may be insufficient to enable the regeneration of healthy ocular surface epithelia.

In all forms of cicatrising eye disease, supportive therapy includes management of the factors that exacerbate the condition. This includes management of inflammation associated with co-existent ocular surface disease. For example, meibomian gland dysfunction and blepharitis may co-exist with the cicatrising disease process. Indeed, blepharitis can lead to colonisation with bacterial pathogens and therefore represents

a risk factor for microbial keratitis.[39] In a study of lid pathogens, 85% of mucous membrane pemphigoid patients were demonstrated as carriers for such pathogens in contrast to 49% in the control group.[46] Dry eye due to mucin and tear deficiency can occur in a many cicatrising eye diseases due to sparse goblet cells and also other dysfunction of other components including the meibomian glands. In turn, this predisposes to poor epithelial integrity and compromised immune defence. Management strategies include tear supplements including autologous serum, punctal occlusion, topical cyclosporine or steroid to address keratoconjunctivitis sicca, and lid surgery to address lid malpositions such as entropion with trichiasis or lagophthalmos.[39]

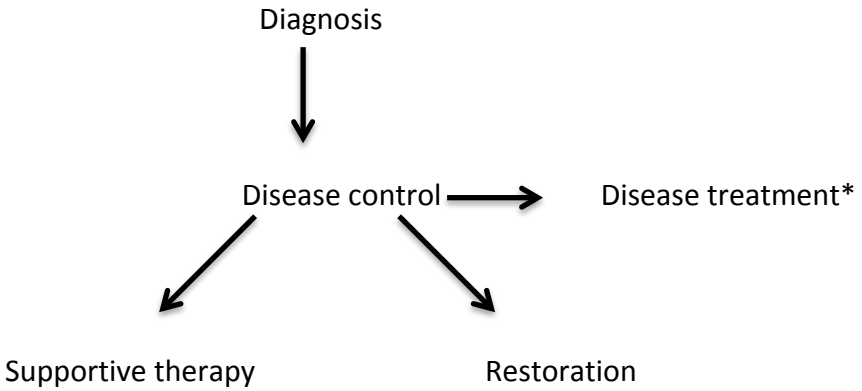

Figure 3: Flow diagram to illustrate that the management of ocular disease involves treatment of the disease process along with supportive therapies and restorative treatment. *Disease treatment may involve removal of the inciting agent, antimicrobials, immunosuppressants or anti-inflammatory agents as described in earlier paragraphs (section 1.2.1).

1.2.2 Surgical ocular surface reconstruction strategies and the clinical need for novel conjunctival equivalents

Poor conjunctival integrity and adnexal abnormalities including dry eye, entropion and trichiasis are prognostic factors for corneal and limbal stem cell transplant failure leading to poor visual outcomes in these patients.[29] It is paramount therefore, that strategies for ocular surface reconstruction include the correction of lid deformities including entropion and also trichiasis, which would otherwise result in continual abrasion and trauma to ocular surface epithelia. Lid deformities together with improvements in conjunctival function must therefore be addressed with surgical interventions to enable the success of a potential corneal or limbal stem cell transplant.

Current strategies for the replacement of conjunctival loss are most commonly conjunctival autografts or amniotic membrane grafts. Conjunctival autografts have been used for the repair of small defects with relative success.[47, 48] These can be taken from the fellow eye or from the same eye, usually the superior bulbar conjunctiva. This approach, however, cannot be used for the repair of larger defects including fornix reconstruction. Furthermore, the trauma to the donor site in retrieving a conjunctival autograft would be detrimental in autoimmune diseases leading to further inflammation and scarring.

Mucosae from the nasal turbinates and oral cavity have been investigated as donor tissues for ocular surface reconstruction. It is recognised, however, that these grafts are associated with poor cosmesis and recurrent scarring.[49] The human oral mucous membrane has been used for the reconstruction of conjunctival fornices with some success.[50, 51] Similarly, nasal turbinate mucosal grafts have also been demonstrated in the successful reconstruction of conjunctival fornices in patients with chemical injury and cicatricial mucosal disease.[52, 53] An increase in mucous production was demonstrated in association with a reduction in symptoms for the majority of patients that received this treatment. This approach, however, is limited by differences in

appearance including the colour of the tissue, which can appear unsightly in comparison to the translucent appearance of amniotic membrane and native conjunctiva.[54] A further consideration is morbidity to the graft donor site, which may be a limitation for its use in patients with mucous membrane pemphigoid due to possible disease involvement of tissue at these extra-ocular mucosal sites.

To date, the most commonly used substrate for ocular surface reconstruction has been amniotic membrane, exemplified by its extensive clinical usage. It is most commonly used in the treatment of large conjunctival epithelial defects where it promotes epithelialisation and reduces scarring.[55] The use of amniotic membrane for the reconstruction of conjunctival fornices, however, has been less successful. In patients with on going inflammation recurrent symblepharon was demonstrated in 10-44% of patients and loss in forniceal depth of 50% or more occurred four months after surgery.[56, 57] Therefore, outcomes of forniceal reconstruction using amniotic membrane grafts are poor due to shrinkage and cicatrisation resulting in recurrent forniceal loss.[58]

The severity of ocular damage to the conjunctiva in mucocutaneous and systemic and inflammatory diseases warrant the development of grafts to regenerate the ocular surface and reconstruct the fornices. Novel robust conjunctival constructs would enable visual and functional rehabilitation in patients with severe ocular surface disease in whom prognosis is poor due to a lack of available therapies. Novel conjunctival equivalents may also assist in surgical procedures associated with conjunctival loss including conjunctival neoplasia, pterygia and glaucoma surgery.

1.3 Substrates for conjunctival regeneration

1.3.1 An ideal conjunctival substrate

An ideal substrate for the expansion of conjunctival epithelium should be elastic to enable free ocular movement, integrate in the host without causing inflammation and support a self-renewing conjunctival epithelium with a sub-population of progenitor and goblet cells. If a small defect requires treatment, a conjunctival equivalent that degrades may be suitable, such that it is eventually replaced by host conjunctiva. Fornix reconstruction however may benefit from a non-degradable substrate that is capable of maintaining long-term forniceal support.

1.3.2 The use of biological substrates for the ex vivo expansion of conjunctival epithelium

Other than autologous tissues including autologous conjunctiva, nasal and oral mucosae, the principal allogeneic biological substrate investigated for conjunctival regeneration has been amniotic membrane. Amniotic membrane is the innermost layer of the membrane that surrounds the foetus in utero. Its use in ophthalmic surgery has been established for over 70 years and it plays a major role in ocular surface reconstruction in current clinical practice.[59] Desirable features include its lack of immunogenicity, antibacterial and anti-inflammatory properties.[60-62] The use of amniotic membrane for the protection of ocular surface defects such as large corneal epithelial defects and chemical burns where it promotes healing has been long established.[63, 64] It can therefore play a major role in the healing process of ocular surface defects. Amniotic membrane been used in both a cellular and decellularised form. Decellularisation may reduce the risk of disease transmission but may disrupt extracellular matrix components and the ultrastructure of the tissue.[65]

The presence of progenitor and goblet cells have been demonstrated in rabbit conjunctival epithelial cell cultures developed on an amniotic membrane substrate.[66] Stratified conjunctival epithelial constructs have also been successfully demonstrated on an amniotic membrane substrate.[67] Studies of ex-vivo expanded human conjunctival epithelium on amniotic membrane have not however, shown the presence of goblet cells.[54, 68] Human amniotic membrane has been transplanted into the eye both with and without the ex-vivo expansion of conjunctival epithelium. The successful reconstruction of conjunctival defects with ex-vivo expanded conjunctival epithelium on amniotic membrane has been demonstrated for small defects including those following the removal of papillomata and pterygia in humans.[69, 70] Studies have shown that amniotic membrane transplantation results in healing without significant inflammation and can result in the regeneration of conjunctiva.[54]

The success of amniotic membrane transplantation, however, depends on the underlying disease process. Fornix reconstruction in particular in the presence of active inflammatory disease is associated with recurrence of symblephara and forniceal loss.[54] In keeping with this, a descriptive study reported 12 of 17 eyes recovered successfully following amniotic membrane reconstruction of shortened fornices. Clinical outcomes were favourable in eyes with symblephara due to traumatic injury in contrast to patients with symblephara due to mucous membrane pemphigoid.[71] Other than amniotic membrane and oral/nasal mucosa, no other cellular or decellularised human allogeneic tissues have been investigated as conjunctival equivalents.[52, 54]

1.3.2.1 Decellularisation of human tissues

'Biological' scaffolds derived from decellularised tissues have been successfully transplanted in humans for a multitude of regenerative therapies including skin, heart valves, vascular repair, bladder and even trachea.[72-75] Extracellular matrices or decellularised scaffolds can be prepared by the removal of cellular components of tissues and organs. Extracellular matrices are relatively conserved across species and

confer the optimal 3D environment providing a platform for recellularisation with the patient's own cells, demonstrated through a variety of organ models.[75, 76] The decellularisation process renders tissues immunologically inert thereby minimising the immunological rejection risk and enables the use of a large donor pool. The key advantages of acellular tissue over synthetic substitutes are that the scaffolds inherently possess the ultrastructure and gross anatomic structure native to the tissue of origin. The precise nature of the 3-dimensional arrangement of matrix proteins may influence cell adhesion with more appropriate ligand specificity.[77] Furthermore the biomechanical properties of the native tissues are also retained and therefore have the potential to influence function.

Decellularised tissues are comprised mainly of extracellular matrix, which is the secreted product of cells native to a particular organ or tissue. It therefore provides a unique opportunity for regeneration with autologous cells in which the unique cues from extracellular matrices may provide the optimal conditions for cell growth. The tissue specificity of the extracellular matrix is proposed to influence and maintain the cellular function and phenotype demonstrated through a variety of organ and tissue models and even includes nerve allografts, which have been used to repair sensory defects in the hand.[78] Interactions with the extracellular matrix have been shown to influence the proliferation and chemotaxis of cells, demonstrated in many tissues and include endothelial and progenitor cell migration.[79] The appropriate differentiation of embryonic stem cells and regeneration of tissues with appropriate function has been demonstrated in studies of several organs including kidney, lung and the adrenal gland.[80-82] Differentiation of tissues along the appropriate lineage together with the appropriate tissue remodelling responses have also been demonstrated in a variety of tissues as described in models including skeletal muscle and vocal cord.[77, 83, 84]

Other than the extracellular matrix, it has also been proposed that the surface topology and the 3-dimensional ultrastructure arrangement also influence cell interaction,

function and phenotype.[77] It is crucial therefore, that there is minimal disruption to acellular scaffold during the decellularisation treatment. Decellularisation can be achieved by several means including physical (e.g. temperature, force and pressure), enzymatic and chemical processes. The most effective agent depends upon features of the tissue including its cellularity, density and lipid content and must be balanced against the adverse effects of extracellular matrix disruption.[77] Chemical agents used in the decellularisation of tissues include alcohols and other solvents, hypertonic and hypotonic agents, acids and bases and detergents. Enzymatic processes often include nucleases, collagenase and dispase.[77] Of these agents, trypsin and collagenase in particular are recognised to result in significant extracellular matrix disruption.[77, 85, 86] Collagenase in particular is generally used for applications in which the ultrastructure of the tissue is not critical.

1.3.1.2 Decellularisation of human amniotic membrane

The human amniotic membrane bears histological similarities in its gross structure to human conjunctiva, as it also comprises an epithelial layer, a basement membrane and substantia propria. A protocol for the decellularisation of human amniotic membrane has been developed using a combination of chemical and enzymatic processes.[87] In this protocol, hypotonic and hypertonic solutions are used which cause cell lysis and the dissociation of DNA from proteins, respectively, whilst causing minimal disruption to the ECM. The detergent sodium dodecyl sulphate (SDS) is used to solubilise cell membranes, dissociates DNA from proteins and is known to be a highly effective decellularisation agent.[77, 88, 89] Finally, the protocol also includes benzonase, an endonuclease, which cleaves nucleic acids and effects the removal of residual nucleotides.[90] Of these described processes, the detergent (SDS) step has the greatest potential for disrupting the extracellular matrix and therefore a low effective concentration should be sought and the residual tissue characterised and tested for cytotoxicity.

An animal study using allogeneic and xenogeneic decellularised cornea and demonstrated successful integration of corneal tissue with maintenance of corneal clarity and cellular ingrowth including nerves [91] The decellularisation of porcine but not human conjunctiva has been reported in literature. In the latter study, decellularised porcine conjunctiva was used as a substrate for the transplantation of limbal stem cells in a rabbit model.[92] To date, the decellularisation of human conjunctiva has not been reported.

The collaborators of this study at NHSBT already produce clinical grade acellular dermal matrix distributed throughout the UK and have experience in decellularisation, characterisation and ex-vivo cellular expansion on human amniotic membrane. An existing protocol for the decellularisation of amniotic membrane will therefore be optimised to enable the decellularisation of human conjunctiva.

1.3.2 Synthetic substrates for ex-vivo expansion of conjunctival epithelium

Numerous synthetic substrates for the development of corneal grafts have been studied in comparison to conjunctival substrates in which relatively few reports exist. The use of a porous glycosaminoglycan co-polymer matrix has been described for the repair of full thickness conjunctival defects in rabbits and the forniceal depth compared with an un-grafted wound in the fellow eye.[93] A similar study describes the use of porous poly (lactide co-glycolide) (PGLA) scaffold modified by hyaluronic acid and collagen.[94] In these studies, forniceal shortening was significantly greater in the un-grafted eyes. In both studies, the un-grafted eyes had irregularly arranged collagen in keeping with scar tissue in comparison to a more regular collagen deposition demonstrated in the grafted eye.[93] Both substrates are examples of a degradable matrix. It should be noted however that both substrates were inelastic and lacked an epithelium.[73] In contrast conjunctival epithelium cultured on collagen matrices was demonstrated to develop with an appropriate cell polarity and even a basement

membrane, but was only an organised monolayer.[95] The latter study confirmed that substrate modulation influences the growth characteristics of human conjunctiva.
A more promising elastic substrate for conjunctival regeneration has been the use of plastic compressed collagen.[96] Laboratory studies have demonstrated confluent growth of conjunctival epithelium including a subpopulation of progenitor cells identified by putative stem cell markers and studies of colony forming efficiency. The authors of this study report the ultimate tensile strength of the substrates and handing was similar to amniotic membrane.[96] Another elastic resorbable polymer demonstrated to support the growth of conjunctival epithelium including goblet cells is ultrathin Poly (ε-Caprolactone).[97] Both substrates are biodegradable.

To date there has not been a non-degradable substrate developed for the regeneration of conjunctiva. This may provide an ideal solution for the epithelialisation following fornix reconstruction and long-term maintenance of fornix depth.

1.3.2.1 Expanded polytetrafluoroethylene (ePTFE)

Polytetrafluoroethylene (PTFE) is a simple polymer composed of carbon and fluorine and is known for its thermal stability and its hydrophobicity. The regular arrangement of fluorine atoms around the carbon backbone confers lack of polarity and therefore chemically inertness.[72] A microporous structure manufactured through heating and expansion is called expanded Polytetrafluoroethylene (ePTFE).[98] The microporous structure allows the free movement of gas and fluid depending upon the pore size, which also determines its flexibility.[72] It has been widely used as a biomaterial as it is non-reactive with surrounding tissues and is nondegradable in a biological environment. Degradation studies of non-expanded PTFE to oxidation and acid hydrolysis found PTFE to be relatively unaffected.[72] Indeed, degradation studies using ePTFE are lacking however no evidence of systemic or local toxicity have been reported as a result of ePTFE degradation in soft tissue applications.[99] Furthermore, there are no known allergic or teratogenic responses to this material.[72, 73] There is considerable

scope to modify the surface chemistry of ePTFE though a number of means including gas plasma, which can render the material more hydrophilic. It can also be impregnated with a number of agents that can prevent bacterial colonisation e.g. with silver and chlorhexidine.[73]

The application of expanded polytetrafluoroethylene (ePTFE) has grown over the last 30 years and it has been widely used in a range of surgical procedures including mesh in hernia repairs, gynaecological surgery, cardiac and vascular surgery. An example is the PRECLUDE^{R} membrane used in the closure and reconstructions within the pericardial space. Adhesions, collagen deposition or cellular infiltration could not been demonstrated following the use of this biomaterial.[100] This is an example in which adhesions with the host tissue were undesirable but a non-degradable and non-immunogenic material was required for the closure of a defect. The PRECLUDE^{R} membrane is an example of an ePTFE membrane in which the pore size <1µm has been cited to limit tissue ingrowth and therefore adhesions.[100, 101]

A number of reports also describe the use of ePTFE in ophthalmic surgery. Expanded PTFE has been successfully used as a 'stent' for the short-term forniceal maintenance in anophthalmic patients.[104] Similarly, it has also been used as a 'spacer' device for the excision of severe symblepharon in which recurrence can be prevented by blocking the physical reapposition of the denuded bulbar and tarsal surfaces when re-epithelialisation occurs in the postoperative period.[105] The ePTFE implant, PRECLUDE^{R} has also been used with low dose mitomycin-C as an adjuvant in preventing excessive bleb leakage in penetrating glaucoma surgery.[106] In the latter study, ePTFE was used as a device to prevent excessive filtration of aqueous humour in a procedure that creates an aqueous draining valve through the sclera to control intraocular pressure. The device was well tolerated and reduced the rate of early hypotony (excessive reduction in intraocular pressure), a common complication following filtration surgery. In these applications however, ePTFE was used as a means of physical support rather

than as a scaffold for cell seeding and epithelialisation. In a laboratory study, the attachment and proliferation of retinal pigment epithelial cells has been demonstrated on ammonia gas plasma treated ePTFE forming a monolayer of functional cells expressing tight junctional protein components including ZO-1 and occludin. [107, 108] These examples, together with reports of endothelial cell epithelialisation demonstrate the potential for ePTFE as a substrate for cellular expansion in tissue engineering applications. The growth of conjunctival epithelium on ePTFE has not previously been reported.

1.3.2.2 Ammonia gas plasma treatment to alter ePTFE surface chemistry

Plasma comprises ionised gas with positive and negatively charged particles. Ammonia gas plasma can be developed as low temperature plasma and requires a vacuum chamber. The gas plasma resonator is a device in which gas plasma can be created and comprises an airtight chamber connected to a vacuum pump, gas flow and electric power supply. The air within the chamber is evacuated by the vacuum pump before ammonia gas is allowed to enter the chamber at low pressure. The gas within the chamber is then energised by an electrical current, which creates a glow discharge and a variety of energetic species. These include ions, electrons, photons and free radicals. Surfaces in contact with plasma are subjected to energy transfer following collisions from the energetic particles. These changes occur only at the surface of the material and therefore do not affect its bulk properties. The surface chemistry of ePTFE can be altered such that a proportion of surface carbon-fluorine bonds are broken. Following plasma treatment, immersion of the samples into distilled water leads to the formation of hydroxyl functional groups in place of broken carbon-fluorine bonds, which renders the material more hydrophilic (Figure 4).

There are many applications in which ePTFE has been chemically modified to promote adhesion and proliferation of epithelia. Cellular proliferation can be promoted by surface modifications including coatings that are specific to the antigenic cues required

by the specific cell type. The successful endothelialisation of vascular ePTFE grafts, for example, have been demonstrated following the use of ePTFE coated with heparin/collagen films comprising functionalised CD133.[102] Similarly, gas plasma modification of ePTFE incorporates hydroxyl (-OH) groups on the surface rendering it hydrophilic and conducive to cell attachment. Furthermore, it has also been found that protein adsorption increases with the -OH group density found on the PTFE surface.[103] When the surface chemistry of these materials is modified, there is potential for tissue ingrowth e.g. mesh in hernia repair in which tissue ingrowth within internodal spaces has been demonstrated histologically and low hernia recurrence and infection rates reported.[73]

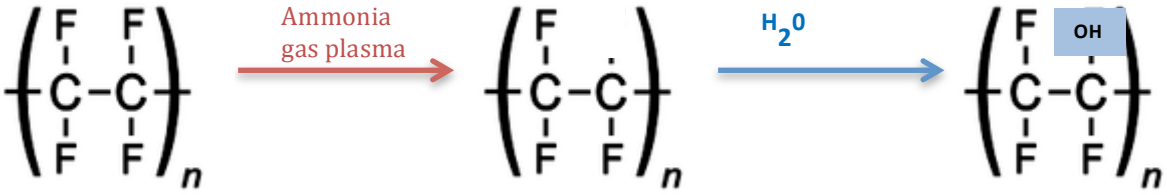

Figure 4: Illustration of the surface chemical change in ePTFE through ammonia gas plasma treatment and immersion in distilled water. Energy from gas plasma breaks some of the surface carbon fluorine bonds, which are replaced by hydroxyl functional groups on contact with water.

1.3.2.3 Determination of the hydrophilicity of materials through contact angle analysis

The contact angle is the angle at thermodynamic equilibrium of a liquid droplet where it meets a solid interface and a gas/vapour interface. This allows estimation of the wettability of the measured surface by the Young equation and defines the molecular interactions of liquid, gas and solid material (Figure 5). The Young-Laplace equation can ascertain the shape of the liquid/gas interface through Young's equation.[109]

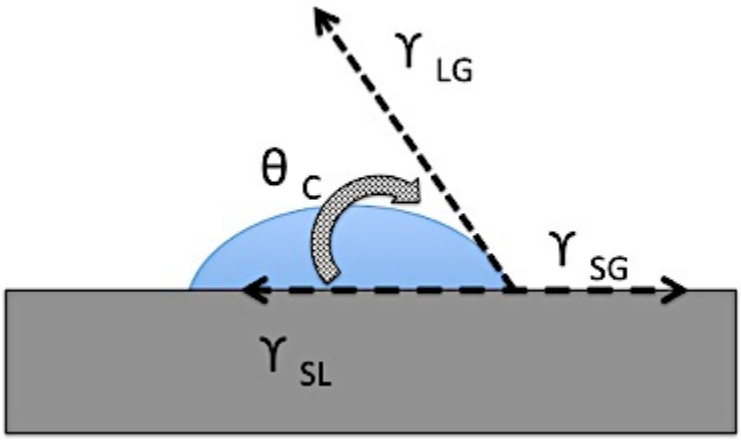

Figure 5: Illustration of a droplet on a solid surface with the measurements required in Young's equation. LG defines the gas-liquid interfacial energy (surface tension), SG defines the solid-vapour interfacial energy and SL defines the solid-liquid interfacial energy. The equilibrium contact angle can be derived from the relationship between these variables through Young's equation:γSG-γSL-γLG cos θc=0.[109]

1.4 Culture conditions for the ex-vivo expansion of human conjunctival epithelial cells

Traditional cell culture methods for the expansion of conjunctival epithelial cells include co-culture with inactivated murine 3T3 feeder layers (immortalised mouse fibroblasts) and the use of foetal calf serum (FCS).[110] Although these culture methods improve cell stratification and morphology, they are not ideally suited to clinical transplant applications given the risk of transfer of xenobiotic proteins and infective agents. Some research groups have demonstrated that successful development of stratified conjunctival epithelium can be achieved through the use of autologous or cord blood serum.[111]

There have been numerous published protocols for the culture of conjunctival epithelia using basal media varying from bronchial epithelial growth medium, RPMI, DMEM/F12 and keratinocyte serum free media.[11, 70, 112-114] The vast majority of recent studies avoiding the use of serum and murine 3T3's, however, have instead used a basal medium of keratinocyte serum free media. Indeed, over recent years, the successful development of conjunctival epithelium has been possible using serum free alternatives. [67, 97, 115, 116] Keratinocyte serum free media does however require bovine pituitary extract (BPE) to promote epithelial proliferation. Interestingly, positive detection of MUC5AC mRNA has been demonstrated in stratified rabbit conjunctival epithelium developed in keratinocyte serum free growth media.[116] Studies have also shown comparable proliferative potential, stratification and differentiation characteristics including a goblet cell subpopulation demonstrated through positive MUC5AC staining of primary conjunctival epithelial cells when cultured in basal media DMEM/F12 with human serum, BPE or FCS.[117] In most culture protocols, the cell primary cell cultures were initiated with a DMEM/F12 media containing FBS and epidermal growth factor (EGF) before changing to the keratinocyte serum free media.[67, 97, 111]

There is no consensus on the optimal growth media for conjunctival epithelium, particularly in the context of the requirement for an optimal subpopulation of progenitor and goblet cells. Marked similarities were also found between culture media protocols established both for the expansion of the HCjE-Gi cell line and primary human conjunctival epithelium.[67-70, 97, 113, 118]

1.5 Characterisation of human conjunctival epithelium

The human conjunctival epithelium is derived from bipotent progenitor cells, which differentiate into stratified squamous epithelial keratinocytes in addition to goblet cells

that resemble glandular epithelia. Proposed markers for the identification of conjunctiva epithelium based on markers of differentiation are described.

1.5.1 Goblet cell markers

Goblet cells have been demonstrated to originate from bipotent progenitor cells which also have the potential to differentiate into keratinocytes.[18] Cytokeratin 7 (CK7) and the intracellular gel forming mucin MUC5AC have been proposed as markers of goblet cells.[11] Only goblet cells amongst all ocular surface epithelia secrete the large gel forming mucin MUC5AC.[28] MUC5AC is found in the tear film and is the result of secretion through the process of exocytosis by goblet cells. [17] MUC5AC is a high molecular weight glycoprotein.

Alternative methods of identifying goblet cells based on their mucin content include UEA-1 (Ulex Europaeus Agglutinin-1) lectin, HPA lectin (Helix pomatia agglutinin), Periodic Acid Schiff (PAS) and Alcian Blue.[11] Lectins are a group of proteins that bind specific carbohydrate groups. UEA-1 binds to glycoproteins and glycolipids containing α-linked fructose residues and glycoconjugates. Cells high in mucins therefore can be identified by the binding of these molecules and have been demonstrated in studies to localise to goblet cells in culture.[11] PAS is a stain used to identify glycolipids, glycoproteins and mucins. Similarly, Alcian blue also identifies polysaccharides and mucopolysaccharides. All of these staining methods other than MUC5AC detection therefore identify transmembrane mucins present on conjunctival epithelial keratinocytes in addition to goblet cells containing MUC5AC. PAS also identifies basement membranes.

1.5.2 Progenitor cell markers

A rapid turnover of conjunctival epithelium occurs throughout life. An earlier study proposed the a uniform distribution of progenitor cells throughout the conjunctiva based upon clonogenic ability of forniceal and bulbar conjunctiva.[18] More recently, however, Immunohistochemical analysis of progenitor cell markers and colony-forming efficiency determined that progenitor cells occur in greatest frequency within the inferior conjunctival fornix and medial canthus.[19, 119]

Conjunctival stem cells may be identified by a number of cell markers through immunological detection and polymerase chain reaction (PCR). A relatively well-studied marker is p63, interest in which initially arose in the 1990's when it was found that the absence of p63 had deleterious effects on the regenerative potential of epidermis and stratified epithelia.[120] It was since suggested that a defect in p63 resulted in a defect in stem cell renewal. Although the precise role of p63 in the differentiation and apoptotic pathways is unclear, cumulative evidence suggests that p63 has a role in epidermal stem cell renewal. Furthermore, a reduction in p63 mRNA expression has been correlated with a reduction in the proliferative capacity of human epidermal epithelium.[121] Its role in progenitor rather than differentiated cells is also supported by the absence of p63 transcription factors in paraclones of limbal and epidermal cells that were present in holoclones.[122] There are 6 isoforms of p63 and the isoform more extensively studied in epithelial cells is ΔNp63α.[9] Indeed, p63 detects basal conjunctival epithelial cells in general whereas ΔNp63α is found in a much smaller population of cells with stem cell like characteristics.[122, 123] Of the p63 isoforms, the ΔNp63α isoform has been identified as the predominant subtype in ocular surface epithelia. [9]

The ATP binding cassette sub-family G member 2 (ABCG2) is the ATP binding and transporter protein and is also a commonly used marker for the identification of progenitor cells in ocular surface epithelia (cornea and conjunctiva). Budak and

colleagues identified ABCG2 as a candidate stem cell marker and demonstrated the active efflux of the dye Hoechst 33342 was mediated by the ABGC2 transporter.[8] This population of cells could be separated as a side population representing <1% of cells by fluorescence activated cell sorting. The cells demonstrated behaviour in keeping with progenitor cells including slow cycling and clonogenic capacity in vitro.[8] Budak and colleagues also demonstrated by immunohistochemistry the presence of ABCG2 basal conjunctival epithelial cells found in clusters.[8]

Putative stem cell markers in of the conjunctiva include ABCG2 and ΔNp63. There are no definitive stem cell markers of the conjunctiva and these markers may detect transiently amplifying cells in addition to true stem cells and therefore will be broadly regarded in this study as progenitor cell markers.

1.5.3 Cytokeratins

Cytokeratins are polypeptides that form the intermediate filament system in epithelia of which there are 30 related polypeptides. They are broadly described within two groups: type 1(neutral-basic) and type 2(acidic). Epithelia may be characterised by the specific pair (type 1 with type 2) of cytokeratins that are expressed in the cells. Cytokeratin expression may be altered in disease states, differentiation and are differentially expressed between epithelia. Furthermore, within conjunctival epithelium, cytokeratin expression can be used to identify conjunctival epithelial cells from goblet cells and therefore can be regarded markers of differentiation. The differential expression of cytokeratins in corneal and conjunctival epithelia has been recognised. The cytokeratin pair CK3/12 have long been recognised as markers of corneal epithelia whereas CK13, CK19, CK7 and MUC5AC have been considered markers of conjunctival epithelia.[10, 124-127] The specificity of some markers such as CK3 and CK19 for corneal and conjunctival specificity, however, has been questioned by a number of authors.[124, 128, 129] In a recent immunocytochemical characterisation study it

was determined that CK13 and CK7 could be locallised to all conjunctival epithelial layers and suprabasal limbal epithelium whereas MUC5AC was specific only to conjunctiva.[124] CK19, however, was found in all conjunctival layers but was also detected in the suprabasal limbus and peripheral corneal epithelia.[124] Qi and colleagues locallised CK4 and CK7 to superficial layers of bulbar conjunctiva, whereas both markers were absent in corneal epithelium.[130] Based upon this evidence, this study will therefore utilise CK4, CK7, MUC5AC and CK19 as markers of conjunctival epithelium.

Cytokeratin 7 (CK7) is characteristic of glandular epithelia and is found in lacrimal tissue amongst other apocrine glands and tracheal epithelium.[125] Studies in animal and human conjunctival epithelium have found that CK7 staining cells have morphological features including secretory vesicles in keeping with goblet cells. It has been suggested that the CK7 filament may facilitate the exocytosis of mucin by interacting more specifically with the contractile apparatus of the goblet cell, which is not otherwise present in conjunctival cells of an epithelial phenotype.[125] Indeed, the upregulation of CK7 has been demonstrated on inductive differentiation of goblet cells in conjunctival epithelial cultures with a γ-secretase inhibitor. CK7 expressing cells in the latter study also expressed MUC5AC and exhibited morphological characteristics in keeping with goblet cells.[131]

Conflicting results have been reported over the expression of CK7 between cells of a goblet cell phenotype and conjunctival keratinocytes.[11, 132] The reason behind this relates to the clone of antibody used in which the OV/TL clone binds to all conjunctival epithelial cells whereas the RCK 105 clone has greater specificity.[133] Cytokeratin 4 (CK4) expression has been found in conjunctival keratinocytes that exhibit an epithelioid rather than a glandular cell morphology suggesting CK4 expressing conjunctival epithelia are keratinocytes that differ both morphologically and phenotypically from conjunctival goblet cells. CK4 positive cells have been locallised to

conjunctival epithelium and often reported within its superficial layers.[134] CK19 however is a recognised marker of conjunctival epithelium and its expression has been reported throughout the conjunctival epithelium in both in vivo and in vitro studies. [10, 124, 127, 130, 135] CK19 is therefore used in this study as a pan-conjunctival epithelial marker.

1.5.4 Proliferation versus apoptotic markers

There are a multitude of candidate markers that may be used to study proliferation and apoptosis. Proliferating cell nuclear antigen (PCNA) and Caspase-3 expression however have been well documented in conjunctival epithelia.

Caspase is a proteolytic enzyme involved in the apoptosis of mammalian cells. Subgroups of caspases also have a recognised role in inflammation (caspase -1, -4, -5, -12). Caspases can also be grouped by function either as initiators or executors of apoptosis.[136] Of these, caspase-3 is known for its role in the execution of apoptosis. The activation of apoptosis occurs via the B-cell lymphoma 2 (Bcl-2) family of proteins and is initiated in response to cellular stress from a variety of stimuli including cytotoxic drugs or irreparable DNA damage.[136] Caspase-3 has been exploited in numerous studies as a marker of apoptosis in conjunctival epithelial cells including human conjunctival cell lines and primary conjunctival epithelial cells.[49, 137-139]

Proliferating cell nuclear antigen (PCNA) is found in all replicating eukaryotic cells and plays a role in the replication of DNA. PCNA had a central role in the s-phase of the cell cycle during which this protein provides a platform for the protein-protein and DNA-protein interactions that occur during DNA replication, repair, chromatin formation and remodelling, and the cohesion of sister chromatids.[140, 141] The immunological detection of PCNA has been extensively used for the characterisation of human cells including conjunctival epithelium.[133, 134]

1.6 Flow cytometry

Flow cytometry is a scientific application that enables the quantitative analysis of cells in suspension. The principle of flow cytometry is that particle detection is based on the light scattering properties of cells when excited by laser.[142] The fluidics within this system is designed to carry a stream of fluid with cells in single file to the lasers within the system. Multiple lasers exist within the flow cytometer, illuminating the particles at varying frequency.[142] Any scattered light and emitted fluorescence is focussed and detected (Figure 6). The technique mostly requires the fluorescent labelling of cells to identify the cell associated marker being studied, whereby the fluorescence emitted by cells is detected after excitation from the respective laser at the required absorbance wavelength. The technique therefore allows multiparametric analysis of cell populations from several lasers simultaneously.

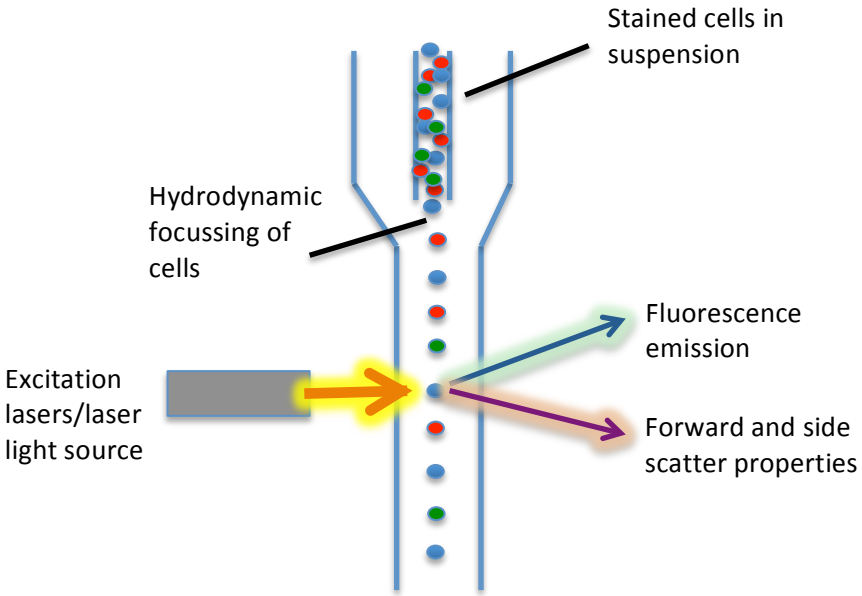

Figure 6: Illustration of the principle of flow cytometry. A heterogeneous population of cells labelled with fluorescent antibodies and markers in solution is directed into single file within a stream of fluid. Laser light sources excite cells and the light scattering characteristics and emitted fluorescence is detected to enable quantitative analysis of heterogeneous cell populations.[142]

Both indirect and direct antibody-staining methods have been employed in the analysis of conjunctival epithelia. Monoclonal or polyclonal antibodies can be directed to the antigen of interest and a fluorochrome conjugated secondary antibody targeted to the specific immunoglobulin and species subtype of the primary antibody. Flow cytometric analysis can be undertaken as single or multicolour analysis involving laser excitation from multiple channels. The fluorochromes are chosen at extremes of wavelengths to each other in multicolour analysis to avoid overlap in detected fluorescence.

1.6.1 Flow cytometry for the analysis of conjunctival epithelial cells

Flow cytometry has been used for the analysis of inflammatory markers in dry eye disease and rosacea.[143, 144] In a murine laboratory cell culture study, conjunctival goblet cells were enumerated by flow cytometry using cytokeratin specific antibodies CK4 (conjunctival epithelial cells), CK7 (goblet cells) and MUC5AC (goblet cells).[145] In another study of conjunctival brush cytology specimens, the side scatter and forward scatter pattern of human conjunctival epithelial cells have been characterised and CK7 used as a marker of conjunctival goblet cells.[146] The application of flow cytometry for the quantitative analysis of intracellular markers characterising progenitor cells in conjunctiva has not however been previously reported.

1.7 Mucous membrane pemphigoid

Of the cicatrising eye diseases, ocular mucous membrane pemphigoid (MMP) is encountered with greatest frequency in patients under review in UK corneal and external eye disease clinics.[36] Furthermore, the risk of sight threatening disease with advancing ocular mucous membrane pemphigoid has been regarded as ‘high risk’ in an international consensus review.[33] For this reason, it will be considered here as a priority treatment group and described in greater detail.

MMP encompasses a group of acquired autoimmune diseases characterised by a type II hypersensitivity response at the epithelial basement membrane zone. There is recognised variation in both clinical presentation and circulating autoantibodies to target auto-antigens in MMP, which suggests significant disease heterogeneity.[147] Suspected antigens include bullous pemphigoid antigens 1 and 2, β4 integrin, type VII collagen and laminins 5 and 6, present in lamina lucida transmembrane hemidesmosomes.[33, 148-150] Clinically, this results in inflammation, blistering and ulceration, which ultimately result in fibrosis and scarring. MMP affects mucous membranes in varying frequency and pattern involving the mouth, upper airway tracts, oesophagus, conjunctiva, anus and genitalia.[147]

Ocular involvement is typically bilateral and characterised by conjunctival injection, blistering and ulceration, which lead to subepithelial scarring and fibrosis. This results in forniceal shortening, further advancing cicatrising change and may ultimately lead to ankyloblepharon (adhesions between the eyelids) and 'frozen globe' (adhesion between the eyelids and globe together with ankyloblepharon). There is wide variation in the presentation of MMP in which it may be seen in the clinical setting with signs of acute inflammation in combination with chronic cicatrisation. Delayed presentation is typical however with low-grade inflammation resulting in slowly progressive cicatrisation.[151, 152] Patients typically present with established cicatrising eye disease and signs including forniceal shortening, conjunctival keratinisation and symblephara. The diagnosis is also often missed due to the non-specific nature of ocular irritation due to dryness, conjunctival injection and sub-epithelial fibrosis that is subtle in early disease.[33] A longitudinal study of ocular mucous membrane pemphigoid patients found younger patients with early onset disease had more signs of conjunctival inflammation and rapidly advancing disease.[36] It is also of interest to note that 42% of patients demonstrated disease progression without detectable signs of conjunctival inflammation based on the degree of conjunctival injection measured at clinic visits.[36] This demonstrates the importance of assessment of disease activity both in terms of

conjunctival inflammation and cicatrisation, which represents chronic change. Early diagnosis and accurate assessment of disease activity and progression is therefore crucial to the management of this challenging condition.

A pro forma was therefore developed for use in corneal and external eye disease clinics at St Paul's Eye Unit, Royal Liverpool University Hospital. A new pro forma was designed with the intention of including relevant aspects of the examination that would assist the clinician in the assessment of both a) disease progression and b) disease activity. Components of existing grading systems have been used or adapted and their pertinent features discussed within sections 1.7.1 and 1.7.2.

1.7.1 Grading systems to detect progression of cicatrisation in ocular mucous membrane pemphigoid

The accurate documentation and staging of ocular MMP is fraught with difficulty due to lack of standardisation of staging methods between clinicians, observer errors in the quantification of cicatricial progression and the insidious nature of the disease process itself. It has been recognised that cicatrisation may advance in the absence of measureable conjunctival inflammatory signs. It follows therefore that ocular MMP warrants assessment both in terms of conjunctival inflammation and cicatricial features to determine disease activity and progression. Several grading systems for cicatrisation have developed to grade the severity of clinical features and are described in this section.

The Foster grading system[153]

The staging system by Foster categorised the disease subjectively into stages I-IV.

Foster stages

I Subconjunctival scarring and fibrosis

II Fornix foreshortening (of any degree)

III Presence of symblepharon (of any degree)

IV Ankyloblepharon, frozen globe

The Mondino and Brown grading system [46]

Mondino and Brown developed a grading system that described forniceal shrinkage in terms of the percentage loss of forniceal depth.

Mondino stages

I 0-25% loss of inferior fornix depth

II 25-50% loss of inferior fornix depth

III 50-75% loss of inferior fornix depth

IV 75-100% loss of inferior fornix depth

Tauber grading system[154]

The Tauber grading system utilised Foster staging I-IV but included sub-divisions for stages II and III to describe the degree of fornix foreshortening (as described by Mondino and Brown) and degree of involvement by symblepharon respectively.

Stage II Percentage loss inferior fornix depth

a-d*

Stage III Percentage horizontal involvement by symblephara

a-d*

*a-d (describes subdivisions within II and III)

a 0-25%

b 25-50%

c 50-75%

d 75-100%

Rowsey grading system[155]

Rowsey developed a system to objectively measure more subtle changes in ocular mucous membrane pemphigoid than previous methods. This was based upon three measurements taken at 5, 6 and 7 o'clock from the limbus to the posterior lid margin with the eye in dextroelevation, upgaze and laevoelevation (Figure 7). The measurements are taken with a rule to the nearest millimetre with the lower lid held under maximal traction before the globe position is affected. An aggregate score was then calculated with a maximal score of 45 whereby the normal score was 15mm for each measurement.

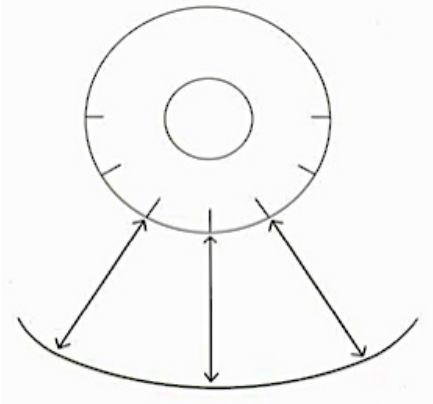

Figure 7: Diagram demonstrating the measured areas for the Rowsey scoring system. The diagram above shows the three measurements that are taken from the limbus to the lid margin at 5, 6 and 7 o'clock from the corneal limbus. Taken from Rowsey et al. Arch Ophthalmol. 2004;122:179-184.

Tauber-Liverpool method[156]

The grading systems described so far (Foster, Mondino and Tauber) grade loss of forniceal depth by estimation of the percentage reduction in the fornix depth, which is the distance from the posterior lower lid margin to the fornix. Difficulties in this estimation may arise due to the poor definition of the fornix itself due to the presence of subtarsal fibrosis and conjunctival corrugations. Furthermore, these staging systems

would not detect subtle change given the levels of staging represent marked changes in fornix depth. The Tauber-Liverpool method is an adaption of the systems previously described by Tauber and Mondino and measures both the vertical forniceal depth and horizontal involvement by measurements taken along the bulbar conjunctival surface.

Vertical forniceal depth

This is measured to the nearest millimetre between the limbus at 6 o'clock and the superior edge of the fibrosis with the lid held gently under traction and the eye held in upgaze. This value is then subtracted from 10 and multiplied by 10 to give the percentage fornix shortening from which grade a-d (Tauber staging) is determined.

Horizontal grading

The horizontal shortening is measured objectively by using a clear rule and measuring the horizontal distance from the medial and lateral canthus 2mm above the start of the inferior fibrosis. The combined width of any symblepharon present is then subtracted from the total conjunctival horizontal width to define the percentage horizontal shortening.

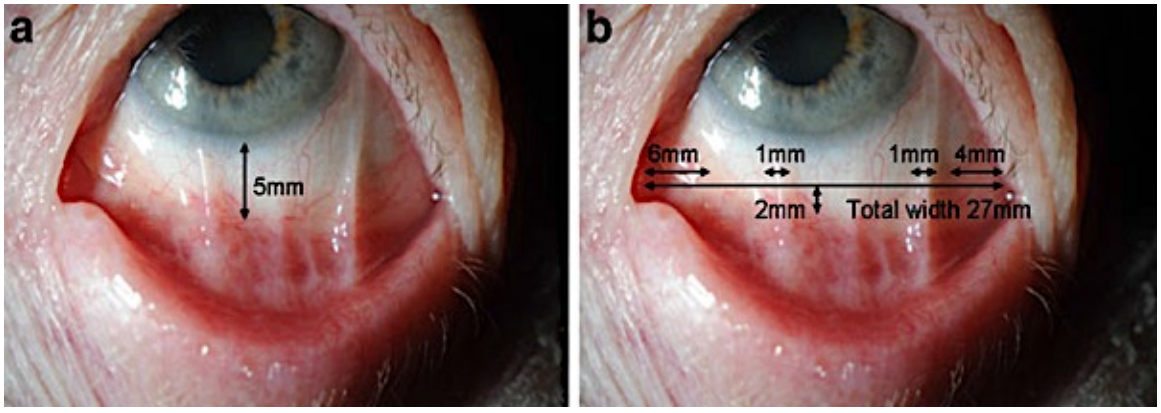

Figure 8: A photographic example of the Liverpool-Tauber grading system. Taken from Reeves. G. Graefes Arch Clin Exp Ophthalmol (2012) 250:611–618. An example of grading is shown in the above photographs with measurements (mm) as follows: a) vertical grading (10-5) x10=50%; b) horizontal grading e.g. (27-(6+1+1+4))/27x100=56%

The main advantage of the Tauber-Liverpool system is that it would allow small changes to be detected. In contrast to the Rowsey system, the Liverpool-Tauber system attempts to quantify the distance of the bulbar conjunctiva between the limbus and the edge of the subtarsal fibrosis using 10mm as an average reference value. This removes potential variation between observers in terms of the degree of traction applied to the eyelid whilst enabling the detection of smaller degrees of change than the traditional Foster, Mondino and Tauber systems.

Given the variation in the described methods thus far and lack of consensus thus far on the appropriate grading system to use for MMP patients, all will be included within the pro forma for comparison. A fornix ruler will also be used to measure the central fornix depth of both the upper and lower fornices as previously described by Williams and colleagues.[157] Staging systems described thus far only measure cicatricial change in the lower fornix. The upper fornix measurement in particular may be of significant clinical value given that it is otherwise notoriously difficult to assess and quantify objectively.

1.7.2 Assessment of the involvement of the ocular surface and eyelids to grade disease progression in MMP

The described staging systems grade cicatrisation but not the level of inflammatory activity present at the time of examination. Several methods have been reported for the grading of bulbar conjunctival hyperaemia including the Oxford grading system, Efron, and International Eye Research grading.[158-161] A grading scheme for conjunctival inflammation specific to ocular MMP has been adapted by Saw et al. from an original report describing inflammatory activity by Elder.[162] The adapted grading scheme has been used in research including clinical trials of ocular MMP patients.[163, 164] This grading system is a five-point scale based on standard photographs, which may be used to grade inflammation in each sector of bulbar conjunctiva (Figure 9). This has

therefore been used as part of the Liverpool pro forma for the assessment of MMP patients (Appendix).

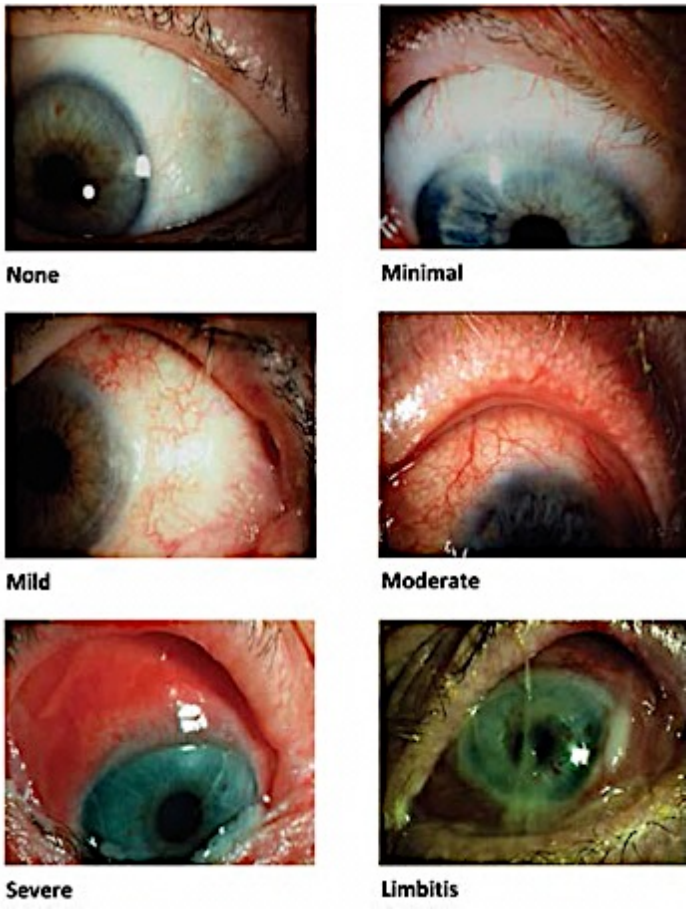

Figure 9: Ocular inflammation grading system by Saw et al. This grading system demonstrates a 5-point grading of ocular inflammation from 'minimal' to 'limbitis'. Taken from: Saw, V. P. Dart, J. K. Rauz, S. et al. (2008) Immunosuppressive therapy for ocular mucous membrane pemphigoid strategies and outcomes. Ophthalmology. 115(2):253-261. [163, 164]

There are no known validated scoring systems for the grading of corneal or lid involvement in MMP patients. A grading system for the assessment of corneal disease was sought from the literature to grade corneal involvement appropriate to MMP patients. Sotozono and colleagues published a grading method for the documentation of disease severity in Stevens-Johnson syndrome, which included grading of conjunctivalisation, neovascularisation, opacification, keratinisation and symblepharon.[165] An observer may grade disease severity by comparing standard photographs to the clinical assessment of the patient undertaken at the slit lamp (Figure 10). As Stevens-Johnsons syndrome is an inflammatory ocular surface disease with a similar ocular signs to that found in MMP, it was felt that this grading system would be appropriate to use. The corneal conjunctivalisation, neovascularisation and opacification components of this grading scheme were therefore included the pro forma. The grading of lid deformities was also included in the pro forma and was an adaptation of existing grading schemes for entropion/ectropion.[166, 167] Unfortunately, no grading schemes specific to cicatrising eye disease could be found in the literature. The adapted entropion/ectropion grading systems are simplified versions of that previously described in the literature and include documentation of whether the medial or lateral aspect of the upper or lower eyelids are involved (Figure 11, Appendix).

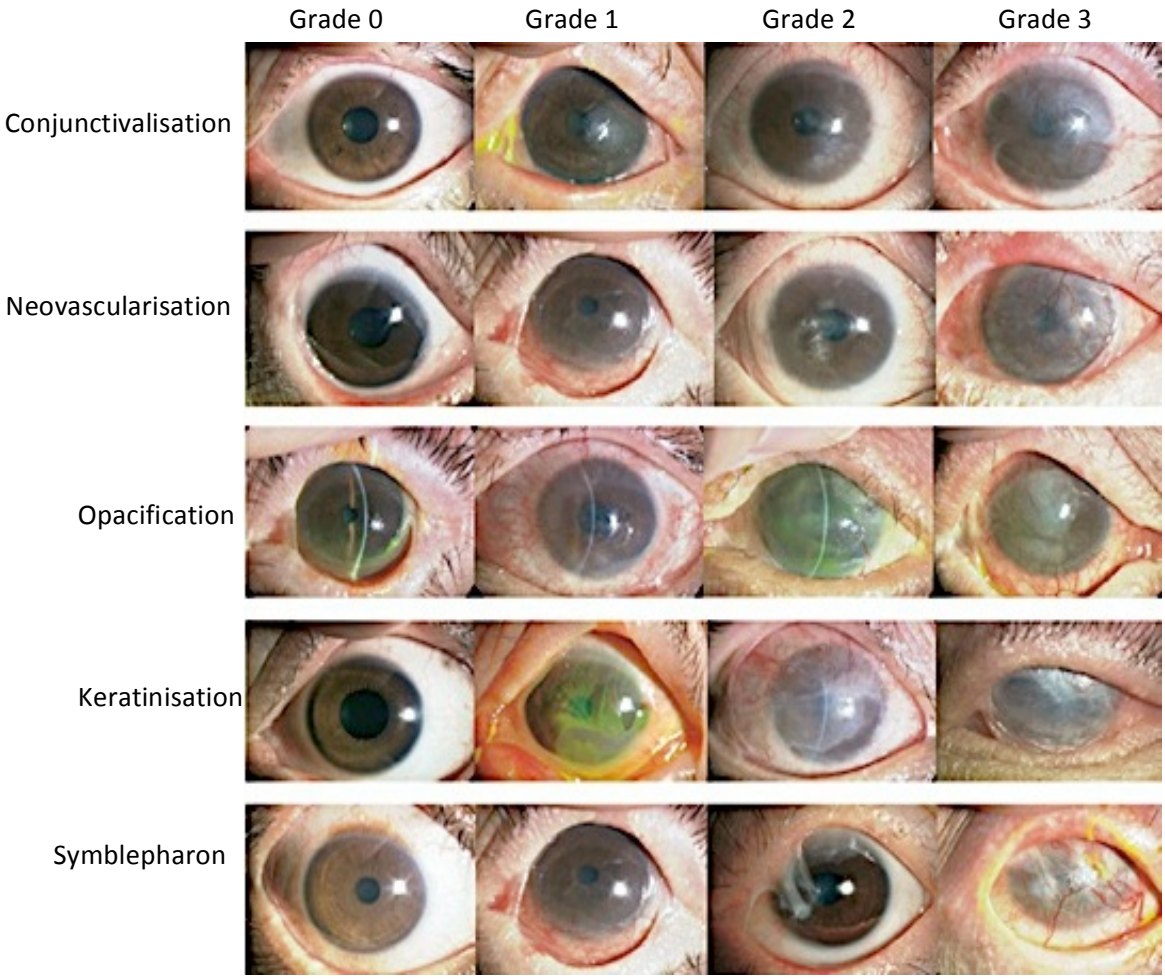

Figure 10: Photographs for the grading of ocular surface manifestations of Stevens-Johnson syndrome as reported by Sotozono et al. (2007). These images were taken from the original publication: Sotozono et al. (2007) New grading system for the evaluation of chronic ocular manifestations in patients with Stevens-Johnson syndrome. Ophthalmology. 114:1294–1302. [165] The conjunctivalisation, neovascularization and opacification components of the grading system were used in the MMP pro forma.

a)

Ectropion Grading Scale

0	Normal eyelid appearance and function
I	Normal appearance but symptomatic; eyelid laxity present on examination
II	Scleral show without eversion of lower eyelid
III	Ectropion without eversion of lacrimal punctum
IV	Advanced ectropion with eversion of lacrimal punctum from lacrimal lake
V	Ectropion with complication (eg, conjunctival metaplasia,retraction of anterior lamella, or stenosis of lacrimal system)
L	Predominantly lateral
M	Predominantly medial
LM	Combined medial and lateral
r	Previous revision*

Entropion Grading Scale

Minimal	-Apparent migration meibomian glands -Conjunctivalisation of lid margin -Lash/globe contact on up-gaze
Moderate	-Apparent migration of meibomian glands -Conjunctivalisation of lid margin -Lash/globe contact in primary position -Thickening of tarsal plate -Lid retraction
Severe	-Gross lid distortion -Metaplastic lashes -Presence of keratin plaques -Lid retraction causing incomplete closure

b)

Adapted ectropion grading scale

- 0-normal appearance
- 1-scleral show without eversion of lower lid
- 2-ectropion with eversion of lid but without eversion of lacrimal punctum
- 3-advanced ectropion with eversion of lacrimal punctum from lacrimal lake

M= Medial, L=Lateral

Adapted entropion grading scale

- 0-normal appearance
- 1-posterior lid border inverted (apparent migration of meibomian glands)
- 2-posterior lid margin inverted to intermarginal strip or lid retraction
- 3-whole lid margin including anterior border inverted or lid retraction resulting in incomplete closure

M= Medial, L=Lateral

Figure 11: Figure to show the original reported grading schemes (a) and the adapted versions (b) for the documentation of entropion and ectropion. The entropion and ectropion scales were taken from and adapted from Kemp et al. (1986) and Moe at al. (2000) respectively. [166, 167]

The grading of ocular dryness is also great importance in MMP (please see section 1.2.1). A grading scheme for the measurement of ocular dryness specific to MMP patients could not be found, however, a number of grading schemes for ocular dryness were obtained from the literature.[158-160, 168] One of the most widely used schemes is the Oxford grading scheme. This was included in the pro forma in its unadapted form (Figure 12).[158] Its advantages include the apparent ease in its administration; especially given the pictorial comparisons seen below and also that it grades both corneal and conjunctival epithelial involvement. It follows therefore that this could be appropriate for use in MMP patients.

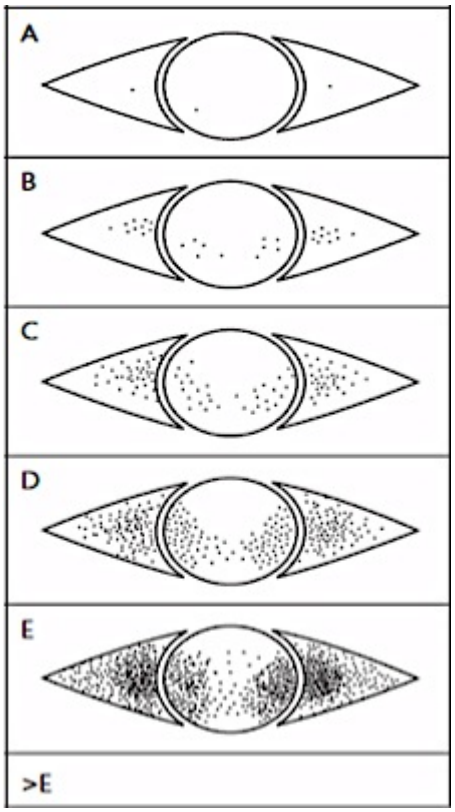

Figure 12: Figure to show the Oxford grading scheme as described by Bron et al. Taken from Bron et al. (2003) Grading of corneal and conjunctival staining in the context of other dry eye tests. Cornea. 22(7): 640-50.

1.8 Aims and objectives

A pliable, degradable graft derived from decellularised conjunctival tissue may suit indications for a conjunctival transplant where structural rigidity is not a requirement, for example following excision of conjunctival lesions. Decellularised conjunctiva would offer all the advantages of an extracellular matrix scaffold, such that it closely resembles native tissue but has the advantage of reduced antigenicity. In contrast, a non-degradable conjunctival construct derived from ePTFE capable of greater physical support may suit applications such as forniceal reconstruction.

This study will develop two such substrates, each with differing physical and biochemical properties that may address a range of transplantation requirements. The aims and objectives of this project are broadly categorised below.

<u>To develop ePTFE as a substrate for conjunctival epithelial expansion</u>

- Investigate the effect of ammonia gas plasma treatment on the proliferation and phenotype of a human conjunctival cell line.
- Investigate the potential of ammonia plasma treated ePTFE to support primary conjunctival epithelium

<u>To develop decellularised human conjunctiva as a biological substrate for conjunctival expansion</u>

- Develop a novel protocol for the decellularisation of human conjunctiva.
- Determine cytotoxicity, biochemical alteration and DNA content of decellularised tissue.
- Cultivate conjunctival epithelium on decellularised conjunctival tissue and characterise the mechanical properties and histology of the tissue in comparison to amniotic membrane and ePTFE.

Clinical application of novel conjunctival substrates

- Develop a pro forma for the documentation of clinical signs and disease activity in MMP patients.
- Describe MMP disease sequelae in a small group of patients attending corneal and external eye disease clinics at the Royal Liverpool Hospital.

2. Methods

2.1 Expanded polytetrafluoroethylene (ePTFE)

2.1.1 Ammonia plasma treatment of ePTFE

Commercially available ePTFE (0.64µm thickness, 0.4µm pore size) was obtained from Goodfellows Ltd (Cambridge, UK), divided into 2x2cm samples and mounted in tissue culture scaffolds; Cell Crown inserts (Scaffdex Ltd); Figure 13. The ePTFE sheets, therefore, derived support from the cell crown rather like a scaffold. It was also straightened such that it was held as a flat sheet on which the surface chemistry was subsequently altered by exposure to ammonia gas plasma. Larger 3x3cm sections of ePTFE were also taken of which some were left untreated and some were subjected to ammonia gas plasma treatment to enable the acquisition of contact angle measurements to measure hydrophilicity.

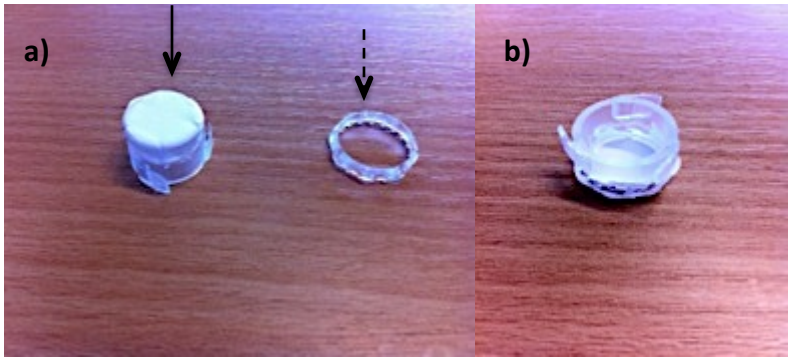

Figure 13: Photographs demonstrating the cell crown cell culture inserts with ePTFE mounted within it. a) Two components of the cell crown. On the left, the cell crown is shown upside down with the ePTFE membrane placed across it (solid arrow). The ring on the right hand side (dashed arrow) fits over the membrane, securing it into place. b) This photograph shows the ePTFE membrane mounted in the base of the cell crown. Each of these was placed within a well of a standard 12-well culture plate for cell culture experiments after sterilisation (section 2.3.2).

Ammonia plasma treatment of samples was achieved by placing the ePTFE mounted cell crowns inside the reaction chamber of helical plasma resonator system, built in-house using a previously described method.[108] The plasma resonator system briefly comprised a half wave helical resonator plasma system assembled by a glass tube around which a 100-turn copper wire was directly wound. The system had a resonant frequency of 13.6MHz and power <1W.[169, 170] Samples were treated at a flow rate of ammonia of 85sccm for two minutes at $1.2x10^{-1}$mbar pressure.[108, 171, 172] Some samples were placed on the stage with the underside of the ePTFE membrane side flush against the stage such that only the inside of the cell culture insert was exposed to ammonia gas plasma (single sided treatment). Samples designated for ammonia plasma treatment on both the inside of the cell culture insert and its underside were placed on the stage on their side to allow exposure to gas plasma on both sides of the membrane (double side ammonia plasma treatment).

After removing the samples from the reaction chamber, samples were immediately immersed in distilled water at room temperature for 24 hours. The cell crowns with the mounted ePTFE were allowed to dry at room temperature before they were sterilised using a ultra violet (UV) cross-linking machine, CL-1000 U.V. Crosslinker, (UVP, Cambridge, UK) for 5 minutes (1500w) each side prior to use in cell culture experiments.

2.1.2 Contact angle analysis of ePTFE

Static contact angle analysis was undertaken on ammonia treated and untreated ePTFE to determine a change in wettability using the DSA 100 Kruss Drop Shape Analyser (Kruss, GmbH). This is an optical contact angle measurement device that estimates the wetting properties of localised areas on a solid surface.

The DSA software supplied with the equipment was used. Prior to analysis the stage was appropriately set and a 'normal sessile drop' selected for analysis from the software options. A live image was visualised on the computer's monitor and the dispensing needle visualised within the centre of the image. A 10µL drop was dispensed and an image of the droplet taken. The contact angle was determined after selecting the contact angle settings for a sessile drop fitting for contact angles greater than 90 degrees and height/width-method for angles less than 90 degrees. This was repeated six times on randomly selected areas of the ammonia plasma treated ePTFE and untreated ePTFE.

2.2 Cells and tissues

All cell culture was undertaken under aseptic conditions in a class II biological safety cabinet (Walker) cleaned with Virkon® (DuPont) and 70% ethanol. Cell incubation was within a 37°C incubator (New Brunswick) maintained with in air with 5% CO_2.

2.2.1 Culture of a human conjunctival cell line

A human conjunctival cell line donated by Gipson laboratories (HCjE-Gi), Schepens Eye Research Institute, Harvard Medical School, Boston, USA was cultured using an adapted protocol from their laboratories. Cells were seeded at the required cell density by dispensing a calculated volume of a solution of even cell suspension. Cell number/density was determined using a haemocytometer.

At an early stage of culture, cells were grown in an 'early grow formula' (Media 1): Keratinocyte serum free medium (K-SFM, Invitrogen), 2ng/ml epidermal growth factor (Invitrogen), 0.25% bovine pituitary extract (Invitrogen), 1% penicillin-streptomycin (Sigma), 0.4mM calcium chloride (Sigma). Approximately 90% of the existing media was

removed and replaced every 2-3 days using media that was pre-warmed at 37°C. Cell cultures were grown in 75cm^2 tissue culture flasks (Greiner) in incubators at 37°C in air with 5% carbon dioxide (CO_2).

At 70-100% confluence, Media 2 was used and comprised a 50:50 mix of the early grow formula and DMEM:F12 (Invitrogen) with 1% penicillin-streptomycin and 10% foetal calf serum (FCS) and cultures were airlifted such that the media fluid level was at the air-liquid interface as described in section 2.3.

2.2.1.1 Passage of conjunctival epithelial cells

Passaging of cell cultures was undertaken at 70-100% cell confluence. Any remaining media in the culture flasks was removed and replaced with TrypLE™ (1x solution, Invitrogen). This agent was used to dissociate cells from the tissue culture plates by incubation in the TrypLE™ solution at 37°C in air with 5% CO^2 for 10 minutes or until complete dissociation was apparent on phase contrast microscopy. A neutralising media was added to the dissociated cell suspension to create a 50:50 mix and centrifuged at 1000rpm/180g for 5 minutes. The neutralising media comprised a 50:50 mix of DMEM and F12 media (Invitrogen), 10% FCS, 3.5g/l HEPES, 1% penicillin-streptomycin (Sigma). The resulting cell suspension was resuspended in media 1 (section 2.2.1) for further culture or storage as required.

2.2.1.2 Cryopreservation

Any surplus HCjE-Gi cells were stored long-term in liquid nitrogen. Cells were dissociated from tissue culture flasks using TrypLE™ (Invitrogen) as described in section 2.2.1.1 and resuspended in 900µl media 1 and 100µl dimethylsulphoxide (DMSO) (Sigma) by continuous mixing of the tube and placed in cryovials (Starlab). All cryovials were subsequently placed in isopropanol containers (Nunc) in a freezer at -80^{o}C. The isopropanol solution subjects the cryovials to gradual temperature decline from room

temperature to -80^{o}C at a rate of 1^{o}C per minute. After 24 hours, the cryovials were placed in liquid nitrogen dewars for long-term storage.

2.2.2 Retrieval of human conjunctival tissue and culture of primary conjunctival cells

2.2.2.1 Retrieval of cadaveric conjunctiva

Ethical approval was obtained from the National Health Service (NHS) Health Research Authority (NRES committee North West) titled 'Isolation, characterisation and expansion of human ocular surface (corneal and conjunctival) stem cells'; REC reference 11/NW/0766 protocol number 4182. The ethical approval enabled the retrieval of human conjunctival tissue from deceased patients at the Royal Liverpool University Hospital in whom consent had been obtained from the next of kin for the use of tissues in research. Consent was obtained either through the University of Liverpool's Research Eye Bank or by the National Retrieval Centre of NHS Blood and Transplant, based in Speke, Liverpool. All practices were in keeping with The Human Tissue Act (Human Tissue Act 2004), the European Union Tissues and Cells Directive (Tissues and Cells Directive 2004) and the Data Protection Act (Data Protection Act, 1998).

Methods for the dissection of conjunctiva were developed following trial of several variations to the technique. In summary, a single long section of tissue was retrieved by performing a 360° peritomy followed by a long temporal relaxing incision and excision of tissue in a clockwise or anticlockwise direction extending as far into the conjunctival fornices as possible to remove all bulbar and as much forniceal conjunctival tissue as possible. This method was in keeping with the Royal College of Ophthalmologists standards for transplantation and research. Conjunctival epithelium was retrieved from both eyes from each donor as soon as possible after death. Tissues were logged

consecutively according to the numbering system of The Research Eye bank, University of Liverpool. The age and gender of the donor was recorded together with the number of hours that lapsed between time of death and retrieval. Retrieved tissue was either stored in 2-3ml phosphate buffered saline (PBS; Invitrogen) at -40°C or dissected for culture immediately.

2.2.2.2 Explant culture of primary human conjunctival cells

Fresh human bulbar/forniceal conjunctival tissue was dissected from its underlying Tenon's capsule layer and divided into approximately 1x1mm tissue sections for use as explants. Five explants were seeded on decellularised conjunctival tissue sections mounted (section 2.5) within tissue cell crowns (Scaffdex Ltd.) orientated such that the basement membrane side faced the substrate. The tissue explants were cultured for the first 24 hours in DMEM/F12 media with 10% fetal calf serum, 1% penicillin/streptomycin (Invitrogen). The subsequent 11 days in culture were in the following serum free media: K-SFM (Invitrogen), 0.2ng/ml EGF (Invitrogen), 25µg/ml BPE (Invitrogen), 0.4mM $CaCl_2$, 1% penicillin/streptomycin. After 12 days in culture, the tissues were airlifted (as per section 2.3) and the following media used up to day 28 in culture: K-SFM (Invitrogen), 10ng/ml EGF, 1.2mM $CaCl_2$, 1% penicillin/streptomycin, transferrin 5µg/ml Insulin 5µg/ml, triiodothyronine 1.4ng/ml, adenine 12µg/ml, hydrocortisone 0.4µg/ml epidermal growth factor 10ng/ml. Media levels were monitored up to twice daily and media replenished as required to ensure that the liquid volume met the air-liquid interface.

2.2.2.3 Culture of cells on decellularised tissues using explants and isolated cell suspensions

Cells from the same tissue donor were used to repopulate decellularised amniotic membrane and conjunctival substrates. Decellularisation of substrates was completed using the described protocol in section 2.5.1 using 0.05% SDS (w/v) and mounted into

Cell Crowns (Scaffdex Ltd.). The conjunctival tissue was divided into explants within hours of eye retrieval. Five randomly selected explants were cultured directly on the decellularised tissues. The remaining explants were seeded on tissue culture plates to allow expansion of conjunctival epithelium over 10 days so that adequate cell numbers developed to enable the seeding of 1 x 10^5 cells/cm^2 isolated cells in suspension onto decellularised substrates at a later date. After 5 days in culture, the explants were removed from the culture plates and the newly developed epithelium continued to divide. After 10 days, the conjunctival epithelium was dissociated with TryPLE for 7 minutes. Agitation of the cell suspension was undertaken by using a pipette to take up and release the suspension repeatedly such that cells disaggregated in a 50:50 mix of neutralising media as previously described (section 2.2.1.1). Both the explants and isolated cells were seeded in DMEM/F12 media with 10% fetal calf serum, 1% penicillin/streptomycin (Invitrogen). After 24 hours, the media was replaced with serum free media as described in section 2.2.1. The experiments were completed in triplicate using both decellularised amniotic membrane and decellularised conjunctiva.

2.3 Cell culture on substrates

2.3.1 Culture of cells on cell culture inserts

Thincerts (Greiner) were used as a positive control in experiments of synthetic substrates. These cell culture inserts are produced from clear polystyrene housings, and polyethylene terephthalate (PET) capillary pore membranes. This was used as a positive control in cell culture experiments were it is referred to as PET membrane. As stated by the manufacturer, the membrane culture surface has undergone a 'physical surface treatment ' to improve cell adherence and growth. Several pore size diameters are available, however, the 0.4 μ m pore size specification was used for consistency between the PET and the ePTFE tested in these experiments. The cell culture inserts were manufactured to fit in culture plates such that there was a space between the

culture insert and bottom of the culture plate where the media fluid level could be controlled (Figure 14). The process of 'airlifting' required the media level to be adjusted to the level of the air-liquid interface at the membrane. This method required regular monitoring of the fluid levels to ensure that the fluid level was maintained at the air-liquid interface.

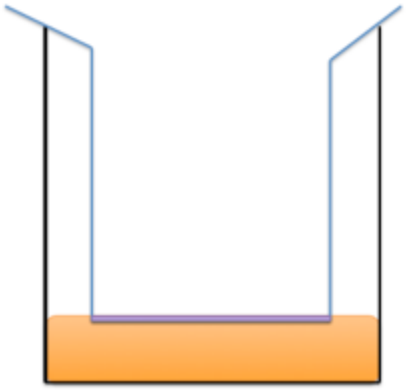

Figure 14: Diagram to illustrate the process of airlifting cell culture inserts. The insert (blue) can be placed in a cell culture well (black) and is supported such that it is suspended within the well. The media (yellow) is inserted and shown here to correspond to the air-liquid interface of the cellular layer (purple).

2.3.2 Culture of cells on ePTFE membrane

In substrate experiments involving the ePTFE membrane, a novel method for airlifting was developed whereby the membrane mounted cell crown was placed on top of a ring shaped device that allowed a higher volume of media in the culture plate whilst airlifting (Figure 15). In preliminary work, it was found that although regular replacement of media was required, the cultures were less likely to dry out using the ring devices than without given that a larger volume of media could be dispensed when airlifting. The ring devices were designed and made by JB, at the University of Liverpool workshop services. During the airlifting culture phase of experiments, media was replaced once to twice per day.

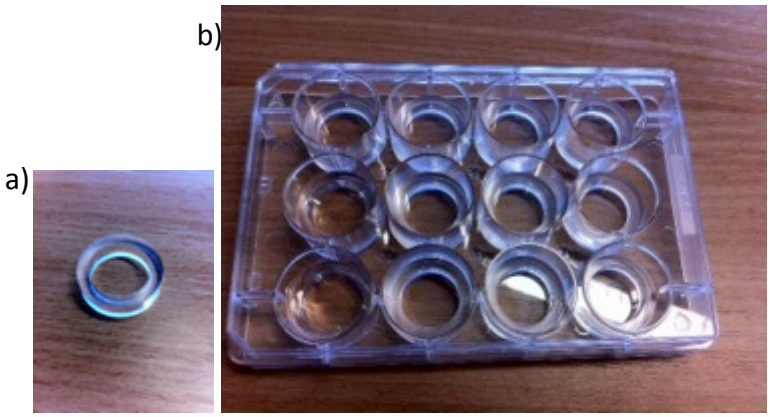

Figure 15: Photographs of the ring device and the placement of these ring devices within culture plates to enable airlifting of cultures. a) This ring shaped device was designed and made by University of Liverpool workshop services (JB). This was sized to enable the cell crown to be positioned 6mm above the base of the well plate. Media was dispensed within this gap, filling the well to the air-liquid interface for the airlifting of cultures. b) This photograph shows a 12-well plate with the ring device in each well. This holds the cell crowns 6mm above the base of each well. These were used for cell culture experiments involving the ePTFE substrates.

2.4 Cell culture and characterisation experiments to assess synthetic substrates

2.4.1 Cell seeding density

Cell seeding density experiments were undertaken to determine an optimal seeding density for all subsequent experimental work. Cell culture protocols used for HCjE-Gi cells describe a change in media after 7 days in culture when cells are 75-100% confluent. This was therefore the optimal goal to reach. The substrates used for this experiment were ePTFE that was ammonia plasma treated on the inner surface (cell culture surface), untreated ePTFE and PET (polyethylene terephthalate) membrane in triplicate. Cells were seeded on triplicates of substrates at a density of $1x10^3$, $1x10^4$ and $1x10^5$ cells/cm^2. Cultures were fixed, stained with DAPI (4', 6-diamidino-2-phenylindole,

Sigma), and photomicrographs taken (Nikon TiE, Japan) after 1,4 and 7 days in culture. The number of cells per area from 5 random areas of each sample were manually counted for each of the substrates in triplicate and expressed as the mean per sample per substrate. Each photographed field was acquired using the x20 magnification microscope lens which produced a photograph with a surface area of 12,420µm^2.

2.4.2 Optimisation of media protocol

Established cell culture protocols using HCjE-Gi cells describe a change in media from an 'early grow' (media 1) to a 'late grow' (media 2) formulation once 75-100% confluent. Given that the substrates used were opaque, the cell density could not be assessed without risk of damage to cells. A number of cell culture protocols were therefore tested using HCjE-Gi cells seeded at 1x10^5/cm^2 on the ammonia plasma treated ePTFE, untreated ePTFE (negative control) and PET membrane (positive control) in triplicate to determine a suitable media protocol for the culture of HCjE-Gi cells on ePTFE. Media protocols were: A) media 2 only; B) media 1 for 7 days followed by media 2; C) media 1 for 3 days followed by media 2; D) media 1 with 1% BSA (Sigma). Cultures were fixed and stained with phalloidin and DAPI after 1,3,7,10 and 14 days in culture. The number of cells per area from 5 random areas of each sample were manually counted for each of the substrates in triplicate and expressed as the mean per sample per substrate.

2.4.3 Comparing cell counts on ePTFE with ammonia plasma treatment on one and both sides

Cell counts were repeated on a further experiment that was repeated on three separate occasions with triplicate samples within each experimental group. This was undertaken to determine with greater accuracy the cell density that would develop on each of the test substrates over a period of 28 days. It was also unknown whether

exposing the ePTFE to ammonia gas plasma within the gas plasma resonator on one side only or both sides would result could influence the cell density. This variable was also therefore introduced. Cell counts were undertaken following 2, 14, 21 and 28 days in culture using the haemocytometer method to determine the number of cells found on the substrate per cm^2 following disassociation. Cultures were also fixed and stained with DAPI, phalloidin, and UAE-1 (Ulex Europaeus lectin; Genetex) at all time points studied and representative photomicrographs taken using a fluorescence microscope (Nikon) and confocal imaging system (Zeiss LSM 510).

2.4.4 Fixation of substrate cultures and staining with fluorescent markers

Samples used for staining were cultured in triplicate and fixed at the time points measured in the experiment. Optimal methods for fixation and permeabilisation were determined together with the optimal concentration of staining agents: UAE-1 lectin, phalloidin and DAPI (Table 2). Fixation was undertaken with 4% paraformaldehyde (Sigma) for 10 minutes prior to staining samples with phalloidin. Samples were also stained with ice-cold methanol (Sigma) for 10 minutes prior to staining with UAE-1 lectin (Genetex). Substrates were washed three times in phosphate buffered saline (PBS; Invitrogen) prior to incubation with phalloidin or UAE-1 lectin stains at varying concentrations as in Table 2, both for 1 hour at room temperature. Substrates were subsequently washed three times in PBS and stained with DAPI for 10 minutes. Stained cells were imaged using confocal microscopy (Zeiss LSM 510).

Staining agent	**Supplier**	**Dilution**
DAPI	Thermo fisher	1:1000
Phalloidin	Abcam	1:1000
UAE-1 Lectin	Vector labs	1:500

Table 2: Details of fluorescent staining agents with their optimised dilutions used for the analysis of cell cultures developed on synthetic substrates.

2.4.5 Determining cell density using a haemocytometer

Cells were dissociated from the substrates using 0.05% trypsin-EDTA (Sigma) under incubation at 37°C with 5% carbon dioxide for 5 minutes. The removal of all cells from the substrates was confirmed by the absence of DAPI staining of substrates following the removal of dissociated cells. Cells suspended in a known volume were counted using a haemocytometer. A 20µl solution was placed within the haemocytometer counting chamber, viewed under a phase contrast microscope and counted within each of the four-1mm2 corner squares of the grid and the mean number of cells in $1mm^2$ calculated. All cells within the grid were counted together with those in contact with the top and left side of all border gridlines. Cells in contact with the bottom and right side of the border gridlines were not included as per standard practice.

2.4.6 Flow cytometry

The data collected by flow cytometry can be presented in histogram format of a single parameter, emission wavelengths or in dot plots or density plots that display the correlation between two parameters. The software (Flowing 2.5, Turku Centre for Biotechnology) allows the selection of one or more cell populations of interest for quantification in terms of the percentage of cells that it represents. All the cell markers used in this study were intracellular markers. The HCjE-Gi cells required dissociation from their culture substrate with TryPLE for 10 minutes at $37^{o}C$. Following dissociation, the cells were fixed with 2% paraformaldehyde for 10 minutes and then washed three times by mixing the cells in wash buffer (gentle vortex) and centrifugation. The wash buffer comprised 1% BSA (w/v) and 0.1% sodium azide (w/v) and centrifugation at 1000rpm/180g for 5 minutes was undertaken. Cells were then resuspended in ice-cold methanol for 30 minutes at $4^{o}C$. Cells were subsequently blocked using 10% goat serum for 30 minutes at room temperature.

Primary antibody incubation was in 1% goat serum for 1 hour at 4^{o}C. All incubation steps were for 30 minutes at 4^{o}C. Following primary incubation with the CK19, CK7, MUC5AC and CK4 antibodies, cells were stained with the secondary antibody (secondary incubation step) with goat anti-mouse IgG H&L Alexafluor 405 (ab175660, Abcam) at a dilution of 1:500. Cells with the primary antibodies ΔNp63 and caspase-3 were stained with the donkey anti-rabbit Alexafluor 647 (Poly 4064, Biolegend) secondary antibody at a dilution of 1:1000. An additional incubation step using FITC-conjugated UAE-1 lectin (Vector labs) at a dilution of 1:500 was undertaken for all samples stained with cytokeratin and MUC5AC primary antibodies. Cells were washed three times between each of the steps described. The optimal dilution for each antibody was initially determined by testing a range of primary and secondary antibody dilutions along with the isotype control at corresponding dilutions to that of the primary antibody; rabbit IgG isotype control (Thermo Fisher Scientific), mouse IgG1 isotype control (ab91353, Abcam), Mouse IgG2 isotype control (ab91361, Abcam).

Antibody	**Clone**	**Supplier**	**Dilution**
CK19	Ab52625	Abcam	1:100
CK7	RCK105	Abcam	1:100
CK4	6B10	Abcam	1:50
MUC5AC	45MI	Abcam	1:25
ABCG2 (FITC conjugated)	5D3	Millipore	1:25
p63	ΔN	Biolegend	1:50
caspase-3	Asp-175	Cell Signalling	1:50
PCNA (FITC conjugated)	PC10	Santacruz	1:50

Table 3: Table of antibodies used for flow cytometry with the respective clone, supplier and optimised dilution

2.4.7 Validation experiment to ensure appropriate use of the HCjE-Gi cell line

A preliminary experiment was undertaken to ensure that immunological detection of the caspase-3 antibody by flow cytometry would increase in HCjE-Gi cells grown under environmental stress. Cultures of HCjE-Gi cells grown on tissue culture that had been deprived of fresh media for one week and left outside the incubator at room temperature for 24 hours were compared with HCjE-Gi cells cultured under optimal conditions (media replaced every 2-3 days and kept in a cell culture incubator in air with 5% CO_2). Quantitative assessment of caspase-3 expression by flow cytometry was undertaken using methods described in section 2.4.6.

The cell line was also validated to ensure that the expression of all the cell markers used in this study did not vary significantly with the passage of cells used. Cells of passage 2 and 28 were analysed by flow cytometry using the full panel of antibodies (section 2.4.6, Table 3) after 14 days culture using standard culture protocols that described in section 2.2.1. The cells were cultured on tissue culture plates in triplicate for each cell marker studied.

2.4.8 Assessing the phenotype of cultures with advancing time and by substrate

An experiment was undertaken to determine the phenotype of HCjE-Gi cells and their subpopulations with advancing time in culture on tissue culture polystyrene and on test substrates. The test substrates studied were: treated ePTFE exposed to ammonia gas plasma (section 2.1.1) on a) one side (single side treatment) and b) both sides (double side treatment), PET membrane (positive control) and untreated ePTFE (negative control). HCjE-Gi cells were seeded at a density of $1x10^5/cm^2$. Samples were analysed in three separate experimental sessions for each marker studied after 14 and 28 days in culture.

An equivalent similar experiment was also undertaken using primary conjunctival cells. The cells were cultured from conjunctival explants expanded on tissue culture polystyrene as described for expansion on decellularised tissue (section 2.2.2.1) over a 10-day period. Cells were subsequently dissociated and seeded at a density of $1x10^5/cm^2$ on double side treated ePTFE and PET substrates. The untreated ePTFE and single side ammonia plasma treated ePTFE from previous experiments could not be used in this experiment owing to the low cell number available for this experiment and the necessity for significant cell numbers per sample required to obtain reliable results by flow cytometry. The experiment was undertaken on three separate occasions using tissue from a different donor for each experimental run.

The cells were fixed and analysed by flow cytometry for a range of conjunctival epithelial markers after 14 and 28 days in culture. Co-staining of CK7 with UAE-1 lectin and ABCG2 with ΔNp63 (see section 2.4.6) was quantified by setting the appropriate voltage gate. The gate determined the percentage of cells with dual fluorochrome staining via a 2-parameter dot plot where the gates were determined with prior analysis of single parameter histograms. For all other samples in which there was only a single antigen of interest, histograms were used for quantification. Flowing software version 2.5 was used for all analyses.

2.5 Decellularisation of human conjunctiva and its characterisation

2.5.1 Decellularisation of human conjunctiva

A protocol for the decellularisation of human conjunctiva was developed by adaptation of an existing protocol by variation of a range of sodium dodecyl sulphate (SDS) dilutions. The original protocol based on a previously optimised protocol for the decellularisation of human amniotic membrane at NHS Blood and Transplant.[87] Fresh

or frozen conjunctival tissue (at -40°C) was allowed to thaw at room temperature and washed in distilled water at 200rpm at 25°C and placed in a hypotonic buffer (0.1% EDTA, 10mM TRIS, 1% penicillin-streptomycin) at 200rpm at 4°C for 21 hours. The tissue was then placed in a detergent buffer (10mM $MgCl_2$, 10mM TRIS, 0.05-0.5% SDS, 0.1% EDTA, pH 8, 1% penicillin-streptomycin) at 25°C for 24 hours, agitated in an orbital incubator (Table 4). Tissue were washed three times in a wash buffer (PBS, 0.1% EDTA) and placed in a nuclease buffer (1U/ml benzonase, 10mM MgCl2, 50 mM TRIS, pH 8, 1% penicillin-streptomycin) for 37°C for 3 hours at 200rpm (Table 4). Tissues were washed twice for 20 minutes at 200rpm at 25°C in the wash buffer and finally twice at 20 minutes in PBS with 1% penicillin-streptomycin.

Reagent	**Source**
Sterile water for irrigation	Baxter
Tris buffered isotonic saline (TBS)	Inverclyde
NaCl	Sigma
EDTA disodium salt	VWR
TRIS	VWR
$MgCl_2$	VWR
HCl 37%	VWR
NaOH	Sigma
Penicillin/streptomycin	Sigma
Benzonase	Novogen

Table 4: Table of reagents used for decellularisation and their source.

2.5.2 DNA extraction and quantification

A 5mm trephine (5mm) was used to cut triplicate samples of tissue and each sample weighed. DNA extraction was undertaken using a commercially available kit (Easy-DNA™ gDNA purification kit, Invitrogen, UK) using a previously described protocol using Easy-DNA solutions and chloroform.[173] In brief, samples were incubated in an orbital incubator (225rpm) for 20 hours at 60°C with in a protein degradation solution. The supernatant following centrifugation was used for DNA precipitation. This involved using 100% and 80% ethanol suspensions and chloroform with repeated centrifugation steps using the upper aqueous phase prior to digestion with RNAse (Easy DNA™ kit, Invitrogen). DNA quantification was achieved using a commercially available kit (PicoGreen, Invitrogen) and a standard curve was drawn following the preparation of a range of calf thymus DNA standards, also stained with PicoGreen. The DNA in cellular and decellularised samples was quantified following the acquisition of fluorescence readings (FLX 800 microplate fluorescence reader, Biotek, UK) whereby absorbance units were converted to the equivalent corresponding DNA concentration using the standard curve from the same experimental run.

DNA quantification was undertaken to determine the DNA in cellular conjunctiva and the resulting tissue subjected to three variations in the decellularisation process based upon the SDS dilution used. Tissue samples were obtained from each experimental group: cellular (untreated) conjunctival tissue and treatment groups: 0.05%, 0.1% and 0.5% SDS (w/v). Three experimental repeats were used for each of the tissues sections, which in turn were also taken in triplicate from each experimental group (n=9 for each test group). The standard curve measurement and calculations were repeated for a subsequent experiment using only the 0.05% (w/v) SDS decellularisation protocol with conjunctival tissue from three separate donors in triplicate with experimental repeats as described earlier. This was undertaken to ensure reproducibility of the decellularisation process using 0.05% (w/v) SDS.

2.5.3 Collagen denaturation

A collagen denaturation assay was undertaken whereby hydroxyproline, a product of collagen denaturation, was detected through colorimetric absorbance values using a previously described technique.[173] In brief, three tissue samples from each test group were used with triplicate experimental repeats from each tissue sample (n=9 for each test group studied). A 5mm trephine was used to cut tissue biopsies. A subgroup of samples were treated with 0.1N NaOH for 16 hours at 25°C and used as the positive control whereas samples treated with 50mM gluteraldehyde at 25°C were used as negative controls for hydroxyproline estimation. The test samples were treated with 10mg/ml alpha-chymotrypsin for 24 hours at 37°C. Denatured collagen results in the release of hydroxyproline into the supernatant along with a corresponding colour change using Elrich's reagent. Controls with pre-determined hydroxyproline concentrations and samples were similarly treated as follows: 12N HCL was added to a sample of each supernatant and autoclaved for 60 minutes at 121°C 18 psi. Chloramine T reagent was then added to each sample at 25°C for 25 minutes. The subsequent addition of Elrich's reagent at 65°C for 20 minutes results in a colour change that corresponds to the concentration of hydroxyproline in solution. Quantification of hydroxyproline was undertaken using a microplate reader (ELX 808, Biotek, UK) whereby a standard curve was drawn from known similarly treated serial dilutions of the hydroxyproline control.

2.5.4 In vitro contact cytotoxicity testing

A standard method for determining contact cytotoxicity was employed as outlined by the Biological evaluation of medical devices- part 5 (2009); ISO 10993-5. Conjunctival tissue decellularised with 0.05% SDS (w/v) (section 2.5.1) was tested for evidence of cytotoxicity in vitro using a culture of primary human skin fibroblasts (kindly donated by S.Rathbone, NHS Blood and transplant, Liverpool) and a human conjunctival cell line (HCjE-Gi cells) in triplicate. A disposable 5mm trephine was used to divide sections of

decellularised tissue, which were attached to 24-well plates with Steristrips™ (3M, UK). Cyanoacrylate glue (RS components, UK) and Steri-strips™ alone were used as negative and positive controls respectively. All samples were tested in triplicate and against two cell types: primary human skin fibroblasts and HCjE-Gi cells. $1x10^5$ cells were seeded in each well and incubated for 48 hours in a cell culture incubator with air and 5% CO_2 at 37°C. HCjE-Gi cells culture was undertaken using earlier described methods (section 2.2.1). Primary human skin fibroblasts were cultured in DMEM (Sigma), 10% Foetal calf serum (Sigma), 1% penicillin/streptomycin (Invitrogen). After 48 hours in culture the samples with fixed in serial ethanol dilutions: 50%, 70%, and 100%, each for 5 minutes at room temperature. After removal of the 100% ethanol, the samples were allowed to air dry before 20% Giemsa solution (Sigma) was added for 5 minutes at room temperature. The samples were then rinsed in distilled water and photographed on an inverted microscope (Leica 090-135-002, UK).

2.5.5 Biomechanical testing

Tensile strength testing is an important test in the field of material science in which a material is subjected to tension at a controlled rate until the material is deformed beyond repair and eventually breaks. The tension is applied by placing the sample between two clamps holding the tissue that move apart at a controlled rate. The elongation of the material is measured against the force applied. The change in gauge length is used to calculate the engineering stress **σ** through the following equation:

$$\sigma = \text{Force (newtons)} / \text{Cross section area } (m^2)$$

Strain (ε) is defined as the deformation of the material due to strain and can be expressed as the following equation:

$$\varepsilon = \text{change in length (extension)} / \text{original length}$$

Young's modulus of elasticity is the resistance that a given material has to deformation in an elastic (non-permanent) manner when a tensile force is applied. It is determined by the stress and strain defined by the following:

$$E = \sigma / \varepsilon$$

The Lloyd Instruments Universal Testing machine (LRX plus, Lloyds instruments, UK was used to determine the tensile strength of tissue samples. Conjunctival sections were divided into approximately 15mm x 3mm sections and held within clamps. The thickness, length and width of each sample were individually measured with Vernier callipers (Digimatic CD-6"C, Mitutoyo UK; resolution 0.01mm). Three measurements of width and thickness were taken from each sample and the average thickness calculated. Each sample was pulled with a 5N load cell and data including stress, strain and elastic modulus were generated by Nexgen software (Canada). A minimum of 4 samples were tested from 3 different donors (n=15 and n=14 respectively) from each of the cellular and decellularised tissue test groups.

2.6 Histology and immunohistochemistry decellularised tissues and recellularised constructs

2.6.1 Preparation of tissues for histology and immunohistochemistry

Tissue samples were unfolded into 1x1cm tissue biopsy capsules (Cell Safe, Leica) and fixed by immersion in 4% paraformaldehyde for 24 hours. The tissue biopsy capsules were then placed into tissue histology cassettes and were processed through a histology tissue processor (Citadel 2000, Thermo Shandon, UK) over a 20 hour cycle comprising serial immersion in 3.7% neural buffered formaldehyde (Sigma), 100% ethanol, xylene (Leica) and Formula R paraffin (Surgipath, UK). Tissue samples were removed from the tissue biopsy capsules following tissue processing and embedded in

a paraffin-embedding unit (Shandon, UK). Following wax embedding, 5-10µm samples were cut using a microtome (Finesse 325, Thermo Shandon, UK). Sections of 5-10µm were used in preference to thinner sections. Mounting and staining with thinner sections (2-5µm) was initially attempted, however, problems were encountered including poor adhesion to slides, shearing and loss of the tissue, which prevented further analysis. Triplicate samples were taken from at least three separate areas of the tissue sections. Tissue sections were mounted onto silanised glass slides (Dako) after placing the tissue sections in an electrothermal tissue float bath (Cole-Parmer) at 40°C. Wet mounted slides were placed onto an electrothermal slide drying bench at 45°C for 10 minutes before leaving overnight in a drying oven at 37°C.

2.6.2 Histology

Tissue sections were deparaffinised using a standard method of serial immersion into 5 minutes in xylene (Leica) and then 100, 90 and 70% ethanol washes. Staining with Haematoxylin and Eosin (H&E, Leica) was performed for 10 minutes, rinsed in running tap water, dipped in 1% acid-alcohol (Leica), rinsed in running tap water and immersed in Eosin (Leica) for 5 minutes. The slides were rinsed again in running tap water, and dehydrated by serial immersion into ethanol 70, 90 and 100% in 30 second intervals prior to further placement into xylene for 10 minutes before mounting onto glass slides with DPX (Sigma) and glass coverslips (Thermo Scientific).

Staining with Periodic acid Schiff (Sigma) was undertaken by de-parrafinisation as described above before slides were immersed in Periodic Acid Solution for 5 minutes, rinsed three times in distilled water, immersed in Schiff's reagent for 15 minutes and finally washed in running tap water. Glass coverslips were mounted as previously described.

Staining with van Gieson's stain was undertaken on deparaffinised and dehydrated tissue sections. Slides were placed in Van Gieson's stain (Surgipath, UK) for 5 minutes and then rinsed in running tap water. Similarly, staining with DAPI (4', 6-diamidino-2-phenylindole) was undertaken following deparaffinisation and dehydration, before mounting the slides with fluorescent mounting medium (Dako).

Tissue sections were examined and imaged using an Olympus BX60 microscope (Olympus, UK) and photomicrographs taken of representative sections from a minimum of 9 stained tissue sections from each tissue block studied.

2.6.3 Immunohistochemistry

Several antigen retrieval methods were tested on tissues for each studied antibody to identify the optimal method. The methods included incubation with trypsin for 30 minutes at 37^{o}C, incubating with 0.01M citrate acetate buffer pH6 (Sigma) in a microwave for 5-15 minutes, and immersion in target retrieval solution (Dako) for 5-20 minutes in a water bath at 95^{o}C. The optimal method for all antibodies studied was the target retrieval solution method. Slides were washed between each step in a wash buffer comprising 0.05% tween (Sigma), 8.76 % NaCl (Sigma), 6.05% TRIS (VWR), pH 7.6. Immunohistochemical staining was undertaken using the Envision^{TM} kit HRP anti-mouse/rabbit (Dako). Slides were incubated with a peroxidase block (0.03% hydrogen peroxide, Envision^{TM} kit) for 10 minutes, followed by blockage with 20% goat serum to prevent non-specific binding for 30 minutes (Dako) prior to incubation with primary antibodies at varying dilutions (Table 5) for 3 hours at room temperature. The appropriate secondary anti-mouse/rabbit horseradish peroxidase (Envision^{TM} kit) was placed on tissue samples for 30 minutes at room temperature. The chomogen, 3-amino-9-ethylcarbazole (AEC, Envision^{TM} kit) produced pigmentation of the immune-positive areas on tissue samples over 5-10 minutes. Slides were mounted in Aquatex mounting media (Merck Millipore) and imaged on an Olympus BX60 microscope. A

representative photograph was taken from the centre of each stained tissue section from a minimum of 9 tissue sections. Each section was taken from triplicate tissue samples each from three separate areas of the paraffin embedded tissue block.

Antibody	Clone	Supplier	Dilution
CK19	Ab52625	Abcam	1:400
CK7	RCK105	Abcam	1:500
CK4	6B10	Abcam	1:200
ABCG2	BXP-21	Millipore	1:50
p63	ΔN	Biolegend	1:50
Caspase-3	CPP-32	Cell Signalling	1:50
PCNA	PC10	Santacruz	1:50
Laminin	L9393	Sigma	1:200
Fibronectin	F3648	Sigma	1:250
Collagen IV	Ab19808	Abcam	1:400

Table 5: Table of antibodies used for immunohistochemistry with the respective clone, supplier and optimised dilution

2.7 Recellularisation of decellularised conjunctiva with primary conjunctival epithelium

2.7.1 Explant culture experiments with and without the orientation of basement membrane of conjunctiva

Initial experiments were undertaken using conjunctival tissue in which the orientation and presence of basement membrane had not been confirmed or marked prior to the decellularisation process. In subsequent experiments, the conjunctiva was examined

under a microscope to confirm the presence of conjunctiva (rather than tenon's or adipose tissue) and was marked by placing 5/0 nylon sutures on the shinier side of the membrane in an attempt to orientate the basement membrane following decellularisation. Five explants were taken from a single donor seeded on each substrate (i) basement membrane present and (ii) basement membrane not present/not easily identifiable, in triplicate.

2.7.2 Comparison of conjunctival epithelial cultures using tissue from different donors for explants and decellularised substrates

This experiment was undertaken to explore the variability in explant tissue outgrowth and whether the decellularised tissue itself has any influence on the degree of outgrowth. Decellularised tissues that had been stored at -40^{o}C were thawed for use in this experiment. Experiments were completed using triplicate samples in which conjunctival explant tissue from three separate donors (15/17/19) was used on each of the decellularised tissue samples from three other donors (9/5/13). Following 28 days in culture, the tissues were fixed and paraffin embedded as described in section 2.6.1. A minimal of 3 tissue sections was taken from 3 areas in each wax paraffin block. Representative photographs from the centre of the tissue sample were taken. Amniotic membrane was used as a control tissue on which explants from each of the donor's conjunctival explants were cultured.

2.8 Statistical analysis

All statistical analysis was undertaken using SPSS 22.0 (IBM). Data was tested for variance homogeneity and distribution. A log transformation of the data was used to meet the variance assumptions for the ANOVA test. This was used to analyse data from the following sets; contact angle analysis, cell count, DNA content, and tensile strength

testing. Bonferroni post-hoc tests were applied to enable a more detailed interpretation of the interactions between individual pairs of treatment groups in the model. The paired t-test was used to analyse hydroxyproline content in the collagen denaturation test between cellular and decellularised samples.

The ANCOVA model for change was used to determine the effect of advancing time and substrate on numerous cell markers assessed by flow cytometry in conjunctival cells. The change in percentage expression of a given marker between day 14 and 28 was the dependent variable, and the interactions calculated for the effect of substrate and time with the value at day 14 as the co-variance factor. The Holm-Bonferroni correction was applied. This accounted for the total number of ANCOVA tests performed and was based upon an initial α value of 0.05. The uncorrected p values have been presented but only the p values significant following Holm-Bonferroni correction are displayed. In tests where statistical significance was determined, post-hoc contrasts were ascertained and a further Holm-Bonferroni correction was applied to determine differences between the substrates studied. All statistical analyses undertaken were verified for their appropriateness by a statistician (GC) in The Department of Eye and Vision Science, Institute of Ageing and Chronic Disease, University of Liverpool.

2.9 Detection and monitoring of ocular mucous membrane pemphigoid patients

2.9.1 Developing a pro forma

A pro forma was developed for the documentation of clinical signs in ocular mucous membrane pemphigoid (MMP) patients to facilitate improved documentation. It was developed in consultation with the Corneal and External Eye Disease team at St Paul's Eye Unit, Royal Liverpool University Hospital NHS Trust. The pro forma may enable

clinicians to standardise the grading of clinical signs and also provides opportunities to establish a database of patients who may benefit from future cellular replacement therapies. Based on the literature review, the Tauber-Kaye method was used. It has proven inter-rater and intra-rater reliability and offers additional quantitative information to those of Tauber, Mondino and Foster. [156] The pro forma also included the traditional Tauber, Mondino and Foster grading systems together with photography and fornix depth measurement using a fornix ruler to determine whether there is any additional value from these methods.

All the aforementioned methods do not include any documentation of the presence of eyelid signs, conjunctival inflammation or corneal involvement. Methods previously used in clinical studies of conjunctival inflammation and corneal involvement and have been included in the pro forma.[33, 163] There have been no validated grading schemes for cicatricial lid disease and therefore a documentation scheme was developed from other (non-cicatrising) entropion and ectropion grading systems so that its severity and location (medial/lateral) could be documented.[166, 174] The presence or absence of lagophthalmos, trichiasis, co-existing ocular pathology and visual acuity was also included.

The aim of this part of the study was to allow a small group of patients with ocular MMP to be assessed to enable discussion of potential treatment strategies for ocular surface reconstruction. It also provided an opportunity to collect pilot data that could help inform further development of the pro forma for use in future clinical studies (Appendix 1).

2.9.2 Assessing MMP using the MMP pro forma

The purpose of the case series was not to obtain a representative sample of MMP patients attending corneal and external eye disease clinics in general, but to obtain a

small sample with any ocular involvement to enable a small pilot study to help develop the MMP pro forma. The cases acquired for this study were recruited opportunistically over a 3-month period. Patients attending a corneal and external eye disease clinic (Professor S B Kaye, St Paul's Eye Unit, Royal Liverpool University Hospital) were examined after the purpose of the examination was explained and consent obtained. Patients were examined at a slit lamp and measurements were taken for the Foster, Tauber, and Tauber-Liverpool grading schemes using a disposable ruler. Corneal dryness grading scores were taken according to the Oxford grading scheme.[158] The corneal and lid grading was undertaken after examination according the pro forma. A perspex fornix ruler was designed and produced by University of Liverpool workshop services (JB): Figure 16. Fornix depth measurements were taken after the application of proxymetacaine 0.5% (w/v) drops (Minims). Measurements were taken on gentle insertion of the fornix rule to the maximum depth of the upper and lower fornix at the midline.

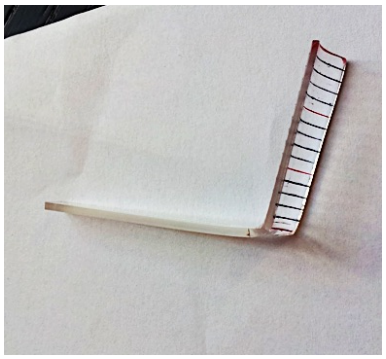

Figure 16: Photograph of the Perspex fornix ruler. Each gradation corresponds to 1mm. The graded section is inserted into the upper and lower fornices. The thickness of the Perspex measuring arm of the fornix ruler is 1mm.

Chapter 3: Results

3.1 Optimisation of culture methods for the ex vivo expansion of conjunctival epithelium on synthetic substrates

3.1.1 Ammonia plasma treatment of ePTFE

Untreated ePTFE as received from the manufacturer is known to be hydrophobic. This was apparent from the formation of a spherical water droplet on its surface when a known volume was dispensed. This was in contrast to a water droplet of the same volume dispensed on ammonia plasma treated ePTFE, which assumed a flatter shape, exhibiting greater spread on the surface of the material. This indicated increased wettability of the treated ePTFE and was confirmed through static contact angle analysis (Figure 6). The contact angle of a droplet of water formed on ammonia treated ePTFE was significantly more acute than those that were untreated (71.08^{o} vs. 131.22^{o} respectively; p=0.02).

	N	Minimum	Maximum	Mean	+/-SD
Untreated ePTFE	6	127.4	135.9	131.2	3.2
Ammonia plasma treated ePTFE	6	67.3	74.8	71.1	2.6

Table 6: Static contact angle analysis of untreated and ammonia gas plasma treated ePTFE. Six readings were taken from randomly selected areas on ammonia plasma treated and untreated ePTFE. 10µl water was automatically dispensed and contact angle between the water droplet and material recorded by an inbuilt video recorder. Statistical analysis showed a difference at a p=0.02 level between treated and untreated ePTFE.

3.1.2 Cell seeding density analysis

The highest cell seeding density was demonstrated on all substrates following 7 days in culture by seeding $1x10^5$ cells/cm^2 cells (Figures 17-19). The highest cell density was noted on the PET membrane (Figure 18) and lowest on the untreated ePTFE (Figure 19). Low cell density was observed on untreated ePTFE, which was approximately 25% of treated ePTFE, even at the highest cell seeding density after 7 days in culture. Cell density on untreated ePTFE was also characterised by markedly high variance owing to patchy growth whereby cells were visualised on some areas within a photographed field, whereas the complete absence of cells was observed in other areas. There was an approximately 4-fold greater cell density after 7 days in culture on ammonia plasma treated ePTFE when cells were seeded at $1x10^5/cm^2$ compared to $1x10^4/cm^2$. This is in contrast to PET membrane whereby the cell density after 7 days in culture when cells were seeded at $1x10^4/cm^2$ was approximately 75% of that seeded at $1x10^5/cm^2$. The representative photomicrographs displayed evenly spaced cell nuclei at a high density on the plasma treated ePTFE at day 7 (Figure 20). The chosen cell seeding density for subsequent experiments was therefore determined as $1x10^5/cm^2$ for subsequent experimental work. Statistical analysis by ANOVA found a significant association between cells per photographed field and time ($p<0.001$), and cells per photographed field and cell seeding density ($p=0.006$) overall across all test substrates.

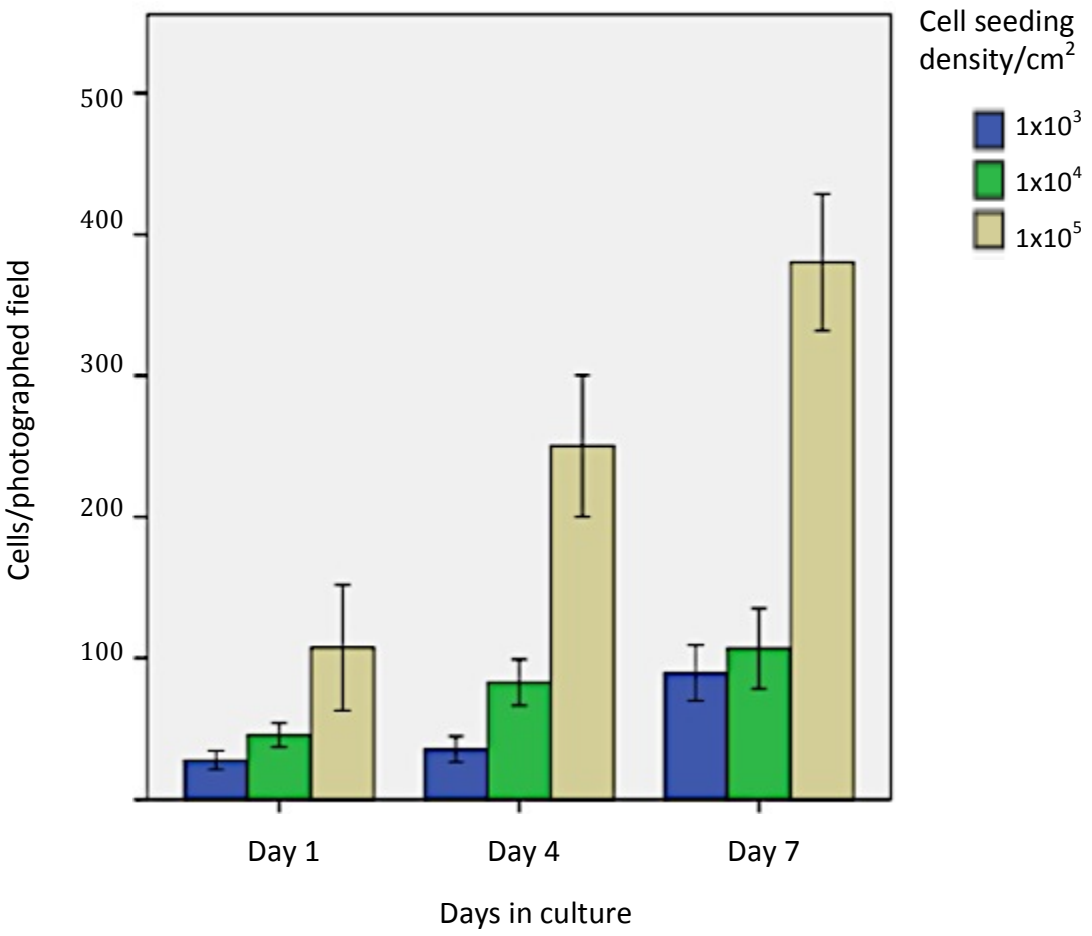

Figure 17: Histogram to show number of cells counted per photographed field with advancing time and increasing cell seeding density on **ammonia plasma treated ePTFE**. This graph shows the number of cells counted manually in each photographed field (+/-SD) at 20x magnification over set time points (day 1, 4 and 7). Each photographed field was 12,420µm^2. Five areas per photographed field were counted from triplicate samples (n=15 within each experimental group).

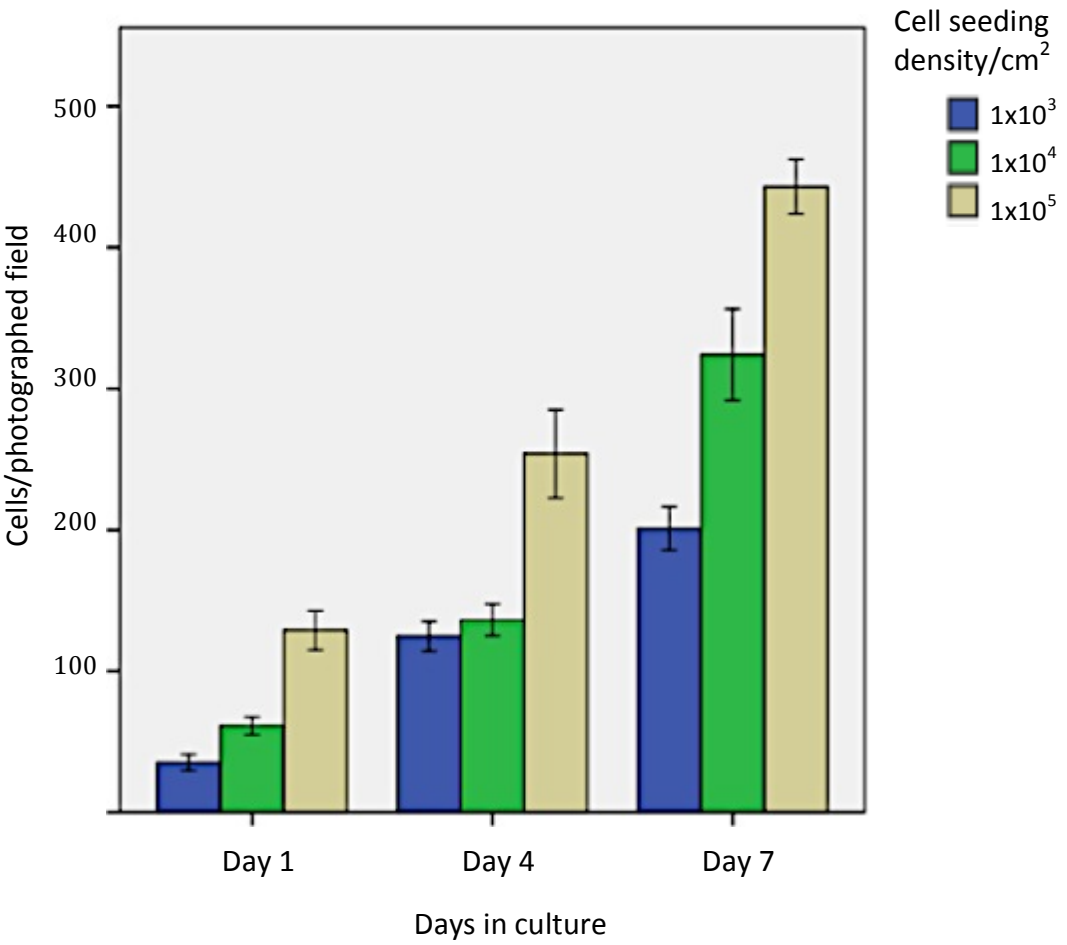

Figure 18: Histogram to show number of cells counted per photographed field with advancing time and increasing cell seeding density on **PET membrane**. This graph shows the number of cells counted manually in each photographed field (+/-SD) at 20x magnification over set time points (day 1, 4 and 7). Each photographed field was 12,420µm^2. Five areas per photographed field were counted from triplicate samples (n=15 within each experimental group).

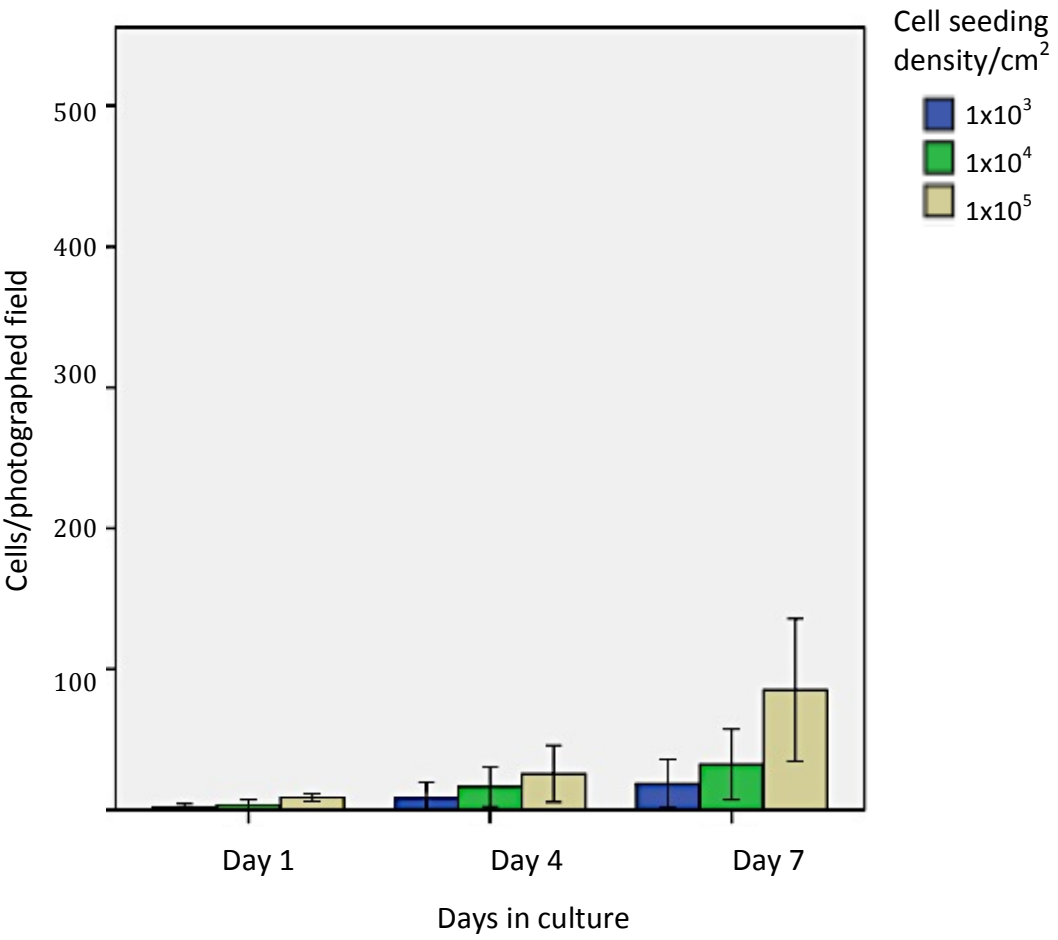

Figure 19: Histogram to show number of cells counted per photographed field with advancing time and increasing cell seeding density on **untreated ePTFE**. This graph shows the number of cells counted manually in each photographed field (+/-SD) at 20x magnification over set time points (day 1, 4 and 7). Each photographed field was 12,420µm^2. Five areas per photographed field were counted from triplicate samples (n=15 within each experimental group).

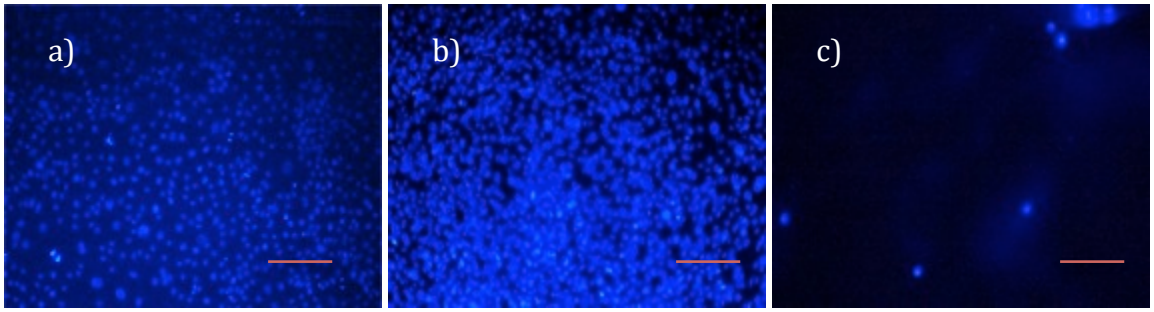

Figure 20: Representative photomicrographs of cultured substrates fixed and stained with DAPI (blue fluorescent nuclear stain) after 7 days in culture. All membranes were seeded at a density of $1x10^5$ cells/cm^2: a) ammonia plasma treated ePTFE b) PET membrane c) untreated ePTFE. Scale bars 100µm.

3.1.3 Effect of media on HCjE-Gi cell proliferation

Four media protocols were tested to determine an optimal protocol for the culture of HCjE-Gi cells and are outlined below. Media 1 was an 'early grow' formula whereas media 2 was used at a later stage when 70-100% confluent to encourage stratification and differentiation (please see section 2.2.1 and 2.4.2).

Media protocol A: Media 2 used.
Media protocol B: Media 1 used and changed to Media 2 after 7 days.
Media protocol C: Media 1 used and changed to Media 2 after 3 days.
Media protocol D: Media 1 supplemented with 1% BSA used.

Statistical analysis by ANOVA found significant associations between cells per photographed field and days in culture ($p<0.001$), and days in culture ($p<0.001$) and media protocol ($p<0.001$) overall across all test substrates. The highest cell density was demonstrated when cells were cultured on PET membrane regardless of the media protocol used (Figures 21, 23, 25, 27). Cells grew at the lowest density using media protocol D (K-SFM media supplemented with 1% BSA) across all substrates (Figure 27).

Cell density was also limited with the use of media protocol A (media 2 only) in which cell density did not rise above 150 cells/photographed field after 14 days in culture on any substrate (Figure 21). Furthermore, the use of media protocols A and D resulted in an overall decline in cell density in contrast to protocols B and C in which an increase was demonstrated with advancing time across all substrates. Cell density was relatively stable from the starting point at day one on PET membrane with use of media protocol A, whereas the cell density on treated and untreated ePTFE declined from day 1 to 14. This is in contrast to cell density on PET using media protocol D in which a higher cell density was demonstrated at day 1, however, a more rapid decline in cell density occurred in comparison to treated and untreated ePTFE where cell density was lower but more stable with advancing time in culture (Figure 27).

Media protocol B and C (media 1 changed to 2 at after 7 and 3 days respectively) resulted in a greater cell density than with the use of media protocols A and D at all time points that increased with advancing time in culture (Figure 23, 25). The greatest cell density developed from the use of media protocol B in which cell density at day 14 was 449 cells/photographed field on ammonia plasma treated ePTFE and 522 cells/photographed field on PET membrane respectively (Figure 23). Cell density on untreated ePTFE reached approximately 2/3 that achieved using ammonia plasma treated ePTFE with media protocol B (Figure 23). Cell density was lower using media protocol C across all substrates, however, increased with advancing time in culture on treated ePTFE and PET membranes (Figure 25). A decline in mean cell density was apparent after 7 days in culture, however, on untreated ePTFE (Figure 25). Qualitative results from nuclear staining undertaken in parallel with cell counts are in keeping with the described observations. Qualitatively, cells appear evenly spread across the materials, demonstrated by even spacing between nuclei demonstrated by DAPI staining (Figures 22,24,26,28). Cells grown on ammonia plasma treated ePTFE and PET membrane at day 14 appeared confluent as demonstrated by the confluence of f-actin staining in contrast to the sparse cell growth observed on untreated ePTFE (Figure 29).

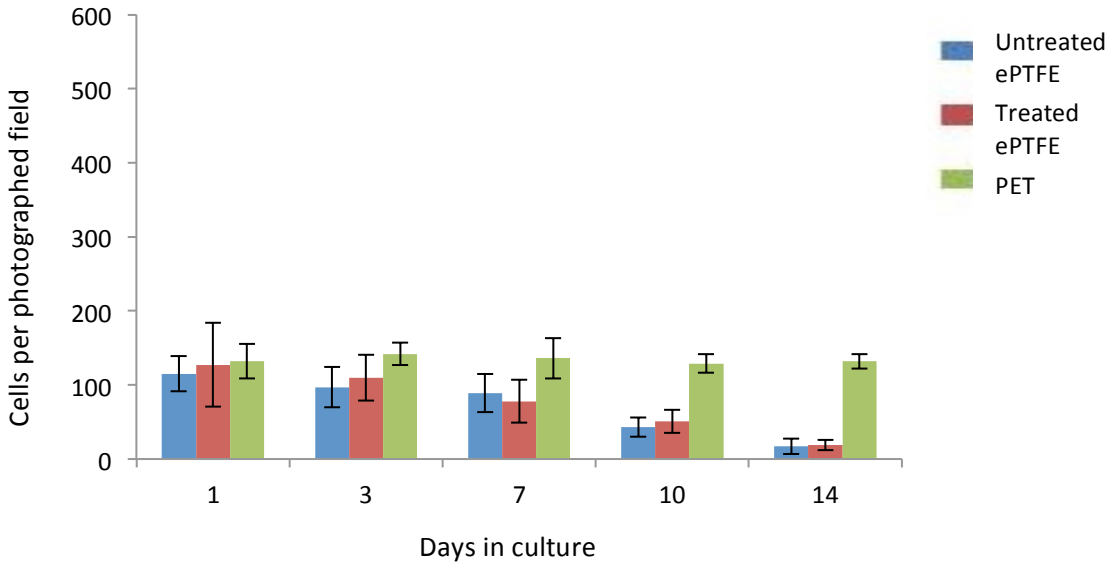

Figure 21: Histogram to show mean number of cells counted per photographed field with advancing time on ammonia plasma treated ePTFE, untreated ePTFE and PET membrane using **media protocol A**. Cells were seeded at $1x10^5/cm^2$ on all substrates. This graph shows the number of cells (+/-SD) counted manually in each photographed field at 20x magnification over set time points day 1,3,7,10 and 14. Each photographed field was 12,420μm^2. Five areas per photographed field were counted in triplicate samples (n=15 within each group).

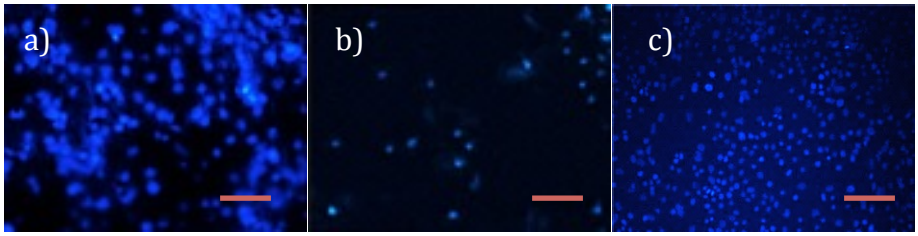

Figure 22: Representative photomicrographs of DAPI stained cells after 14 days in culture using media protocol A. All substrates were seeded at a density of $1x10^5$ cells/cm^2: a) ammonia plasma treated ePTFE b) untreated ePTFE c) PET. Scale bars 100µm.

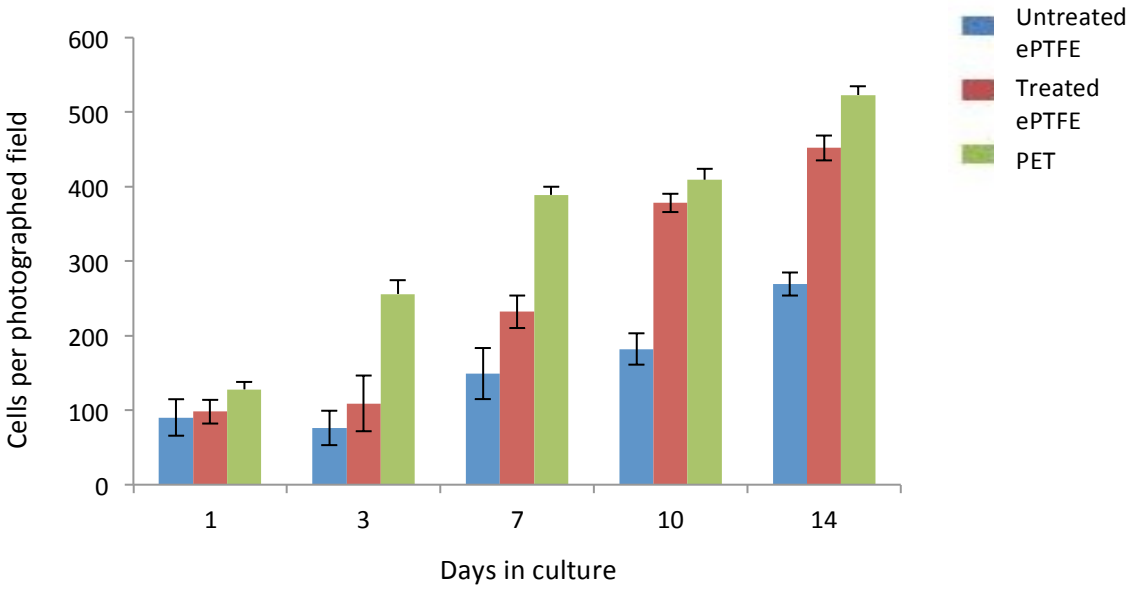

Figure 23: Histogram to show the mean number of cell photographed per photographed field with advancing time on ammonia plasma treated ePTFE, untreated ePTFE and PET membrane using **media protocol B**. Cells were seeded at $1x10^5/cm^2$ on all substrates. This graph shows the number of cells (+/-SD) counted manually in each photographed field at 20x magnification over set time points day 1,3,7,10 and 14. Each photographed field was 12,420µm^2. Five areas per photographed field were counted in triplicate samples (n=15 within each group).

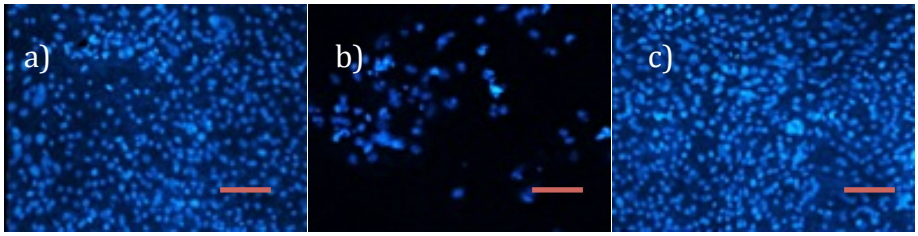

Figure 24: Representative photomicrographs of cultured substrates fixed and stained with DAPI after 14 days in culture using media protocol B. All substrates were seeded at a density of $1x10^5$ cells/cm^2: a) ammonia plasma treated ePTFE b) untreated ePTFE c) PET. Scale bars 100µm.

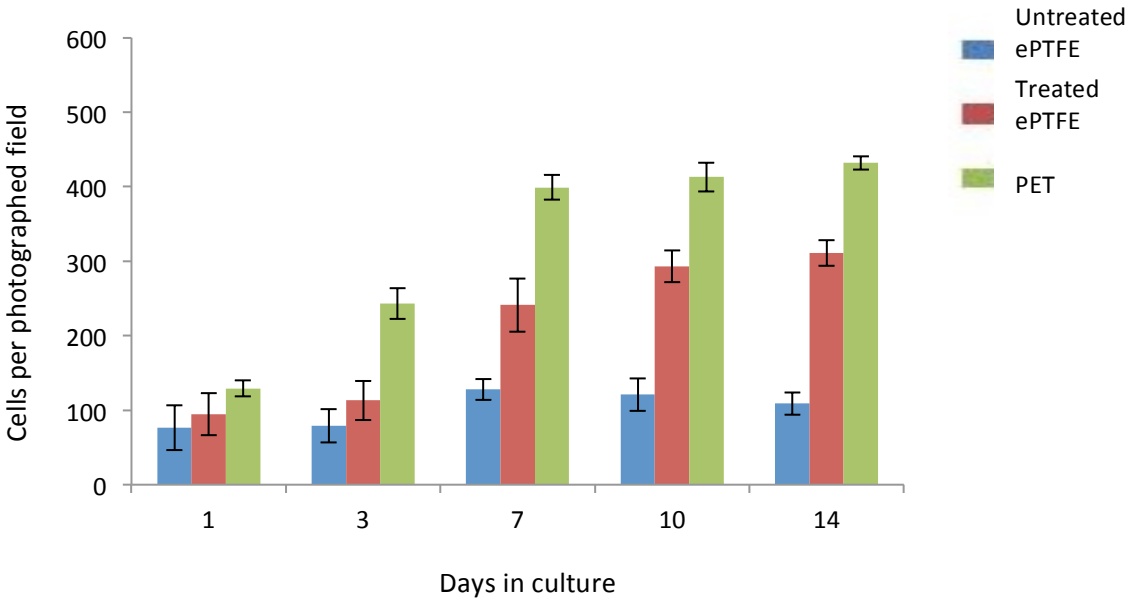

Figure 25: Histogram to show the mean number of cell photographed per photographed field with advancing time on ammonia plasma treated ePTFE, untreated ePTFE and PET membrane using **media protocol C**. Cells were seeded at $1x10^5/cm^2$ on all substrates. This graph shows the number of cells (+/-SD) counted manually in each photographed field at 20x magnification over set time points day 1,3,7,10 and 14. Each photographed field was $12,420\mu m^2$. Five areas per photographed field were counted in triplicate samples (n=15 within each group).

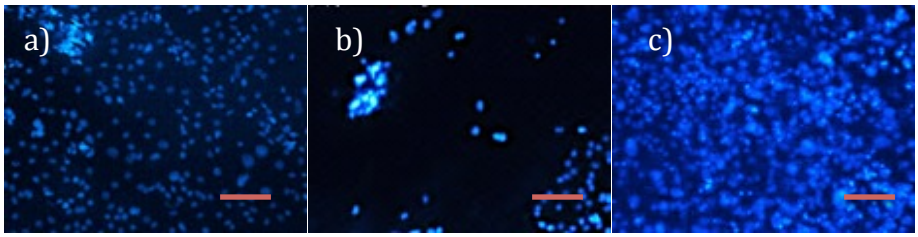

Figure 26: Representative photomicrographs of cultured substrates fixed and stained with DAPI after 14 days in culture using media protocol C. All substrates were seeded at a density of $1x10^5$ cells/cm^2: a) ammonia plasma treated ePTFE b) untreated ePTFE c) PET. Scale bars 100µm.

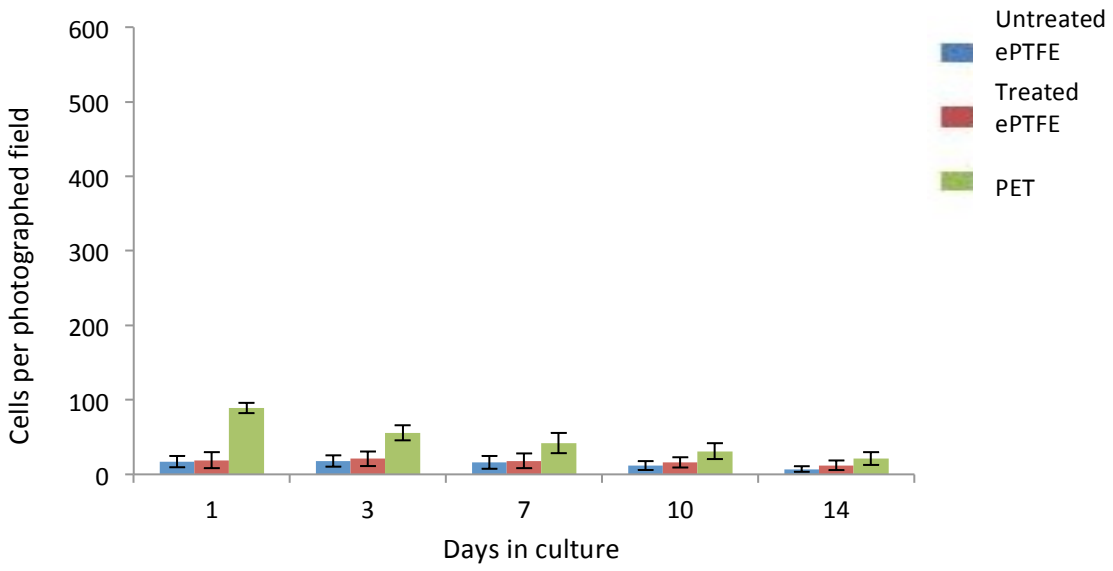

Figure 27: Histogram to show the mean number of cell photographed per photographed field with advancing time on ammonia plasma treated ePTFE, untreated ePTFE and PET membrane using **media protocol D**. Cells were seeded at $1x10^5/cm^2$ on all substrates. This graph shows the number of cells (+/-SD) counted manually in each photographed field at 20x magnification over set time points day 1,3,7,10 and 14. Each photographed field was 12,420μm^2. Five areas per photographed field were counted in triplicate (n=15 samples within each group).

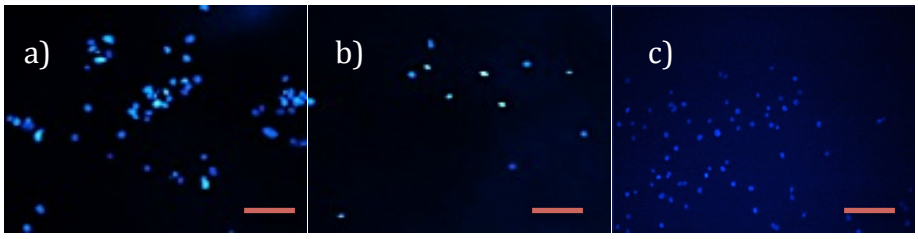

Figure 28: Representative photomicrographs of cultured substrates fixed and stained with DAPI after 14 days in culture using media protocol D. All substrates were seeded at a density of $1x10^5$ cells/cm^2: a) ammonia plasma treated ePTFE b) untreated ePTFE c) PET. Scale bars 100µm.

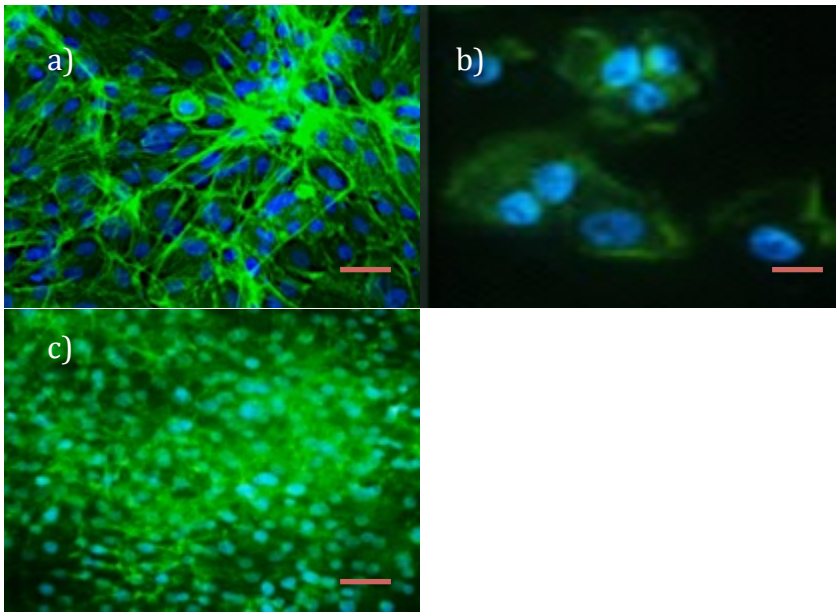

Figure 29: Representative photomicrographs of HCjE-Gi cells after 14 days in culture using media protocol B on ammonia plasma treated ePTFE (a), untreated ePTFE (b) and PET membrane (c). Green staining is phalloidin (f-actin) and blue nuclear staining is the result of DAPI uptake. Confluent morphology was demonstrated on both treated ePTFE and PET and sparse growth found on untreated ePTFE. Phalloidin staining was abundant however individual fibres were difficult to visualise with this stain on PET membrane. Nuclei appear smaller in size on the PET compared with treated ePTFE substrates. Scale bars 50µm.

3.2 Ex vivo expansion of conjunctival epithelium on synthetic substrates

3.2.1 Comparison on cell density between substrates including ammonia plasma treatment of one or both sides of ePTFE

The cell density at day 28 was higher when the ePTFE was exposed to the ammonia gas plasma on both sides of the material rather than treatment only on the side intended for cell seeding; $p<0.001$ (Figure 30). This difference was marked after 14 days in culture. Cell counts at all time points studied were lowest on the untreated ePTFE and

highest on the PET membrane (Figure 30). Statistically significant differences were found between all substrates studied (P<0.0001).

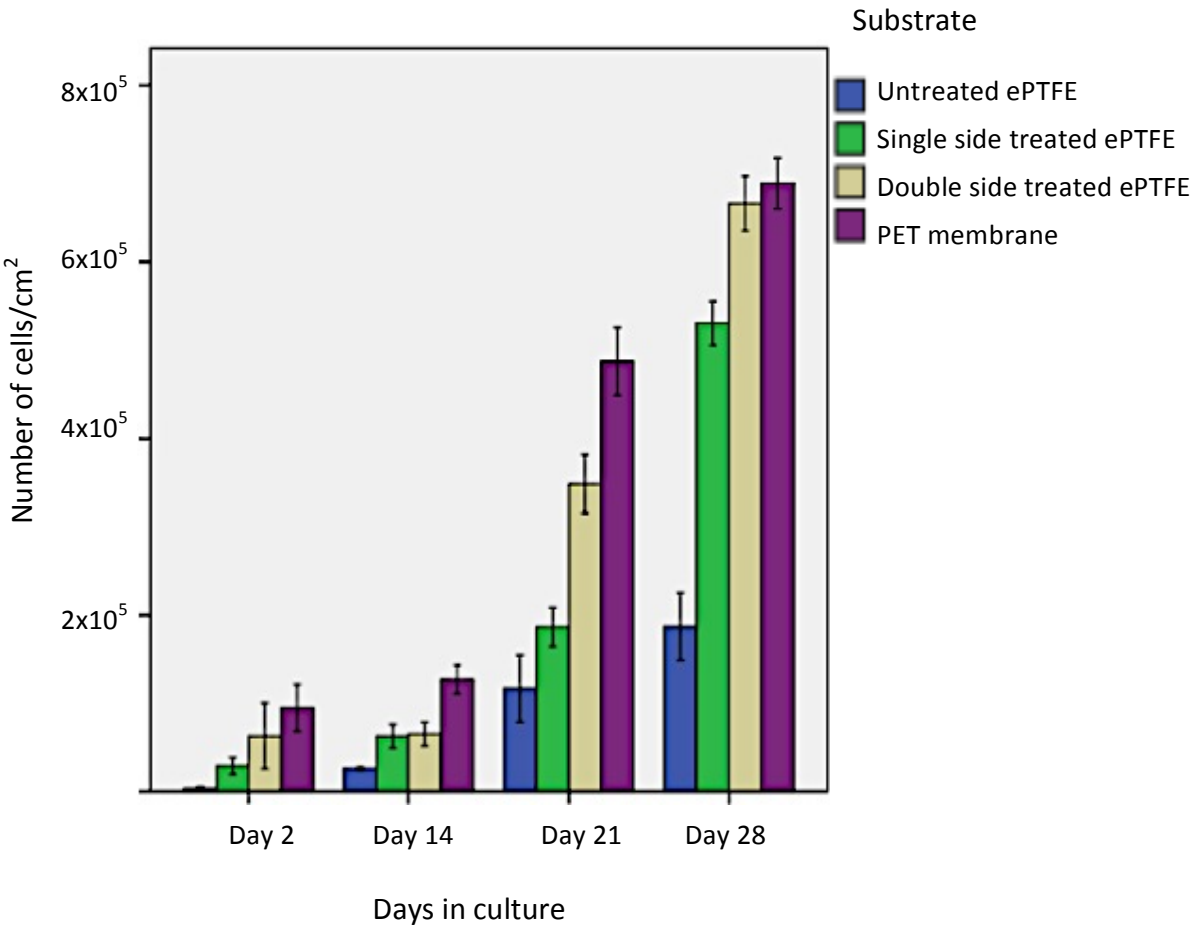

Figure 30: Cell density of HCjE-Gi cells grown on ammonia plasma treated ePTFE, PET membrane and untreated ePTFE with advancing time. Cells were cultured using media protocol B seeded at $1x10^5/cm^2$. Data has been log transformed to allow parametric statistical analysis by ANOVA. The overall model was significant p<0.001 for the effect of both time point and substrate. Bonferroni post-hoc tests of the difference between pairs (both time points an substrate) in any combination were also highly significant; p<0.001.

3.2.2 Morphology of conjunctival cultures developed on synthetic substrates

Along with cell density, the morphology of cultures was also studied. F-actin staining demonstrated by red fluorescent staining with phalloidin together with the blue nuclear staining from DAPI shows confluent growth on PET and treated ePTFE towards the mid to late time points (Figures 31-37). Sparse growth was demonstrated on untreated ePTFE at all time points studied. Phalloidin staining was somewhat difficult to assess in PET cultures, as the actin fibres were not visible as discretely as they were with cells imaged on ePTFE substrates. This was overcome by UAE-1 lectin, which demonstrated the cell morphology of HCjE-Gi cells on all the substrates clearly by staining of cell membranes together with intracellular mucin (Figures 38-44). The morphology of cells on PET membrane demonstrated that cultured cells were smaller in size with proportionally smaller nuclei in comparison to those cultured on ammonia treated ePTFE indicated by the outline of the cells through UAE-1 lectin staining (Figure 40). The shapes of the cells were epithelioid and assumed 'cobblestone' morphology on all the substrates. Although the cells and their nuclei were smaller on PET membrane, no other significant morphological differences in HCjE-Gi cell morphology were qualitatively demonstrated between PET and all other ePTFE substrate cultures. This was demonstrated through UAE-1 lectin and phalloidin staining (Figures 31-44). Although the cells on untreated ePTFE appeared 'rounded' in appearance initially, they became more epithelioid in appearance with advancing time in culture as the cell density increased. The cell density appeared the lowest on untreated ePTFE and lower on single sided treated than double side treated ePTFE, qualitatively, in keeping with the cell density analysis (Figure 30).

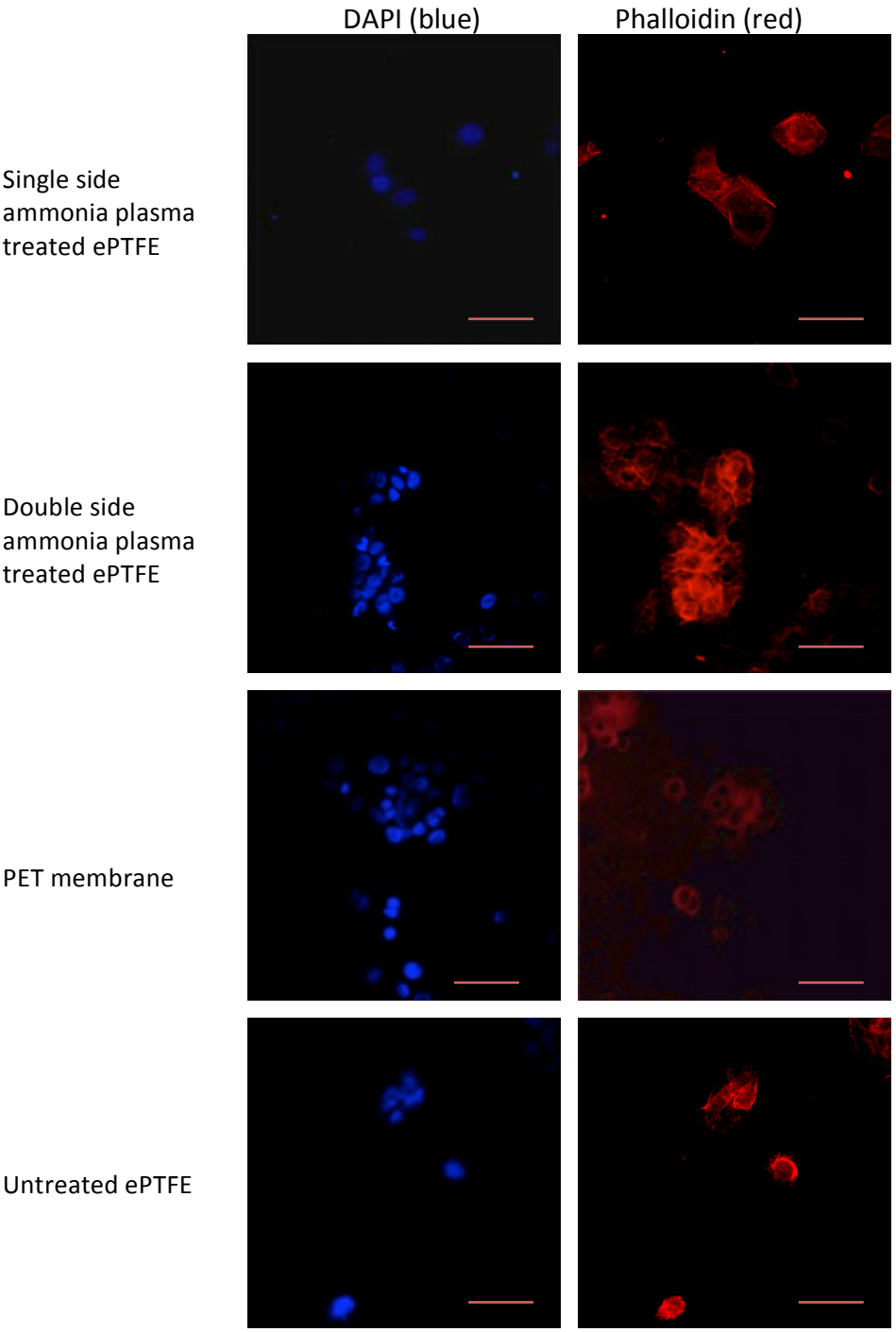

Figure 31: Representative photomicrographs of nuclear and f-actin staining of HCjE-Gi cells cultured on ammonia plasma treated ePTFE, PET and untreated ePTFE after **2 days** in culture. Cell size appears smaller on PET membranes however cell density appeared greatest. Lowest cell density was apparent on untreated ePTFE with cells more 'rounded' in appearance than on ammonia plasma treated ePTFE substrates. Scale bars 50µm.

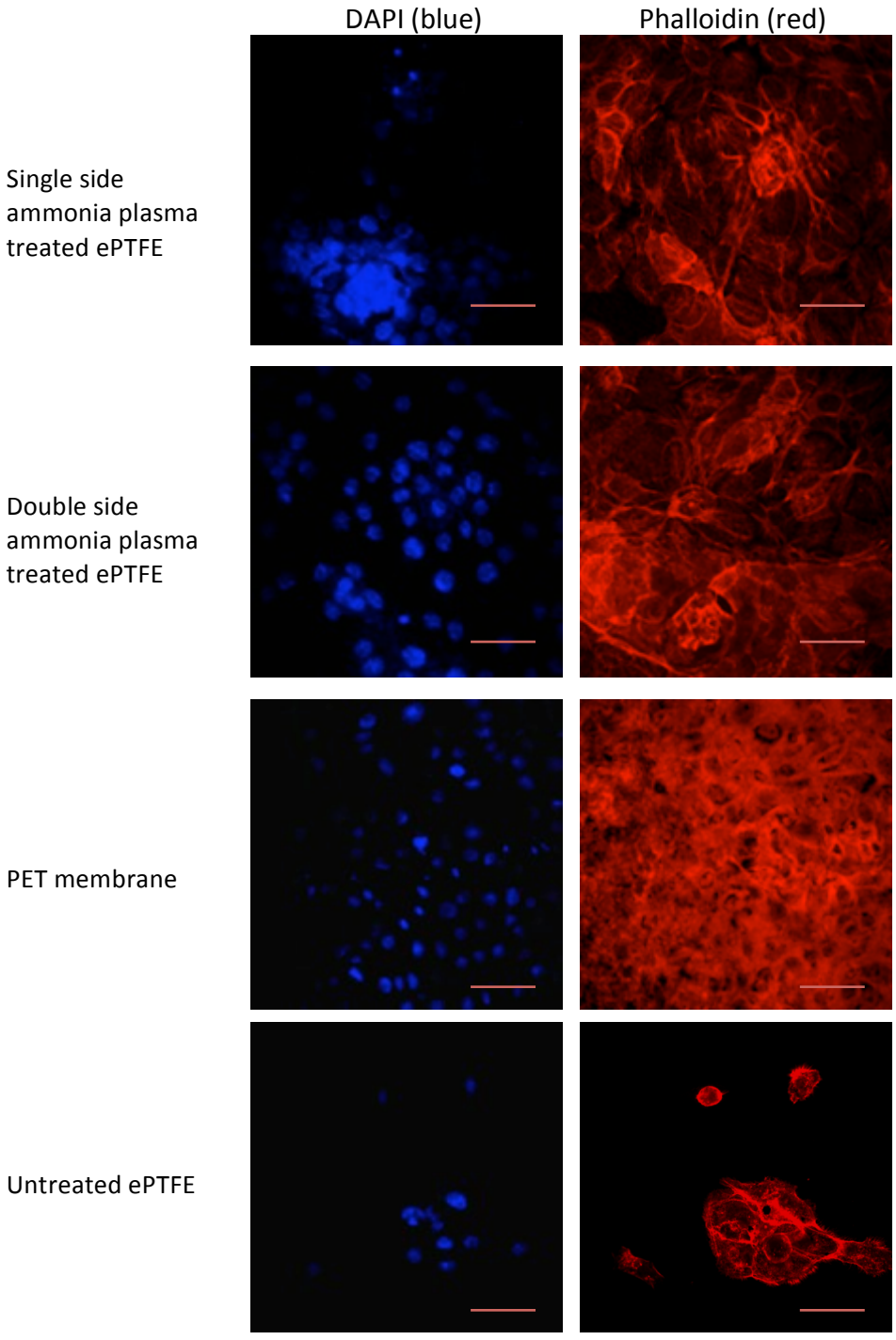

Figure 32: Representative photomicrographs of nuclear and f-actin staining of HCjE-Gi cells cultured on ammonia plasma treated ePTFE, PET and untreated ePTFE after **14 days** in culture. Cell size appeared the smallest with greatest density on PET membrane. Similar morphology was apparent on treated ePTFE and PET membrane. Lowest cell density with 'rounded' cells was apparent on untreated ePTFE. Cultures were more confluent on double-side treated ePTFE than single side treated ePTFE. Scale bars 50µm.

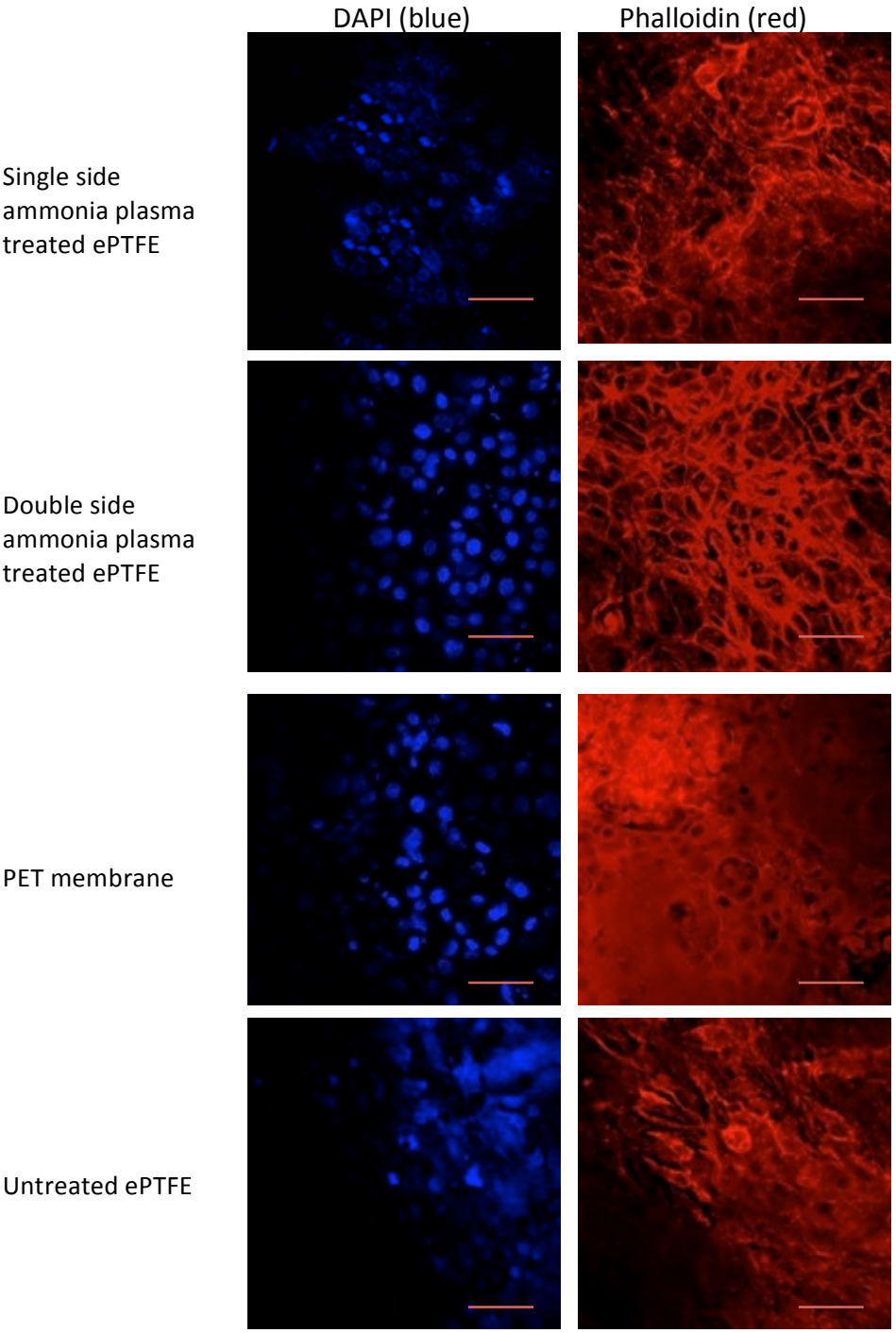

Figure 33: Representative photomicrographs of nuclear and f-actin staining of HCjE-Gi cells cultured on ammonia plasma treated ePTFE, PET and untreated ePTFE after **21 days** in culture. Lowest cell density was apparent on untreated ePTFE however there is greater variation in the size and shape of the nuclear material than on any other substrate. Cultures were more confluent on double side treated ePTFE than following single side-treatment and cells appear to have more of cobblestone morphology than on other substrates. Scale bars 50µm.

a)

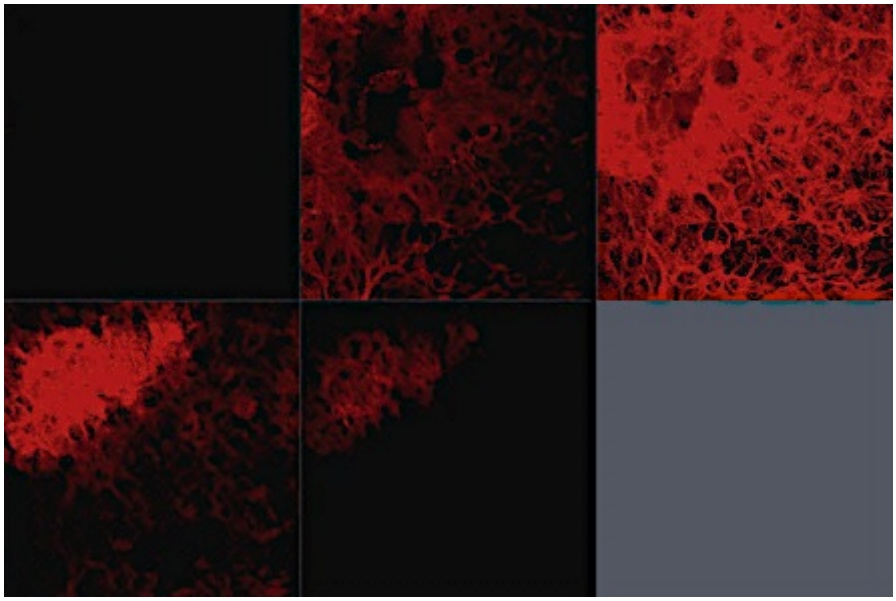

b)

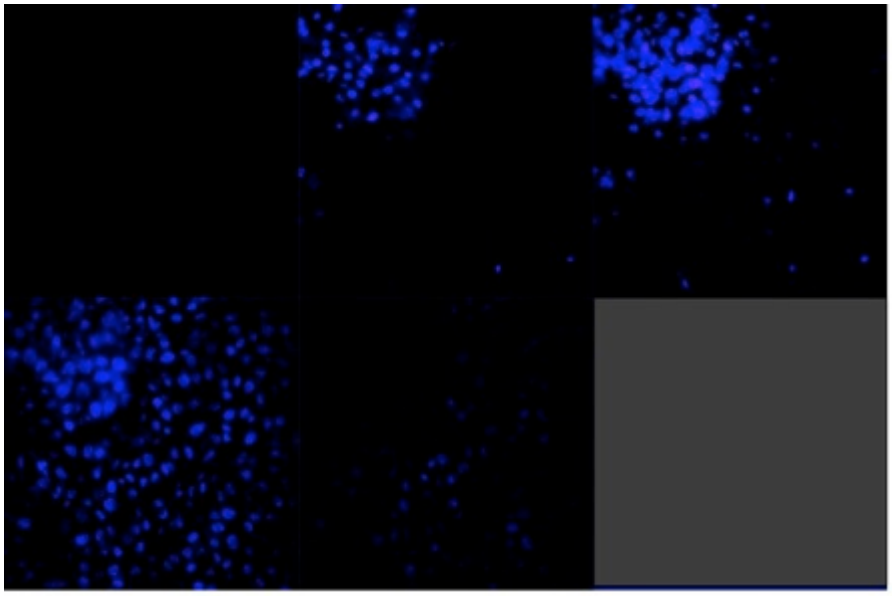

Figure 34: Representative confocal z-stack series of **single side ammonia plasma treated ePTFE** after 28 days of HCjE-Gi cell culture: a) phalloidin (f-actin staining) (b) DAPI (nuclear) staining. Five slices have been taken, each in 4.5-5µm intervals whereby the top and bottom of the z-stack had been manually set after the focus points at the top and bottom of the cell cultures were located. Scale bars 50µm.

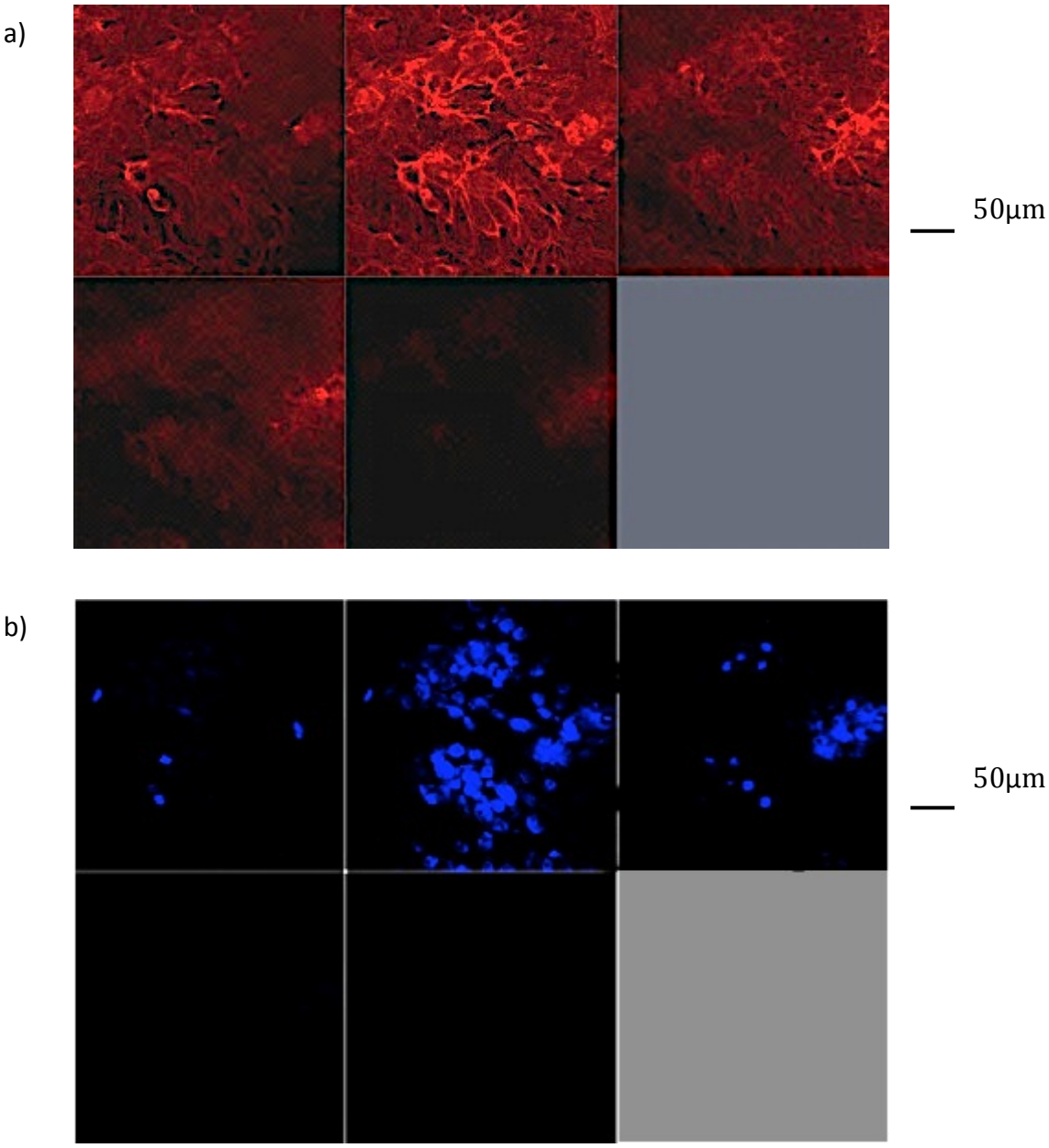

Figure 35: Representative confocal z-stack series of **double side ammonia plasma treated ePTFE** after 28 days of HCjE-Gi cell culture: a) phalloidin (f-actin staining) (b) DAPI (nuclear) staining. Five slices have been taken, each in 4.5-5µm intervals whereby the top and bottom of the z-stack had been manually set after the focus points at the top and bottom of the cell cultures were located. Scale bars 50µm.

a)

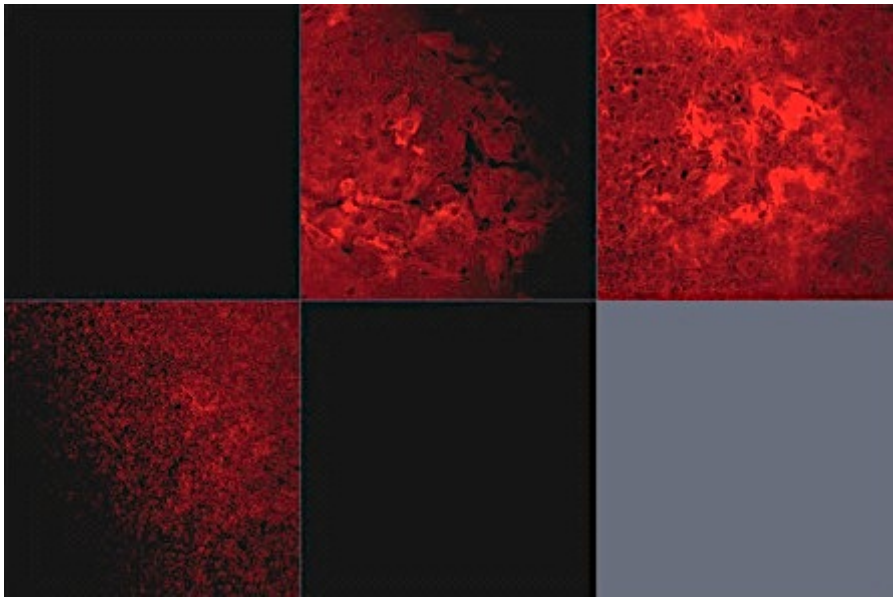

50µm

b)

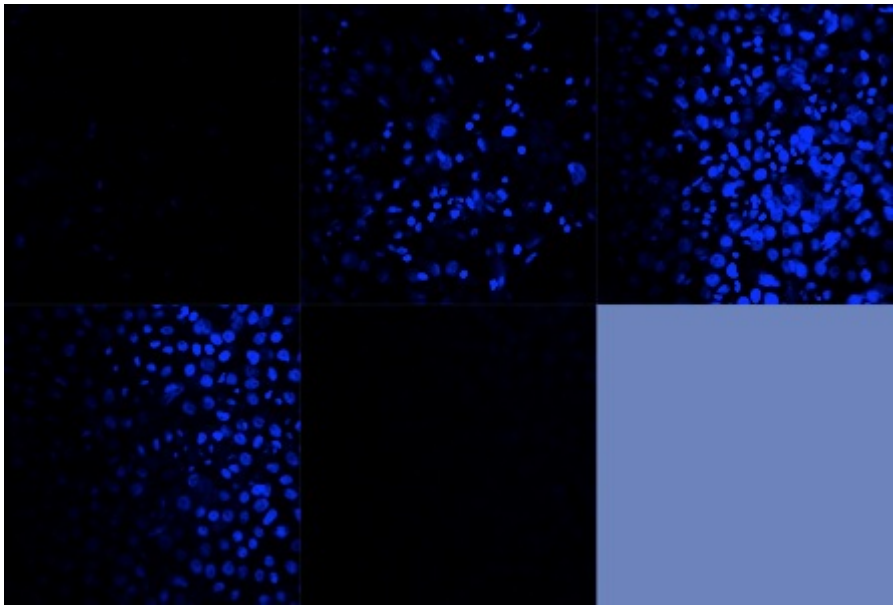

50µm

Figure 36: Representative confocal z-stack series of **PET membrane** after 28 days of HCjE-Gi cell culture: a) phalloidin (f-actin staining) (b) DAPI (nuclear) staining. Five slices have been taken, each in 4.5-5µm intervals whereby the top and bottom of the z-stack had been manually set after the focus points at the top and bottom of the cell cultures were located. Scale bars 50µm.

a)

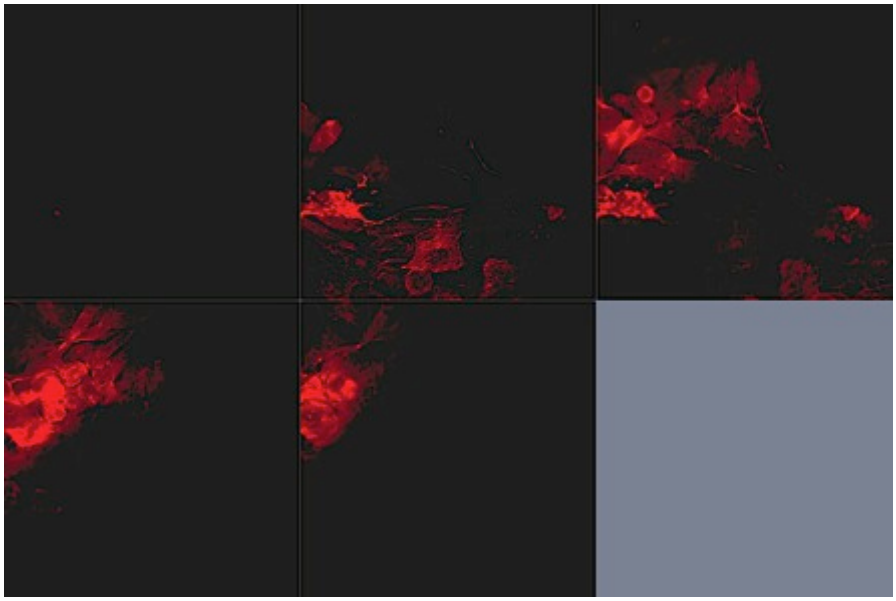

50µm

b)

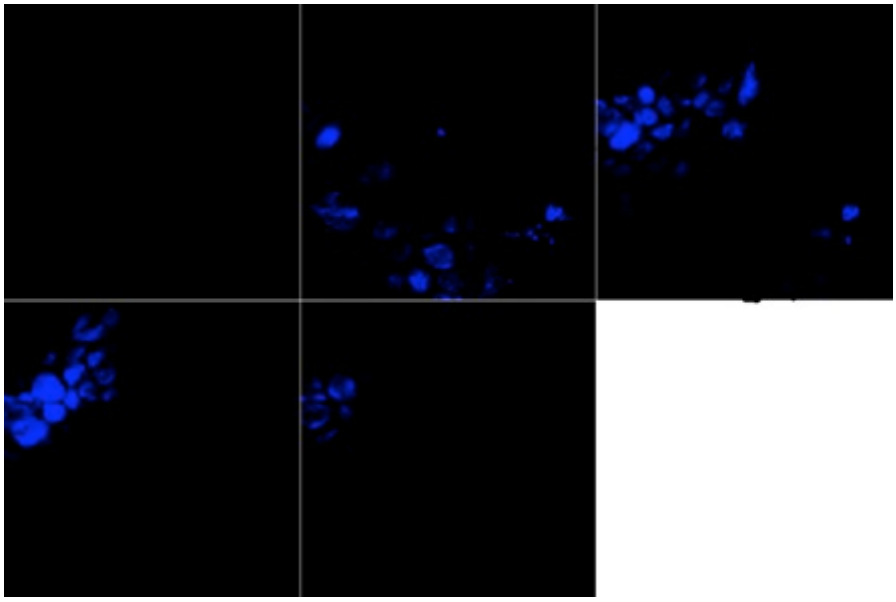

50µm

Figure 37: Representative confocal z-stack series of **untreated ePTFE** after 28 days of HCjE-Gi cell culture: a) phalloidin (f-actin staining) (b) DAPI (nuclear) staining. Five slices have been taken, each in 4.5-5µm intervals whereby the top and bottom of the z-stack had been manually set after the focus points at the top and bottom of the cell cultures were located. Scale bars 50µm.

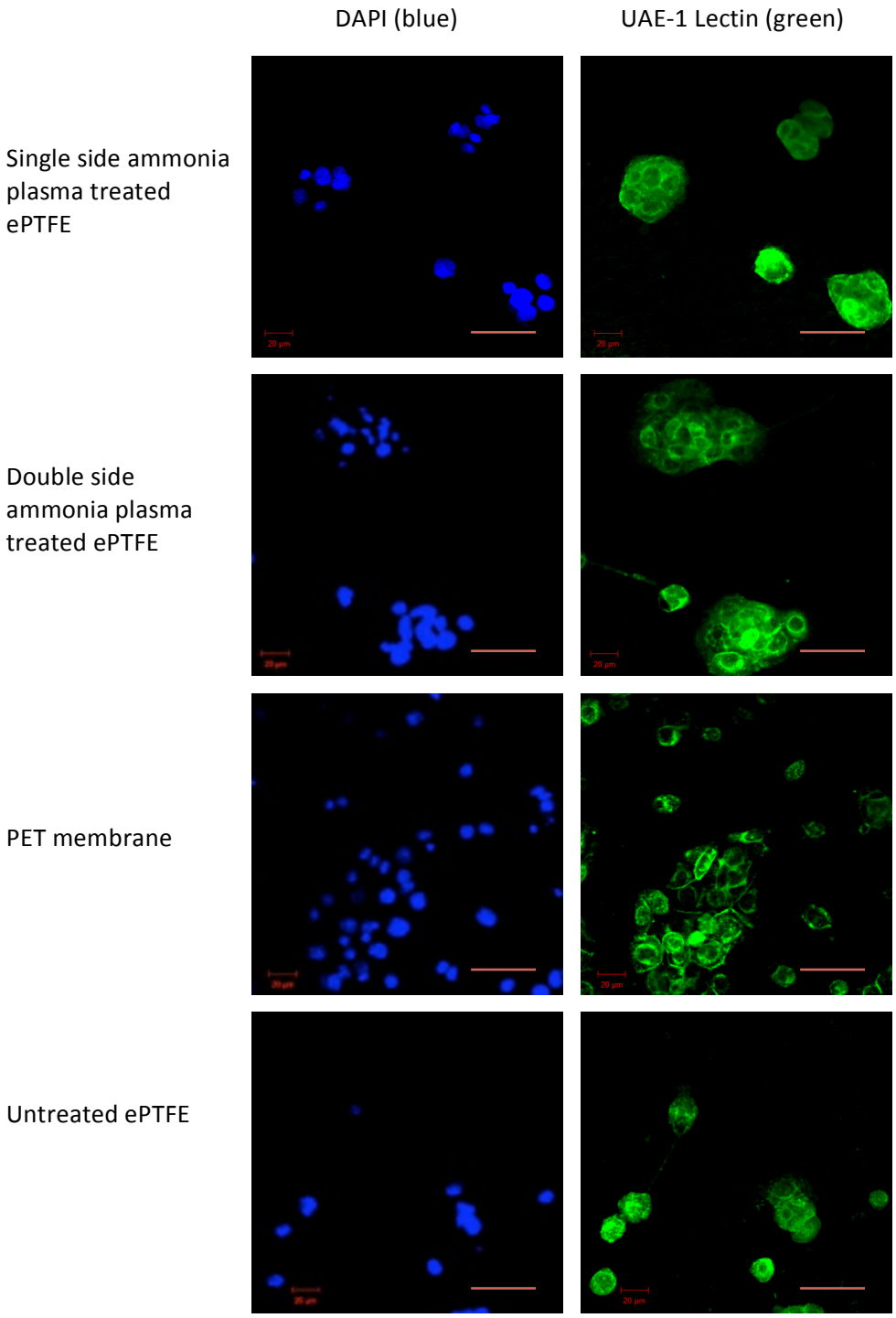

Figure 38: Representative photomicrographs of nuclear and UAE-1 staining of HCjE-Gi cells cultured on ammonia plasma treated ePTFE, PET and untreated ePTFE after **2 days** in culture. Lowest cell density was apparent on untreated ePTFE. Overall greater UAE-1 (intracellular and membrane associated) staining was apparent on cells cultured on ePTFE than PET membrane in which staining appeared more discrete and mostly membrane associated. Scale bars 50µm.

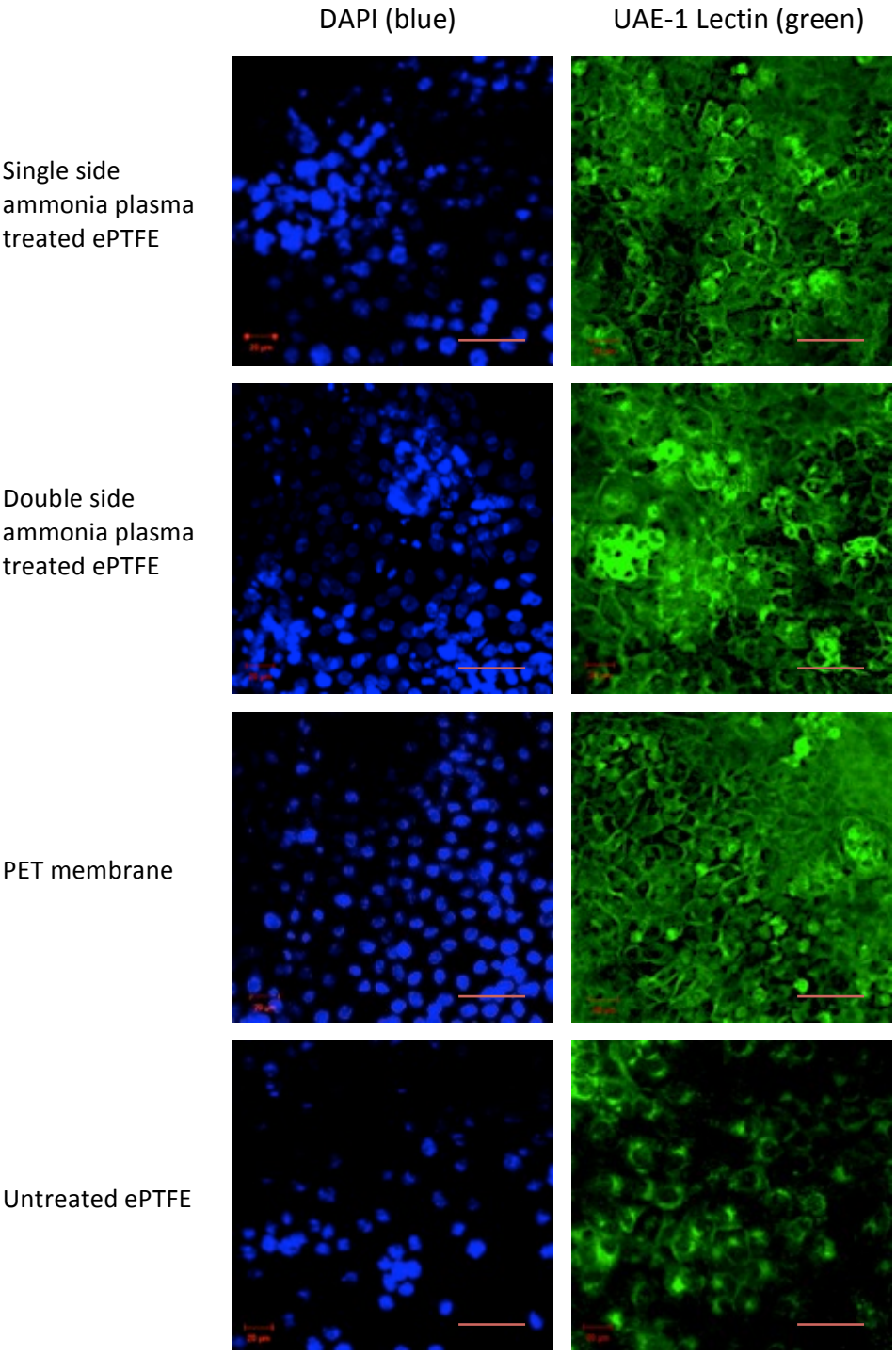

Figure 39: Representative photomicrographs of nuclear and UAE-1 staining of HCjE-Gi cells cultured on ammonia plasma treated ePTFE, PET and untreated ePTFE after **14 days** in culture. Lowest cell density was apparent on untreated ePTFE. The greatest intensity of UAE-1 staining appeared on PET membrane and double side treated ePTFE. Staining of cell membranes showed the cell size was greater on ePTFE cell cultures than PET cell cultures. Scale bars 50µm.

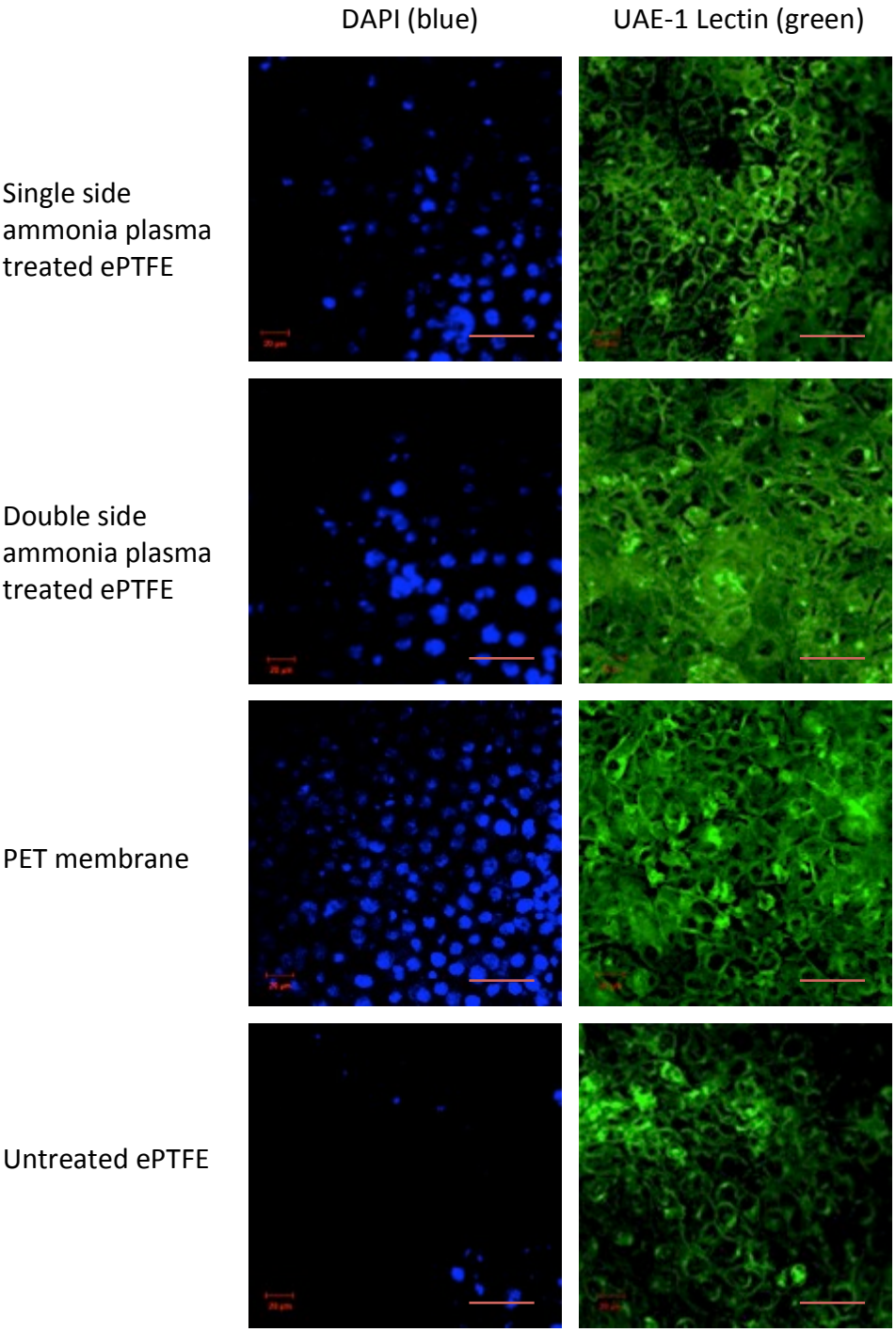

Figure 40: Representative photomicrographs of nuclear and UAE-1 staining of HCjE-Gi cells cultured on ammonia plasma treated ePTFE, PET and untreated ePTFE after **21 days** in culture. Lowest cell density was demonstrated on untreated ePTFE, whereas the greatest density was demonstrated on PET membrane and double side treated ePTFE. Cell size was greater on ePTFE cell cultures than PET cell cultures, and was more pronounced on double side treated ePTFE, especially amongst the cells with greater intracellular staining. Scale bars 50µm.

a)

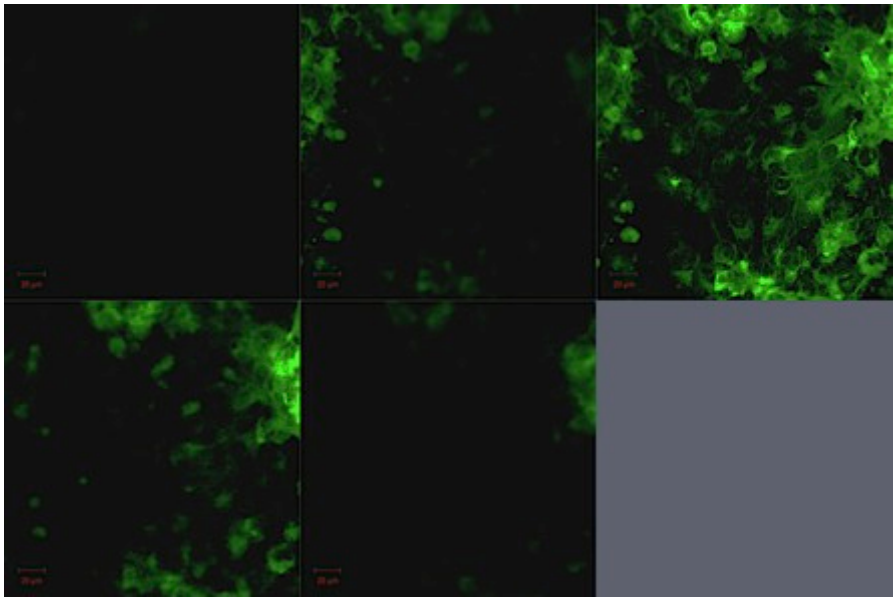

b)

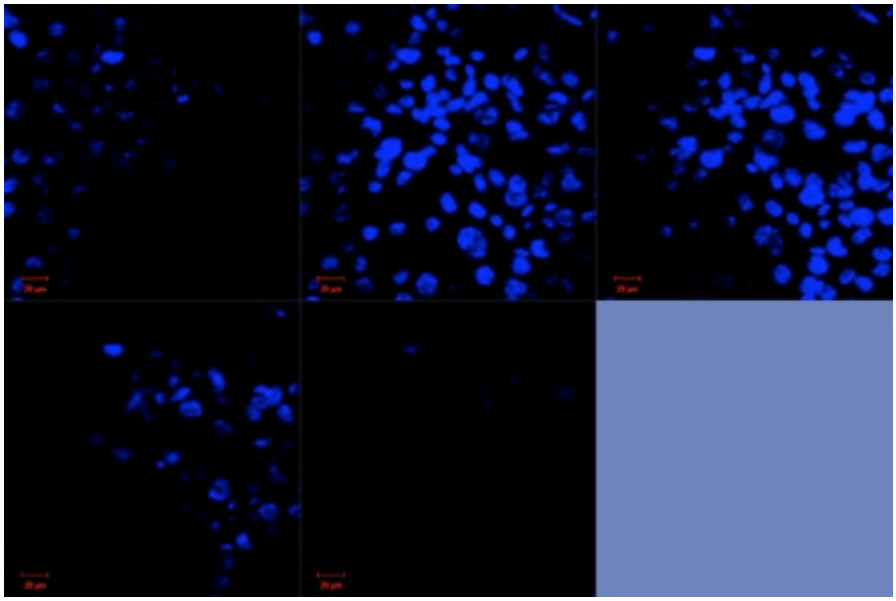

Figure 41: Representative confocal z-stack series of **single side treated ePTFE** after 28 days of HCjE-Gi cell culture: a) UAE-1 lectin staining, b) DAPI (nuclear) staining. Five slices have been taken, each in 4.5-5µm intervals whereby the top and bottom of the z-stack had been manually set after the focus points at the top and bottom of the cell cultures were located. Scale bars 50µm.

a)

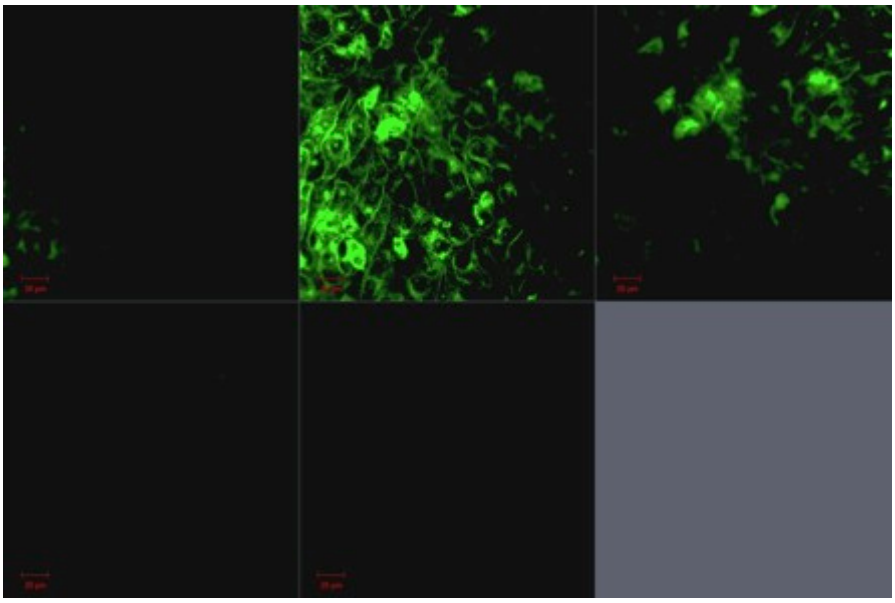

b)

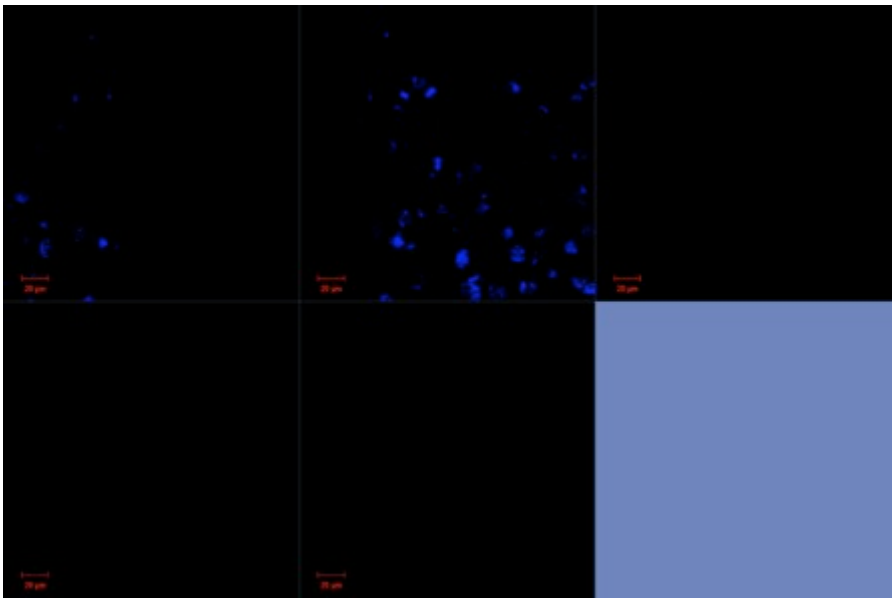

Figure 42: Representative confocal z-stack series of **double side treated ePTFE** after 28 days of HCjE-Gi cell culture: a) UAE-1 lectin staining, b) DAPI (nuclear) staining. Five slices have been taken, each in 4.5-5µm intervals whereby the top and bottom of the z-stack had been manually set after the focus points at the top and bottom of the cell cultures were located. Scale bars 50µm.

a)

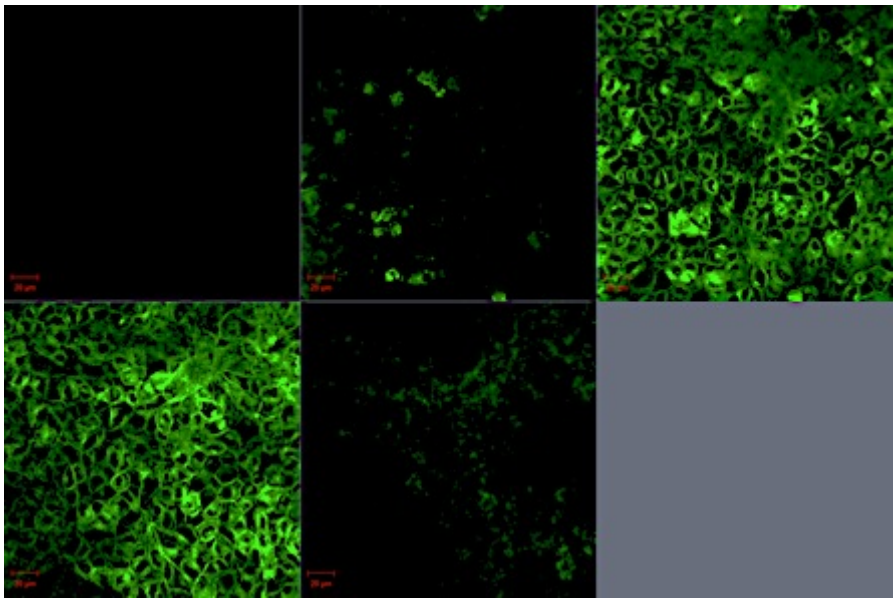

50µm

b)

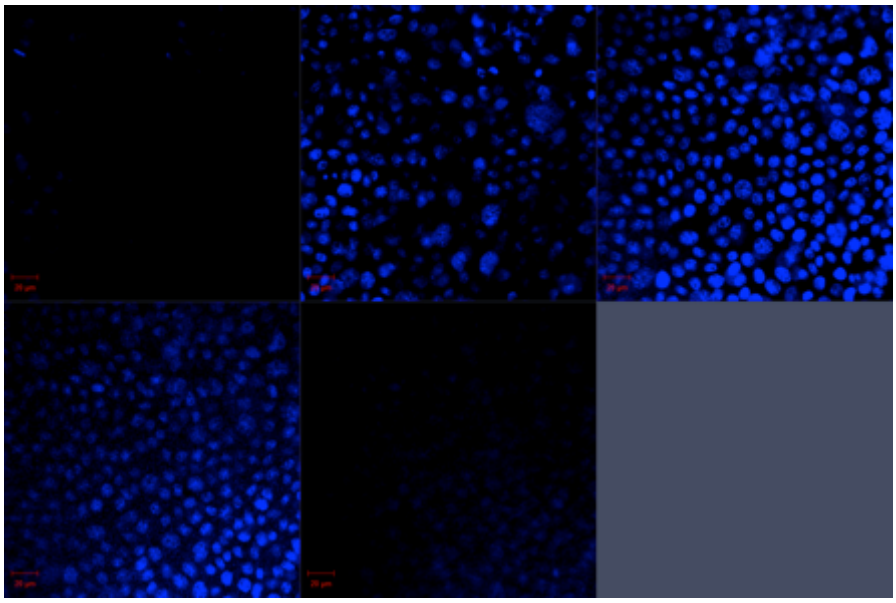

50µm

Figure 43: Representative confocal z-stack series of **PET membrane** after 28 days of HCjE-Gi cell culture: a) UAE-1 lectin staining, b) DAPI (nuclear) staining. Five slices have been taken, each in 4.5-5µm intervals whereby the top and bottom of the z-stack had been manually set after the focus points at the top and bottom of the cell cultures were located. Scale bars 50µm.

a)

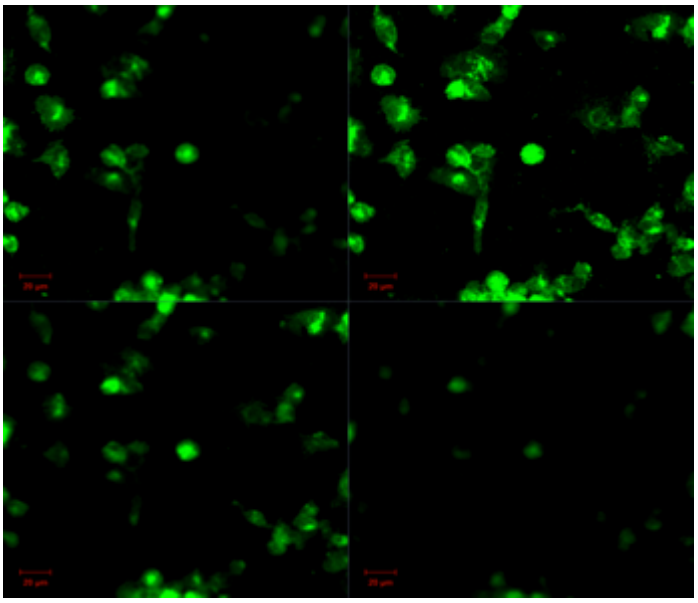

50µm

b)

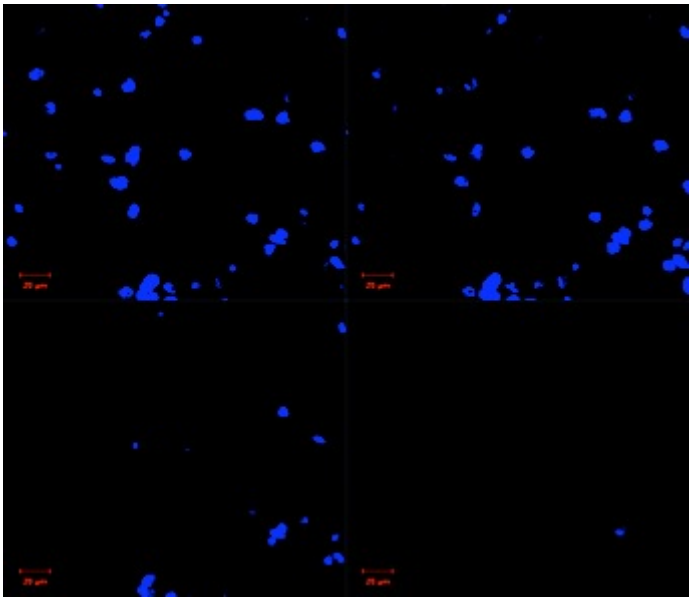

50µm

Figure 44: Representative confocal z-stack series of **untreated ePTFE** after 28 days of HCjE-Gi cell culture: a) UAE-1 lectin staining, b) DAPI (nuclear) staining. Four slices have been taken, each after 3µM whereby the top and bottom of the z-stack had been manually set after the focus points at the top and bottom of the cell cultures were located. Scale bars 50µm.

3.3 Retrieved human conjunctiva

Human conjunctiva was retrieved from 26 eyes of 13 tissue donors. Six donors were male and 7 donors were female with a mean age of 84.2 years (range 65-92). The mean time to retrieval was 20.4 hours (range 7-32 hours).

Donor number	Gender	Age	Time to retrieval (hours)
1, 2	Male	84	19
3, 4	Male	87	7
5, 6	Female	96	29
7, 8	Male	76	26
9, 10	Female	80	16
11, 12	Female	90	12
13, 14	Male	92	24
15, 16	Male	77	9
17, 18	Female	88	19
19, 20	Female	65	23
21, 22	Female	85	28
23, 24	Male	84	22
25, 26	Female	91	32

Table 7: Table of the age and gender of tissue donors together with the post-mortem retrieval time. The donor eyes were designated numbered sequentially, left eye followed by right eye.

3.4 Preliminary optimisation and validation of the HCjE-Gi cell line and flow cytometry

3.4.1 Optimisation of antibody staining for flow cytometry

Many of the antibodies identified for this study were not conjugated to a fluorochrome. Testing the optimal dilution for both the primary and secondary antibody was undertaken before any experimental work was conducted. The incubation period was also optimised. The optimal protocol was determined when a shift in fluorescence was clearly detectable with minimal overlap from a non-stained population. For example, several concentrations of UAE-1 lectin were tested with variations in length of incubation, however, this did not have a significant effect (Figure 45). In contrast, greater separation of cell populations was observed by variation in the dilution of UAE-1 lectin. An optimal concentration of 1:500 at an incubation time of 30 minutes was determined.

The detected fluorescence of samples treated with unconjugated primary and secondary antibodies were compared against their respective isotype controls. In addition, the secondary antibody alone was also tested at varying dilutions to find an optimal balance between bright staining and non-specific binding. The percentage of the cell population that represented a positively stained population was determined by quantitative analysis of the cell population that emitted fluorescence at a greater intensity to the control samples: i) the respective isotype control in combination with its secondary antibody ii) the secondary antibody alone. Experiments for each antibody were therefore undertaken using secondary antibody alone in addition to with each dilution of the primary and the secondary antibody combination and the corresponding concentration of isotype control. The example of antibody optimisation shown in Figure 46 demonstrates a degree of non-specific antibody binding. This optimisation step determined that the greatest separation in cell populations was detectable (and

therefore least non specific binding occurred) when the dilution of primary and secondary antibody was used at 1:50 and 1:1000 respectively.

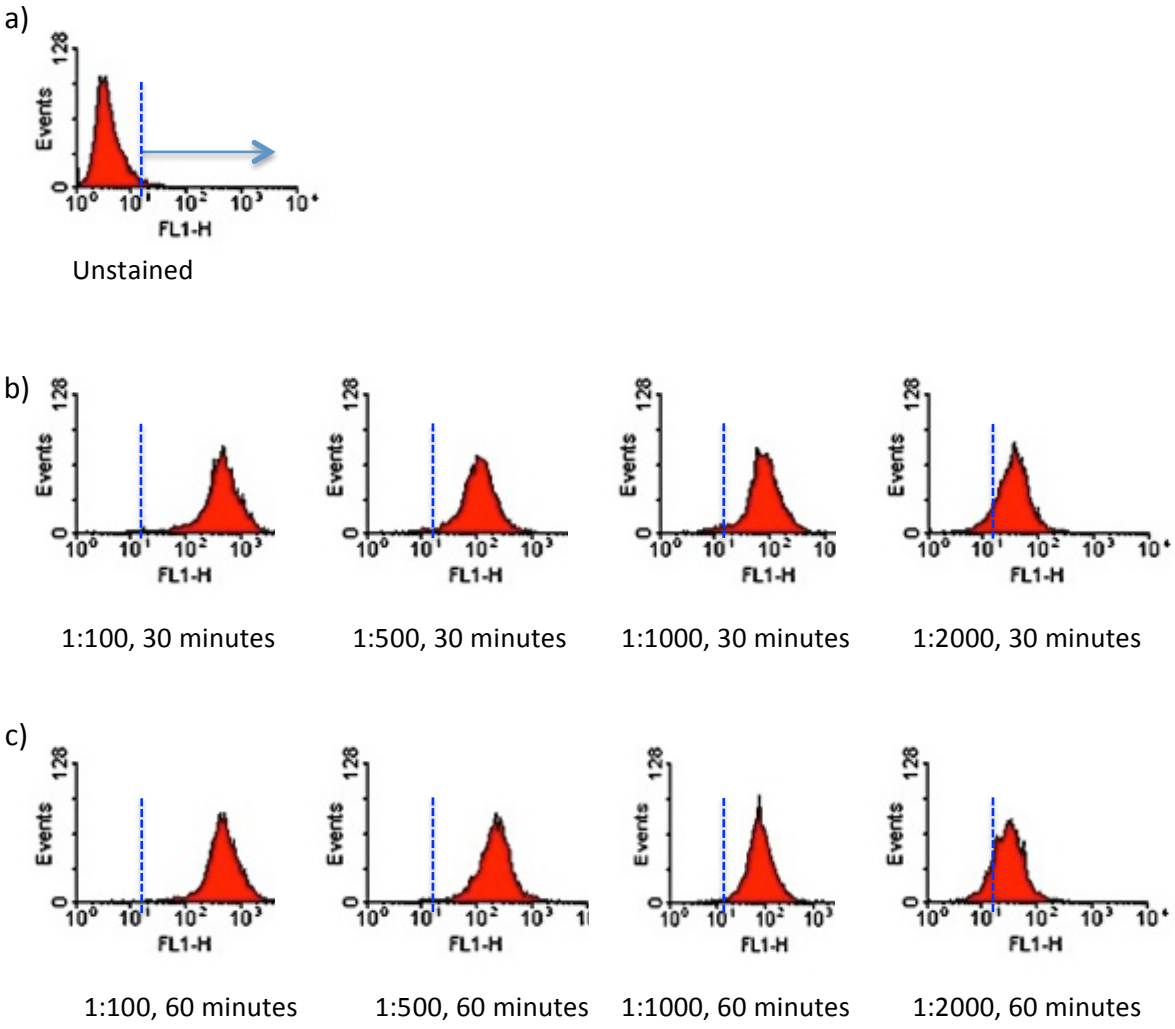

Figure 45: Fluorescence channel histograms of HCjE-Gi cells demonstrating the resulting fluorescence after staining with various concentrations of UAE-1 lectin over 30 (b) and 60 (c) minutes. The dashed line on all the histograms and arrow on the histogram of the unstained control sample (a) indicates the fluorescence beyond which staining was regarded as positive. These histograms demonstrate that there was little effect of incubation time and therefore 30 minutes was sufficient. At all the antibody dilutions studied, there was marked separation of the histogram from an unstained (control) sample of cells, however, the 1:500 dilution was optimal.

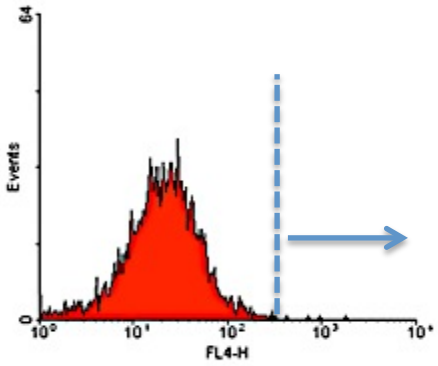

Isotype control with secondary antibody 1:1000

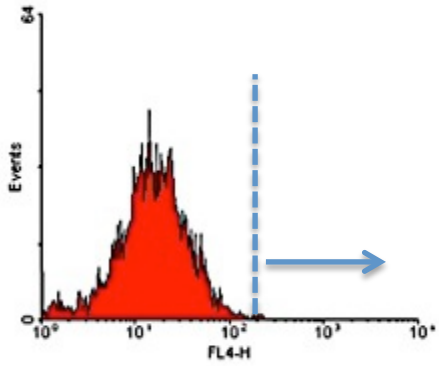

Secondary antibody only 1:1000

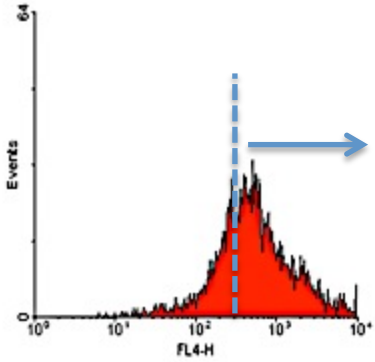

ΔNp63 1:50, secondary antibody 1:1000

Figure 46: The histograms above show the results at the optimal determined dilutions of the primary ΔNp63 antibody and secondary antibody (1:50 primary and 1:1000 secondary) compared with an isotype control and the secondary antibody in isolation. Other variables tested but not displayed above included: primary antibody dilutions 1:100, 1:250: in all combinations with secondary antibody dilutions 1:100, 1:500, 1:1500. The positively stained peak was determined from primary and secondary antibody combinations, which exceeded the fluorescence of both the isotype control and secondary antibody in combination and to the secondary antibody alone at the same dilutions. Importantly, the shift in the histogram curve was such that there was minimal overlap with the histogram curve of the control samples described. The dotted lines and arrows indicate the area of histogram from which a logical 'gate' was placed to determine the percentage of cells that were deemed positive for ΔNp63 expression.

3.4.2 Characterisation of primary HCjE-Gi conjunctival cell line with flow cytometry

The antibody optimisation experiments shown in previously described section (3.4.1) enabled the determination of optimal primary and secondary antibody staining protocols to undertake flow cytometry. Optimisation was undertaken for all the antibodies studied and representative experiments have been displayed to illustrate how this was conducted. Characterisation of the prepared sample began with adjusting the forward and side scatter voltages and compensation to obtain optimal scatter characteristics from which the cell population was identified (Figure 47). The same voltage settings were used for all subsequent experimental work. Figure 47 displays the cell population that was gated for subsequent analysis. Each stained cell sample was analysed in conjunction with its relevant isotype control. An isotype control of a corresponding dilution was included in each experimental run for each antibody that was used. The antibody staining characteristics together with the relevant isotype controls are shown in histograms for both primary conjunctival cells and the HCjE-Gi cell line (Figure 48). The gating criteria regarded as positive antibody staining was determined from the point on the x axis at which the histogram curve for the isotype control tapers with increasing fluorescence. Illustrative examples are shown in Figure 48.

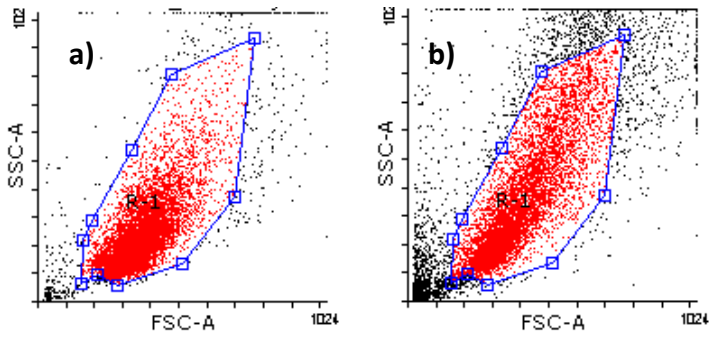

Figure 47: Dot plot of side scatter-height (SSC-H) against forward scatter height (FSC-H) of HCjE-Gi (a) and primary conjunctival cells (b). The dots occurring at the bottom left of the plot (low FSC-H and SSC-H) are particulates/debris.

Figure 48 (displayed below and over pages 110-114): Histograms to show the fluorescence detected in primary conjunctival epithelial cells and HCjE-Gi cells after staining as described in section 2.4.6: a) CK19, b) CK4, c) CK7, d) UAE-1 lectin, e) MUC5AC, f) PCNA, g) caspase-3, h) ΔNp63, i) ABCG2. The dotted lines and arrows indicate the region the 'gates' were set such that cells emitting fluorescence above that detected in the relevant isotype controls (all histograms on the left hand side) were deemed positively stained. The red arrows on the histograms on the right hand side demonstrate the positive antibody stained population determined by setting a logical gate based on the emitted fluorescence of the isotype control samples illustrated on the histograms on the left hand side with blue arrows. The percentage of cells positively stained for the antigen of interest were quantified using an analytical software tool for flow cytometry data (Flowing 2.5).

a) CK19

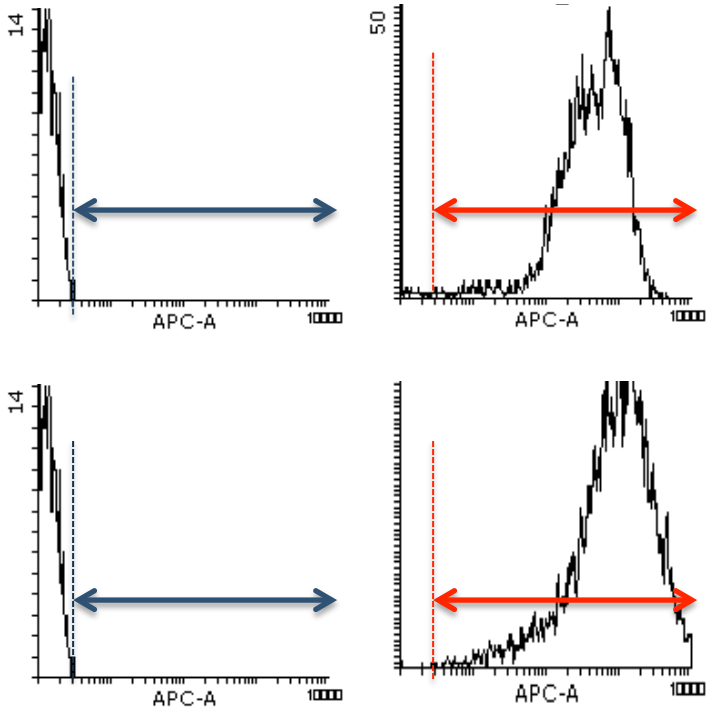

Primary conjunctival cells

HCjE-Gi cells

b) CK4

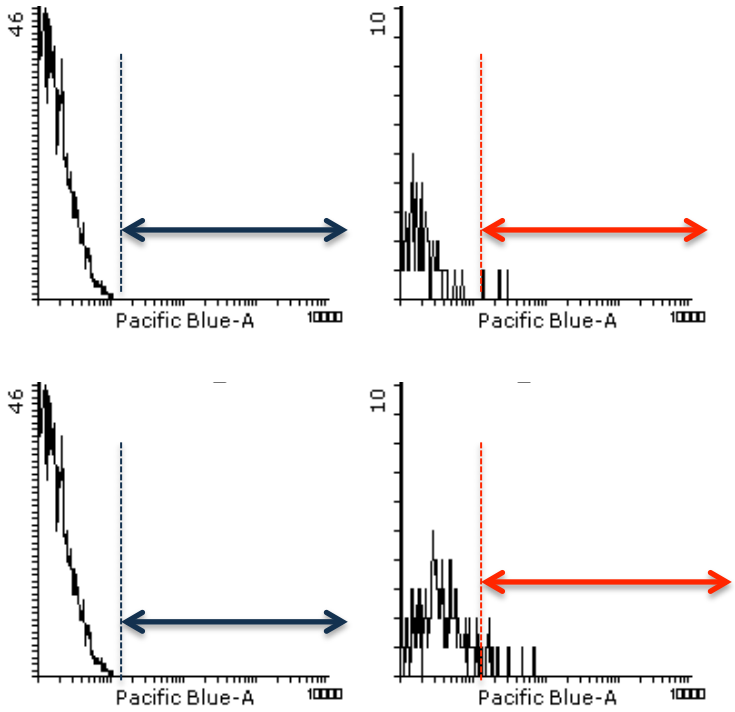

Primary conjunctival cells

HCjE-Gi cells

c) CK7

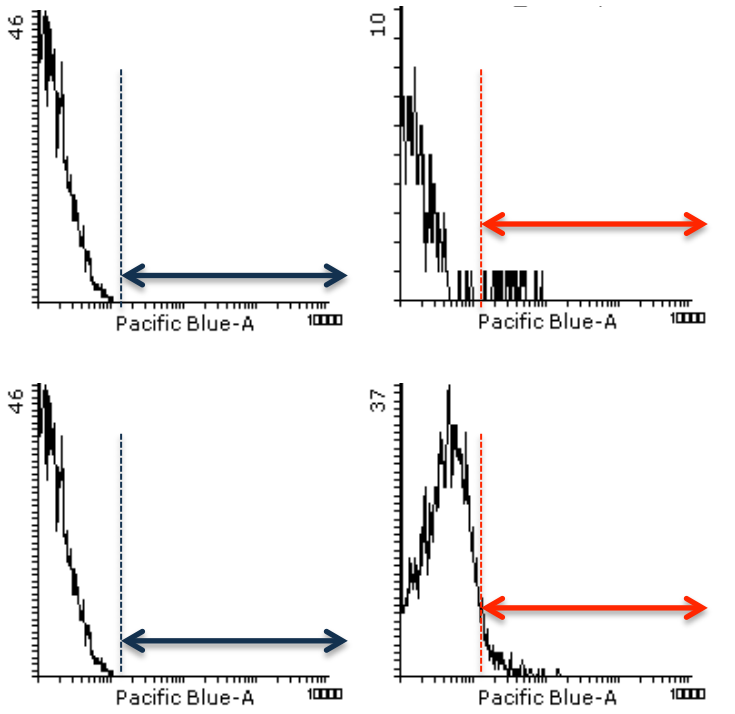

Primary conjunctival cells

HCjE-Gi cells

d) UAE-1 lectin

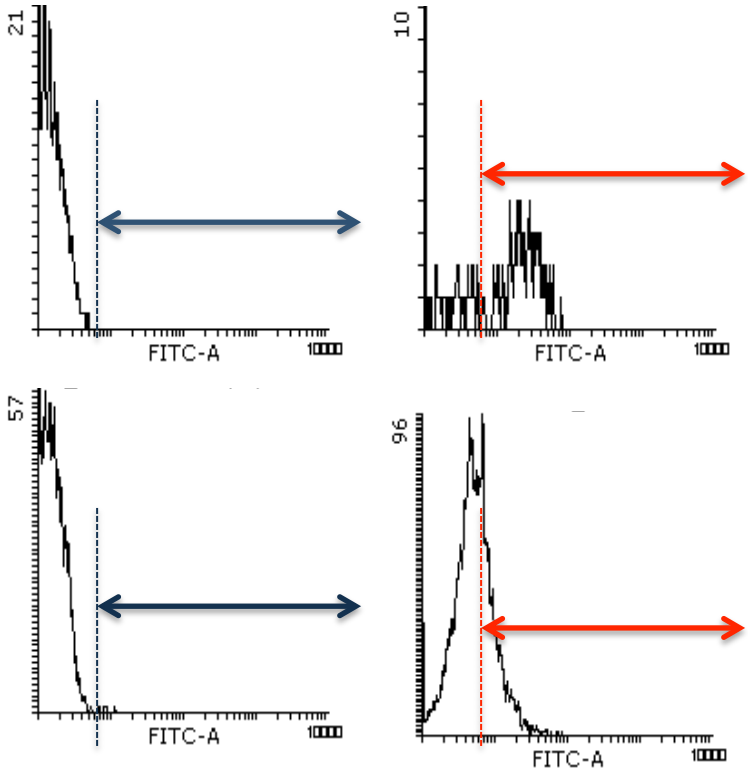

Primary conjunctival cells

HCjE-Gi cells

e) MUC5AC

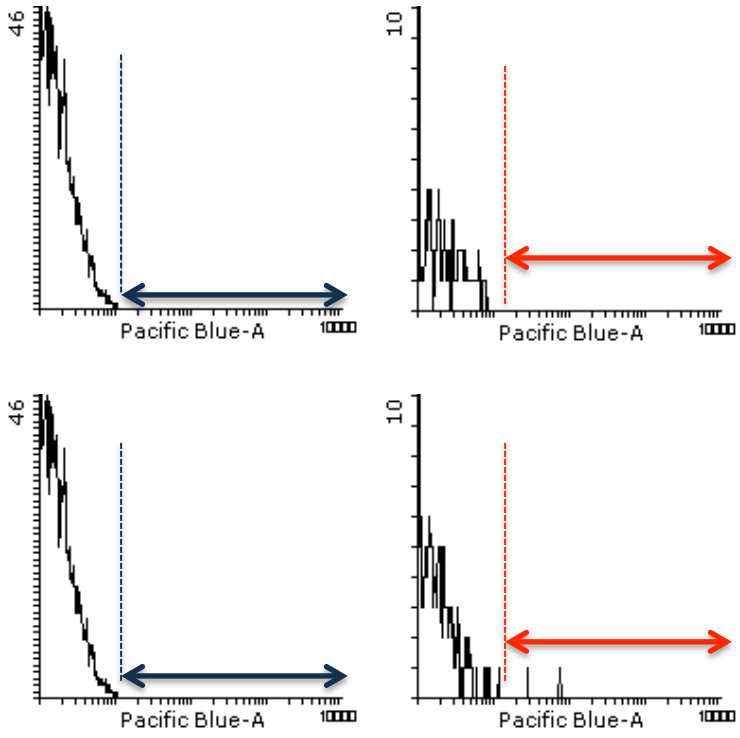

Primary conjunctival cells

HCjE-Gi cells

f) PCNA

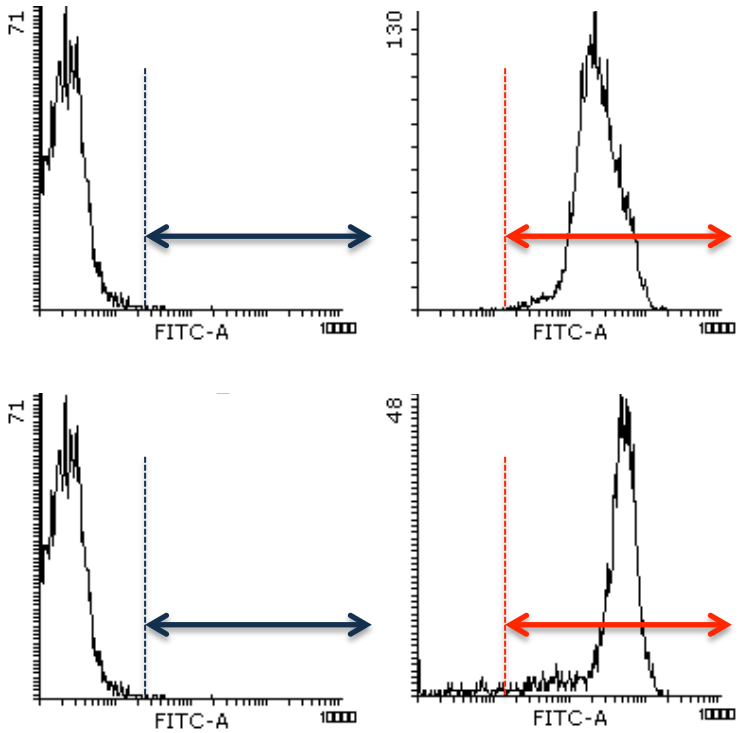

Primary conjunctival cells

HCjE-Gi cells

g) Caspase-3

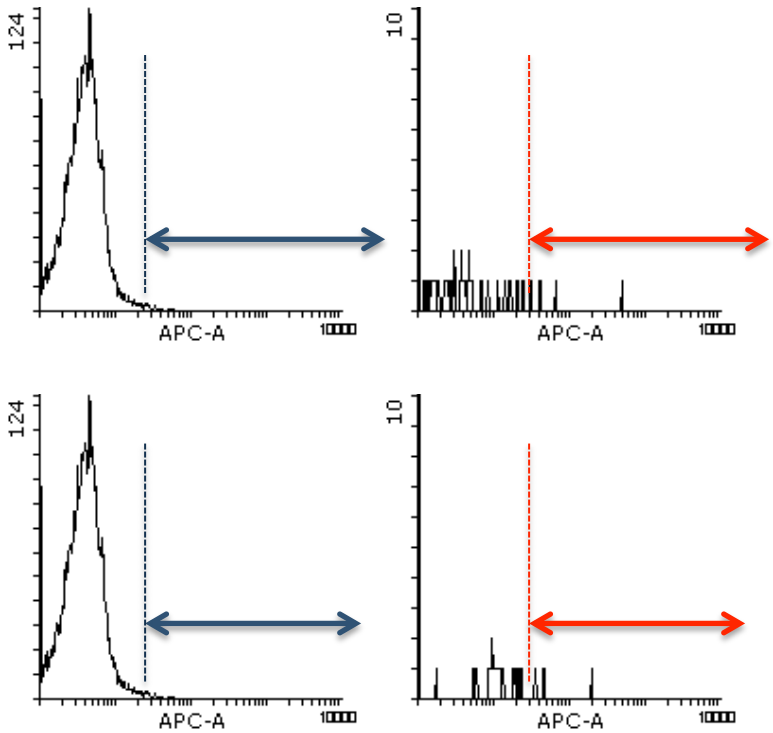

HCjE-Gi cells

Primary conjunctival cells

h) ΔNp63

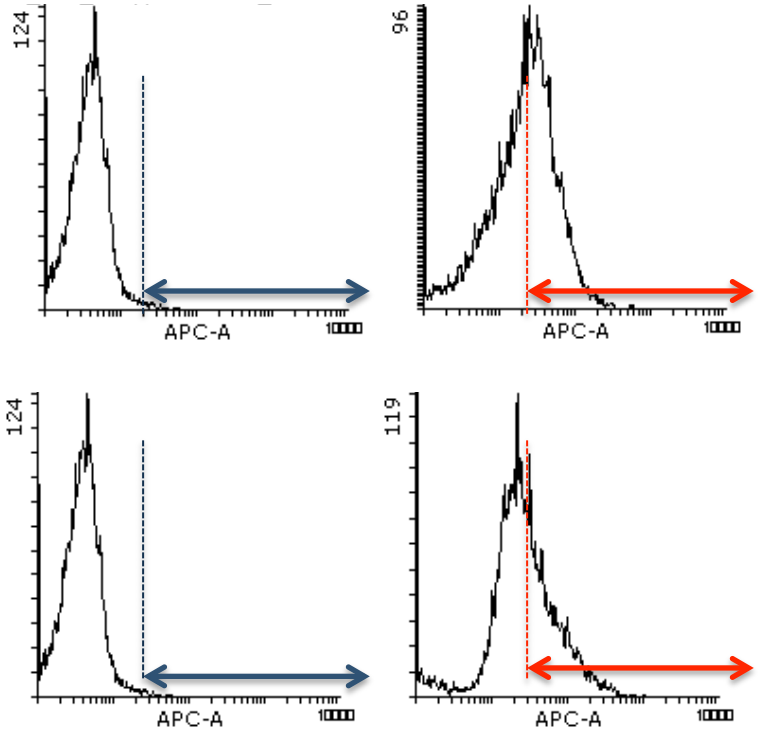

Primary conjunctival cells

HCjE-Gi cells

i) ABCG2

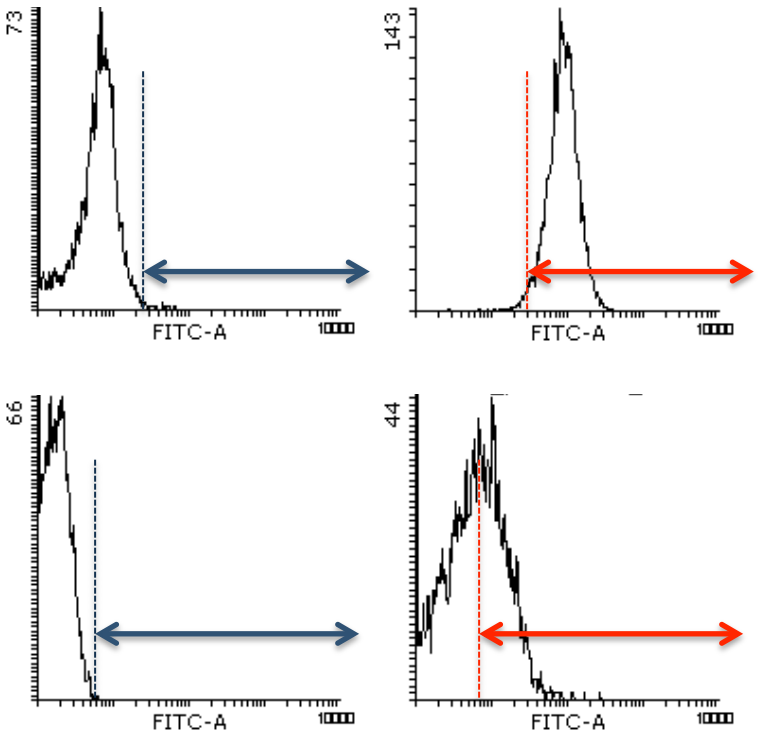

Primary conjunctival cells

HCjE-Gi cells

3.4.3 Determining the utility of caspase-3 as a marker for the identification of apoptotic cells in conjunctival epithelia

Figure 49 shows the shift in fluorescence along the APC (far-red) channel of the cell population stained with caspase-3 with the isotype controls. This revealed greater than 100-fold expression of caspase-3 in the deprived cells (43.5%) compared to those that had been maintained in optimal culture conditions (0.36%).

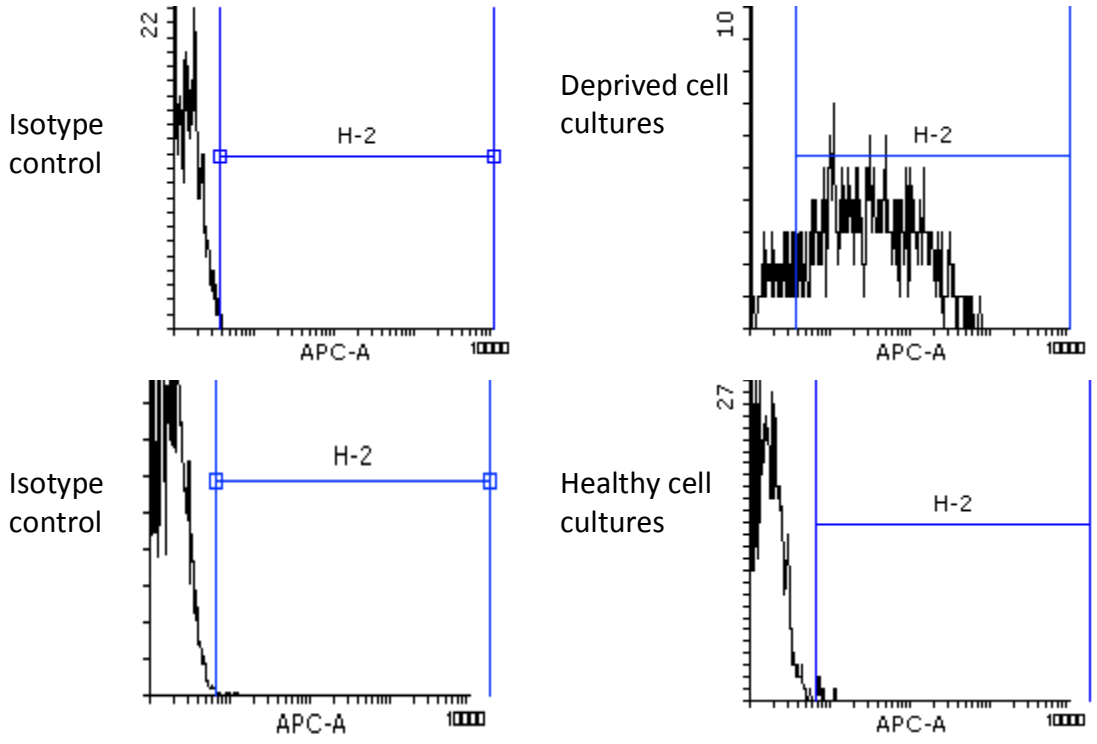

Figure 49: Histograms of fluorescence detected following staining with caspase-3 in healthy and deprived cultures. H2 indicates the 'gates' set using a flow cytometry analysis software program such that cells emitting fluorescence levels above that detected in the isotype controls (in the range indicated by H2) were regarded as positively stained. This enabled the quantification of the cell population in terms of the percentage of the cells present in this gated region.

3.4.4 Validation of the cell line

Quantitatively, the expression levels of all cell markers were very similar between HCjE-Gi cells of passage 2 and 28 at arrival from source (donated cell line), and no statistically significant differences were demonstrated. Based on this data, HCjE-Gi cells between passages 2 and 28 were deemed suitable for use in subsequent experiments.

	Passage 2 mean (+/- SD) percentage of cells	**Passage 28 mean (+/- SD) percentage of cells**	**p value**
CK4	0.22 (0.07)	0.23 (0.09)	0.89
CK7	2.63 (0.78)	2.58 (1.11)	0.95
CK19	98.8 (0.61)	99.1 (0.21)	0.47
MUC5AC	0.18 (0.04)	0.17(0.08)	0.87
Lectin	44.59 (2.61)	46.3 (3.35)	0.52
Δ Np63	54.9 (11.2)	53 (15.6)	0.78
ABCG2	25.4 (3.63)	22.2(4.5)	0.39
ABCG2 + Δ Np63	24 (3.29)	21.7 (4.75)	0.54
Caspase3	0.15 (0.03)	0.12 (0.03)	0.41
PCNA	98.9 (0.02)	98.3 (0.12)	0.41

Table 8: Table to show percentage expression of conjunctival markers in HCjE-Gi cells of passage 2 and 28. Triplicate samples for each marker within each cohort (passage 2 and passage 28) were analysed by flow cytometry. Similar levels of markers in terms of the percentage of cells detected was apparent between cells of passage 2 and 28 with no differences confirmed by statistical analysis (ANOVA).

3.5 Analysis of conjunctival epithelial phenotype with advancing time on synthetic substrates by flow cytometry

3.5.1 HCjE-Gi cell phenotype with advancing time in culture on synthetic substrates

Almost all HCjE-Gi cells were found to express CK19 (≥96%) across all substrates at 14 and 28 days in culture. No statistically significant differences in CK19 or CK4 expression were observed with respect to advancing time. The highest expression of CK4 was demonstrated on PET and untreated ePTFE substrates, whereby significant post-hoc test differences were found: PET had greater CK4 expression than double side treated ePTFE, and untreated ePTFE had greater CK4 expression than double side treated ePTFE; $p<0.01$ (Figure 50, Table 11). CK7 expression increased with advancing time in culture together with the proportion of cells co-expressing CK7 and UAE-1 lectin across all substrates studied with significant differences demonstrated between the untreated ePTFE and all other substrates studied; $p<0.0001$ (Figures 51 and 55). CK7/CK7+ UAE-1 lectin expression on untreated ePTFE (mean 78%) was more than 3-fold higher than that on double side ammonia plasma treated ePTFE (mean 25%) and more than double that on PET and single side ammonia treated ePTFE (mean 32% and 38% respectively): Figure 55.

UAE-1 lectin expression varied significantly with substrate but not with advancing time: $p=0.001$, $p=0.64$ respectively (Figure 54). After 28 days in culture, highest UAE-1 expression was found on double side treated ePTFE and untreated ePTFE. Significant differences were found in post-hoc tests between untreated ePTFE and both PET membrane and single side ammonia plasma treated ePTFE ($p<0.007$). Significant differences were also demonstrated between double side ammonia plasma treated ePTFE and PET membrane; $p<0.007$ (Figure 54).

MUC5AC detection was low at both day 14 and day 28 on all substrates whereby it represented less than 0.75% of all cells (Figure 53). No statistically significant differences in MUC5AC detection were demonstrated between the substrates studied however expression significantly increased with advancing time in culture overall; $p=0.33$, $p<0.001$ respectively. The highest MUC5AC levels were detected on double and single side ammonia treated ePTFE at day 28, which were almost twice that expressed in PET membrane cultures.

ΔNp63 was expressed in large proportion of cells (≥90%) and this level remained high with advancing time in culture (Figure 56). No significant variation with respect to substrate or advancing time in culture could be demonstrated after Holm-Bonferroni correction: $p=0.096$, $p=0.007$ respectively. In contrast, the ABCG2 expression was lower than ΔNp63 at day 14 and appeared to decline with advancing time in culture, however this was not statistically significant and variance was relatively high (Figure 57). Significantly higher ABCG2 expression was found on double side treated ePTFE than that on single side treated ePTFE and untreated ePTFE after 28 days in culture: $p=0.008$ and $p=0.004$ between double side ammonia plasma treated ePTFE and untreated ePTFE and double side ammonia treated ePTFE and single side ammonia treated ePTFE respectively (Figure 57, Table 11). No significant difference in ABCG2 expression was demonstrated between cultures from double side ammonia plasma treated ePTFE and PET membranes. A significant difference was however demonstrated in the co-expression of ABCG2 and ΔNp63 (Figure 58). The highest ABCG2/ ΔNp63 co-expression was demonstrated on double side treated ePTFE. This was significantly higher than on any other substrate studied; $p<0.01$ in post-hoc tests between double side treated ePTFE and all other substrates studied (Table 11).

PCNA levels did not change significantly with advancing time: $p=0.024$ (Figure 60). No statistically significant differences in PCNA expression were demonstrated between substrates ($p=0.146$), however the lowest levels were found on untreated ePTFE at 14

and 28 days in culture. Caspase-3 expression was relatively low across all substrates at 14 days in culture and did not increase with advancing time overall: p=0.163 (Figure 59). There was, however, an almost 10-fold greater caspase-3 expression at 28 days in culture on untreated ePTFE than any other substrate. Caspase-3 expression was significantly higher on untreated ePTFE than all other test substrates; p<0.0001 (Table 11).

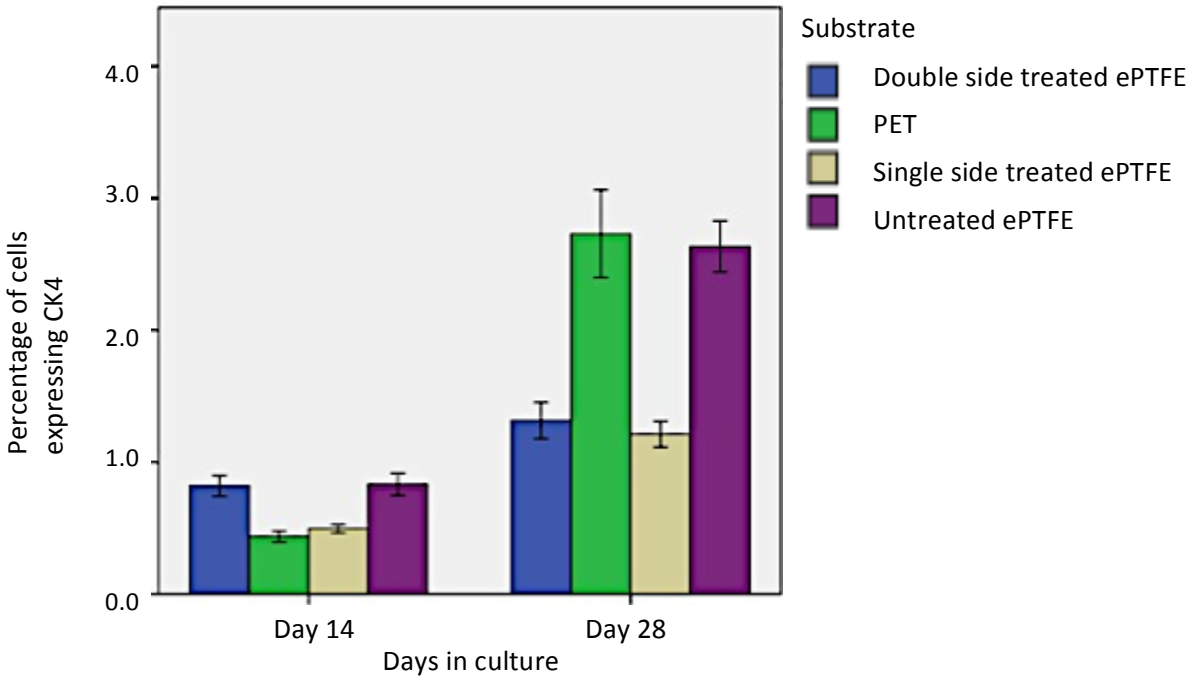

Figure 50: Histogram to show **percentage expression of CK4** on ammonia plasma treated ePTFE, untreated ePTFE and PET after 14 and 28 days in culture. ANCOVA overall model substrates; p<0.0001; time p=0.152. Error bars +/-SD.

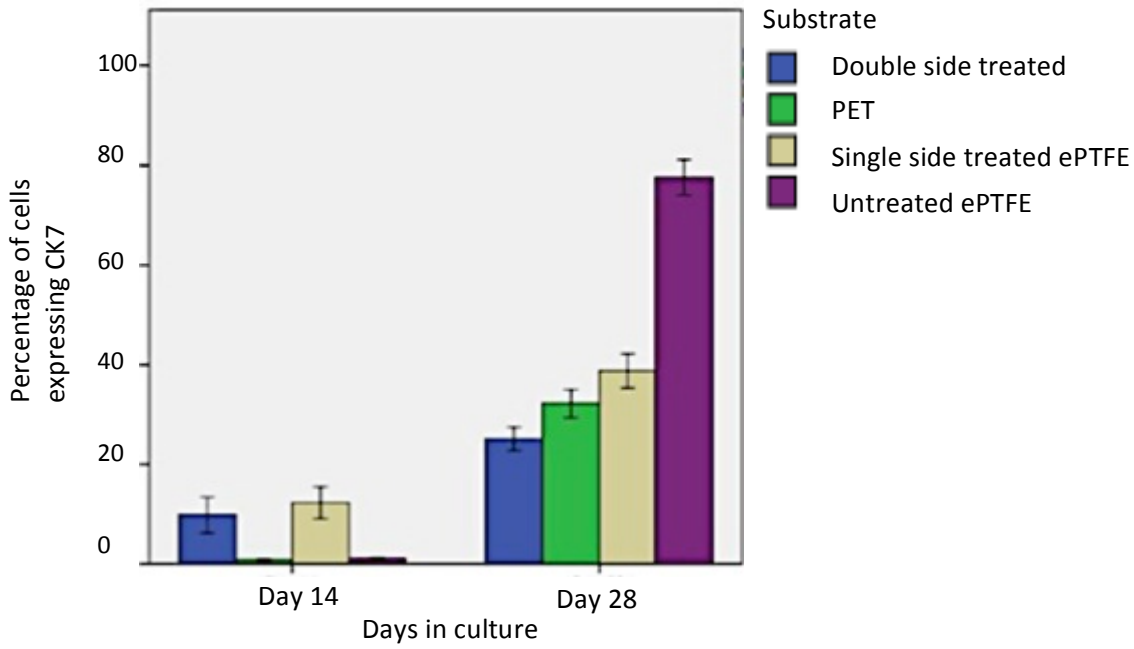

Figure 51: Histogram to show **percentage expression of CK7** on ammonia plasma treated ePTFE, untreated ePTFE and PET after 14 and 28 days in culture. ANCOVA overall model substrates and time; $p<0.001$. Error bars +/-SD.

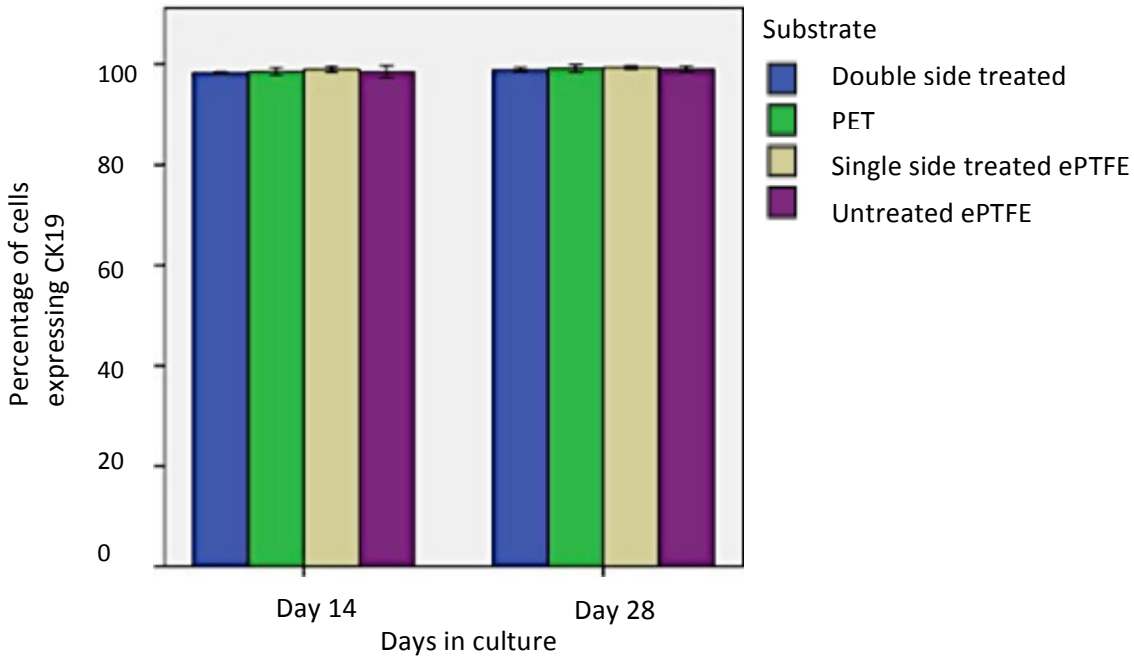

Figure 52: Histogram to show **percentage expression of CK19** on ammonia plasma treated ePTFE, untreated ePTFE and PET after 14 and 28 days in culture. ANCOVA overall model substrates $p=0.975$; time $p=0.88$. Error bars +/-SD.

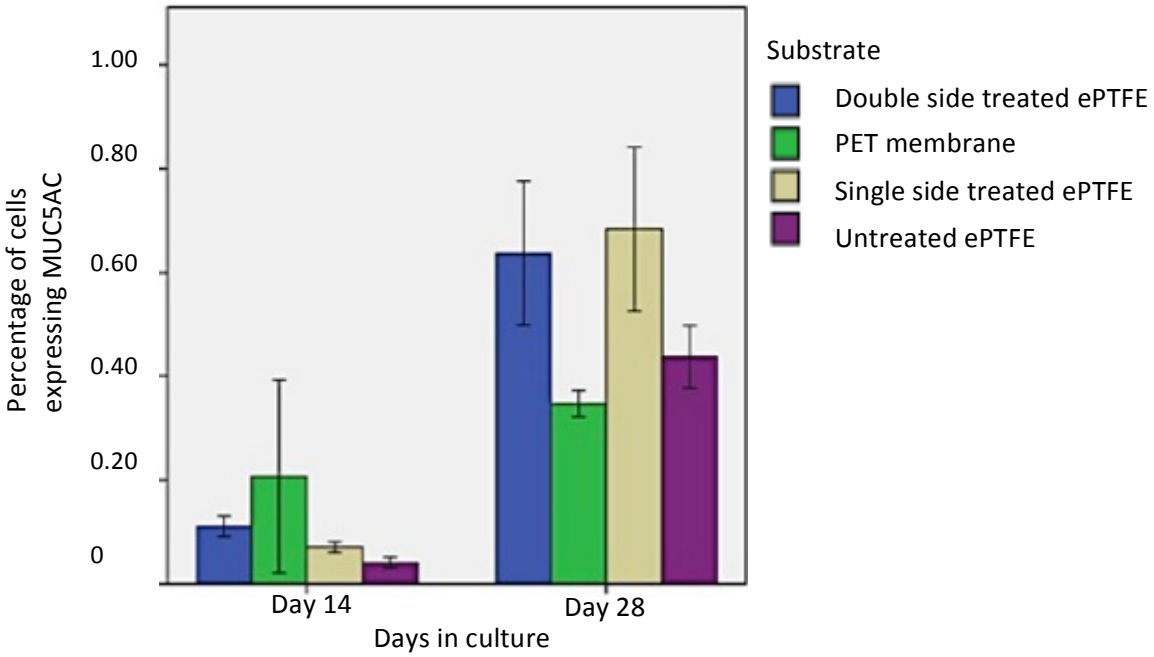

Figure 53: Histogram to show **percentage expression of MUC5AC** on ammonia plasma treated ePTFE, untreated ePTFE and PET after 14 and 28 days in culture. ANCOVA overall model substrate p=0.033; time p<0.0001. Error bars +/-SD.

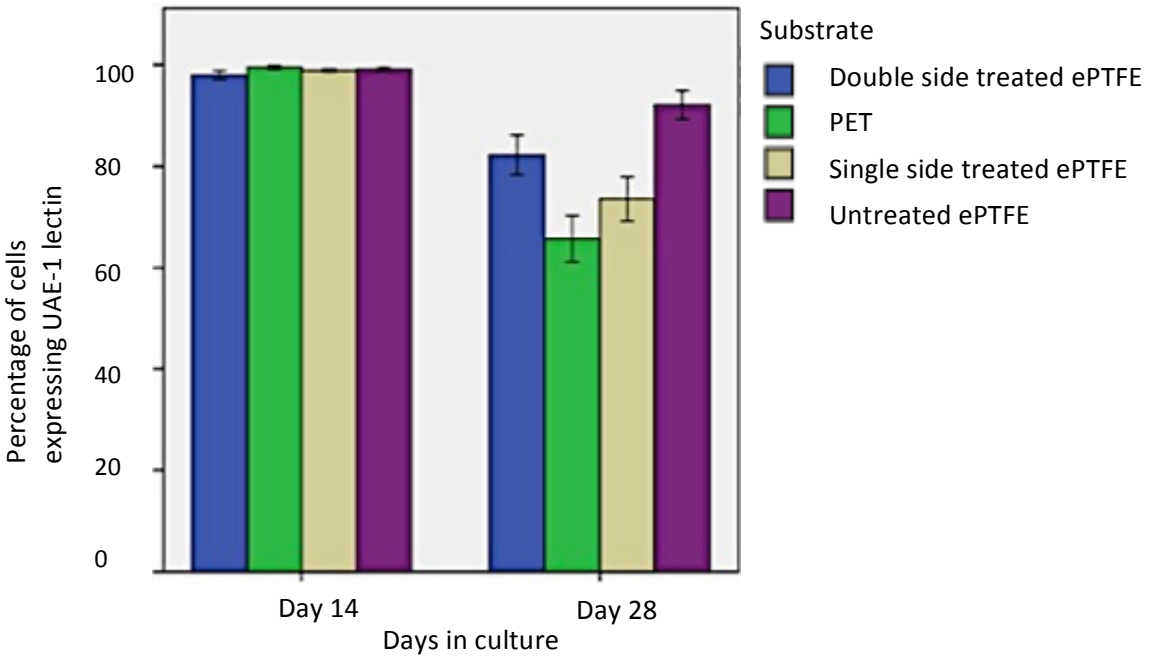

Figure 54: Histogram to show **percentage expression of UAE-1 lectin** on ammonia plasma treated ePTFE, untreated ePTFE and PET after 14 and 28 days in culture. ANCOVA overall model substrate p=0.001; time: p<0.641. Error bars +/-SD.

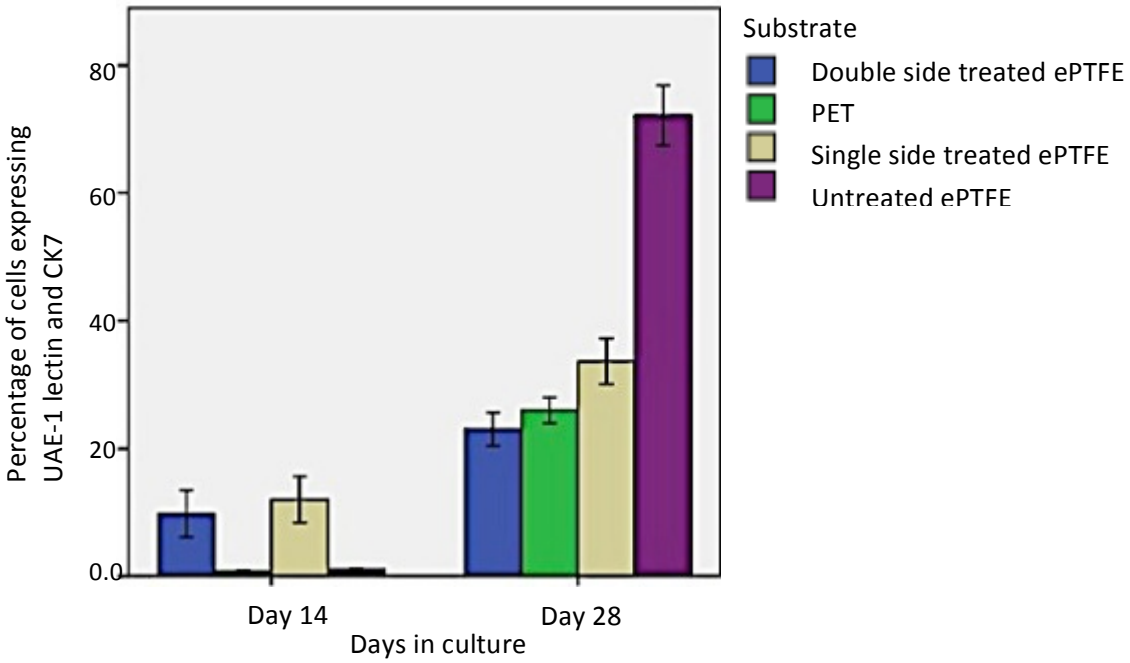

Figure 55: Histogram to show **percentage expression of CK7 and UAE-1 lectin** co-expression on ammonia plasma treated ePTFE, untreated ePTFE and PET after 14 and 28 days in culture. ANCOVA overall model substrate and time point: $p<0.0001$. Error bars +/-SD.

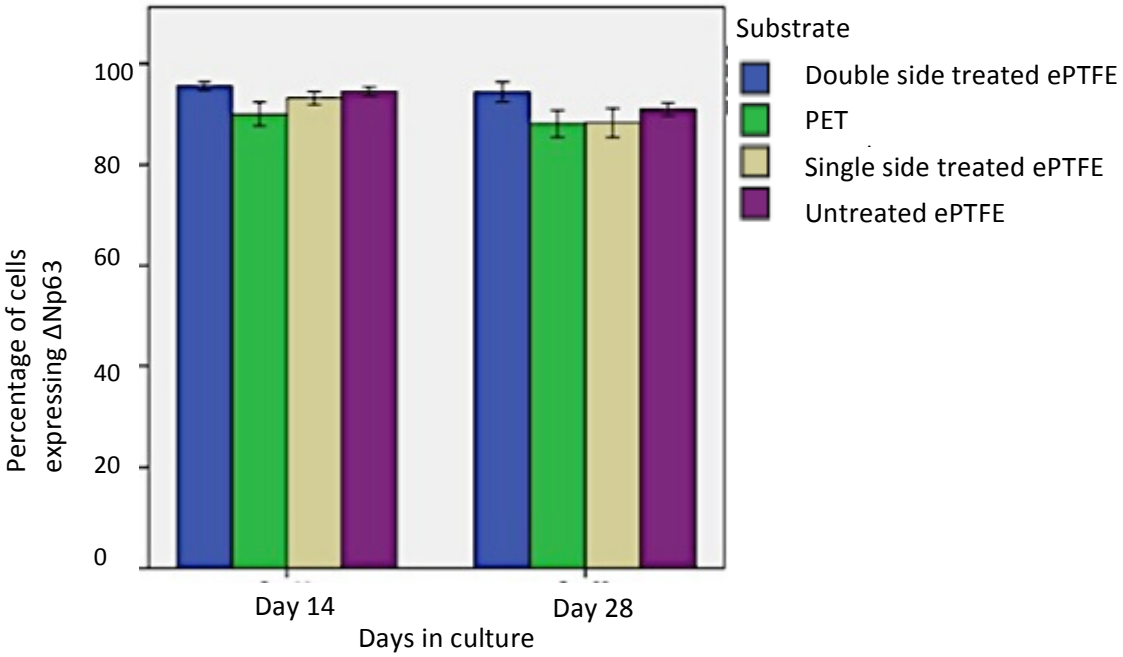

Figure 56: Histogram to show **percentage expression of ΔNp63** on ammonia plasma treated ePTFE, untreated ePTFE and PET after 14 and 28 days in culture. ANCOVA overall model substrates $p=0.007$; time $p=0.096$. Error bars +/-SD.

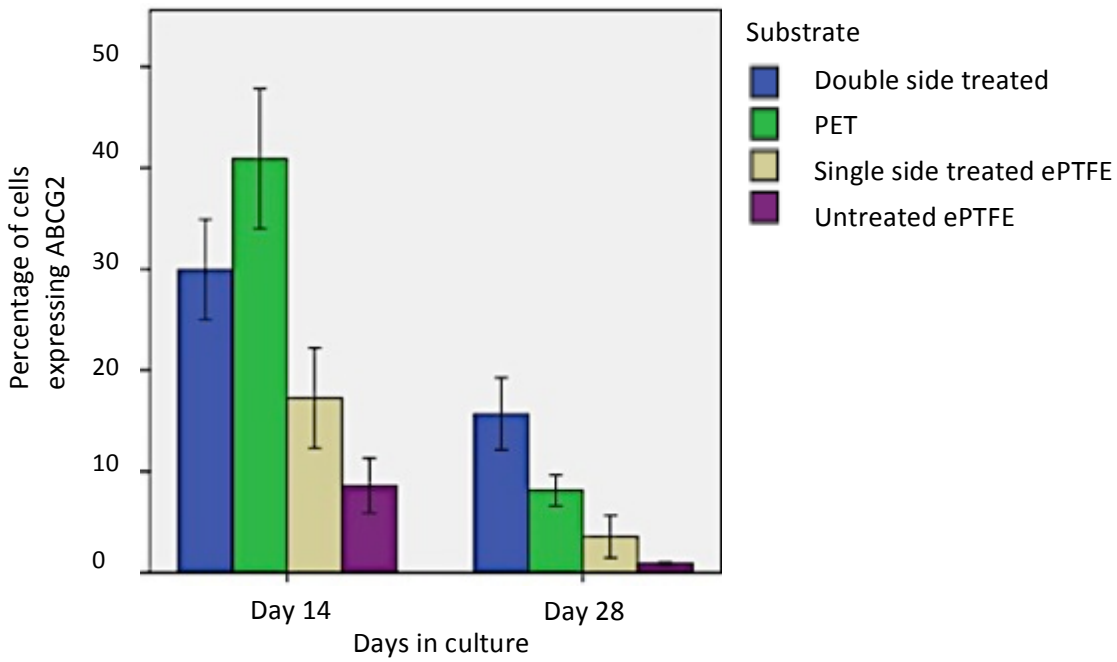

Figure 57: Histogram to show **percentage expression of ABCG2** on ammonia plasma treated ePTFE, untreated ePTFE and PET after 14 and 28 days in culture. ANCOVA overall model substrates p=0.003; time p=0.137. Error bars +/-SD.

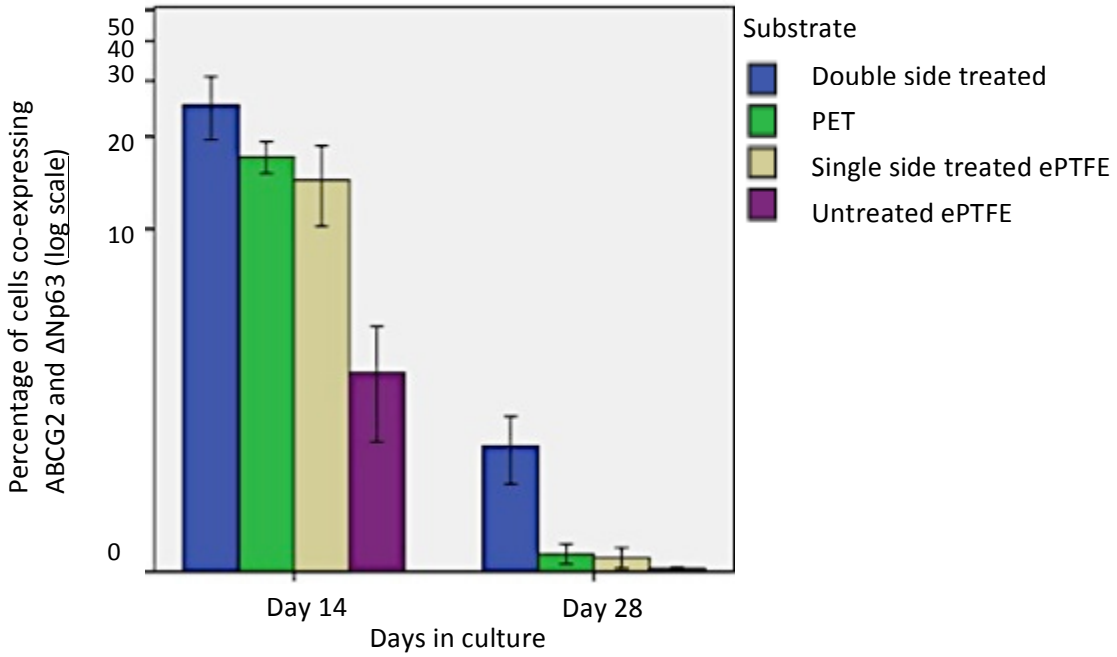

Figure 58: Histogram to show **percentage expression of ABCG2 and ΔNp63** on ammonia plasma treated ePTFE, untreated ePTFE and PET after 14 and 28 days in culture. ANCOVA overall model substrates p=0.001; time p=0.008. Error bars +/-SD.

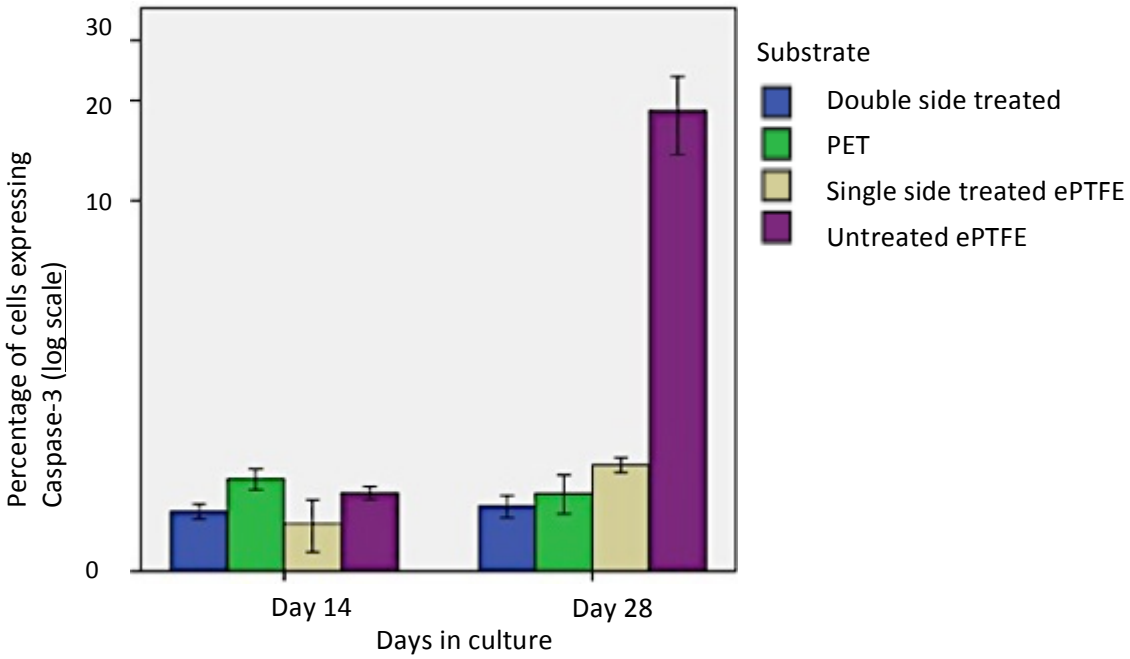

Figure 59: Histogram to show **percentage expression of Caspase-3** on ammonia plasma treated ePTFE, untreated ePTFE and PET after 14 and 28 days in culture. ANCOVA overall model substrates p=<0.0001; time p=0.163. Error bars +/-SD.

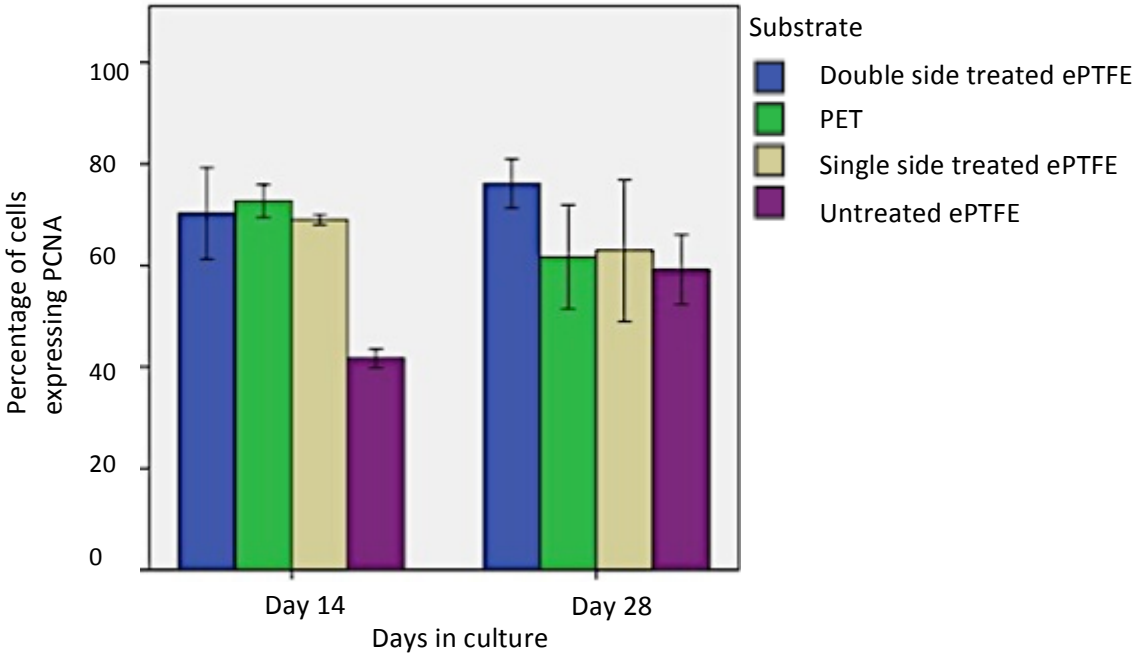

Figure 60: Histogram to show **percentage expression of PCNA** on ammonia plasma treated ePTFE, untreated ePTFE and PET after 14 and 28 days in culture. ANCOVA overall model time p=0.024; substrates p=0.146. Error bars +/-SD.

Marker	P value
CK7	0.0001
CK7/UAE-1 lectin co-expression	0.0001
MUC5AC	0.0001

Table 9: Table of cell markers in which a statistically significant change was demonstrated with advancing time in culture. Raw p values from the ANCOVA are displayed. Only p values statistically significant following correction by Holm-Bonferroni for multiple testing hypotheses are displayed.

Marker	P value
CK7	0.0001
CK7 + UAE-1 lectin	0.0001
UAE-1 lectin	0.001
CK4	0.0001
Caspase-3	0.0001
ABCG2	0.003
ABCG2+ NP63	0.001

Table 10: Table of cell markers in which a statistically significant difference was demonstrated between substrates. Raw p values from the ANCOVA are displayed. Only p values statistically significant following correction by Holm-Bonferroni for multiple testing hypotheses are displayed.

Marker	Post-hoc contrasts; p value and pairs of data
CK7	p<0.0001: U vs. D; U vs. S; U vs. P
CK7 + UAE-1 lectin	p<0.0001; U vs. D, U vs. S, U vs. P
UAE-1 lectin	p<0.007: D vs. P, U vs. S, U vs. P
CK4	p<0.01: D vs. P, D vs. U
Caspase-3	p<0.0001: D vs. U, U vs. P, U vs. S
ABCG2	p=0.008 D vs. U p=0.004 D vs. S
ABCG2+ ΔNp63	p≤0.001 D vs. U, D vs. S, D vs. P

Table 11: Table of cell markers in which a statistically significant difference was demonstrated between substrates: U=untreated ePTFE, D=double side treated ePTFE, S=single side treated ePTFE, P=PET membrane. Raw p values from the ANCOVA post-hoc contrast tests are displayed. Only p values statistically significant following correction by Holm-Bonferroni for multiple testing hypotheses are displayed.

3.5.2 Cell density and morphology of primary cell cultures on double side ammonia plasma treated ePTFE and PET membrane

Primary cells from a single donor (donor 10) were expanded and seeded at $1x10^5/cm^2$ on ammonia plasma treated ePTFE (double side treated) and PET membrane (positive control) in triplicate. The cell density expanded up to 14 days in culture, after which a decline occurred (Figure 61). At all time points studied, the cell density on PET membrane was more than double that found on ePTFE. This was in keeping with the qualitative appearance of nuclear staining density observed in DAPI stained samples (Figure 62). Morphologically however, the cells appeared larger in cultures developed on ePTFE than PET membrane at day 14 giving the impression of a similar degree of cell confluence despite a lower cell density on the ePTFE substrate (Figures 61 and 62). Other notable morphological features include greater variation in nuclear size and shape in cells developed on ePTFE substrate in comparison those on PET membranes at

day 14. F-actin staining of cells on both substrates demonstrated that cells appeared more elongated with cell processes visible on day 14 which were no longer present at day 28 when cells appeared sparse with a more 'rounded' appearance on both substrates.

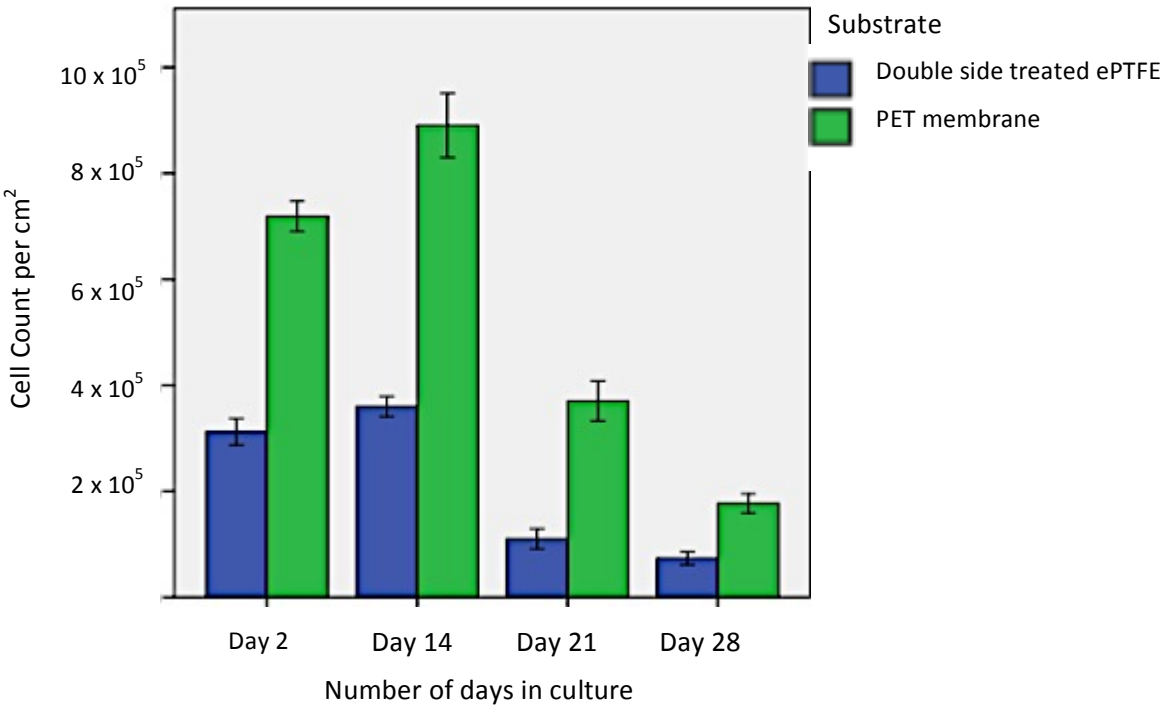

Figure 61: Histogram to show number of cells per cm^2 with advancing time in culture on double side ammonia plasma treated ePTFE (both sides exposed to plasma) and PET membrane. Primary cells used in this experiment were from a single donor and were seeded at $1x10^5/cm^2$. Scale bars +/- SD.

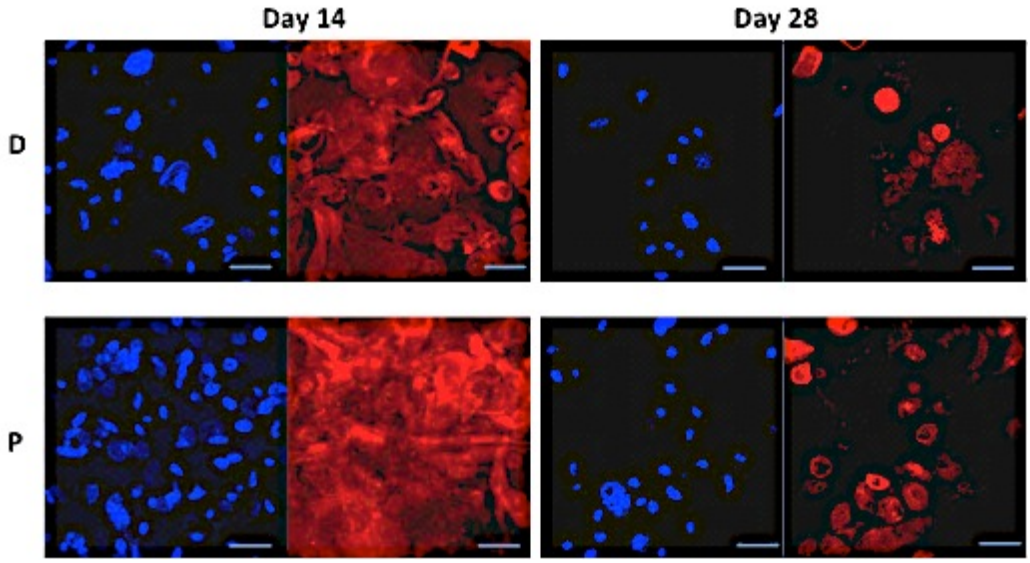

Figure 62: Representative photomicrographs of primary conjunctival cells on double side ammonia plasma treated ePTFE (D) and PET (P) membrane at after 14 and 28 days in culture. Scale bars 50µM. Phalloidin (f-actin staining): red. DAPI (nuclear staining): blue.

3.5.3 Phenotype of primary cells expanded on double side plasma treated ePTFE and PET membrane by flow cytometry

The conjunctival epithelial cells used in this experiment were derived from explants from three separate tissue donors (tissue donors 4, 8 and 12: Table 7). The majority of cells (≥97%) expressed cytokeratin 19 (Figure 63). No significant effect was found either with respect to time in culture (day 14 versus day 28) or the substrate on which cells were grown (double side ammonia treated ePTFE or PET substrate); p=0.079, p=0.123 respectively. Similarly, no statistically significant differences could be found in CK7, CK4, UAE-1 lectin or co-expression of CK7/UAE-1 lectin with respect to advancing time or substrate (Figures 64-67). The histograms of CK7 expression alone and CK7 and UAE-1 lectin co-expression were quantitatively similar (Figures 65 and 67). UAE-1 lectin expression alone, however, was greater than CK7 expression alone (Figure 66). The expression of both MUC5AC and UAE-1 lectin were on average higher at 28 days than

14 days in culture, however, this was not statistically significant; p=0.12, p=0.51 respectively (Figures 66 and 68). No significant differences could be could be demonstrated in MUC5AC or UAE-1 lectin expression between cells cultured on PET and ePTFE substrates; p=0.46, p=0.26 respectively.

No statistically significant differences in ΔNp63, ABGC2 expression or co-expression of ΔNp63 and ABGC2 were demonstrated with advancing time in culture or between substrates (Figures 69-71). The proportion of cells expressing either ABCG2 or ΔNp63, however, less than halved between day 14 and day 28, and the proportion of cells co-expressing ABCG2 and ΔNp63 also diminished markedly. It should be noted that variance in the test samples was relatively high. Similarly, caspase-3 expression appeared to more than double with advancing time and higher levels were found on ammonia plasma treated ePTFE (Figure 72). The variance, again, was high and therefore no statistically significant differences with respect to advancing time in culture or substrate were demonstrated. PCNA expression declined with advancing time in culture and was found to be statistically significant following Holm-Bonferroni correction; p=0.003 (Figure 73). Levels of PCNA expression were similar between double side ammonia plasma treated ePTFE and PET membrane.

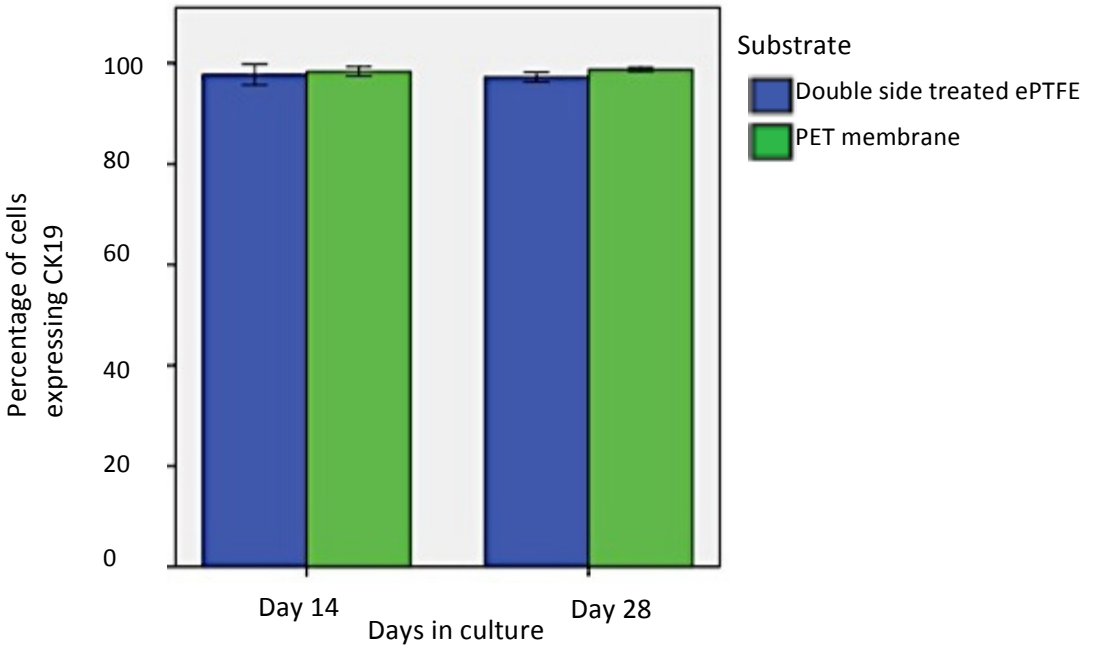

Figure 63: Histogram to show **percentage expression of CK19** in primary cells cultured on double side ammonia plasma treated ePTFE and PET membrane after 14 and 28 days. ANCOVA time p=0.079; substrate p=0.123. Error bars +/-SD.

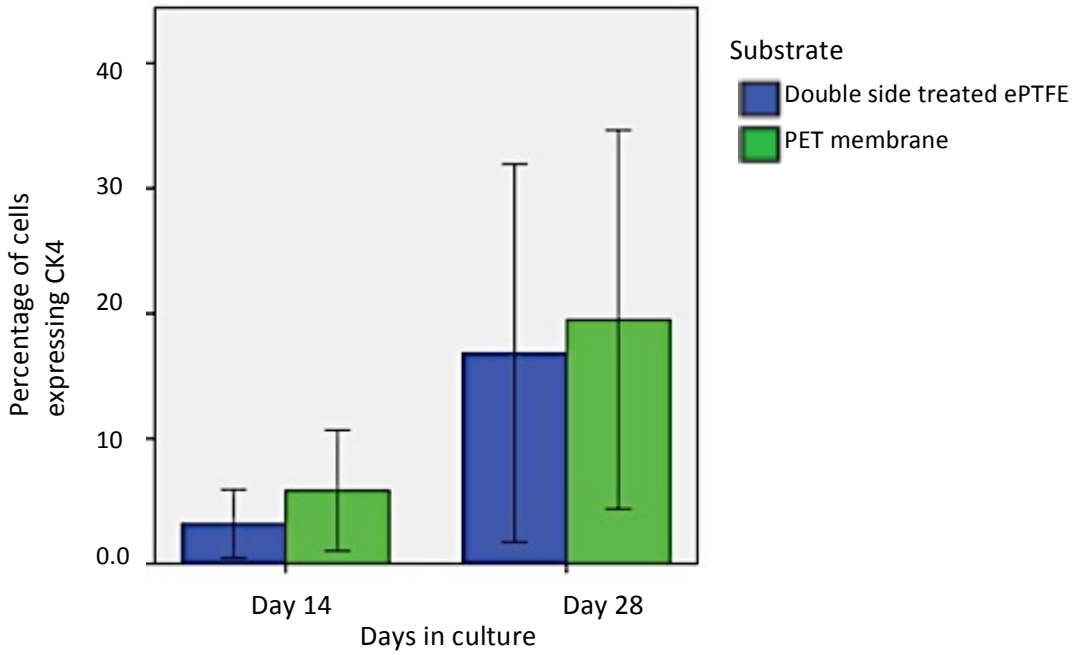

Figure 64: Histogram to show **percentage expression of CK4** in primary cells cultured on double side ammonia plasma treated ePTFE and PET membrane after 14 and 28 days. ANCOVA time 0.52; substrate 0.753. Error bars +/-SD.

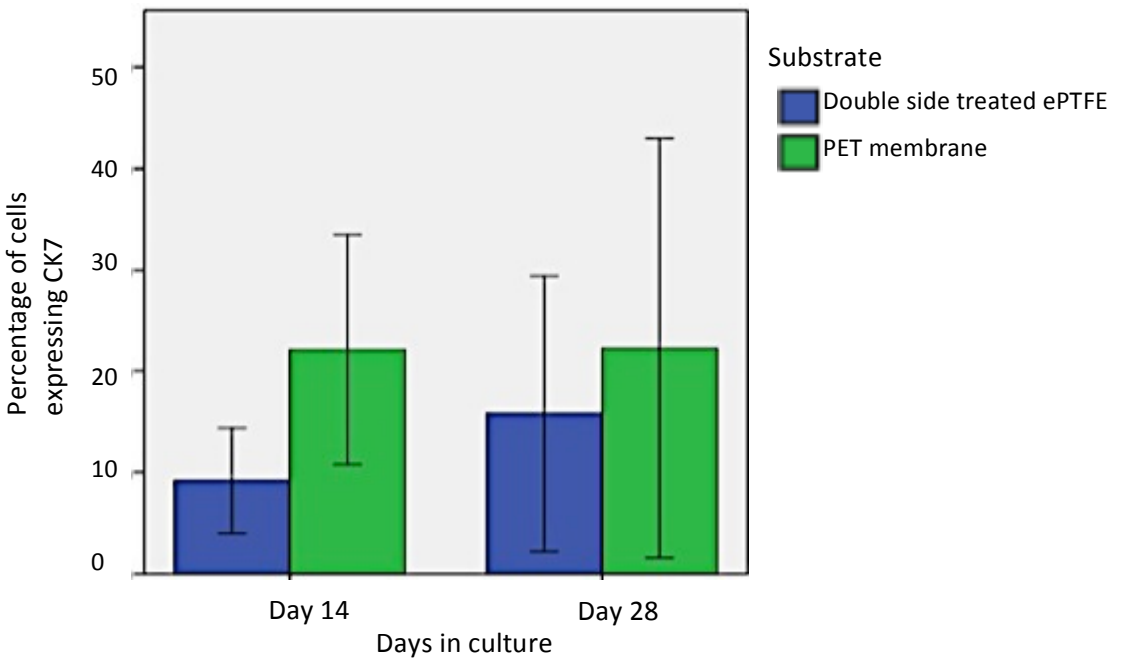

Figure 65: Histogram to show **percentage expression of CK7** in primary cells cultured on double side ammonia plasma treated ePTFE and PET membrane after 14 and 28 days. ANCOVA time 0.647; substrate p=0.25. Error bars +/-SD. Error bars +/-SD.

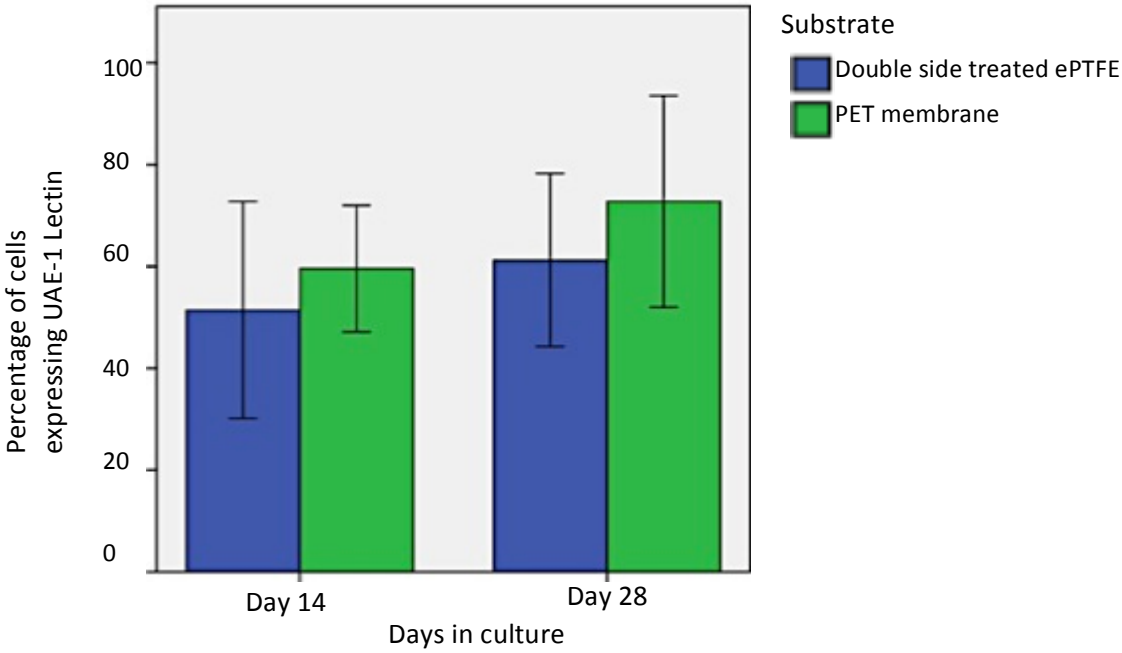

Figure 66: Histogram to show **percentage expression of UAE-1 lectin** in primary cells cultured on double side ammonia plasma treated ePTFE and PET membrane after 14 and 28 days. ANCOVA time 0.39; substrate p=0.712. Error bars +/-SD.

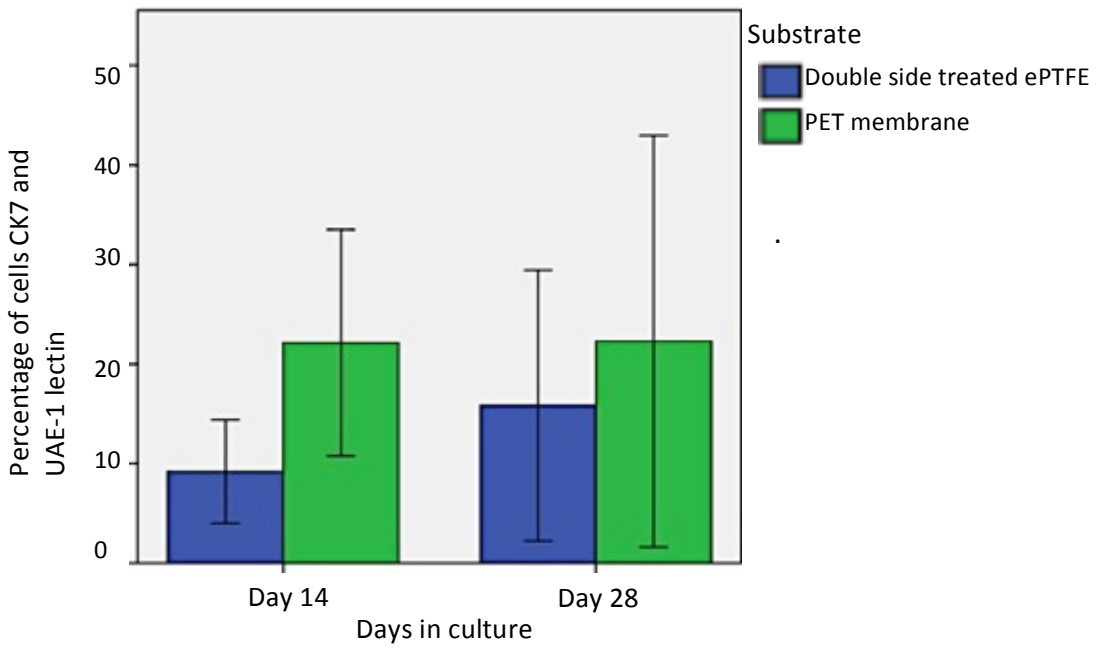

Figure 67: Histogram to show **percentage expression of UAE-1 lectin and CK7** in primary cells cultured on double side ammonia plasma treated ePTFE and PET membrane after 14 and 28 days. ANCOVA time p=0.505; substrate p=0.263. Error bars +/-SD.

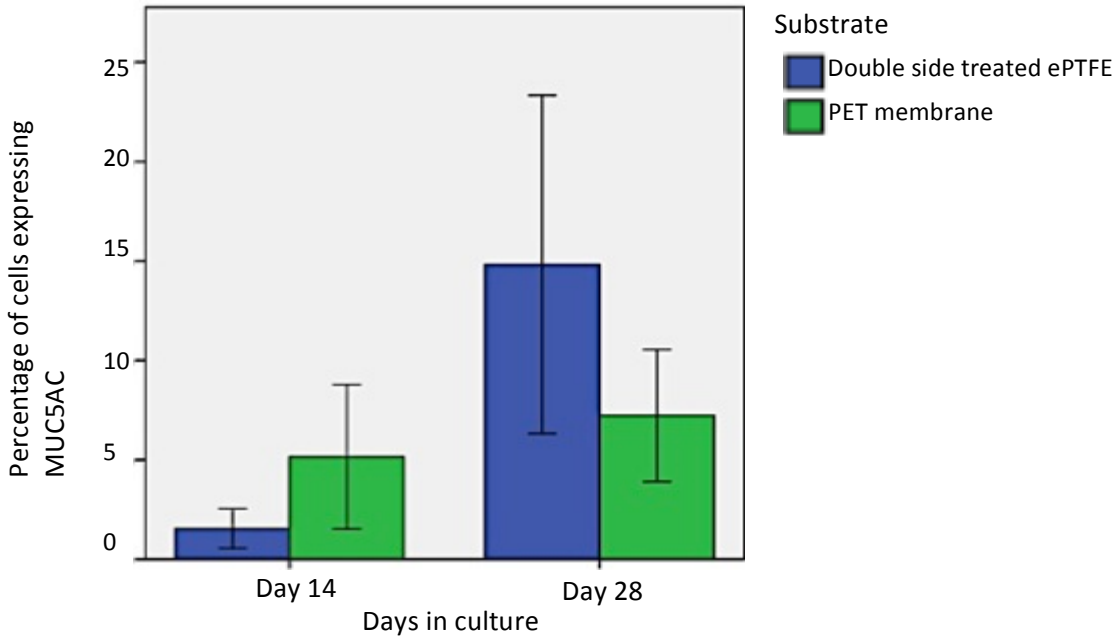

Figure 68: Histogram to show **percentage expression of MUC5AC** in primary cells cultured on double side ammonia plasma treated ePTFE and PET membrane after 14 and 28 days. ANCOVA time p=0.124; substrate p=0.456. Error bars +/-SD.

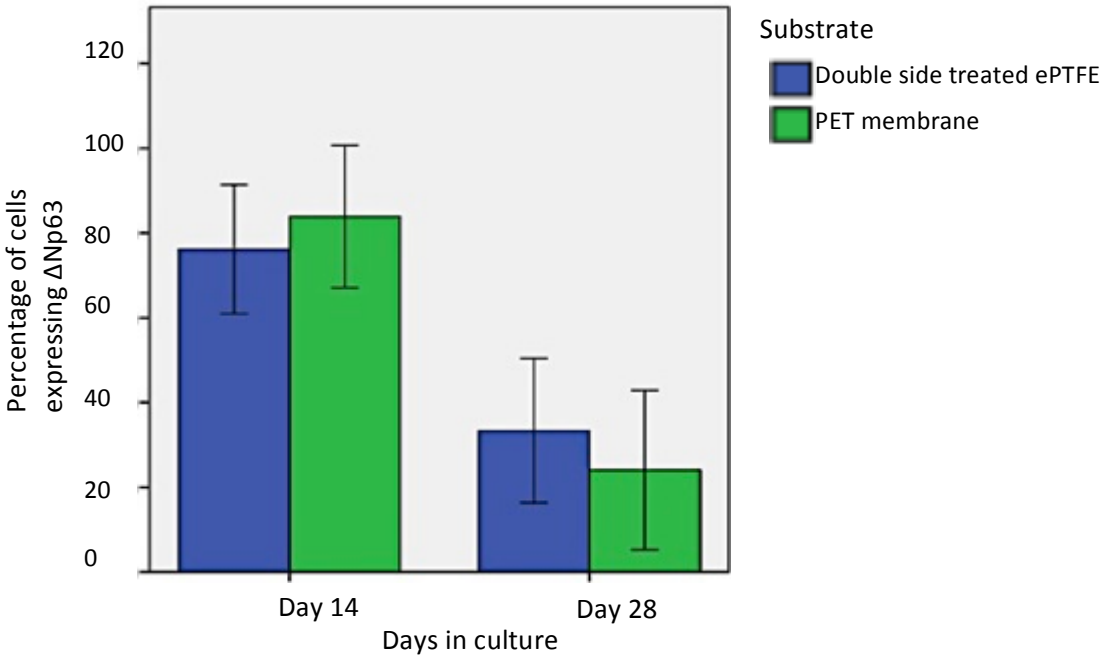

Figure 69: Histogram to show **percentage expression of ΔNp63** in primary cells cultured on double side ammonia plasma treated ePTFE and PET membrane after 14 and 28 days. ANCOVA time p=0.945; substrate 0.537. Error bars +/-SD.

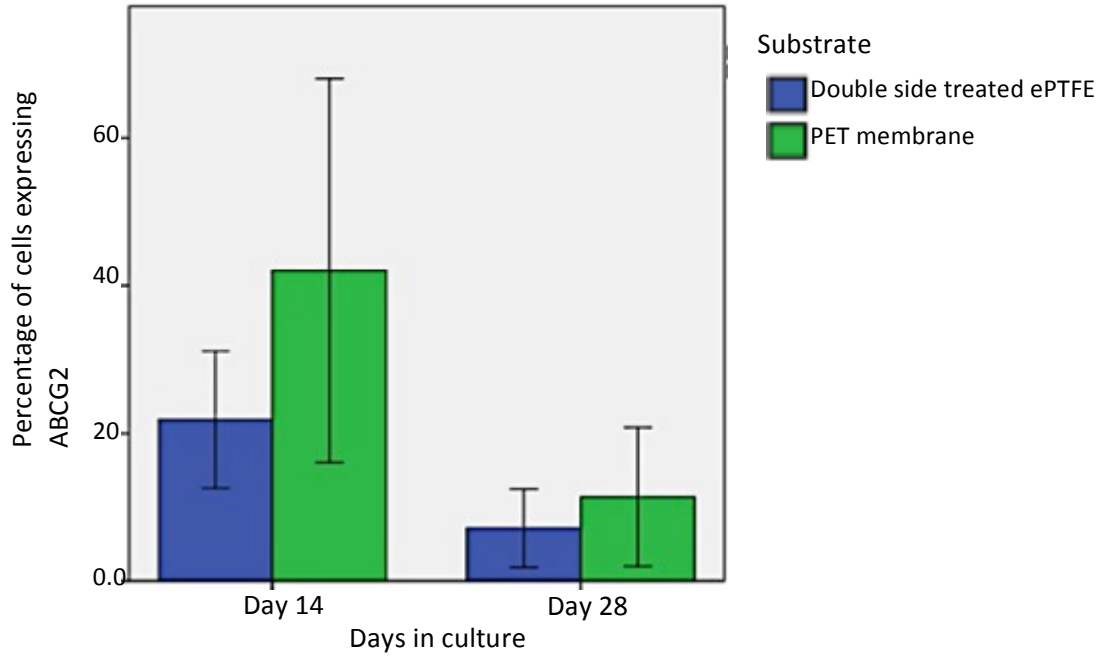

Figure 70: Histogram to show **percentage expression of ABCG2** in primary cells cultured on double side ammonia plasma treated ePTFE and PET membrane after 14 and 28 days. ANCOVA time p=0.753; substrate p=0.611. Error bars +/-SD.

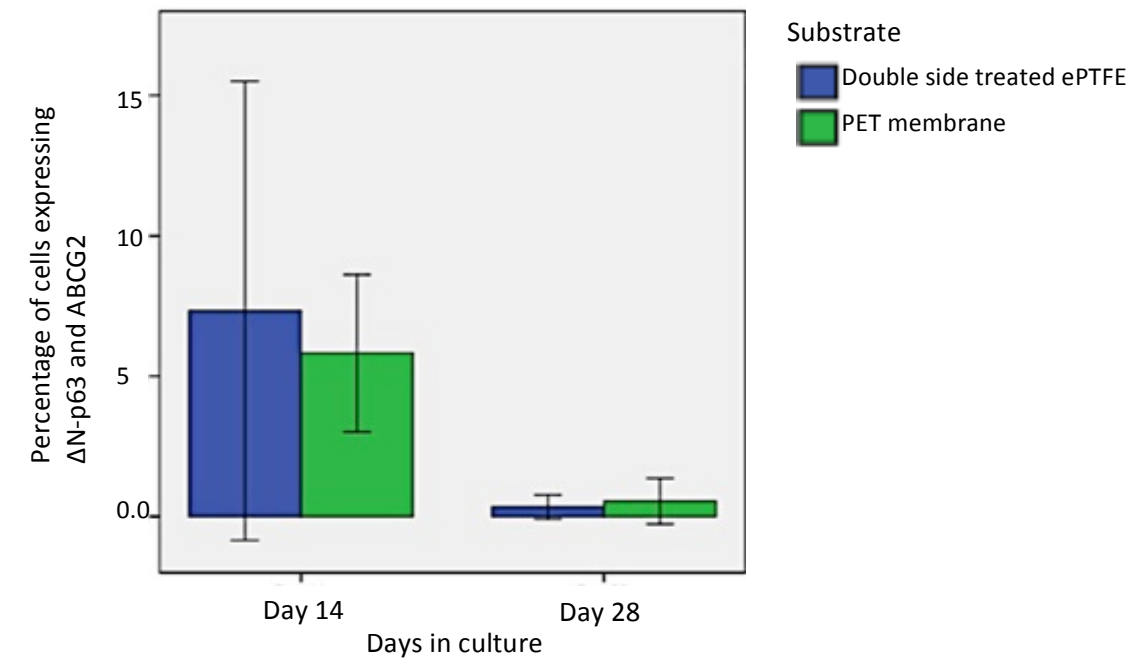

Figure 71: Histogram to show **percentage expression of ΔNp63 and ABCG2** in primary cells cultured on double side ammonia plasma treated ePTFE and PET membrane after 14 and 28 days. ANCOVA time p=0.328; substrate p=0.787. Error bars +/-SD.

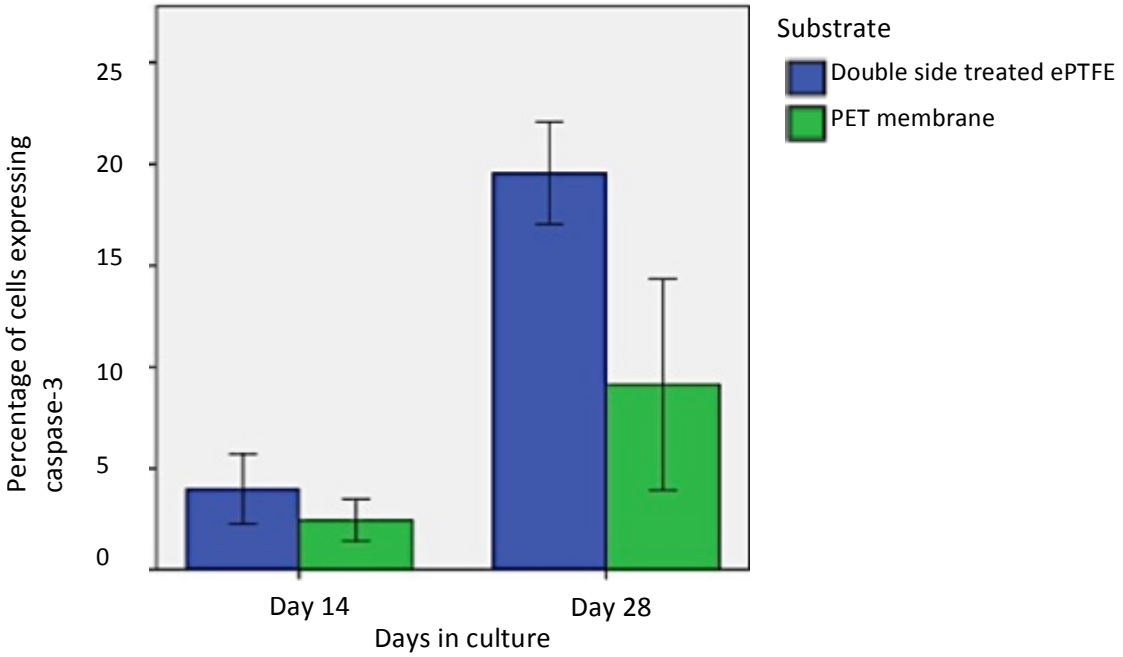

Figure 72: Histogram to show **percentage expression of caspase-3** in primary cells cultured on double side ammonia plasma treated ePTFE and PET membrane after 14 and 28 days. ANCOVA time p=0.138; substrate p=0.134. Error bars +/-SD.

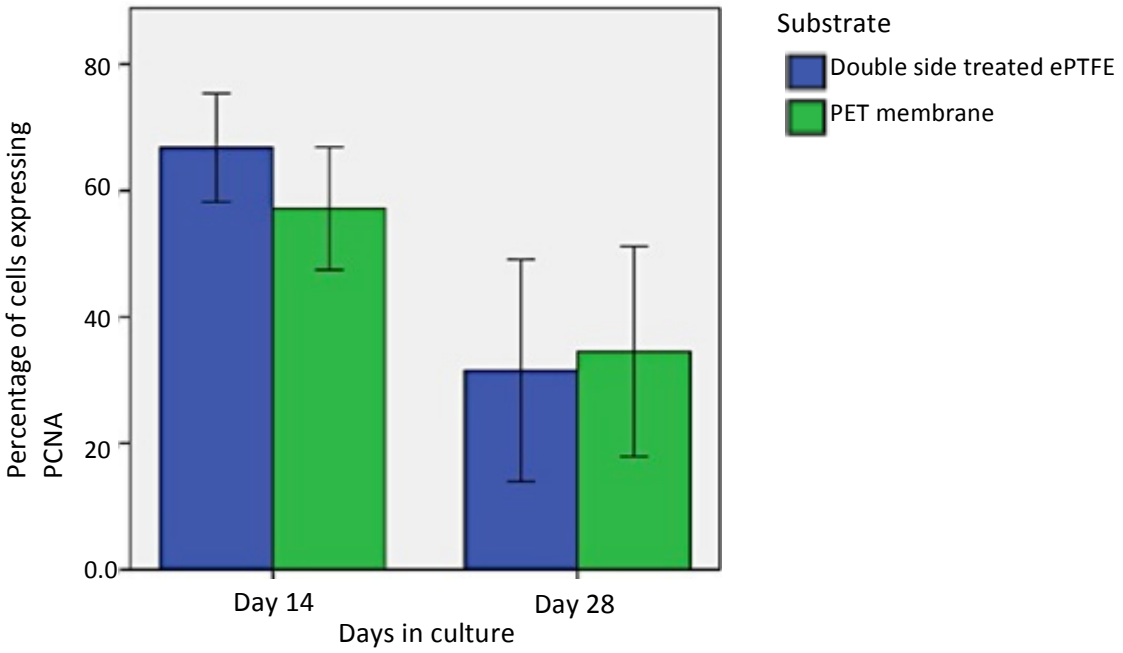

Figure 73: Histogram to show **percentage expression of PCNA** in primary cells cultured on double side ammonia plasma treated ePTFE and PET membrane after 14 and 28 days. ANCOVA time p=0.003; substrate p=0.04. Error bars +/-SD.

3.6 Decellularisation of human conjunctiva and its characterisation

3.6.1 DNA quantification of decellularised conjunctiva

A commercially available kit was used to degrade conjunctival tissue and isolate double stranded DNA so that it was present in solution for quantification with a fluorescent nucleic acid stain. Calf thymus DNA standards were used in known serial dilutions to enable the acquisition of a standard curve (Figure 74). The standard curve displays the relationship between the measured absorbance values and known concentrations of DNA. This enabled calculation of the gradient and intercept from the equation **y=mx+c** so that DNA could be quantified from each test sample from the measured absorbance value.

The effective decellularisation of tissues was demonstrated in all treatment groups defined by SDS dilution in the decellularisation process ($p<0.001$). No difference could be demonstrated between SDS treatment groups in Bonferroni post-hoc tests ($p>0.1$) indicating there was no difference in efficacy with variation in dilution of SDS (Table 12). The reproducibility of decellularisation using the 0.05% SDS (w/v) concentration ($p<0.001$) was confirmed by no significant difference in DNA levels detected between tissues obtained from 3 separate donors (Table 13). In all treatment groups, 98.9% (mean 99.1%) or greater DNA removal was achieved. Effective decellularisation was also indicated by the absence of fluorescent nuclear staining, otherwise detectable by DAPI (4', 6-diamidino-2-phenylindole, dihydrochloride) in decellularised tissue (Figure 75). In contrast, abundant blue fluorescent staining of nuclei was demonstrated in the cellular (control) tissue samples.

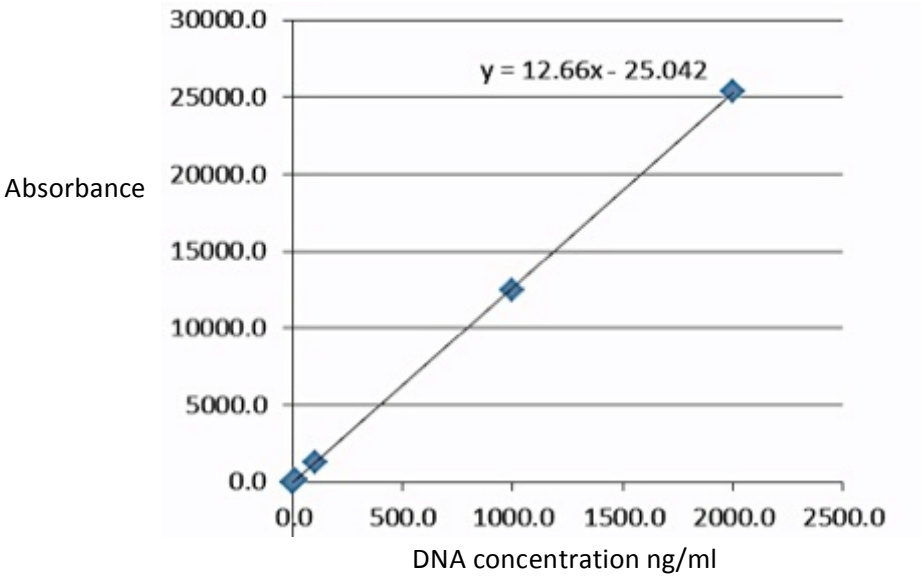

Figure 74: Standard curve of fluorescence absorbance values with increasing DNA concentration in control samples (known dilutions of calf thymus DNA). The standard curve shown enabled calculation of the gradient and y intercept in the equation y=mx+c to determine the DNA content in experimental samples.

Treatment group	DNA ng/mg (SD)	Percentage DNA removal
Cellular control	54.5 (10.4)	-
0.05%	0.4 (0.2)	99.3
0.1%	0.2 (0.1)	99.7
0.5% SDS	0.3 (0.3)	99.4

Table 12: Table to show DNA content of cellular tissues and decellularised tissues using SDS of varying concentration. The overall ANOVA model was significant; $p<0.001$. Data was log transformed to enable parametric data analysis and ANOVA model was satisfied following Levene's test of equality of variance ($p=0.1$). Bonferroni post hoc tests between 0.05%/0.1/0.5% SDS (w/v) treatment groups; $p\geq0.1$.

Tissue	DNA ng/ml (SD)	Percentage DNA removal
Cellular control	42.3 (7.4)	-
Donor a	0.4 (0.2)	98.9
Donor b	0.3 (0.1)	99.2
Donor c	0.3 (0.1)	99.3

Table 13: Table to show DNA content of cellular tissues and donor tissues decellularised with 0.05% SDS (w/v). Overall ANOVA model was significant $p<0.001$. Data log was transformed to enable parametric data analysis and ANOVA model satisfied following Levene's test of equality of variance ($p=0.28$). Bonferroni post hoc tests between donor a/b/c; $p\geq0.1$.

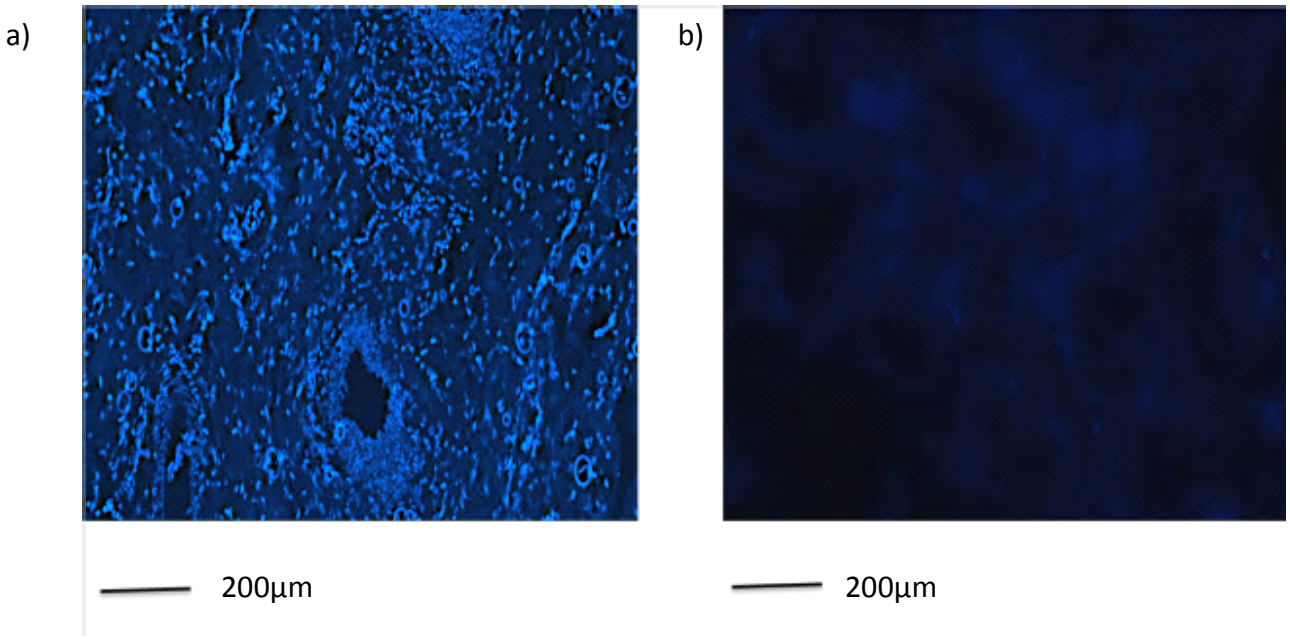

Figure 75: Representative photomicrographs of deparrafinised tissue sections stained with DAPI. Bright fluorescent blue staining indicates the presence of DNA/nuclei a) cellular conjunctival cellular tissue: b) conjunctival tissue decellularised with 0.05% SDS (w/v).

3.6.2 Contact cytotoxicity of decellularised conjunctival tissue

Photomicrographs taken of fixed Giemsa stained cultures demonstrated both HCjE-Gi cells and primary human skin fibroblasts were present in close proximity, seen within and around decellularised tissue in the absence of a zone of inhibition or any cellular debris that would have indicated the presence of non-viable cells (Figure 76). In contrast, cellular debris indicating non-viable cells were demonstrated surrounding the cyanoacrylate glue sample that served the role of a positive (cytotoxic) control in this experiment. A large zone of inhibition was found when primary human fibroblasts were cultured with cyanoacrylate glue (Figure 76).

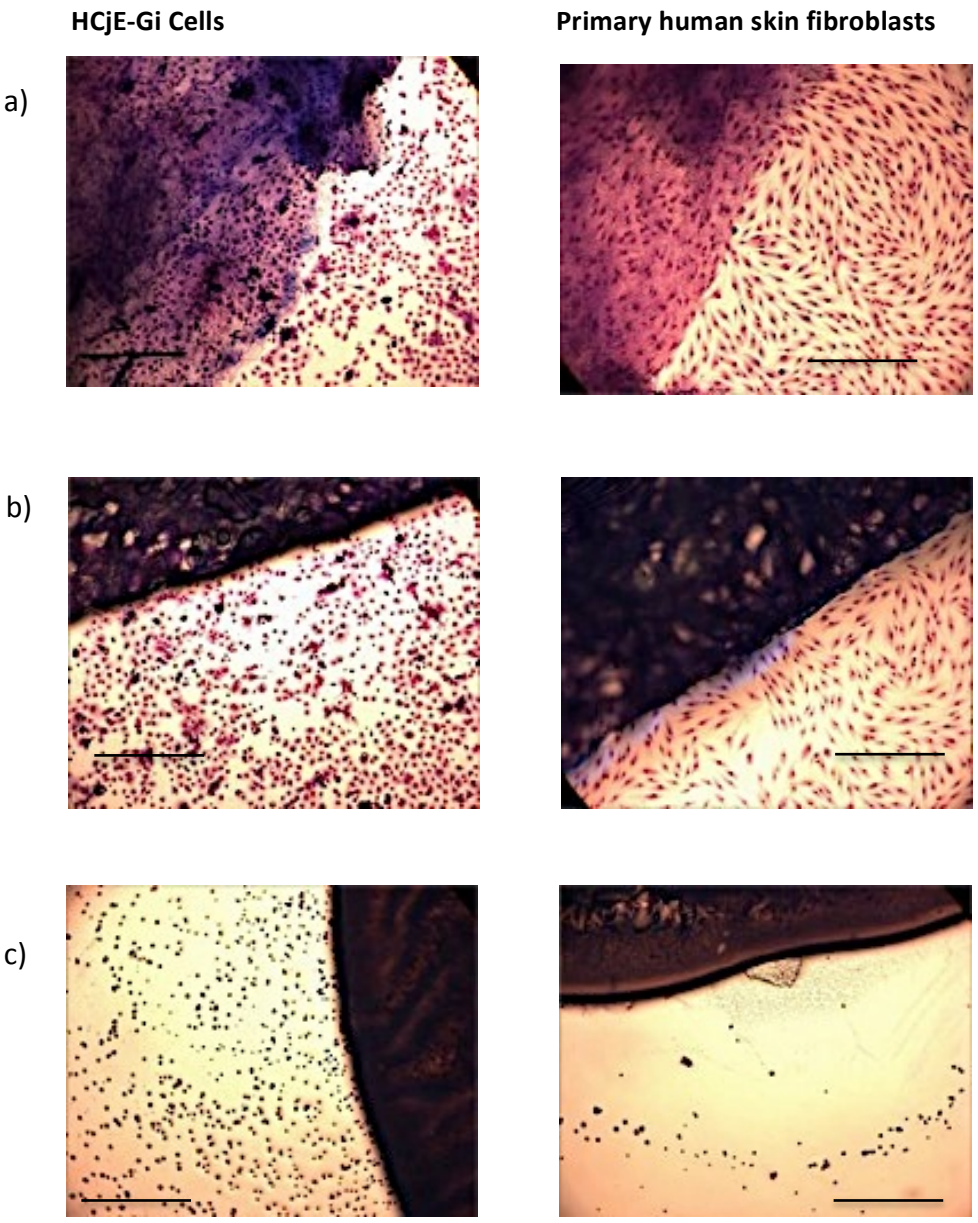

Figure 76: Representative photomicrographs of fixed Giemsa stained cells from a human conjunctival cell line (HCjE-Gi cells) and primary human skin fibroblasts in culture with decellularised conjunctiva, Steri-strips™ and cyanoacrylate glue after 48 hours. a) Decellularised conjunctiva with cells seen in contact with tissue b) Steri-strips™, experimental negative control known not to exhibit cytotoxicity, seen here with cells visible in contact c) cyanoacrylate glue, experimental positive control showing cytotoxicity with cellular debris of HCjE-Gi cells surround it and a large zone on inhibition apparent with cellular debris. Scale bars 200µm.

3.6.3 Tensile strength testing

The tensile strength of cellular and decellularised conjunctiva were tested in comparison to ePTFE and cellular and decellularised amniotic membrane (Table 14). The mean ultimate tensile stress values were greatest for ePTFE; however, there was no significant difference between ePTFE and cellular or decellularised amniotic membrane. The ultimate tensile strength was least for cellular and decellularised conjunctiva and significant differences were demonstrated between: conjunctiva and amniotic membrane ($p<0.0001$); and conjunctiva and ePTFE ($p=0.01$).

Decellularised amniotic membrane had the greatest Young's modulus (12.0 MPa), which was more than 3-fold higher than ePTFE and decellularised conjunctiva, indicating greater stiffness. Young's modulus was similar between ePTFE and conjunctiva: 2.7 and 3.0 MPa respectively ($p=1$). Marked variance in conjunctival and amniotic membrane tensile stress data was demonstrated by high standard deviation values in all measured parameters. No significant difference in ultimate tensile stress or Young's modulus could be demonstrated between cellular and decellularised conjunctiva or between cellular and decellularised amniotic membrane, which suggests no change in stiffness following decellularisation (Figure 77).

Tissue	Ultimate tensile stress MPa (+/-SD)	Young's modulus MPa (+/-SD)
ePTFE	1.2 (0.01)	2.7 (0.2)
Cellular conjunctiva	0.7 (0.5)	3.9 (5.6)
Decellularised conjunctiva	0.5 (0.9)	3.0 (3.6)
Cellular amniotic membrane	1.7 (1.1)	11.5 (6.1)
Decellularised amnion	1.8 (0.7)	12.0 (5.1)

Table 14: Table of results from tensile strength testing of ePTFE, cellular and decellularised conjunctiva and amniotic membrane. Data shown in this table was normalised by log transformation prior to ANOVA analysis. Overall ANOVA model for both ultimate tensile strength and Young's modulus between tissues; $p<0.0001$. No significant differences were found in both parameters studied between cellular and decellularised tissues; $p=0.354$ ultimate tensile strength; $p=0.561$ Young's modulus.

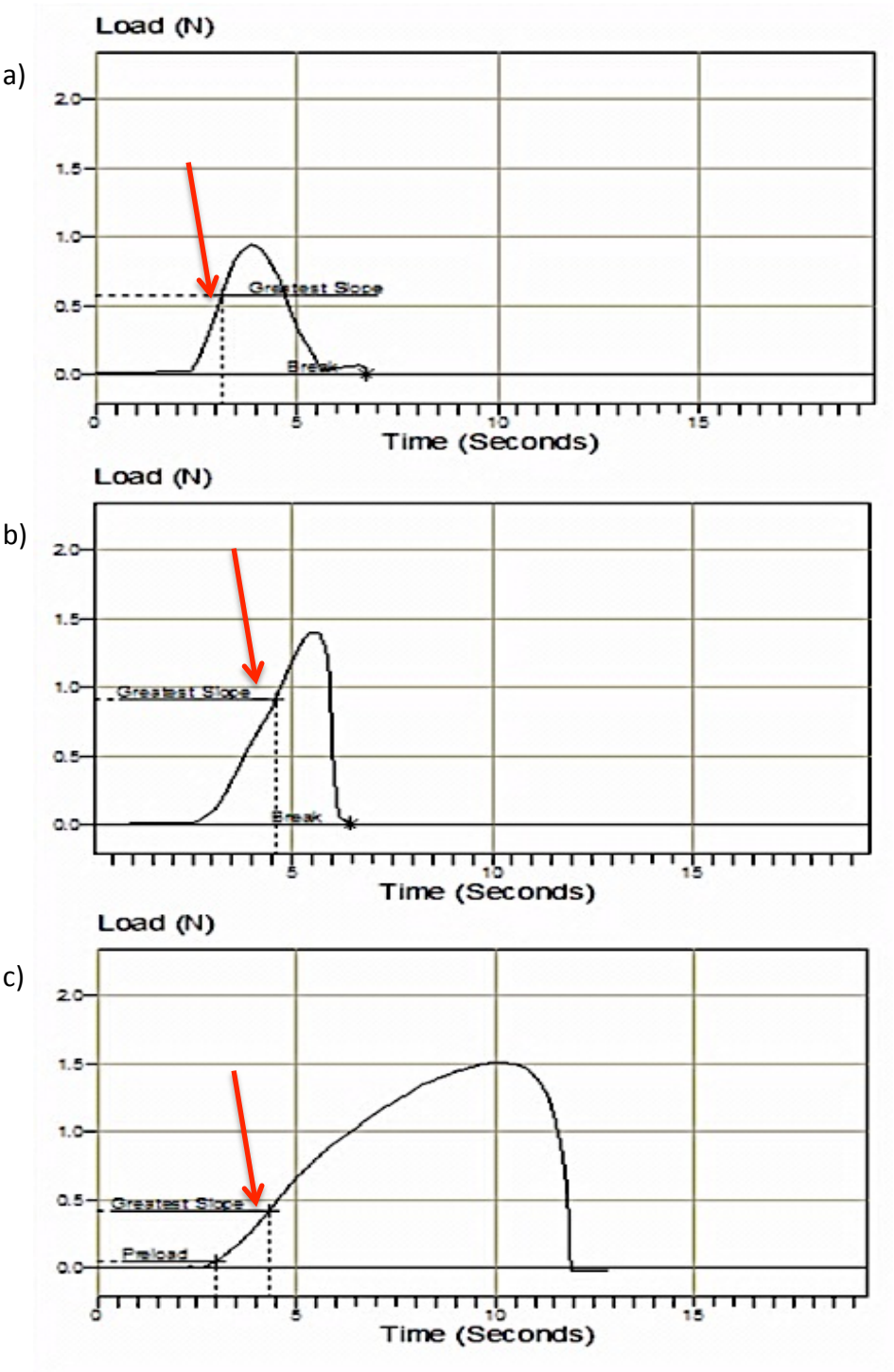

Figure 77: Representative histograms of load (N) against advancing time (seconds) during the tensile strength test: a) conjunctiva b) amniotic membrane c) ePTFE. Each histogram also demonstrates the section of the curve from which the gradient for the greatest slope was determined (see 'Greatest slope' marked on each graph by the red arrows).

3.6.4 Collagen Denaturation Assay

A standard curve from the measured absorbance values of known concentrations of a hydroxyproline standard enabled the determination of the gradient and intercept from the equation **y=mx+c** (Figure 78). These values allowed hydroxyproline quantification from test samples. Minimal collagen denaturation was observed in all tissue samples studied demonstrated by low hydroxyproline values (range 3.12-6.24 hydroxyproline ng/mg). The negative control values were 2.82 hydroxyproline ng/mg. No difference in hydroxyproline was found between paired samples of cellular and decellularised conjunctival tissue suggesting collagen was not denatured by decellularisation (p=0.74, paired t-test).

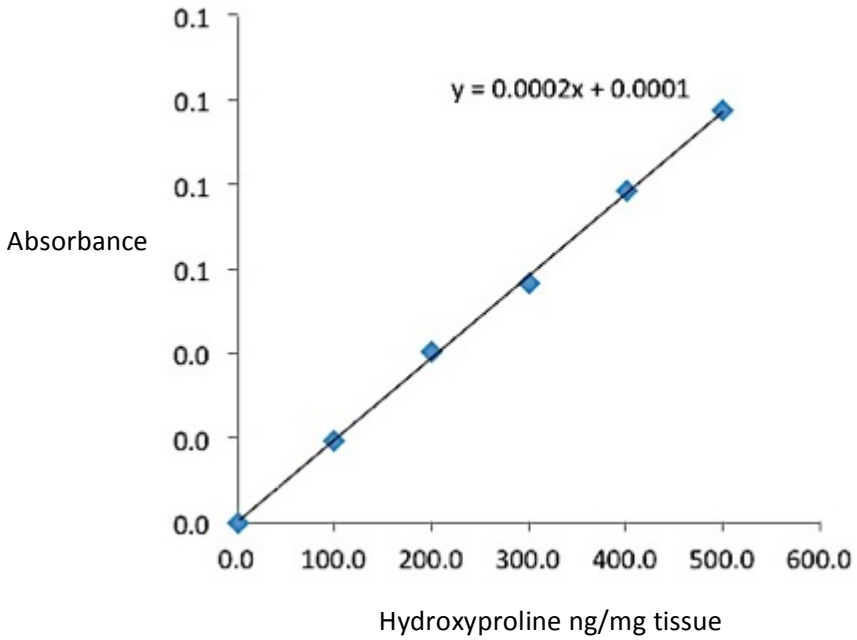

Figure 78: Standard curve of colorimetric absorbance values with increasing hydroxyproline concentration from known concentrations of the control standard. The standard curve shown enabled calculation of the gradient and y intercept in the equation **y=mx+c** to determine the hydroxyproline content of each of the experimental samples.

	Hydroxyproline ng/mg	SD
Positive control	196.8	31.9
Negative control	2.8	0.9
Cellular tissue donor a	3.1	0.9
Decellularised tissue donor a	4.0	1.1
Cellular tissue donor b	4.2	1.2
Decellularised tissue donor b	3.6	0.8
Cellular tissue donor c	6.2	4.6
Decellularised tissue donor c	5.2	1.6

Table 15: Table to show hydroxyproline (ng/mg) found in assays of paired samples of cellular and decellularised tissue. P=0.74: paired samples t-test between cellular and decellularised donor tissue (n=3 in each group).

3.6.5 Histology of decellularised conjunctiva

Haematoxylin and Eosin (H&E) staining of cellular and decellularised tissues demonstrated marked similarities in the Eosin staining patterns and the notable absence of basophilic Haematoxylin staining in keeping with the absence of nuclei in decellularised tissue (Figure 79). Van Gieson's stain demonstrated the absence of brown staining in decellularised tissue indicating the absence of nuclear material and preserved collagen extracellular matrix architecture, as shown by the red-purple staining (Figure 80).

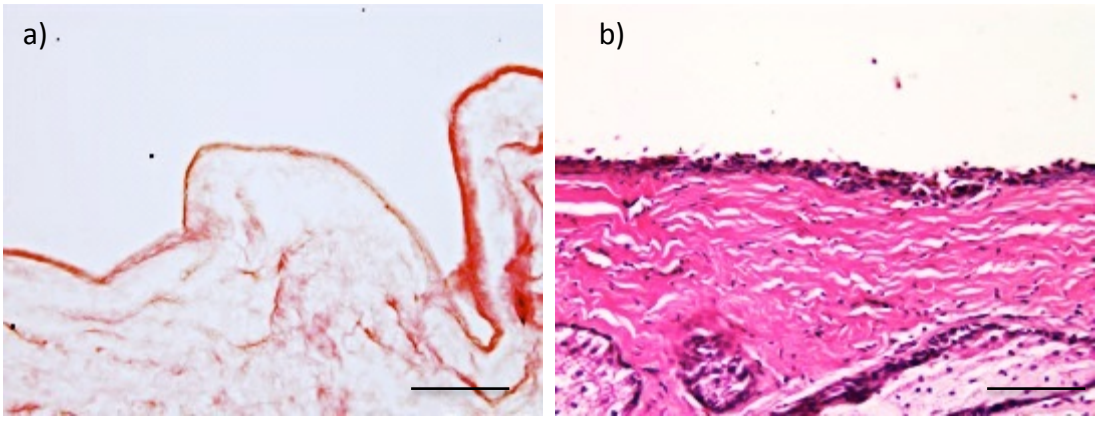

Figure 79: Representative photomicrographs of Haematoxylin and Eosin stained paraffin embedded tissue sections: a) decellularised tissue; b) cellular tissue. Scale bars 200µm.

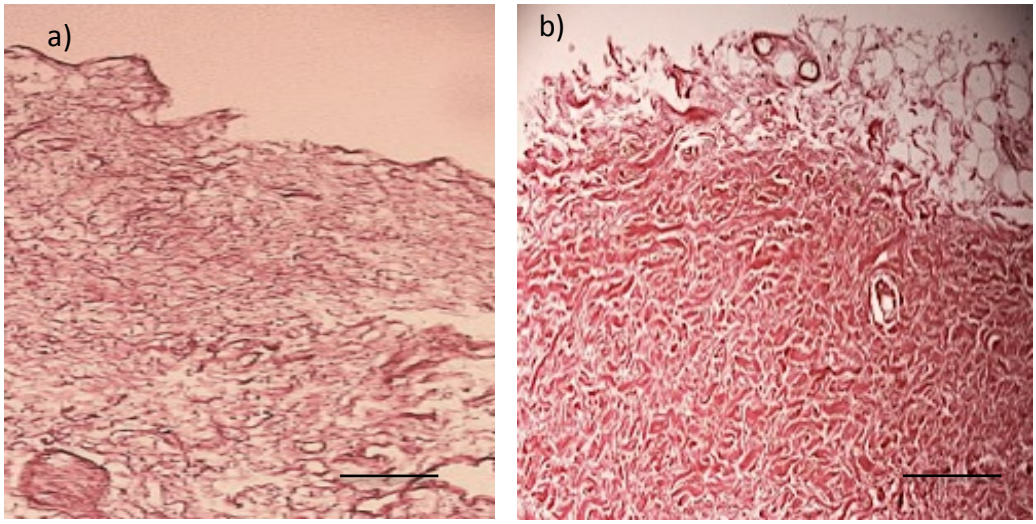

Figure 80: Representative photomicrographs of conjunctiva tissue stained with Van Gieson's stain: a) decellularised tissue; b) cellular tissue. Scale bars 100µm.

3.7 Culture of primary human conjunctival epithelial cells on decellularised conjunctiva

3.7.1 Cell culture on decellularised tissue substrates with primary conjunctival epithelial cells using explant and suspension cultures

The conjunctival explants used for this experiment were taken from donor eye 5. The isolated cells cultured on amniotic membrane were sparse and grew in concentrated areas in comparison to explant cultures in which a more confluent cell culture developed (Figure 81). Similar results were obtained using decellularised conjunctiva in which explant cultures resulted in a qualitatively higher cell density in comparison to the culture of an isolated cell suspension using cells from the same donor. This difference was more notable on amniotic membrane whereby cells were also qualitatively found in greater density than on conjunctiva overall. The basement membrane, however, in the decellularised tissue appeared to be absent based on the H&E staining in these photomicrographs.

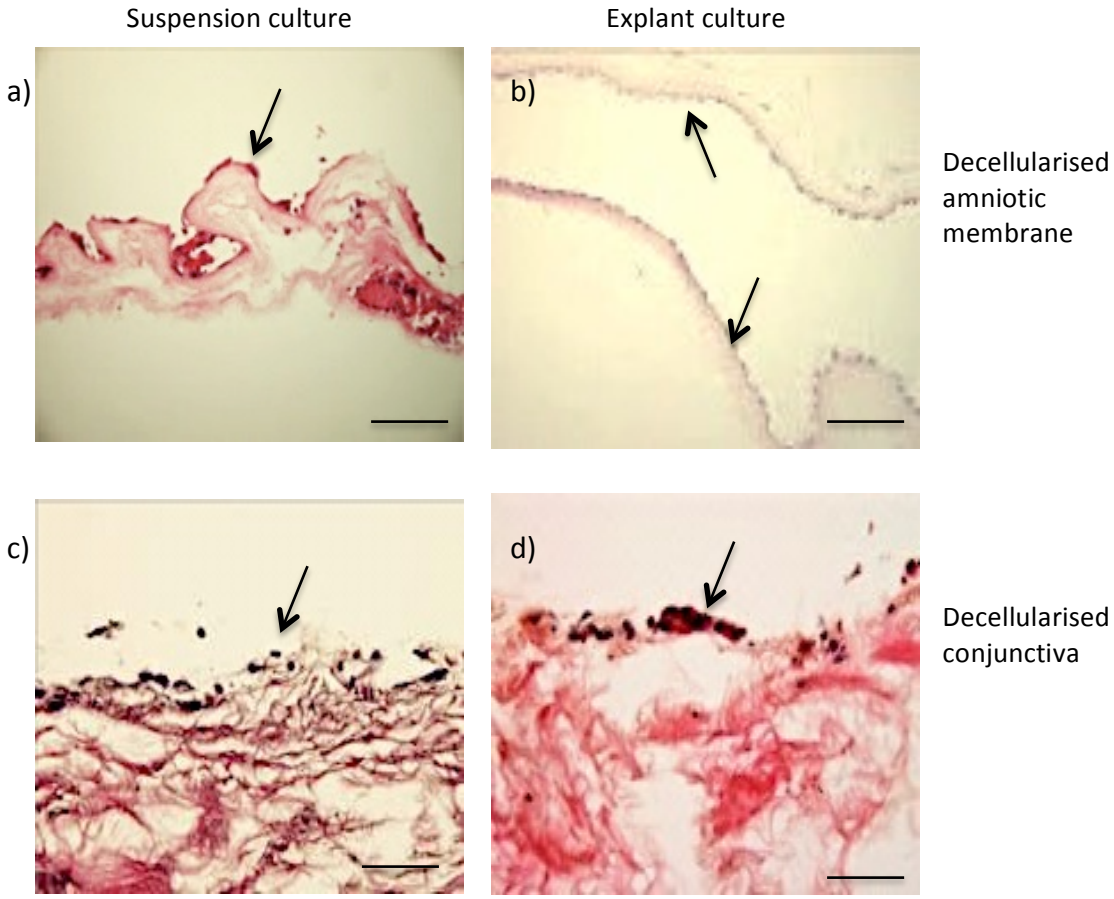

Figure 81: Representative photomicrographs of decellularised amniotic membrane and conjunctival tissue sections recellularised with conjunctival epithelial cells. Greater cell density was evident qualitatively following explant culture (b and d) than that following suspension culture (a and c). Scale bars 100µm. Arrows point to purple nuclei in cells.

3.7.2 Explant culture with attention to conjunctival basement membrane orientation

Confluent cell growth was demonstrated with qualitatively greater cell density from explant cell culture following the confirmation and orientation of the basement membrane in comparison to tissue in which the basement membrane could not be identified (Figure 82). The explant cultures used in this experiment were taken from donor eye 7.

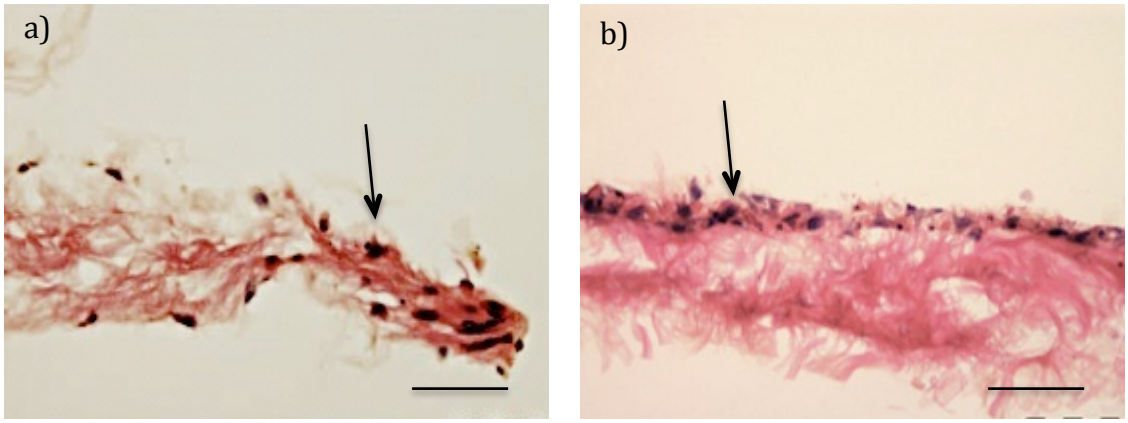

Figure 82: Representative photomicrographs of explant cultures grown on decellularised tissue: a) basement membrane not present b) basement membrane present. Arrows are pointing to nuclei (purple). Scale bars 100µm.

3.7.3 Comparison of conjunctival epithelial cultures using tissue from different donors for explants and decellularised substrates

Conjunctival tissues from donor eyes 9, 5 and 13 were decellularised for use in this experiment. The explants cultured on these substrates were taken from tissue donor eyes 15, 17 and 19. Results from these experiments showed that growth was sparse from all three explant donors. The best results qualitatively based upon confluence and the apparent density of cells was demonstrated using decellularised tissue from donor 13 and explants from donor 19 (Figure 83-86). Consistent cellular expansion from explant donor 19 however was not evident across all decellularised tissue samples. Donor 19, however, also produced the greatest density of cells qualitatively on the amniotic membrane control tissue (Figure 86). In some tissue sections, the explant itself was visible with minimal outgrowth from its edge.

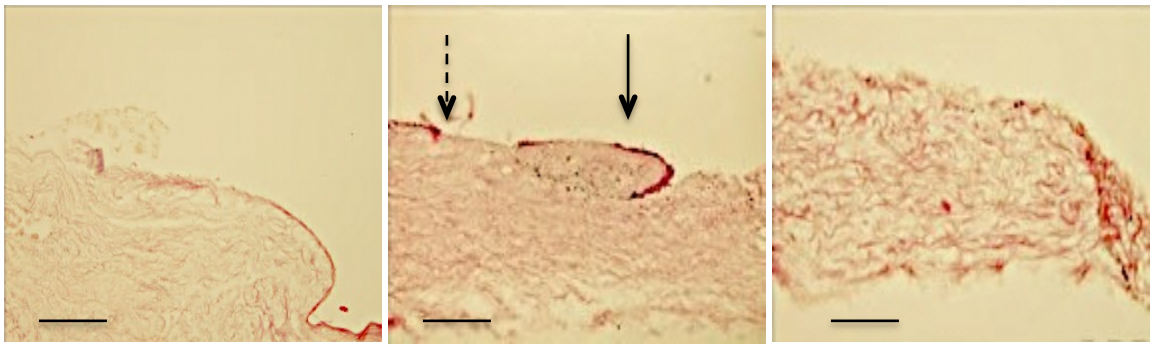

Tissue donor 9 **Tissue donor 5** **Tissue donor 13**

Figure 83: Representative H&E stained photomicrographs of **explants from donor 15** cultured on decellularised conjunctiva from tissue donors 9/5/13. The photomicrograph of decellularised tissue donor 5 has captured the presence of explant (solid arrow) with conjunctival epithelium that had developed on the left hand side of this photomicrograph (dashed arrow). In contrast minimal and no nuclei were visible in photos from decellularised tissue donors 9 and 13. Scale bars 200µm.

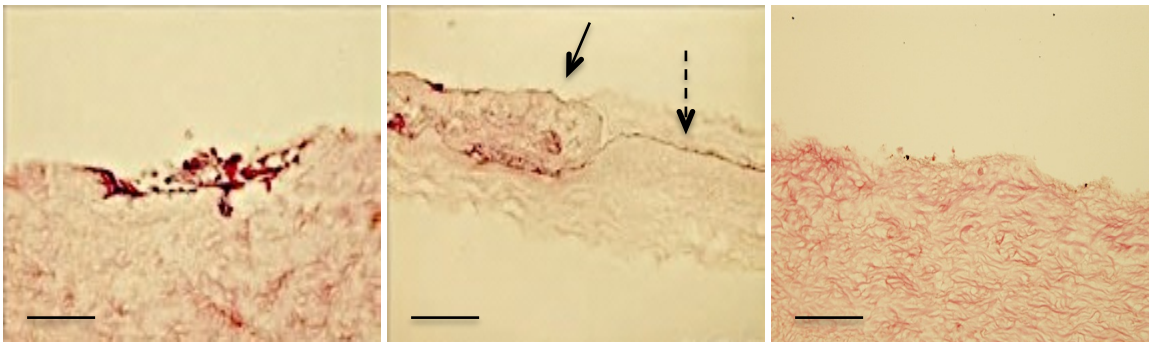

Tissue donor 9 **Tissue donor 5** **Tissue donor 13**

Figure 84: Representative H&E stained photomicrographs of **explants from donor 17** cultured on decellularised conjunctiva from tissue donors 9/5/13. No cells are evident from on tissue sections derived from decellularised tissue donor 13. Occasional areas of epithelial growth were demonstrated on decellularised tissues from donor 9 and 5. In the centre photo from decellularised tissue donor 5 an explant (solid arrow) can be seen with cellular outgrowth (dashed arrow). Scale bars 200µm.

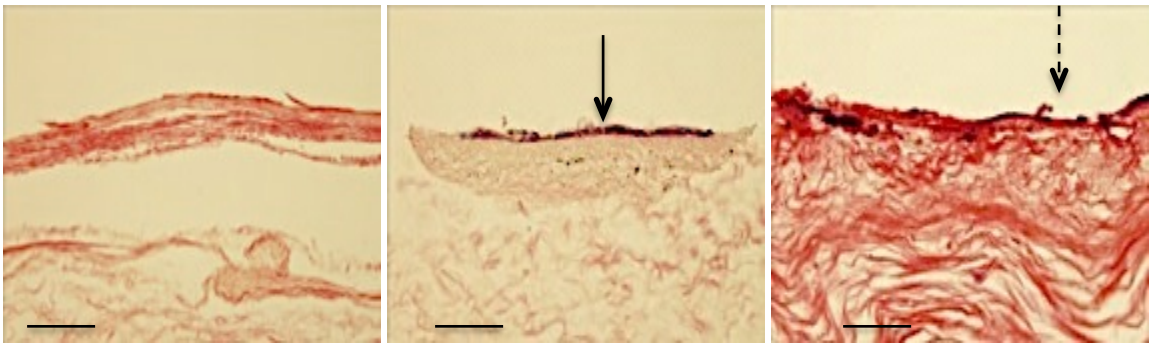

Tissue donor 9 **Tissue donor 5** **Tissue donor 13**

Figure 85: Representative H&E stained photomicrographs of **explants from donor 19** cultured on decellularised conjunctiva from tissue donors 9/5/13. No cells were evident from on tissue sections derived from decellularised tissue donors 9 or 5 (donor tissue 5 shows only the explant with no outgrowth; solid arrow). Cellular growth was observed in most tissue sections derived from explant culture on decellularised tissue donor 13 (dashed arrow). Scale bars 200µm.

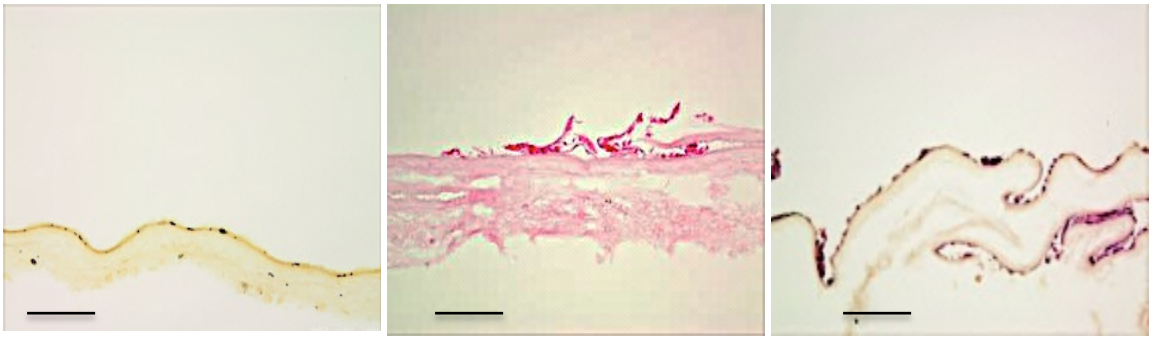

Explant donor 15 **Explant donor 17** **Explant donor 19**

Figure 86: Representative H&E stained photomicrographs of **explants from donors 15/17/19** cultured on a decellularised amniotic membrane substrate (same donor). Cellular growth is evident from all the explants; however, qualitatively the greatest density of cells was evident from explants derived from donor 19. Scale bars 200µm.

3.7.4 Further conjunctival explant cultures on freshly decellularised tissues

Further conjunctival explant cultures were undertaken using decellularised tissues stored in phosphate buffered saline supplemented with 1% penicillin/streptomycin, used within one week of decellularisation. In previous experiments, decellularised conjunctival tissues were stored at -40^{o}C and allowed to thaw prior to use. The decellularised tissues from the same donor (21) were seeded with explants acquired within hours of tissue retrieval. This was undertaken twice using two separate donors (23 and 25). Both these experimental runs resulted in more confluent growth of conjunctival epithelium across the entire sectioned tissue samples on both decellularised conjunctiva and the amniotic membrane. The formation of a multi-layered epithelium was also evident on the decellularised conjunctiva but not on the amniotic membrane (Figure 87).

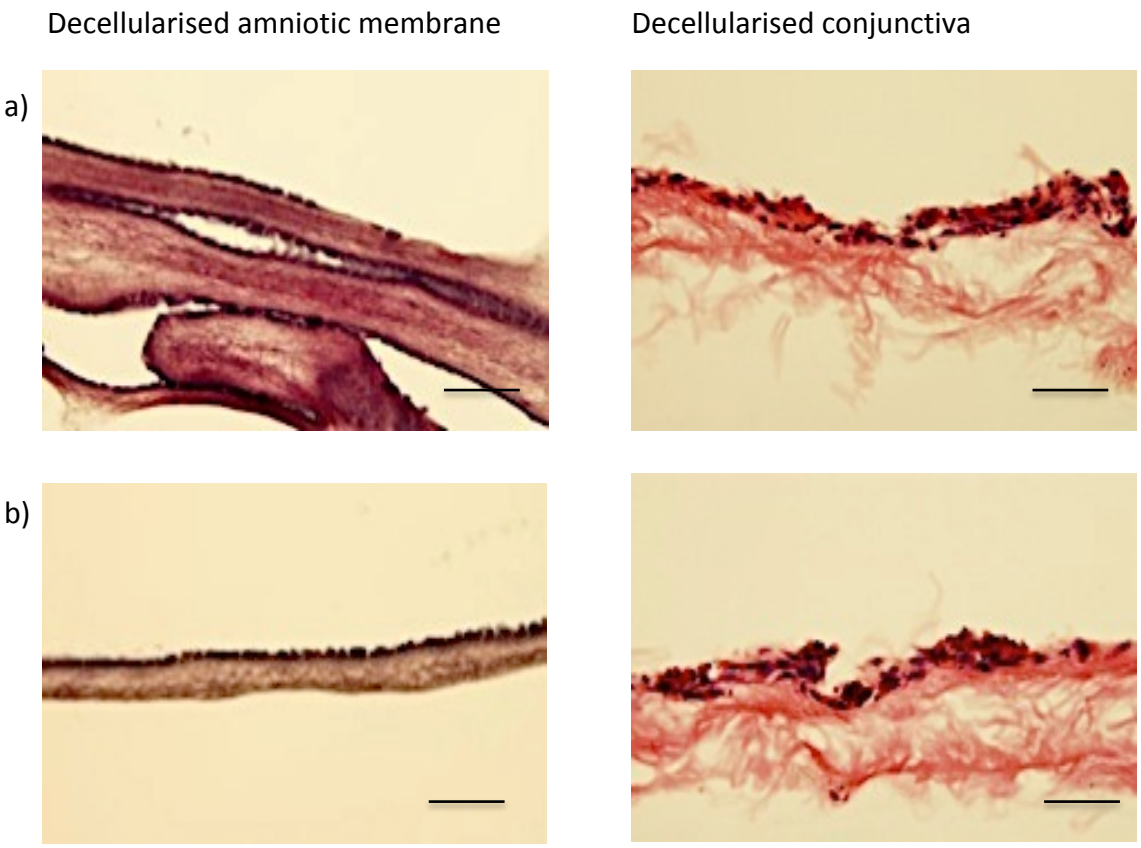

Figure 87: Representative photomicrographs of stained tissue sections following conjunctival explant culture using donor 23 (a) and 25 (b) on decellularised conjunctiva (from donor 21) and amniotic membrane. Stratified cells were demonstrated on decellularised conjunctiva in contrast to monolayer formation on amniotic membrane. Qualitatively, the cell density and morphology of the epithelium appeared similar between the donors (23 and 25) on both tissue substrates. Scale bars 100µm.

3.7.5 Characterisation of the cellular phenotype of conjunctival epithelium cultured on decellularised conjunctiva

An embedded tissue wax block from the previous experiment; donor 21 with explants from donor 23 was further sectioned to allow immunohistochemical identification of markers associated with conjunctival epithelial cells. Figure 89 demonstrates abundant expression of CK19 throughout the tissue sample. In contrast, CK7 and CK4 were

expressed in a qualitatively lower proportion of cells. MUC5AC expression was qualitatively sparse, however detectable, within the tissue sections examined. Markers of progenitor cells ΔNp63 and ABCG2 were also present in lesser frequency, and ABGC2 expression appeared less abundant than ΔNp63 (Figure 90). Levels of PCNA expression appeared similar to that of ΔNp63. Caspase 3, a marker of apoptotic cells was also present and appeared to be expressed in apical rather than basal cells, in contrast to the other cell markers studied which appeared more evenly distributed.

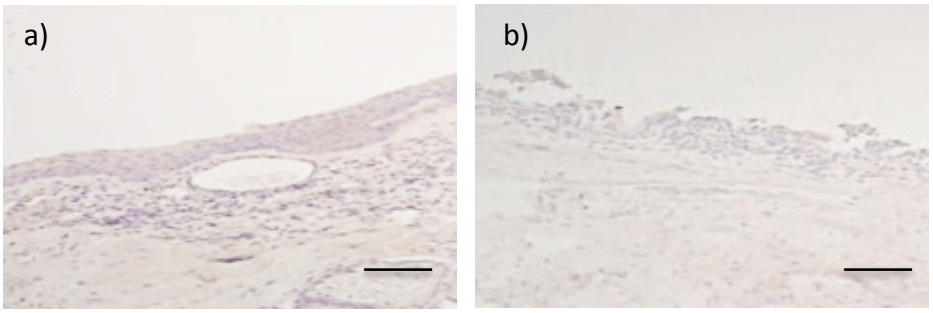

Figure 88: Representative photomicrographs of tissue sections of conjunctival tissue (a) mouse IgG isotype control, (b) rabbit IgG isotype control stained with Mayers haematoxylin only. These representative images display the level of background staining detected for immunohistochemistry samples in this section and are the negative controls. Scale bars 100µm.

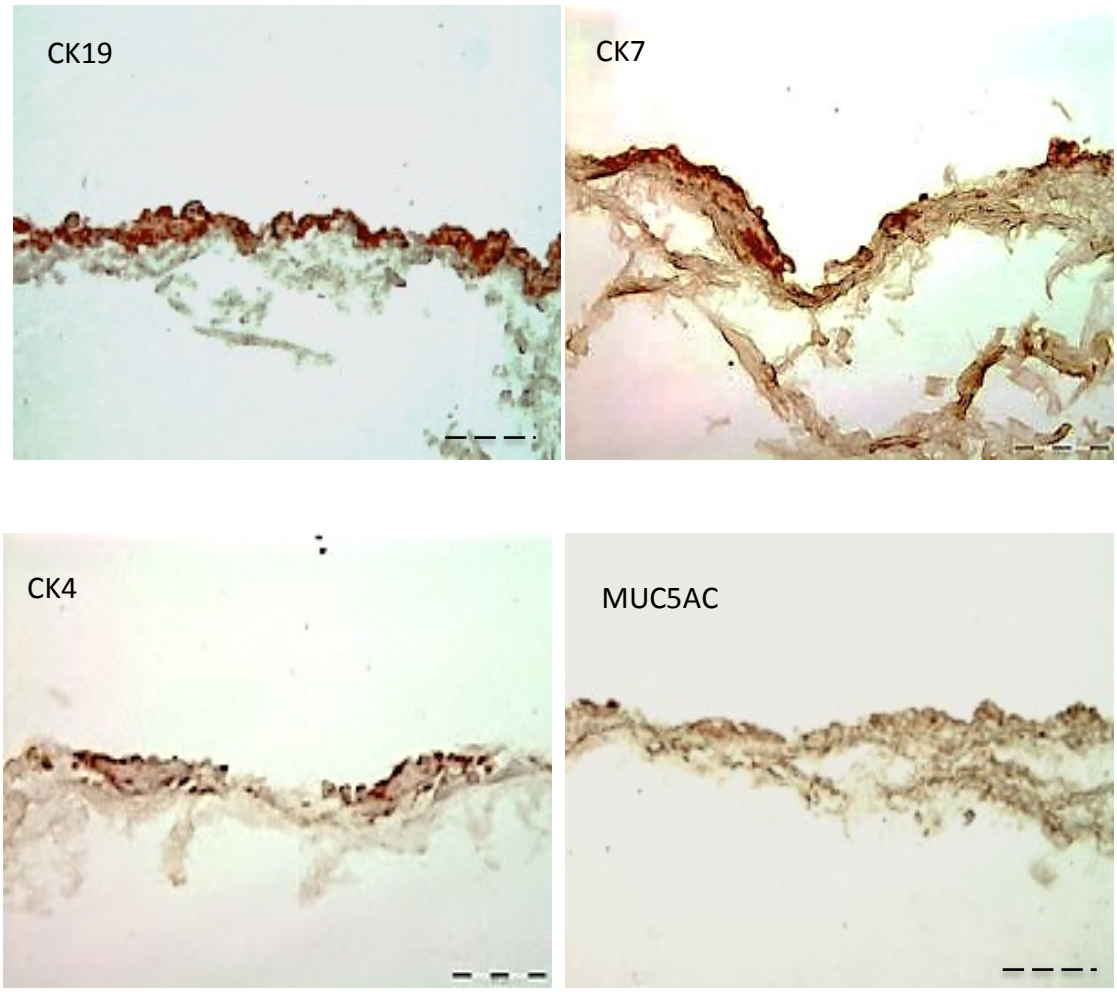

Figure 89: Representative photomicrographs of immunohistochemical staining of tissue sections of decellularised conjunctiva 21 recellularised using explants from donor 23. All brown staining represents positive immunolocalisation of the respective marker studied. Scale bars 100µm.

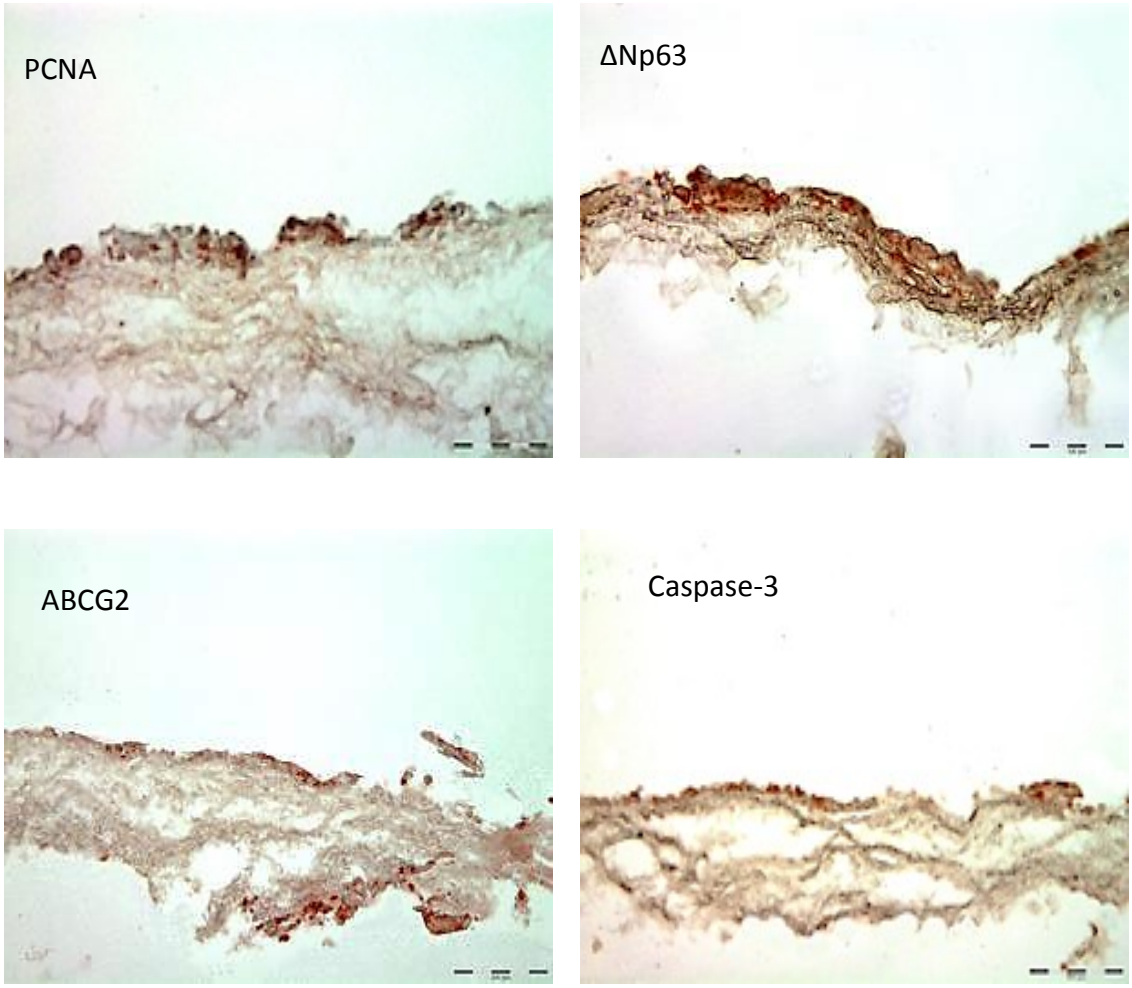

Figure 90: Representative photomicrographs of immunohistochemical staining of tissue sections of decellularised conjunctiva 21 recellularised using explants from donor 23. All brown staining represents positive immunolocalisation of the respective marker studied. Scale bars 100µm.

3.8 Identification and characterisation of basement membranes of human conjunctiva and amniotic membrane

3.8.1 Characterisation of basement membrane with PAS

Conjunctiva from three tissue donors and amniotic membrane from three tissue donors were stained with periodic acid Schiff (PAS) stain to identify glycoproteins within basement membranes. PAS also stains transmembrane and goblet cell associated mucins in conjunctival epithelium. The thickness of the basement membrane and intensity of staining were qualitatively similar between paired samples (cellular and decellularised tissue) of both amniotic membrane and conjunctiva (Figure 91 and 92). The outline of cells were also visualised and demonstrated on cellular tissue samples of both conjunctiva and amniotic membrane. This was notably absent in decellularised tissue samples. Representative photomicrographs taken from the centre of the slide mounted stained tissue section are shown (Figures 91 and 92).

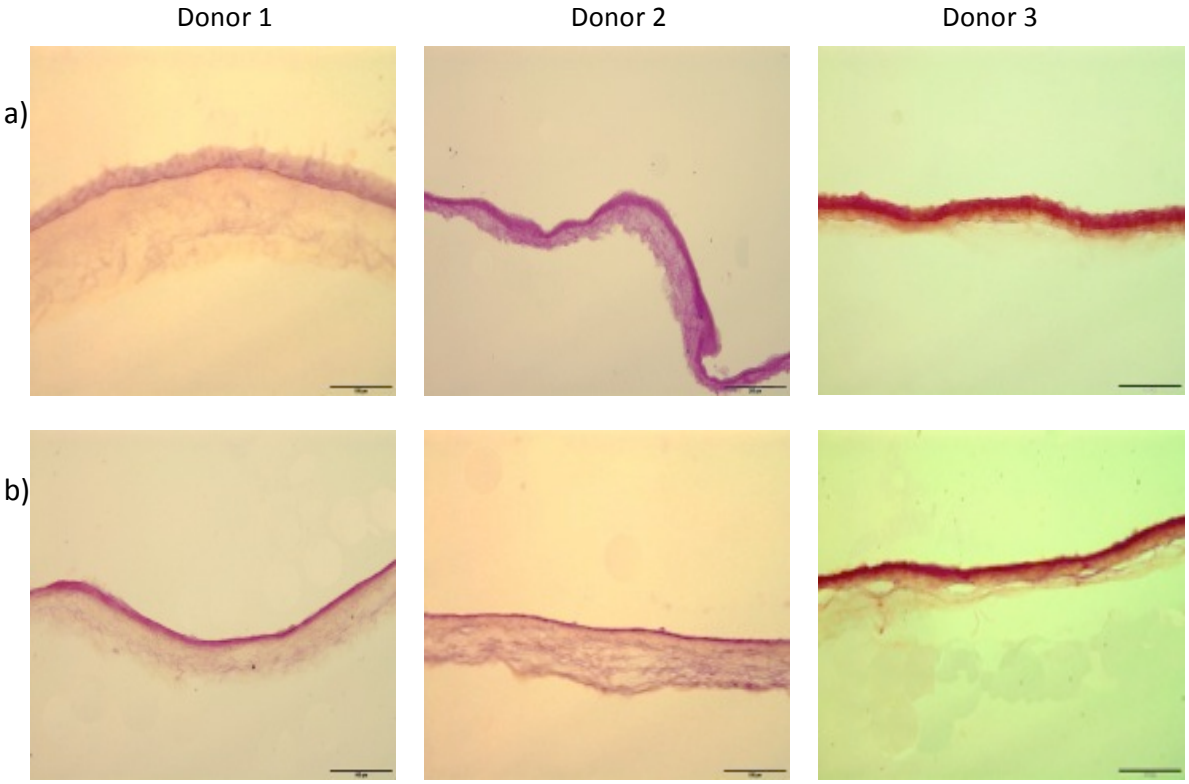

Figure 91: Representative photomicrographs tissue sections of cellular (a) and decellularised amniotic membrane (b) from three tissue donors stained with PAS. The basement membrane tissues appear stained and similar between cellular and decellularised tissue sections suggesting it was preserved following decellularisation. Scale bars 100µm.

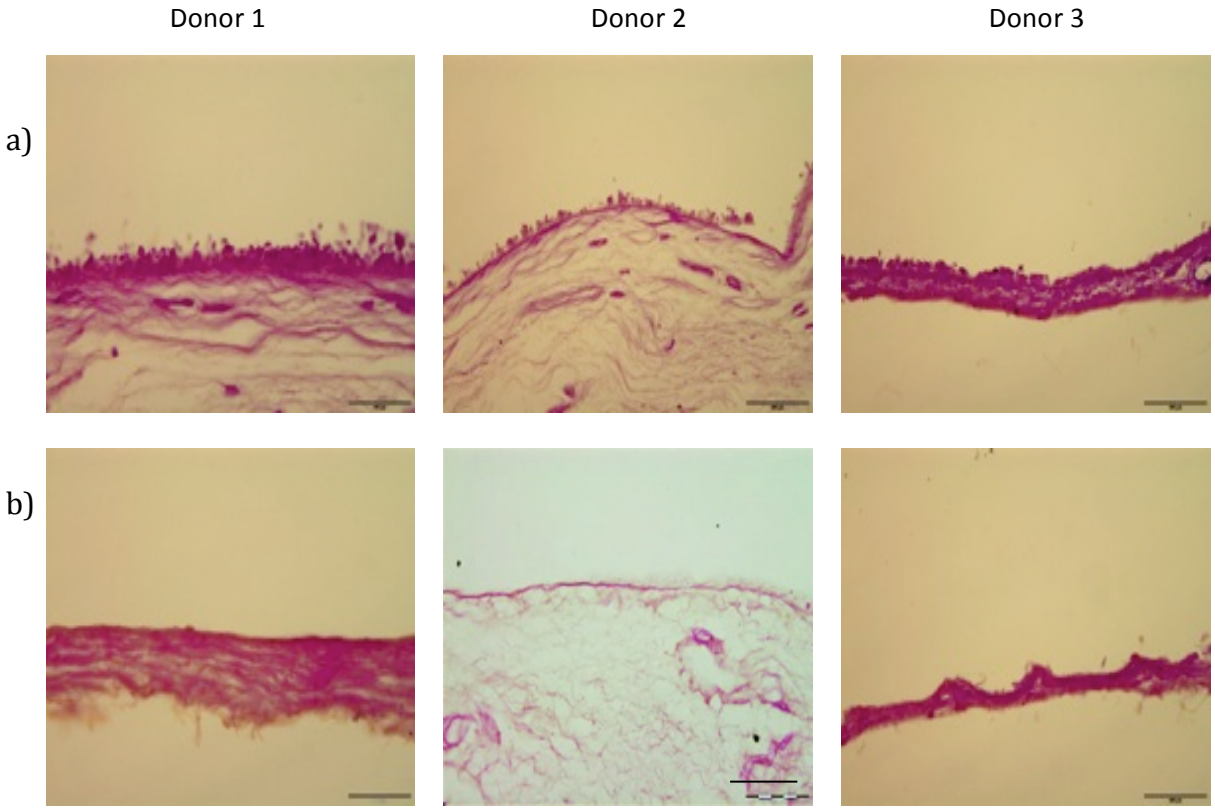

Figure 92: Representative photomicrographs tissue sections of cellular (a) and decellularised conjunctiva (b) from three tissue donors stained with PAS. The basement membrane PAS staining in all the cellular and decellularised tissues appeared similar between tissue sections suggesting it was preserved following decellularisation. Scale bars 100µm.

3.8.2 Characterisation of cellular and decellularised tissue with laminin, collagen IV and fibronectin

Deparaffinised tissue sections from three conjunctival epithelial donors and three amniotic membrane donors were characterised for collagen IV, fibronectin and laminin by immunohistochemical staining. Both cellular and decellularised tissues were stained to ascertain whether decellularisation qualitatively affected the immunohistochemical detection of extracellular proteins. Three different donors have been studied for each tissue type. The images (Figures 93-99) demonstrate that collagen IV, laminin and fibronectin were detectable in the epithelial tissue basement membranes and stromal tissue. The strongest staining, qualitatively, was present in the basement membranes. Overall, there did not appear to be any significant difference in the detection of these proteins between donors. Furthermore, decellularisation did not reduce the intensity or distribution of staining by qualitative observation. The gross morphology of the tissue, specifically the thickness and appearance of underlying stromal tissue, however, appeared to differ more significantly between the conjunctival donor tissues (Figure 97-99) than the amniotic membrane tissues (Figure 94-96).

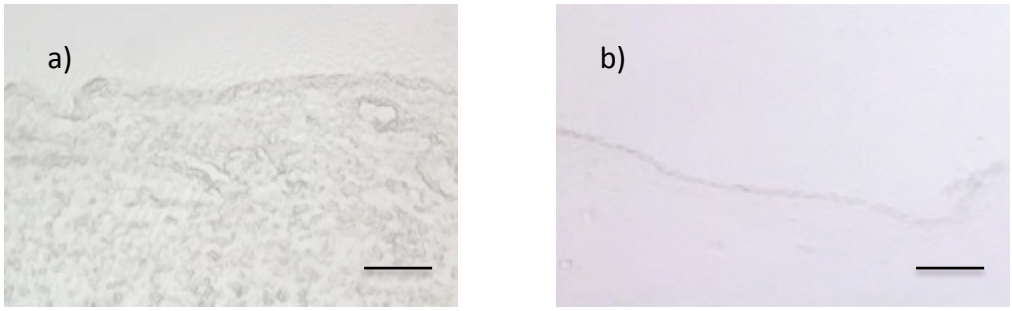

Figure 93: Representative photomicrographs of tissue sections of conjunctival tissue (a) and amniotic membrane (b) incubated with isotype controls and stained with Mayer's haematoxylin only. These representative images display the level of background staining detected for immunohistochemistry samples in this section. All primary antibodies were raised in rabbit. Scale bars 100µm.

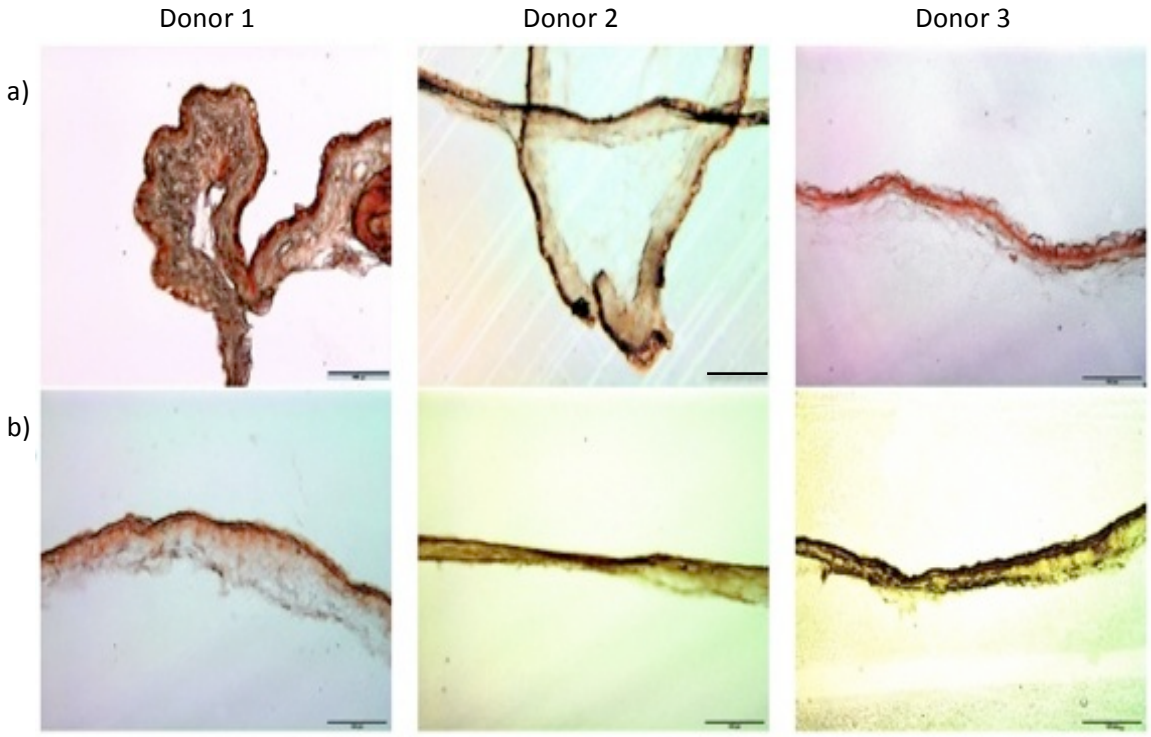

Figure 94: Representative photomicrographs of cellular (a) and decellularised (b) amniotic membrane tissue sections from three separate donors examined for laminin by immunohistochemistry. All brown staining represents positive immunolocalisation of laminin. Scale bars 100µm.

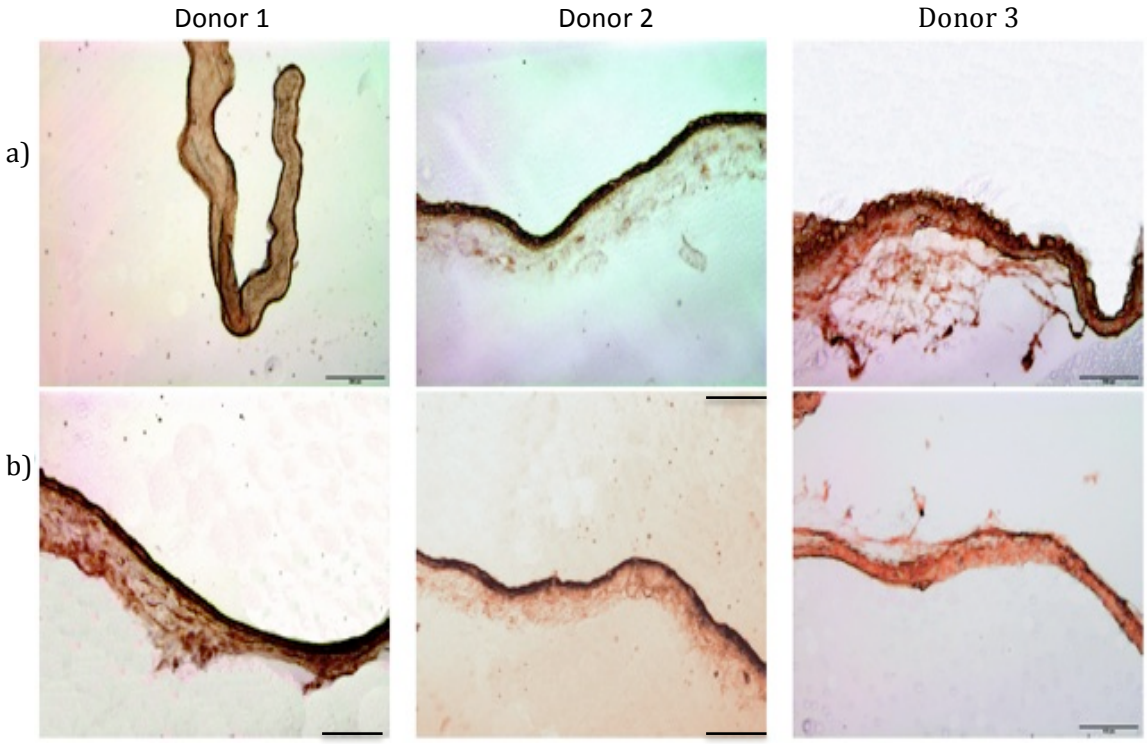

Figure 95: Representative photomicrographs of cellular (a) and decellularised (b) amniotic membrane tissue sections from three separate donors examined for fibronectin by immunohistochemistry. All brown staining represents positive immunolocalisation of fibronectin. Scale bars 100µm.

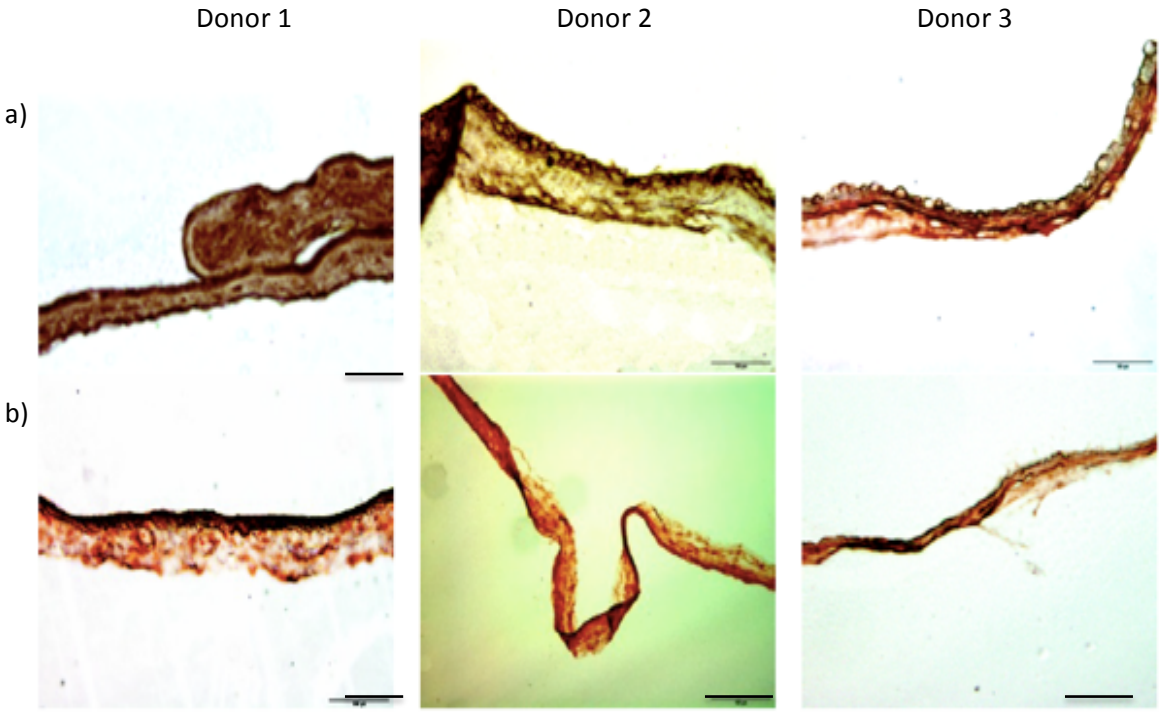

Figure 96: Representative photomicrographs of cellular (a) and decellularised (b) amniotic membrane tissue sections from three separate donors examined for collagen IV by immunohistochemistry. All brown staining represents positive immunolocalisation of collagen IV. Scale bars 100µm.

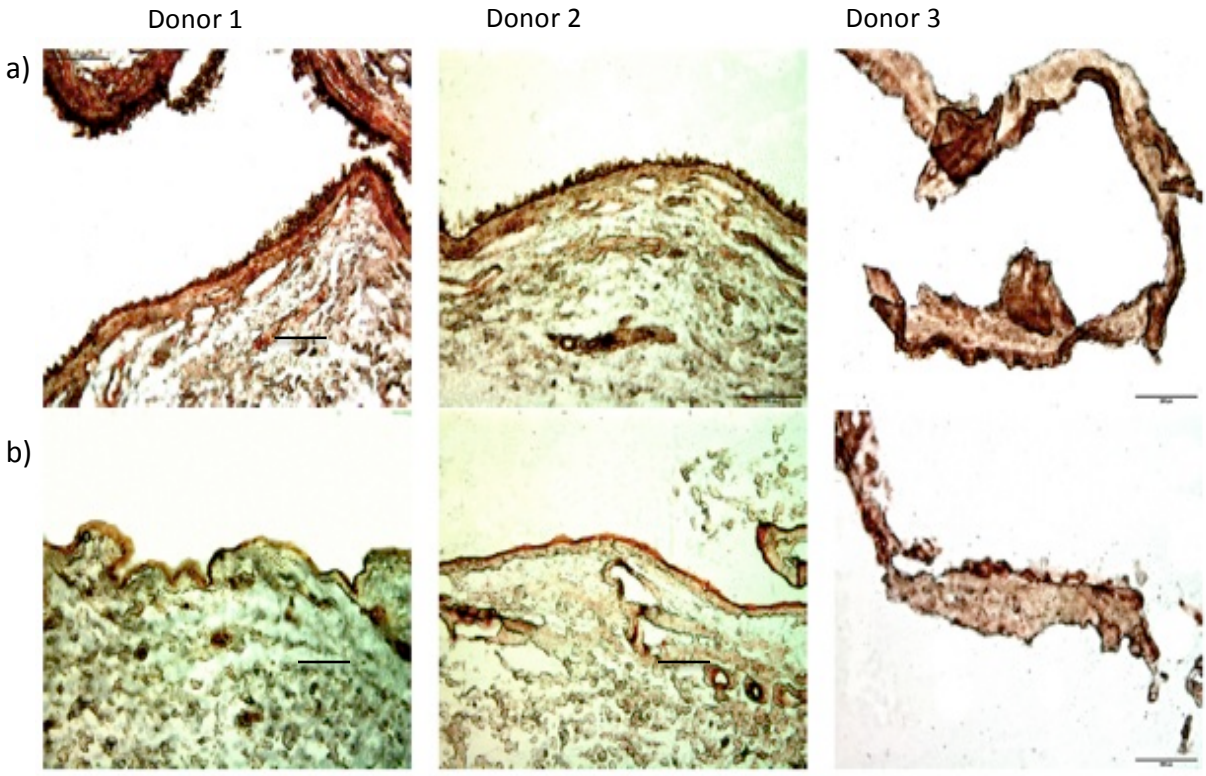

Figure 97: Representative photomicrographs of cellular (a) and decellularised (b) conjunctival tissue sections from three separate donors examined for laminin by immunohistochemistry. All brown staining represents positive immunolocalisation of laminin. Scale bars 100µm.

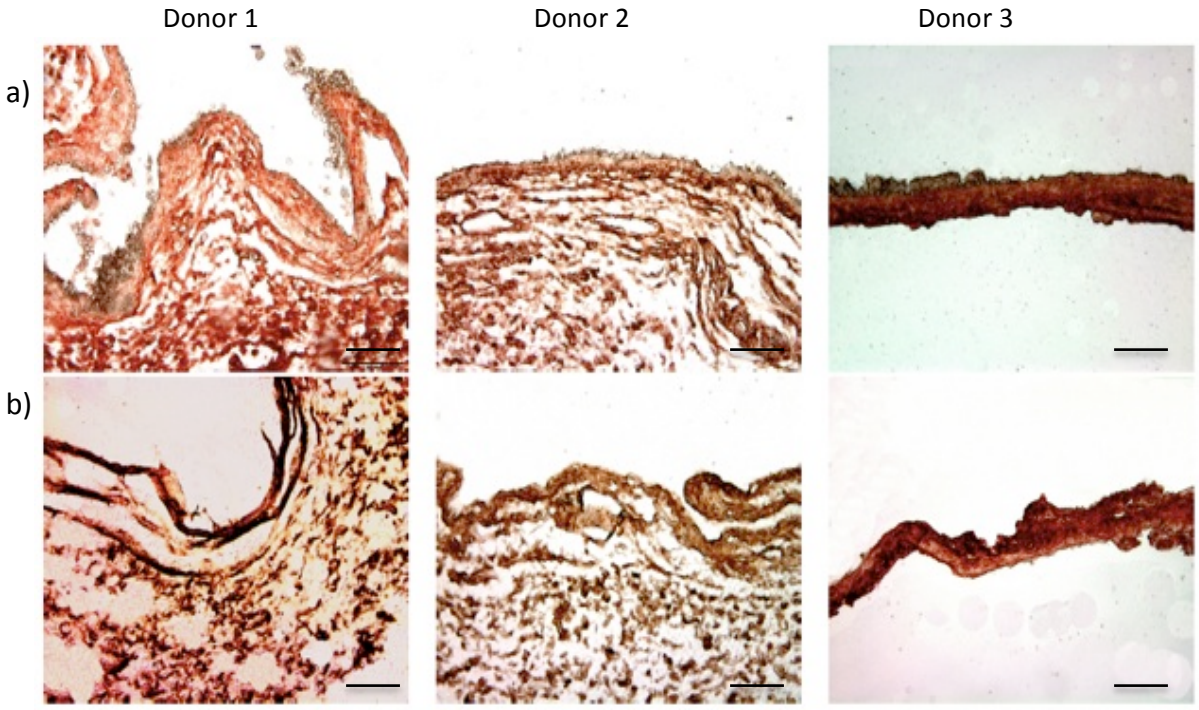

Figure 98: Representative photomicrographs of cellular (a) and decellularised (b) conjunctival tissue sections from three separate donors examined for fibronectin by immunohistochemistry. All brown staining represents positive immunolocalisation of fibronectin. Scale bars 100µm.

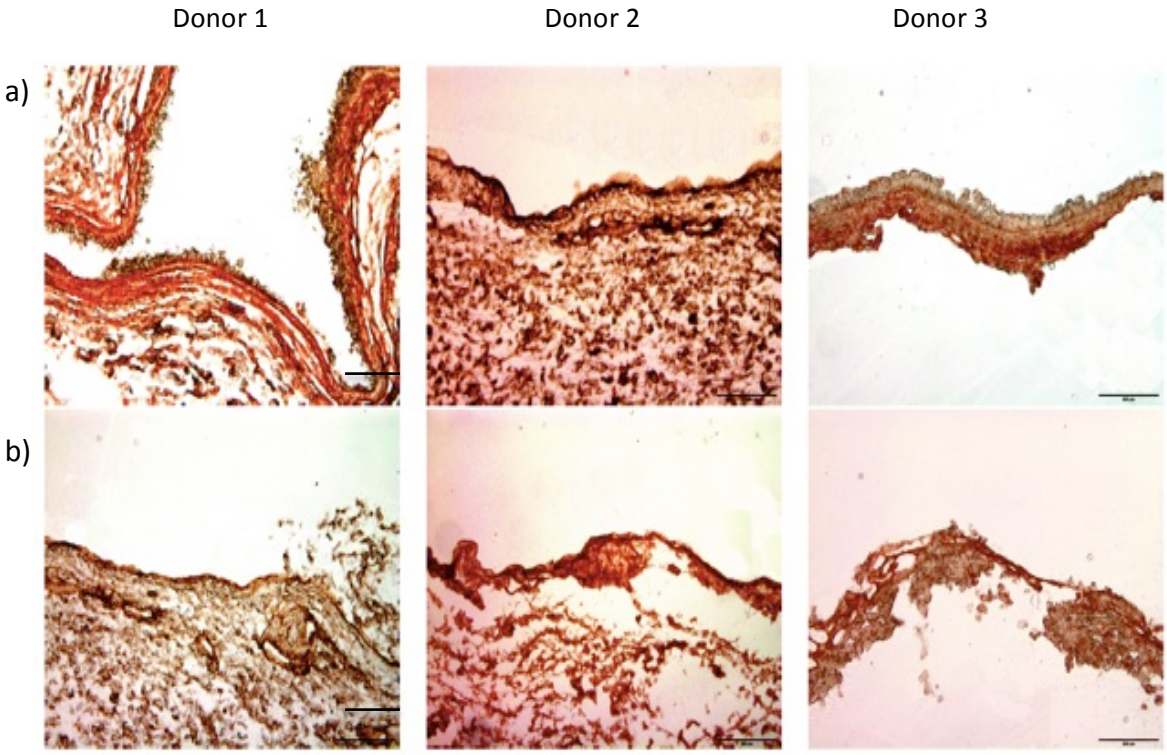

Figure 99: Representative photomicrographs of cellular (a) and decellularised (b) conjunctival tissue sections from three separate donors examined for collagen IV by immunohistochemistry. All brown staining represents positive immunolocalisation of collagen IV. Scale bars 100µm.

3.9 Characterisation of patients with ocular MMP

Five patients were examined and are described in this section. Two of five patients examined had visual acuities of 6/9 Snellen acuity or lower in one or both eyes. In both cases there was co-existing ocular pathology that accounted for the visual impairment. Patient 1 had normal tension glaucoma and visual acuity of 6/18 and 6/9 right and left eyes respectively. Patient 2 had age related macular degeneration with geographic atrophy and visual acuity of 6/12 and 6/60 right and left eye respectively. Four patients had an inflammatory score ≥5 in one or both eyes. The score “0” and “1” were difficult to differentiate when assessed at slit lamp examination. All patients had one or both

eyes grade III involvement by Foster.[153] Assessment by Tauber grading found only 1/10 eyes had no involvement and this was in keeping with the Tauber-Liverpool score.[154, 156] All patients had in one or both eyes ≥60% vertical involvement and ≥50% horizontal involvement. Four patients had a Rowsey score ≤50% of the total score.[155] All patients had grade II or less oxford grading score (mild). No eyes had corneal involvement exceeding grade 1 on any of the measured parameters (conjunctivalisation/ neovascularisation /opacification). No eyes had lagophthalmos or any upper lid deformity. Only one patient had a lower lid deformity, which was a grade 1 lateral and medial entropion that was in keeping with the degree of their bilateral conjunctival cicatrisation. Eight of ten eyes had trichiasis of any degree.

Patient number	1; OD and OS	2; OD and OS	3; OD and OS	4; OD and OS	5; OD and OS
Conjunctiva					
Inflammatory score totals (limbitis)	5; 7 (n; n)	5; 5 (n; n)	4; 2 (n; n)	4; 10 (n; n)	7; 2 (n; n)
Tauber score	IIcIIIb; IIcIIIb	IIdIIId; IIdIIId	IIcIIIb; IIbIIIa	IIdIIId; IIbIIIb	IIcIIIb; IIaIIIa(nil)
Tauber-Liverpool (% II/III)	65/30; 70/35	75/100; 75/83	60/25; 50/13	85/83; 50/25	70/46; 0/0
Rowsey (score/45)	22; 24	16; 19	29; 36	14; 29	28; 45
Foster	III; III	III/III	III/III	III/III	III/0
Fornix upper/lower (mm)	6/3; 6/4	5/0.5; 6/0.5	6/2; 6/3	0/6; 8/4	6/2; 8/5
Cornea					
Oxford dryness score	2; 2	1; 1	2; 2	2; 1	1; 2
Conjunctivalisation/ neovascularisation	1/1; 1/0	1/0; 1/0	0/0; 1;0	1/1; 0/0	1/0; 0/0
Opacification peripheral/central	0/0; 0;0	0/0; 0/0	0/0; 0/0	1/0; 0/0	1/0; 0/0
LIDS					
Lagophthalmos	n; n	n; n	n; n	n; n	n; n
Lashes	T; T	T; n	T; T	T; T	T; n
Upper lid deformity and grade	n; n	n; n	n; n	n; n	n; n
Lower lid deformity and grade	n; n (laxity but grade 0)	Entrop G1 L+M; Entrop G1 L+M	n; n	n; n	n; n

Table 16: Table displaying conjunctival, corneal and lid involvement in ocular MMP patients examined using the new pro forma: OD=right eye, OS=left eye, n= none/no involvement, T= trichiasis (any degree), Entrop= entropion; G=grade L=lateral, M=medial. See appendix 1 for full details of grading.

a) 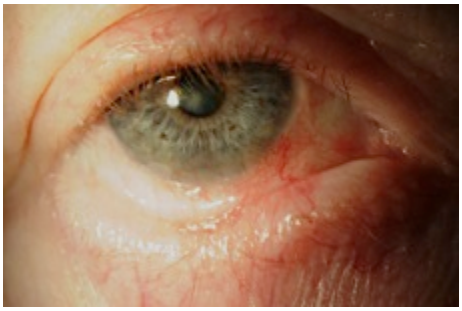 b) 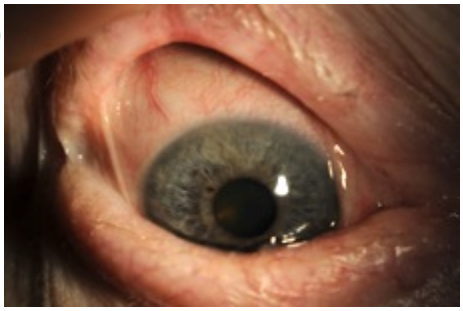

Figure 100: Photographs of the right eye of patient 4. The extent of horizontal symblepharon involvement was 20mm extending medially from the lateral canthus: a) lower lid held at tension b) upper lid held at tension. The distance between the inferior limbus at the midline to the edge of the subconjunctival fibrosis was 1.5mm. The fornix ruler could not be inserted into the inferior conjunctival fornix.

4 Discussion

4.1 Overview

The conjunctiva is a mucous membrane that is an important component of the ocular surface. In a range of conjunctival diseases leading to cicatrisation, it may become irreversibly damaged. This leads to dryness and desiccation of the ocular surface and may ultimately lead to corneal blindness. To restore vision, any potential corneal or limbal stem cell transplant is likely to fail in the presence of significant conjunctival disease. This study sought to develop novel substrates on which conjunctival epithelium could be expanded for use as conjunctival grafts.

Two novel substrates have been developed, each with differing properties to suit a different range of clinical indications. A conjunctival construct developed from the ex vivo expansion of conjunctival epithelium on a decellularised conjunctival substrate is degradable and therefore may suit indications where smaller grafts are required. This is in contrast to a conjunctival construct developed from the expansion of conjunctival epithelium on ePTFE, which is non-degradable and available in large quantities to suit indications where a larger graft is required. In particular, this may suit forniceal reconstruction whereby the substrate would remain in situ to prevent recurrent forniceal loss.

Described in the following sections is the process whereby ePTFE and decellularised conjunctival substrates have been developed as culture substrates. Ammonia gas plasma modification of ePTFE and its effect on hydrophilicity is described along with an exploration of the optimal culture media for the growth of conjunctival cells. The cell density of cultured cells has also been compared when ePTFE is treated on one or both surfaces (surface and underside). Finally, the phenotype of conjunctival cells developed on plasma treated ePTFE is compared with untreated ePTFE and an established cell

culture material, Thincert, in which the cell culture surface is a chemically modified PET membrane. In all experiments, PET membrane is used as a positive control given that it is an established product designed for cell culture. Chemically modified PET is sucessfully utilised in medical applications such as capillary membranes for dialysis and implantable medical devices such as vascular stents.[175] It would not serve as a potential substrate for conjunctival transplantation, however, due to its rigidity. In contrast, ePTFE can be manufactured into thin and durable sheets with a high degree of elasticity and making it ideally suited to soft biological tissue applications with demonstratrable superiority to other polymers.[175, 176] PET membrane is therefore utilised as a positive control in this study rather than being investigated as an alternative substrate for conjunctival epithelial expansion.

The decellularisation of human conjunctiva has not been previously reported. Described within the following sections are the development of a suitable protocol for the decellularisation of human conjunctiva and its characterisation in terms of DNA content, collagen degradation, tensile strength, basement membrane composition and contact cytotoxicity. Several attempts have also been made to develop conjunctival cultures on the decellularised substrate with some success when the explant cultures are developed on decellularised tissue with an intact basement membrane. The expression of a range of conjunctival markers in the developed conjunctival construct is also described.

4.2 Ammonia gas plasma treatment increases the hydrophilicity of ePTFE

Expanded polytetrafluoroethylene (ePTFE) is a relatively hydrophobic material. Ammonia gas plasma was used as a treatment in this study to increase the hydrophilicity of ePTFE to improve its ability to support cell adhesion and proliferation.

Indeed, ammonia gas plasma has been previously shown to increase the surface wettability of a range of polymers including PTFE and PDMS.[108, 177] The results from this study confirm that radio-frequency glow discharge (RFGD, also referred to as gas plasma) followed by the post-treatment modification in distilled water resulted in a significant reduction contact angle to 71^{o}, which is 54% of the original static contact angle of untreated ePTFE. These contact angle measurements are in keeping with previous studies on the ammonia plasma treatment of ePTFE, which also demonstrated that the substrate supported the growth of functional retinal pigment epithelium.[107] In general, contact angles <90^{o} are considered highly wettable surfaces in which significant spread of a droplet of water can be observed, whereas those with contact angles >90^{o} are considered to be less wettable.[109]

A potential limitation in this study is the use of static contact angle measurements rather than dynamic contact angle measurements. Potential advantages of the dynamic contact angles are the assessment of both advancing and receding measurements of the contact angle. These act as surrogate measures of hydrophobicity and hydrophilicity respectively.[109] This allows additional information on the hysteresis and therefore the roughness of the material.[109] Dynamic contact angle measurements have however, been obtained previously for ammonia gas plasma modified ePTFE in an earlier study.[178] The main remit of contact angle measurement in the present study was to ensure that the treatment had the desired effect on hydrophilicity. Features to optimise reliability of static contact angle measurement in the present study included a motorised drop dispenser to ensure a droplet was dispensed in a controlled rate and volume, an enclosed chamber to reduce airborne contamination, optical measurement based upon an image taken by an in-built camera and automated process to reduce problems with observer determined tangent lines.[109]

The RFGD followed by the post-treatment modification in distilled water has been demontrated by x-ray photoelectron spectroscopy to result in breakage of the carbon-

fluorine bonds which are replaced by hydroxyl groups (OH).[179] Defluorination has also been shown to result in the addition of other nitrogen and oxygen containing moieties, which also result in an increase in surface wettability though ammonia gas plasma.[108, 171, 172, 180]

The specific chemical composition of the polymer, including the 'functional' groups present on its surface as a result of plasma treatment and the resulting wettability greatly influence the nature of interactions with both cells and proteins. [108] Studies have shown that materials with terminal functionalities including hydroxyl (-OH) groups and substrates with increased wettability, in general, adsorb peptides to the material surface more easily and positively influence cell attachment and proliferation.[181, 182] Alternative gas plasma modifications include modification with oxygen and air.[108] These were not explored in this study as ammonia gas plasma modification was shown to be successful in supporting retinal pigment epithelium.[178] Given that ammonia gas plasma treatment also increased the cell density of cultured conjunctival epithelium, further modifications were not attempted. Investigation of alterative gas plasmas however may warrant consideration in future work.

An ideal synthetic substrate should allow the adherence of cells and support cell proliferation and differentiation along an appropriate lineage. To this end, a multitude of factors are responsible for optimal cell culture in vitro including media and its supplements, the surface topology, roughness and stiffness of the substrate, porosity and surface chemistry.[77, 183-185] Scanning electron microscopy of ePTFE, suggested that RFGD may result in a mild degree of surface etching of the surface ridges that was not apparent on ePTFE when examined as-received.[108, 171, 172, 180] The effect of this together with other surface topology features warrant consideration.

Other modifications to consider in future work include the immobilisation and adsorption of extracellular matrix proteins on the material surface to mimic native

basement membranes.[183] To this end, differential signalling in conjunctival epithelial cells have been determined when adherent to different isoforms of laminin.[186] This therefore confirms the potential for cell-matrix interactions of conjunctival epithelial cells and their influence on cellular phenotype and behaviour.[187]

The production of a basement membrane has been reported in mature endothelial cell cultures in vascular grafts developed from synthetic substrates.[185, 188] It has been proposed that basement membrane deposition would occur from most cell types when cultured on synthetic substrates.[189] Although beyond the remit of the present study, it would be of interest to determine the timescale required for the development of a basement membrane from conjunctival epithelium on ePTFE and to explore the specific components deposited in comparison to conjunctival basement membrane.

4.3 Experimental use of the HCjE-Gi Cell line

4.3.1 Characteristics of the HCjE-Gi cell line

The HCjE-Gi cell line was chosen for this study given its similarity to primary human conjunctiva in terms of its keratin repertoire and mucin gene expression including goblet cell specific MUC5AC.[190] Alternatives such as the IOB-NHC cell line and Chang cell line were excluded as there were concerns that the IOB-NHC was showing signs of senescence (personal communications with Dr. Diebold) and the Chang cell line was recognised to have HeLa cell contaminants displaying a more fibroblastic phenotype. Characterisation studies by the Gipson group acknowledged that HCjE-Gi epithelia were similar to native conjunctiva, but they did not achieve the normal morphologic differentiation observed in native conjunctiva. A small subpopulation of HCjE-Gi cells expressed MUC5AC mRNA when developed on type 1 collagen and fibroblast co-culture, however, there was no morphological evidence of goblet cell presence or

secreted mucin within cultures. Despite the culture of HCjE-Gi cells under the kidney capsule of SCID mice, the cell line still did not develop mature goblet cells. The Gipson group suggested that it was likely that the differentiation pathway had been deleteriously altered such that goblet cell differentiation would not take place, in keeping with other reports on the phenotypic outcome of cell transformation. [191]

Similar to the present study, the HCjE-Gi cell line has also been used in studies of substrate development for conjunctival expansion and in studies of mucin gene expression.[190] Despite evidence that the cell line may not fully differentiate, the HCjE-Gi cell line was used for the present study as the upregulation and therefore the relative increase/decrease in conjunctival epithelial markers may serve as the best available indication of the expected response in primary conjunctival epithelium. In this study, consistency and repeatability of cellular response was of particular importance given that numerous substrates and experimental repeats were required for experiments. The alternative of using primary conjunctival epithelial cells from a single donor would have been insufficient. The detection of MUC5AC by flow cytometry had not been previously reported in the HCjE-Gi cell line and was therefore also investigated.

4.3.2 Surface modified ePTFE allows human conjunctival cell attachment and proliferation with an appropriate cell seeding density and cell culture media

4.3.2.1 Determination of the optimal cell seeding density

Determination of an optimal cell seeding density is crucial in the context of repopulating synthetic scaffolds with cells. Studies on the cell seeding density of primary endothelial cells found that between 20-70% of cells that initially adhered to synthetic materials were lost after one hour.[192] This is likely to occur in most cell types and depends upon the substrate used for culture.[185] The residual cells may partially replace cell loss by proliferation and migration but this would depend on the density of

residual cells.[185] It follows therefore, that initial cell seeding experiments enable the development of cultures within a suitable time frame and rate but importantly, ensure that the development of confluent cell growth is possible.

In the present report, it was noted that the cell seeding density was more crucial for cultures seeded on ammonia plasma treated ePTFE than those on PET membrane (polyethylene terephthalate; Thincert). A cell seeding density of $1x10^4$cells/cm^2 versus $1x10^5$cells/cm^2 on plasma treated ePTFE led to a more than 3-fold difference in cell density after 7 days in culture. This contrasts with PET membrane in which the difference in cell density at 7 days after seeding at $1x10^4$cells/cm^2 was approximately 30% less than an initial seeding density of $1x10^5$cells/cm^2. The observed differences suggest a superior ability of PET to support greater cell adherence following seeding.

In models of bone regeneration, the cell seeding density was regarded as a critical factor to the synthesis of extracellular matrix and subsequent induction of new bone.[193] The role of cell seeding density has also been shown to influence the differentiation of pluripotent stem cells and in particular, the expression of tight junctional proteins.[194] It seems likely therefore, that the cell density is of critical importance to ensure cell-cell contact and signalling.[185] This was proven by Chen and colleagues, who demonstrated that proliferation of cells in culture was dependent upon cell-cell contact, and not just soluble factors within media. This was demonstrated through experiments designed to control the space and contact between pairs of cells.[195]

4.3.2.2 Determination of the optimal culture media

The original protocol for culture of the human conjunctival cell line HCjE-Gi had described the use of ‘early’ and ‘late’ grow media formulae, which were replicated in the present study.[190] The purpose of testing a change in media from the ‘early’ to ‘late’ formula after 3 days (protocol C) and 7 days (protocol B) in culture were to

ascertain which protocol would lead to a greater cell density. Furthermore, it was also of interest to quantify cell density using the 'late grow' media alone to determine whether the initial early grow media was required. A further cohort also included the 'early grow' media with 1% BSA (w/v) in the place of bovine pituitary extract and epidermal growth factor. The 1% BSA cohort (protocol D) was included to determine its effect on cell density since to the best of my knowledge, it has not been previously reported as a media constituent used in the culture of epithelial cells.

Gipson and colleagues had described a protocol in which the 'early grow' media was changed to the 'late grow' formula when HCjE-Gi cells were 70-100% confluent.[190] As the ePTFE substrate is opaque, phase microscopy could not be used when an experiment is in progress to determine cellular confluence. The use of media protocols A and D led to an overall decline in cell density in contrast to protocols B and C, in which the cell density increased with advancing time in culture. In protocols B and C, the media was changed from 'early' to the 'late grow' media after 7 and 3 days respectively. The experiment determined that the greatest cell density can be achieved if the media is changed from an 'early grow' to the 'late grow' formula on day 7 (protocol B) when cells are seeded at $1x10^5$ cells/cm^2. This was in keeping with existing protocols for the culture of the HCjE-Gi cell line in which the late grow formula was used once cells were 70-100% confluent.[190] This was evident and in keeping with the cell density and spacing demonstrated on DAPI stained photomicrographs, which demonstrate confluent cultures on treated ePTFE and PET membrane but sparse cell growth on untreated ePTFE. Interestingly, even untreated ePTFE supported a slowly increasing population of HCjE-Gi cells in culture with media protocol B. This was in contrast to culture in media protocol C, in which a decline in cell density was demonstrated after 7 days in culture. The PET membrane was demonstrated to support a steady cell density with media protocol A in comparison to ePTFE substrates in which a more obvious decline is notable with advancing time. It follows therefore, that the PET membrane may be supplying factors that enable a higher rate of initial cell

adherence and maintenance of a higher cell density in comparison to cultures developed on ePTFE. These data also demonstrate that untreated ePTFE supports a very limited population of cells and the resulting cell density is influenced by factors in the culture media. It is unlikely that untreated ePTFE would serve as a useful substrate in cell culture applications given the sparse cell density of cells after 14 days in culture.

For optimal cell growth in vitro, the osmolality and pH of the media must be tightly controlled. In addition, the media must contain sugars, salts, amino acids, growth factors and hormones specific to the cell type being cultured.[185] In a variety of media, growth factors and hormones are supplied through the addition of foetal calf serum to constitute 10% of the media.[185] Disadvantages of this approach are the potential for the transmission of infection and the potential variability in batches of serum.[185] Bovine serum albumin (BSA) is commonly used in media studies of gametes including the ovine oocytes model (0.04% w/v) and spermatogonal stem cells.[196, 197] Media used in the culture of spermatogonal stem cells contains 0.2%BSA and a number of cytokine constituents have been identified including fibroblast growth factor-2, glial cell-line derived neurotrophic factor and GDNF family receptor alpha 1.[198, 199] Indeed other media designed for stem cell culture have been developed for haemopoietic stem cell culture which include 0.5% BSA in StemPro34-SFM media, but this also contains 1% foetal calf serum.[200]

Given the above examples of the use of BSA in media, it seems to have greater utility in the context of maintaining undifferentiated cells and therefore its use in the promotion of proliferation and differentiation of epithelia may be limited. In other experimental models BSA underwent a reaction with glucose to produce advanced glycation end products, which were found to drive lymphocytes towards a pro-inflammatory response.[201] Indeed in the present report, in contrast to the other media protocols tested, the cell density with use of media protocol D resulted in a decline in cell density across all substrates with advancing time. The cell density on treated and untreated

ePTFE was similar but four-fold greater on PET membrane suggesting far greater initial adherence on PET membrane. It would be of benefit to ascertain the nature of the surface chemistry on the Thincert PET membrane however this has been protected from the public domain given that it is a commercial cell culture product.

The initial cell density is similar on PET membrane regardless of the media used suggesting that the initial adherence is superior due to its surface modification rather than media factors. This study also confirmed that cell density is greater on ammonia plasma treated than untreated ePTFE regardless of the media used suggesting that superior adherence occurs on treated ePTFE in comparison to untreated ePTFE. These differences in cell density became increasingly marked with advancing time in culture.

Epithelia are arranged as a sheet of cells on a basement membrane. In general epithelia are recognised to be relatively short in vertical height whereas they are relatively wide and therefore flat in shape.[185] The cell morphology demonstrated following culture in media protocol B on treated ePTFE and PET was therefore in keeping with the expected appearance of epithelial cells in contrast to cells imaged on untreated ePTFE, which were sparse. The phalloidin staining, however, was poor with diffuse staining of cells cultured on the PET membrane. It may be that there is an unknown chemical component, which prevents effective phalloidin staining or that the chemical composition of the membrane itself results in a high degree of background staining. This may be due to the presence of proteins on the polymer surface as part of the surface modification process. The cell morphology on both treated ePTFE and PET membrane demonstrated cellular confluence. A notable difference however was the size of both the nuclei and the size of the cells overall whereby HCjE-Gi cells cultured on treated ePTFE were considerably larger.

4.3.2.3 Summary of the optimisation experiments for the culture of conjunctival epithelium on ePTFE

In summary, these experiments determined that the greatest cell density could be achieved at 14 days in culture with the use of media protocol B and a cell seeding density of $1x10^5/cm^2$. A further advantage of cell culture protocol B is that it is similar to that that defined in other studies used for primary conjunctival epithelial cells.[97, 111, 115]

4.3.3 Consistency of marker expression between passages and demonstration of caspase-3 upregulation in HCjE-Gi cells

4.3.3.1 The HCjE-Gi cell line is consistent in the expression of the range of tested markers between passages 2-28

The HCjE-Gi cell line was used at several passages in this study. Passages 2 and 28 (from arrival of the donated cell line) were developed under the same experimental conditions and the phenotype analysed through flow cytometry. This was undertaken to ensure that there would be consistency in expression of the range of phenotypic markers used in this study between passages.

There are many reports of phenotypically stable cell lines with advancing serial passage, which can be propagated indefinitely. This enables us to exploit the consistency and proliferative capacity of cell lines in experimental work. This was of particular importance in the present study in which it was not possible to derive large cell numbers from the same primary cell source, especially as numerous replicates and variables were required. There are also reports of cell lines such as a human bronchial epithelial cell line, which became spontaneously tumorigenic at passage 184 in vitro-culture.[202] Furthermore, other than a marked transformation, more subtle differences

in phenotype including those due to epigenetic changes (e.g. architecture of chromatin) are recognised caveats of the use of cell lines in experimental conditions.[203]

An alteration in telomerase activity is regarded as a key component in establishing immortality in cells lines.[204] Indeed, the HCjE-Gi cell line was telomerase transformed with hTERT, a telomerase holoenzyme reported to induce replicative immortality without shortening telomeres and without loss of potential to differentiate.[190, 204, 205] Gipson and colleagues developed the HCjE-Gi cell line and confirmed the expression of cytokeratins, membrane associated mucins and MUC5AC mRNA determining that this cell line could be useful in studies of conjunctival mucin gene repertoire.[190]
The cytokeratin markers, together with progenitor cell markers, MUC5AC, PCNA and caspase-3 had not been characterised in the HCjE-Gi cell line. These preliminary experiments therefore sought to determine the 'baseline' level of expression of these markers after 14 days in culture and the proportion of cells expressing these markers with advancing passage. The expression of a range of markers associated with proliferation (PCNA), apoptosis (Caspase-3), progenitor cell markers (ΔN-p63 and ABCG2), cytokeratins 19/7/4 and the goblet cell marker MUC5AC were tested in cells of passage 2 and 28 to ensure consistency. Indeed, no significant difference between cells of passage 2 and passage 28 were demonstrated. It was therefore determined that all subsequent work could be undertaken with the HCjE-Gi cell line within this range of passage without concerns relating to phenotypic change.

4.3.3.2 Caspase-3 expression increases in response to environmental stress

Caspase-3 is involved in the apoptotic pathway and can be found in the cytoplasm of cells destined for apoptosis.[136] The downregulation of caspase-3 has been reported in the context of cancer including breast carcinoma.[206] Caspase-3 has been used as marker of apoptosis in in a variety of cells including cell lines.[207, 208] Nevertheless, since the use of caspase-3 as a marker of apoptosis had not been previously reported in the

HCjE-Gi cell line, this experiment sought to characterise its expression prior to use in subsequent experimental work.

To ensure that caspase-3 would be a useful marker to assess the viability of HCjE-Gi cultures, staining was compared in healthy cells with those exposed to environmental stress to ensure that caspase-3 was up regulated.[209] The findings of this experiment determined a 100-fold increase in expression of caspase-3 with environmental stress. This marker was therefore appropriately upregulated in the cell line and was used as a marker of apoptosis in subsequent experiments.

4.4 Culture of HCjE-Gi and primary conjunctival cells on ammonia plasma treated ePTFE

Preliminary experiments determined that ammonia plasma treated ePTFE could support a growing population of conjunctival epithelial cells as described in section 4.3.2. Initial experiments were also undertaken to determine the optimal seeding density and media that would enable this. The work described in this section describes how HCjE-Gi cell density can be influenced by the exposure of ePTFE to ammonia gas plasma on both sides of the material.

4.4.1 HCjE-Gi cell density is greater on ePTFE subjected to ammonia gas plasma on both sides

An experiment was undertaken to determine how ammonia plasma treatment on one or both sides (referred to here as single or double side treated) of the ePTFE substrate would compare with PET membrane and untreated ePTFE as positive and negative controls respectively. This was undertaken as it was hypothesised that additional ammonia gas plasma modification on the underside of the culture surface could

improve the passage of nutrients from media through the ePTFE membrane. The cell density was determined together with cell morphology and analysis of the cellular phenotype by flow cytometry. The latter is described in section 4.5.1.

The results of this experiment demonstrated a gradual increase in cell density with advancing time across all substrates, which was greatest on PET membrane. Significantly higher cell density however could be cultured on double-side ammonia plasma treated ePTFE than single side ammonia plasma treated ePTFE. Another example of a hydrophobic polymer treated by ammonia gas plasma treatment on both sides of the material to enable cell culture was poly (L -lactide). A study investigated the depth of plasma treatment such that it penetrated both sides of the material and found that the latter enabled the proliferation of cells and promoted proliferation within the scaffold itself.[210] This may be more relevant to this particular type of scaffold, which is biodegradable and therefore cell growth and infiltration from both sides and within the body of the material was desirable. It was hypothesised in the present study, however, that treatment on both sides of the ePTFE material would result in improved transport of water, solutes and proteins across the pores from the basal portion of the ePTFE in contact with culture media and the apical portion supporting epithelia. This was most likely to have an effect after the process of airlifting had begun. Indeed, a marked difference in cell density between single and double side treated ePTFE was apparent but only after 14 days in culture when cultures were in the airlifting phase of the culture protocol.

The cell cytoskeleton comprises intermediate filaments, microtubules and microfilaments.[185] The microfilaments are composed of actin whereas intermediate filaments represent cytokeratins in epithelial cells.[185] The cell cytoskeleton is crucial to cell function including division and movement and therefore also influences the shape of the cell. [185] The microfilaments considered the most abundant protein in animal cells, comprised of actin polymers and are arranged in different ways based upon their

function e.g. as a contractile ring in cell division.[185] Phalloidin stains f-actin and was therefore used to assess the cytoskeletal structure in cells. Unfortunately the phalloidin staining on the PET membrane did not stain the cytoskeletal fibres as clearly as those on ePTFE substrates. Preliminary experiments in the present study found UAE-1 stained the HCjE-Gi cell line such that the cell outline became clearly visible and was also accompanied by variable intracellular staining on both ePTFE and PET substrates. It was therefore was used as a surrogate marker to qualitatively assess cell morphology in addition to phalloidin staining.

The morphology of cells on PET membrane show that cultured cells were smaller in size and assume an epithelioid 'cobblestone' morphology after 14 days in culture that are in keeping with typical conjunctival epithelium.[211] In earlier time points when the density was lower cells appear more 'rounded' across all the substrates. This would be expected given this was at a time when the cell population was expanding e.g. day 2 in culture. Indeed, it has been observed that mammalian cells become round and may even almost detach as they divide.[185] The key morphological differences demonstrated were the appearance of larger cells with proportionately larger nuclei on ePTFE compared with PET membranes by qualitative assessment of representative photomicrographs. Larger cells, high nuclear cytoplasmic ratio, and heterogeneity in the nuclear appearance have been reported as measures of squamous metaplasia in impression cytology specimens. [37, 211, 212] To this end, the cells developed on ePTFE substrates were larger and although this feature may be regarded to constitute as a feature of squamous differentiation, the nuclear cytoplasmic ratios did not appear qualitatively greater. Furthermore, heterogeneity in nuclear appearance was not apparent on ePTFE or PET membrane samples. In squamous metaplasia, the nuclei are also considered to become pathologically altered and described aberrations include double nuclei, nuclear fragmentation and 'snake like' chromatin.[211] Again, these features have not been noted in HCjE-Gi cells on any of the substrates.

All of the grading schemes developed to date are based upon impression cytology and therefore it must be taken into account that the descriptions may be based on loosely adherent cells on the most superficial layers of the conjunctival epithelium and therefore may not be representative of the conjunctival epithelium overall.[37, 211, 212] There are no known grading systems for the assessment of the cross section of conjunctival epithelium or cytoskeletal staining. Nevertheless, the appearance of larger cells may represent a greater degree of squamous metaplasia in the cultures developed on ammonia plasma treated ePTFE. To corroborate these findings it would be imperative in future work to assess the expression of involucrin, a marker of terminal differentiation, squamous metaplasia and keratinisation.[213]

4.4.2 Primary cell culture is similar on double side ammonia plasma treated ePTFE and PET membrane

Through use of the HCjE-Gi cell line, it was demonstrated that greater cell density could be found on ePTFE exposed to gas plasma on both sides of the material rather than treatment of the culture side only. This was repeated using primary conjunctival epithelial cells to determine how cultures developed on double side ammonia plasma treated ePTFE would compare with the PET membrane. The phenotype in terms of a range of intracellular conjunctival epithelial markers was also undertaken and is described in section 4.5.2. This experiment was undertaken to demonstrate the potential of double side ammonia plasma treated ePTFE as a cell culture substrate in comparison to PET, a commercially available cell culture product used in this experiment as a positive control. A limitation of this experiment was the inability to include single side ammonia plasma treated and untreated ePTFE substrate (negative control) cohorts due to lack of available cell number. Unfortunately, only a limited number of cells could be derived from a single donor. Indeed it was imperative to use cells from a single donor for consistency and comparability. The experiment showed that the trend in cell density developed on treated ePTFE mirrored that of PET

membrane, in which both cultures supported a degree of proliferation from day 2 to day 14 in culture, following which a decline occurred. The primary cells may therefore require further exogenous factors and improved culture techniques to enhance their proliferative potential and maintain a population of progenitor cells. Possible methods may include the use of fibroblast conditioned media and/or enrichment with human serum, both of which were shown to increase cell numbers with advancing time in contrast to EGF enriched media shown by Garcia-Posadas and colleagues.[132]

The morphology of cultures on double side treated ePTFE demonstrated cells of similar size and elongated cell processes visible at day 14 that are no longer present at day 28 when cells appear more rounded. Notably, however there was greater variation in nuclear size and shape on ePTFE in comparison to cells on PET membrane. This suggests that these cells were undergoing squamous differentiation based upon conjunctival cytology grading classifications described in the previous section (4.4.1).[37, 211, 212] Another study comparing primary human conjunctival cells with a cell line reported the appearance of elongated shapes to be in keeping with a 'fibroblastic morphology'.[214] A limitation of the present study was that analysis of the presence of fibroblast-associated markers was not undertaken. Given that flow cytometry demonstrated that of 96% or greater cells expressed CK19 (of the same cells in this experiment: section 4.5.2) it seems unlikely that these cells represent fibroblasts per se rather than conjunctival epithelia.

4.5 Phenotype of conjunctival epithelial cultures developed on ePTFE and PET membranes

Flow cytometry was undertaken using the HCjE-Gi and primary cell cultures developed on ePTFE and PET membrane as described in sections 4.4.1 and 4.4.2. This was undertaken to enable quantitative assessment of the expression of a range of

conjunctival intracellular markers to determine the presence of goblet and progenitor cells and to determine whether cells were actively proliferating or undergoing apoptosis. The described analysis was undertaken with respect to the substrate used and advancing time in culture. Comparisons have also been made with regard to overall levels of expression of markers between HCjE-Gi cells and primary conjunctival cells. This was undertaken as these differences were unknown prior to these experiments and would be important for future work.

4.5.1 Differential expression of cytokeratins, UAE-1 lectin and MUC5AC in HCjE-Gi cells and primary human conjunctival cells

Analysis of primary cell cultures was limited to those developed on double side ammonia plasma treated ePTFE and PET membrane whereas the HCjE-Gi cell line was additionally cultured on untreated ePTFE and single-side ammonia plasma treated ePTFE. This was due to a limitation in the number of cells available for primary cell culture since all cells were derived from a single tissue donor. The experiment was repeated on three occasions with cells from a different donor. Determination of the cell density and morphology was undertaken using the same cohort of HCjE-Gi/primary conjunctival cells as that described in this section and has been discussed in sections 4.4.1 and 4.4.2.

4.5.1.1 Expression of cytokeratin 19

- The majority of HCjE-Gi and primary conjunctival cells expressed CK19
- No differences in CK19 expression were determined between substrates or advancing time in culture

In the present study, detection of the CK19 antigen was demonstrated in 96% or greater of the gated cell populations demonstrated by flow cytometry for both HCjE-Gi and primary conjunctival cells on all substrates. There was no significant difference in

CK19 expression between the time points or substrates studied. This indicates that the cells were of a conjunctival epithelial phenotype as CK19 is a recognised marker of conjunctival epithelia, and is not expressed by conjunctival fibroblasts.[125, 132] A study of explant cultures on gelatin sponges found that CK19 was not expressed by the basal layer of cells, which expressed in greater frequency, markers associated with a progenitor phenotype.[215] In contrast, other studies have found CK19 expression in all epithelial layers when developed with serum on a 3T3 feeder layer.[49] The described differences in the literature are likely to be due to differences in culture protocols. Given that a small proportion of cells did not express CK19 in the present study, it may provide an explanation for the less than 100% CK19 expression if it could be further verified that progenitor cells do not express CK19. It would also be in keeping with the proportion of cells expressing ABCG2 alone or ABCG2/ ΔNp63 co-expression discussed in the next section of this thesis (section 4.5.2). Multichannel flow cytometry may provide future opportunities to verify these observations and achieve a better understanding of conjunctival cell developmental biology.

4.5.1.2 Expression of cytokeratin 4

- CK4 expression was markedly higher in primary cell cultures than HCjE-Gi cell cultures
- HCjE-Gi expression of CK4 was lower on double side treated ePTFE on PET membrane
- No significant effect of CK4 expression was found with respect to time in culture in primary cell cultures or HCjE-Gi cell cultures

CK4 expression was almost a 10-fold greater in primary cells in comparison to HCjE-Gi cells after 28 days in culture. It should be noted however that variance was high in primary cell cultures and no significant difference was demonstrated with respect to substrate or advancing time in culture. CK4 expression in HCjE-Gi cultures was greatest on PET membrane and untreated ePTFE and lowest on single and double side ammonia

plasma treated ePTFE. Statistically significant differences were only demonstrated however between double side ammonia plasma treated ePTFE, untreated ePTFE and PET membrane in post hoc analyses. CK4 is used as a marker for non-goblet conjunctival epithelia and is considered to be specific.[11] There have however been variable reports in relation to the patterns of CK4 expression in conjunctival epithelium. Eidet and colleagues found no immunoreactivity to CK4 in primary human conjunctival cell cultures when testing a serum free cryopreservation storage protocol.[139] Garcia-Posadas and colleagues also used the CK4 marker in the characterisation of conjunctival cultures but did not comment on its qualitative or quantitative detection.[132] In contrast, Schrader and colleagues reported CK4 expression through all but the basal epithelial layers in cryopreserved epithelial cultures developed in serum containing media on a growth arrested 3T3 layer, whereas Qi and colleagues reported CK4 in superficial layers of bulbar conjunctiva.[49, 130] Differences in the frequency of CK4 detection between the present study and that by Schrader and colleagues may be due to substrate related factors, differences in media, the specificity of the antibody clone used within experiments or a combination of these. To date, there has not been a study that has characterised the frequency and spatial distribution of CK4 throughout native conjunctival epithelium. Therefore, it is not possible to comment on how the cultures developed on substrates in the present report compare with expression patterns in vivo. Furthermore, the functional relevance of the proportional of cells expressing CK4 is unclear from the existing body of literature. If regarded as a marker of differentiation, it is notable that a significantly greater proportion of primary cells express CK4. The HCjE-Gi cell line data would suggest that cultures may be more differentiated when cultured on untreated ePTFE and PET membrane than ammonia plasma treated ePTFE. This is in keeping with and is inversely proportional to the proportion of progenitor cells and those of a proliferating phenotype described in the next section (4.5.2).

4.5.1.3 Expression of cytokeratin 7

- CK7 expression was similar between HCjE-Gi and primary cell cultures
- A significant increase in expression of CK7 and CK7/UAE-1 lectin co-expression was noted with advancing time in HCjE-Gi cell cultures

CK7 expression was similar in primary conjunctival cells and HCjE-Gi cells after 28 days in culture. In HCjE-Gi cell cultures, however, the percentage of CK7 and CK7/UAE-1 co-expressing cells demonstrated on untreated ePTFE was more than double that of other substrates. In HCjE-Gi cell cultures, but not primary cell cultures, a statistically significant increase in expression of CK7 and CK7/UAE-1 lectin co-expression was found with respect to advancing time in culture. The absence of a statistically significant increase with advancing time in primary cell cultures may relate to the high levels of variance as shown by standard deviation values. In contrast to HCjE-Gi cell cultures, no significant difference was found between substrates investigated in primary cell culture experiments. For both cell types, a similar proportion of cells co-expressed UAE-1/CK7. Interestingly, these values are remarkably similar to the percentage expression of CK7 alone in both HCjE-Gi and primary cells. This would suggest that most CK7 positive cells express UAE-1 lectin but not vice versa. Indeed this is in keeping with existing knowledge that mucin is present in all conjunctival epithelia (e.g. transmembrane mucins on epithelial cells) and is not limited to goblet cells.[17]

Dartt and colleagues have localised the presence of CK7 with Ulex Europaeus Lectin-1 (UAE-1).[11] UAE-1 is a glycoprotein that is recognised to bind with oligosaccharides on the membranes of blood group O erythrocytes but also on human epithelial cells. Given the results by Dartt and colleagues together with the present study, it appears that CK7 and UAE-1 lectin localise to the same cells making it highly likely that these cells are of a goblet cell phenotype. Indeed, Dartt and colleagues hypothesise that CK7+/UAE-1 negative cells may represent a population of immature and actively proliferating goblet cells in their study of the migration patterns from conjunctival explant outgrowth and

differentiation.[134] In this study, the percentage of conjunctival cells co-expressing CK7/UAE-1 lectin increases with advancing time in culture, suggesting the maturation of a subset of goblet cells was in progress. It was also determined that double side ammonia plasma treated ePTFE appears to support a subpopulation of immature goblet cells similar to cultures developed on PET membrane. Improvements in culture techniques, optimisation of biopsy site location and cell purification may result in improved cell density and the development of mature goblet cells on ammonia plasma treated ePTFE in future studies. Further application of multichannel flow cytometry and cell sorting in future studies would also enable verification and further analysis of specific sub populations of cells and further our understanding of conjunctival cell biology and the development of goblet cells in conjunctival epithelial cultures.

4.5.1.4 Expression of MUC5AC

- MUC5AC expression was markedly greater in primary cell cultures than HCjE-Gi cells
- MUC5AC expression was similar between substrates
- MUC5AC expression increased with advancing time in HCjE-Gi cell cultures

MUC5AC was expressed in a 20-fold or greater proportion of primary conjunctival cells in comparison to HCjE-Gi cell cultures regardless of substrate after 28 days in culture. A significant increase in MUC5AC detection in HCjE-Gi cells was found with advancing time in culture but the substrate did not have a statistically significant effect. In primary cell cultures, no statistically significant difference was demonstrated in MUC5AC expression between substrates or time points.

Ang and colleagues developed an ultrathin poly (ε-caprolactone) (PCL) membrane and found marginally higher goblet cell density after seeding primary rabbit conjunctival cells on PCL membrane treated with sodium hydroxide.[97] They suggested that goblet

cell numbers were similar to that developed on amniotic membrane (2-3% of cells), but lower than that observed in vivo (21%).[97] By comparison, the finding in the present study that 15% of cells developed on double side ammonia plasma treated ePTFE express MUC5AC, is the highest reported goblet cell density developed on a synthetic or biological substrate with the use of human primary conjunctival cells. It should be taken into account however that the variance in these measurements was high, which suggests that consistency may be a problem associated with the use of primary cell cultures. Given that variance is markedly lower in HCjE-Gi cells, it would suggest that variance is due to the cells themselves rather than substrate or media factors. It would be of interest to investigate the effect of media constituents, time and culture conditions to improve goblet cell density. Furthermore, it is likely that the location of origin of the explants seeded on the substrate may influence the resulting goblet cell density.[134] It is possible therefore that the random selection of explants contributed to the high variance in primary cell data in this study.

Tsai and colleagues found that mucin antigen and Periodic Acid Schiff was detected in cultures of primary rabbit conjunctival cells developed on collagen and matrigel but not on plastic and glass.[95] The latter study concluded collagen and matrigel as permissive environments for goblet cell differentiation by demonstrating mucin detected using an anti-mucin antibody but did not quantify MUC5AC. A distinction must be made between mucins overall and goblet cell specific markers to enable investigation of goblet cell differentiation. Indeed this is an area that needs developing in future studies and investigation into alternative markers of goblet cells are warranted given that immature goblet cells may not be identified using MUC5AC.[11, 134]

It is known that airway goblet cell differentiation is influenced by the transcription factors SAM-pointed domain–containing ETS-like factor (SPDEF) and forkhead ortholog A3 (FOXA3) resulting in an inflammatory response and goblet cell hyperplasia.[216] The role of SPDEF in conjunctival goblet cell proliferation has been partly characterised,

however its role in chronic inflammation may differ to that observed in airway epithelia given that SPDEF mRNA was deficient in patients with Sjogrens disease in comparison to normal subjects.[217] In future studies, investigation of factors that drive goblet cell differentiation would also be important for conjunctival tissue engineering applications.

4.5.2 Differential expression of markers of progenitor cells, proliferation and apoptosis in the HCjE-Gi cell line and primary human conjunctival cells

4.5.2.1 Expression of ΔNp63

- Expression of ΔNp63 was markedly greater in cultures of HCjE-Gi cells than primary conjunctival cells after 28 days in culture
- No significant effect was found with respect to substrate or advancing time in culture

ΔNp63 expression was almost 3-fold greater in HCjE-Gi cell cultures than primary cell cultures at 28 days and no significant difference was demonstrated with respect to substrate or advancing time in culture. Similarly, in primary cell cultures, no significant differences could be demonstrated in expression of ΔNp63 expression between substrates or advancing time in culture. ΔNp63 has been studied as a marker of progenitor cells in primary cell cultures but not in the HCjE-Gi cell line to the best of my knowledge.[18, 19] The greater percentage ΔNp63 expression in HCjE-Gi cell cultures overall may be accountable to the original telomerase transformation in the production of the cell line and therefore its upregulated replicative ability.

Indeed, ΔNp63 may be a marker that can be identified in both progenitor cells in addition to transiently replicative cells. This would explain the markedly higher levels of expression in the cell line than primary conjunctival cells. Furthermore, it may also explain the higher than expected levels of ΔNp63 in primary conjunctival cells after 28

days in culture. Indeed, the majority of tissue donors from which the primary cells originated were elderly and therefore would be expected to have a lower proportion of progenitor cells. In keeping with this, it has been shown by Stewart and colleagues that the colony forming efficiency was inversely correlated to donor age.[19]

It would therefore be of interest to further investigate the appropriateness of ΔNp63 alone as a marker of progenitor cells. It may be that ΔNp63 must be used in combination with other markers to identify with greater accuracy a true population of progenitor cells. In view of this, the co-expression of ΔNp63 together with ABCG2 has been described (section 5.2.2.2). Future studies using multichannel flow cytometry may be used to determine the true nature of ΔNp63 by analysis of other co-expressed markers of differentiation/proliferation. This may also be confirmed in future work through clonal analysis of individual subgroups of cells defined by their marker expression after fluorescence activated cell sorting.

5.2.2.2 Expression of ABCG2 and co-expression with ΔNp63

- ABCG2 expression and co-expression with ΔNp63 was similar in HCjE-Gi and primary conjunctival cells
- ABCG2 expression and co-expression with ΔNp63 in HCjE-Gi cell cultures was highest on double side treated ammonia plasma treated ePTFE after 28 days in culture

In contrast to ΔNp63, ABCG2 was expressed at similar frequency in both the HCjE-Gi and primary conjunctival cells at 14 and 28 days in culture. No significant effect of substrate or time in culture could be determined with respect to ABCG2 expression in primary cell cultures. Amongst HCjE-Gi cell cultures, ABCG2 expression was highest on double side ammonia treated ePTFE and statistically significant differences were found between this, untreated ePTFE and single-side ammonia treated ePTFE in post hoc analyses. In both cell line and primary cultures, ABCG2/ ΔNp63 co-expression was

remarkably low at 1% or less after 28 days in culture. No statistically significant difference was found with regard to ABCG2/ ΔNp63 co-expression in primary cultures with respect to advancing time or substrate. In HCjE-Gi cell cultures however, the percentage of cells co-expressing ABCG2/ ΔNp63 was highest on double-side ammonia plasma treated ePTFE and statistically significant differences were found between this, untreated ePTFE, single sided ammonia plasma treated ePTFE and PET membrane on post hoc analysis. Although this pattern mirrors that of ABCG2 expression alone in HCjE-Gi cells, it should be noted that the proportion of cells co-expressing ABCG2 and ΔNp63 is markedly lower than that expressing ABGC2 alone in both primary and HCjE-Gi cultures. It follows therefore that not all ABCG2 expressing cells also express ΔNp63. The results from our study would suggest that the highest proportion of progenitor cells developed on double side ammonia treated ePTFE, however this was confirmed only with cell line data. Variance is high in the primary cell data and is likely to be due to differences in the seeded explants in terms of the biopsy site from which the explant originated. Further studies using greater numbers of donors and consistency in the tissue biopsy site are warranted to corroborate the findings of this experiment. The optimisation of culture conditions together with improvements in techniques to isolate and seed a purified sample of conjunctival epithelial cells may enable primary cell cultures in the future to be developed on ammonia plasma treated ePTFE with a greater proportion of progenitor cells and potential for self-renewal.

ABCG2 and ΔNp63 have been studied together in a study of the colony efficiency assays of conjunctival tissues from various sites.[19] The latter report demonstrated highly significant correlations between the clonogenic ability of conjunctival explants and the levels of both ABCG2 and ΔNp63 expression.[19] In keeping with this, it has been observed in other studies that the density of cells expressing these markers reduce with advancing passage.[49] Although there are no definitive markers of conjunctival stem cells, the markers used here within the present studies have been the most extensively studied. As findings from this study show, not all cells expressing ABCG2

appear to express ΔNp63. The use of both markers, however, may identify with greater sensitivity, a subpopulation of cells that represents a true progenitor cell population. Furthermore, it also suggests that ABCG2 alone may be superior to ΔNp63 in its ability to detect progenitor cells. In keeping with results in the present study, ABCG2 expression, but not ΔNp63 has been shown to correlate significantly with the colony forming efficiency of primary conjunctival epithelial cultures and is inversely correlated to donor age.[19] It is of interest to note that the ΔNp63 antibody would identify ΔNp63α that is otherwise considered a stem cell marker.[9] The results of the present study however together with observations by Stewart and colleagues would suggest otherwise.[19] To investigate stem cell marker expression and corroborate the observations of the present study, the clonogenic ability of cultures of cells in relation to the expression and co-expression of candidate stem cell markers warrants further study. Furthermore, the use of a more specific antibody clone, for example ΔNp63α instead of ΔNp63, which detects all isoforms (α/β/γ), should also be undertaken to determine the precise location and phenotype of progenitor cells and the relative frequency and relevance of cells of each of the ΔNp63 isoforms.

4.5.2.3 Expression of caspase-3

- Caspase-3 expression is greater in primary conjunctival cell cultures
- Greater caspase-3 expression was demonstrated on untreated ePTFE in HCjE-Gi cultures

Caspase-3 expression was more than double in primary conjunctival cells overall compared to HCjE-Gi cells at the time points studied. In primary conjunctival cell cultures, no significant effect could be demonstrated with respect to advancing time in culture or substrate. Similarly, there was no significant difference in caspase-3 expression in HCjE-Gi cell cultures with advancing time in culture but substrate had a significant effect whereby the highest levels of caspase-3 expression were found on untreated ePTFE. Given that statistically significant differences were found only

between untreated ePTFE and all other substrates studied in post-hoc tests for HCjE-Gi cells, it would suggest that all substrates with the exception of untreated ePTFE were equally capable of supporting conjunctival cell cultures without inducing high levels of apoptosis.

A limitation of this work is that the untreated ePTFE substrate was not tested using primary cell cultures owing to a shortage of available cells to use. It is therefore not possible therefore to comment on the expression of the apoptosis marker on primary cells cultured on untreated ePTFE. These data, however, suggest that there was no significant difference between primary conjunctival epithelia developed on treated ePTFE and the PET cell culture membrane. This represents proof of concept that double side ammonia plasma treated ePTFE could be an effective substrate for primary conjunctival cell expansion and warrants further investigation. To the best of my knowledge, there are no other reports in the literature describing use of caspase-3 in the development of conjunctival substrates. There is therefore no available comparison to determine the relative caspase-3 expression in the present study. A study of the effect of hypoxia and staurosporine on endothelial cells however also determined the levels of caspase-3 as a percentage of the cell population by flow cytometry.[218] This study demonstrated 5.9% caspase-3 expression in a healthy population, compared with 9% in endothelial cells exposed to hypoxia and 24% in cells exposed to staurosporine (an inhibitor of protein kinases used as a research tool to induce apoptosis). Similarly, in the present study around 20% of HCjE-Gi cells expressed caspase-3 at 28 days in culture when developed on untreated ePTFE compared with <5% expressing caspase-3 on treated ePTFE and PET membrane. These observations would also suggest that caspase-3 would be an appropriate marker of apoptosis to use in future studies of conjunctival epithelial cultures.

4.5.2.4 Expression of PCNA

- PCNA expression is markedly higher in HCjE-Gi cell cultures at day 28
- PCNA expression declines in primary conjunctival cells but not HCjE-Gi cells with advancing time in culture

No significant difference was found with respect to the percentage PCNA expression in HCjE-Gi cell cultures with advancing time in culture or between substrates. Similar levels of PCNA expression were found in primary conjunctival cell cultures developed on treated ePTFE and PET substrates after 28 days suggesting an equivalent ability of double side treated ePTFE to support cell proliferation. In contrast to HCjE-Gi cells, however, a statistically significant difference in PCNA expression occurred whereby expression levels approximately halved from 14 and 28 days in culture. The percentage PCNA expression in HCjE-Gi cells was approximately double that of primary cell cultures at 28 days in culture.

The observed trend of PCNA expression in HCjE-Gi cells with advancing time was similar to that of ΔNp63. The reasons of the observed differences in the primary cells and the HCjE-Gi cell line may be due to reasons mentioned in earlier sections. It would be of interest in future studies to correlate PCNA expression to markers associated with stem cells to determine methods to distinguish transiently amplifying cell populations from 'true' stem cells.

Eidet and colleagues described PCNA expression by immunohistochemistry in conjunctival tissue samples in approximately ¾ of cells through a semi-quantitative analysis.[139] This study was designed to determine the effect of storage free media after 4 and 7 days. It must be noted however that the time points, media used and technique used (immunohistochemistry) differs to the present study. It follows therefore that the optimal or baseline frequency of PCNA expression in conjunctival epithelial cell cultures has yet to be established in the context of developing substrates.

Nevertheless, the finding of similar levels of PCNA expression between double side ammonia plasma treated ePTFE and PET membrane even in primary cell cultures suggests that the former warrants further investigation.

4.6 Decellularised human conjunctiva

Decellularised tissues have been used as scaffolds for the re-population of cells in a variety of tissue and organ models. The decellularisation of human conjunctiva, however, has not been previously. Described in this section is the developed protocol for the decellularisation of human conjunctiva and characterisation of the resulting tissue in terms of its cytotoxicity, DNA content, collagen denaturation, basement membrane and tensile strength. Comparisons have been made between the basement membrane of amniotic membrane and human conjunctiva. The tensile strength of conjunctiva is also compared with amniotic membrane and ePTFE.

4.6.1 Decellularisation and cytotoxicity of human conjunctiva

Decellularisation can be achieved using a variety of chemical, enzymatic and physical processes. Sodium dodecyl sulphate (SDS) was the agent of choice to optimise in the present study. This step was part of an established decellularisation protocol used for the decellularisation of amniotic membrane. Decellularisation of amniotic membrane has been previously described by physical removal alone or in combination with chemical agents and detergents including ammonium hydroxide, SDS, sonication and trypsin.[219-222] Of these methods, only SDS achieved high levels of cellular removal from the tissue matrix.[77] This detergent has been also been reported to successfully decellularise other tissues including porcine heart valves.[223] The lack of observed cell mediated or humoral immune response in the recipient to decellularised tissue has

been proposed to be due to the removal of soluble proteins during the decellularisation process.[224]

In this report, the decellularisation protocol that utilised SDS at a concentration of 0.05% (w/v) removed 99% or greater DNA with reproducibility across donors. This was also confirmed in histology specimens, whereby the absence of nuclear DAPI staining in decellularised tissue sections was demonstrated. Adequate decellularisation is of paramount importance as the presence of DNA has been directly correlated to adverse responses in the recipient, an effect that is most notable in xenogeneic transplantation.[225, 226]

Decellularised tissue per se has not been strictly defined in terms of residual DNA content. Results from in vivo studies in which tissue remodelling has been demonstrated in the absence of an adverse host immunological response suggest 90-95% decellularisation is adequate.[77, 173] It follows therefore that a decellularisation protocol using 0.05% SDS (w/v) to decellularise conjunctival tissue meets these previously defined standards.[77] Amniotic membrane closely resembles conjunctiva given that it also comprises an epithelial cell layer, basement membrane and a thin layer of underlying loose connective tissue.[54] Amniotic membrane can be decellularised with 0.03% SDS which removes 95% of the DNA.[227] This is comparable to DNA removal shown in the present study. A limitation of the present study, however, was that SDS at a concentration lower than 0.05% was not studied. In future work, it would be of interest to test lower SDS concentrations and correlate the DNA removal against additional parameters such as elastin and glycosaminoglycan quantification.

In the present study, decellularisation was achieved through a combination of chemical, detergent and enzymatic steps. In the first stage cell lysis was achieved through osmosis using a hypotonic buffer. It has been suggested that this occurs with minimal alteration in the architecture of the tissue.[89] In the second stage, dissolution

of the lipid bilayer of the cell membrane and removal of cellular residues was achieved through the use of SDS. In the final stage, Benzonase was used to remove any residual nuclear material from the tissue matrix. Hypotonic and hypertonic reagents are known to be effective in lysing cells but may leave cellular residues.[77] The removal of cellular residues however is known to be effected by SDS.[77] It has been demonstrated to effectively remove nuclear and cytoplasmic remnants from even dense tissues, but a disadvantage is that it may damage collagen matrices.[77, 228] Of these described stages, the SDS is known to have the greatest potential for cellular cytotoxicity.[77] Indeed, multiple washes and rinses of the tissue take place as part of the protocol to leach as much of the SDS out of the residual tissue as possible. The results from the contact cytotoxicity experiments in this study demonstrated that both primary human skin fibroblasts and the human conjunctival cells proliferate in close contact with the decellularised tissue demonstrating that the tissues lack cytotoxicity. In later sections, this is also demonstrated by the culture of explants on decellularised tissues (section 4.7).

4.6.2 Quantification of collagen denaturation

To test whether the decellularisation process would disrupt conjunctival collagen matrices, an assay to test collagen denaturation was undertaken. This rationale for undertaking this experiment was that exposure to SDS is known to disrupt collagen matrices.[77, 228] Our study found however that at a concentration of 0.05% (w/v) SDS, there was no increase in hydroxyproline within the supernatant in the collagen denaturation assay. This indicated that there was no disruption of conjunctival collagen matrix as a result of decellularisation. Hydroxyproline was detectable in this assay following exposure to α–chymotrypsin, an enzyme that selectively denatures only degraded collagen.[229] These data therefore suggest that an SDS concentration of 0.05% (w/v) may represent a favourable balance between decellularisation and tissue disruption in human conjunctival tissue. This collagen degradation assay is useful as it

provides quantitative data to support the qualitative examination of other extracellular matrix proteins through histology, described in later sections (section 4.6.4). More detailed studies investigating the degradation of other components such as elastin and glycosaminoglycan content are warranted in future work. Importantly, examinations of the ultrastructural features of the tissue are also warranted to confirm the integrity and examine the 3-dimensional architecture following decellularisation. The ultrastructure may be studied by scanning electron microscopy in future work.

4.6.3 Tensile strength of conjunctiva, amniotic membrane and ePTFE

The effect of decellularisation on the tensile strength of conjunctival tissue was determined together with data of the tensile strength of amniotic membrane and ePTFE for comparison. Tensile strength results demonstrated no significant difference in the ultimate tensile stress (MPa) or Young's modulus (MPa) between cellular and decellularised tissue suggesting that biomechanical strength is not altered by the decellularisation treatment. This is in keeping with other tissue models comparing cellular and decellularised tissue.[173, 230, 231] The tensile strength measurements are relatively low for both conjunctiva and amniotic membrane in terms of their absolute values in comparison to other characterised tissues such as dermis and cartilage.[173, 230, 231] No other published work can be found in which the tensile strength of conjunctiva has been characterised.

Stress at failure measurements have been previously reported for amniotic membrane and were approximately half the reported values in this study.[227] It is recognised that differences between observed values may be derived when using different equipment, and that such differences have not been entirely explained in other reports.[232] There are a however, a number of crucial differences in the testing method, in the present study compared to that by Wilshaw et al. In general, the methodology for tensile strength testing involves the cutting of dumbbell shaped sections that are therefore

constant in length and also width, and the wider portion at both ends are inserted into the clamps. This method was not possible for the assessment of both conjunctival and amniotic membrane in the present study as the standard dumbbell shapes were small, leaving thin friable sections of tissue that would break or become damaged during the process of insertion into the test clamps or would slide through the test clamps altogether. To enable testing to take place, larger rectangular sections of tissue were divided and measured for the test. The tests in this report measured the thickness of the amniotic membrane at 3 different points by placing the tissue flat between two glass coverslips. This method resulted in mean thickness values for amniotic membrane of 0.055 mm in this study, which contrasts to that by Wilshaw and colleagues, who measured mean thickness values of amniotic membrane as 0.16mm. Although the stress measurements would normalise the effect of thickness, the method used to measure thickness of the tissues differs between the present study and that by Wilshaw and colleagues. In addition, the speed of tensile test, which was not reported, may have differed in addition to other factors including the type of grips used to hold the material. It is possible that these factors, in particular the thickness measurements of amniotic membrane may explain the observed differences.

The young's modulus has not been previously characterised for amniotic membrane. Young's modulus is a measure of stiffness of an elastic material. The stiffness of a material itself has been recognised to influence the cellular phenotype.[233] It is of interest to note a 3-fold greater Young's modulus of amniotic membrane in comparison to conjunctiva indicating greater stiffness. Indeed it has been recognised that amniotic membrane has a thick basement membrane, which may account for these observations.[49]

It would be of interest to undertake further tensile strength testing to ascertain the suture pull out strength. This may be of particular relevance given that the materials investigated are intended for eventual surgical use. Tensile strength characterisation is

useful given the current scientific climate in which synthetic materials are also under investigation as conjunctival substrates.[97] Importantly, the stiffness of materials is known to influence cell attachment, proliferation and differentiation.[228, 233, 234] The precise subtypes of extracellular matrix components and stiffness of the decellularised conjunctiva are not greatly altered by decellularisation. This 3-dimensional scaffold would otherwise be difficult to replicate in synthetic materials. It might be expected therefore, that decellularised conjunctiva would possess the greatest potential to support conjunctival epithelium with a subpopulation of progenitor and goblet cells by providing the most appropriate niche for these cells.

4.6.4 Characterisation of the extracellular matrix components and basement membrane of cellular and decellularised tissues

Decellularisation may reduce the risk of disease transmission but may disrupt extracellular matrix components and the ultrastructure of the tissue.[77] The histology and immunohistochemistry qualitatively demonstrate that there is no disruption of the extracellular matrix as a result of the decellularisation process.
Histology of the tissue sections stained with H&E and Van Gieson's stain demonstrate that there is preservation of the architecture of the tissue including the major structural proteins elastin and collagen. Glycosaminoglycans were also strongly localised to the basement membranes and conserved following decellularisation.

The extracellular matrix components laminin, fibronectin and collagen IV do not appear changed following decellularisation. This is apparent qualitatively in terms of the distribution of laminin, fibronectin and collagen IV staining through immunohistochemistry. The absence of collagen degradation is also supported quantitatively in terms of the detection of denatured collagen as described in the previous section (section 4.6.2). Laminin, fibronectin and collagen IV was found in the basement membrane zone and epithelium of conjunctival tissues, a staining pattern

that has been previously described by immunohistochemistry.[15] The PAS and H&E staining also confirmed that the basement membrane layer appears unchanged by decellularisation.

Tissue samples from three different donors were examined for distribution of collagen IV, laminin and fibronectin in both conjunctival tissue and amniotic membrane. This qualitatively demonstrated that there were no significant differences in the distribution of these proteins in either tissue between different donors. Differences were observed, however, in the distribution of collagen IV, laminin and fibronectin between conjunctiva and amniotic membrane. The basement membrane of amniotic membrane had greater qualitatively staining than the substantia propria for all three proteins studied. All the investigated proteins were present in the basement membrane of conjunctiva; however, their presence in the substantia propria was present qualitatively to a greater degree than amniotic membrane. Laminin appears mostly within basement membranes of conjunctiva whereas fibronectin appears almost as abundant within the basement membrane as the substantia propria of conjunctiva. The distribution of type IV collagen and laminin isoforms in amniotic membrane have been studied and reported to be similar to that of conjunctiva but differ from corneal basement membrane.[3] It has therefore been suggested that amniotic membrane may therefore act as a suitable substrate for conjunctival expansion.[12] The latter study by Fudaka and colleagues highlights potentially important differences in extracellular matrix composition between amniotic membrane and conjunctiva. In particular, the greater fibronectin composition of the substantia propria of the conjunctiva could serve as a preferential environment to the co-culture of conjunctival fibroblasts.[235] The results in this study also demonstrated that there is far greater variability in the tissue thickness and architecture of the conjunctival samples in comparison to amniotic membrane between the donor samples studied. Ultimately, this may limit its future utility given limitation in the availability of large sections of tissue of an optimal quality.

The qualitative methods used for the characterisation of extracellular matrix have their merits as they provide information about the distribution patterns and microscopic appearance of tissues, which quantitative assays such as the collagen degradation assay cannot provide. It is imperative therefore that both qualitative and quantitative analysis occurs in parallel. A limitation of the immunohistochemical methods are the variability of staining that is observed under the same experimental conditions and even along the same tissue section. The grading of tissue sections for strength of staining therefore may be unreliable. It follows therefore, that immunohistochemical staining serves more utility in being able to identify the absence or presence of staining in comparison to a negative control. It does however provide useful information regarding the distribution of the antigen of interest. As stated previously, a more detailed study of the ultrastructure, degradation of other components such as elastin, glycosaminoglycan content and importantly, ultrastructural features are warranted. Furthermore, only the major groups of extracellular proteins have been characterised in this study. There are opportunities in future work to characterise precise isoforms e.g. of laminin in comparison to other biological substrates and amniotic membrane.

4.7 Culture of primary human conjunctival cells on decellularised conjunctiva and amniotic membrane

The protocol for the decellularisation of human conjunctiva was developed and the resulting tissue characterised (section 4.6). The tissue was not cytotoxic and the extracellular matrices and tensile strength were not significantly altered by decellularisation. Techniques for the culture of human conjunctival epithelium on decellularised conjunctiva were developed in this study. Experimental findings are discussed together with the limitations of the study and opportunities for further research. The key findings from this study are summarise overleaf.

- Seeding decellularised tissues with conjunctival tissue explants resulted in qualitatively greater cell density in comparison to seeding a cell suspension.
- Confluent epithelial growth occurred when explants were cultured in contact with the basement membrane of decellularised conjunctival tissue.
- There was marked variability in the conjunctival epithelial cell growth from explants from different donors and decellularised conjunctiva from different sources.
- A stratified conjunctival epithelium was developed from explant culture on freshly decellularised conjunctival tissue.
- The stratified conjunctival epithelial construct was demonstrated to express conjunctival epithelial markers including CK7, sparse MUC5AC staining and progenitor cell markers

4.7.1 Cell culture experiments and characterisation of the developed tissue constructs

Preliminary primary cell culture experiments found that seeding decellularised tissue with conjunctival explants resulted in confluent epithelial cell growth whereas seeding the decellularised tissue with a cell suspension resulted in sparse cell growth. Indeed, the isolated cell suspension had been initially expanded on tissue culture plates from explants. The cells were therefore at a more advanced passage and seeded after 7 days in culture in comparison to explants, which were seeded within hours of retrieval. One of the reasons that the explant cultures develop more successfully than isolated cells may be that any stem cell 'niche' may have been preserved in its native state and was therefore more capable in supporting proliferation and differentiation.

The orientation of tissue was crucial such that cellular expansion occurred more effectively when cells were cultured in direct contact with the basement membrane. In the earlier section, the distribution of laminin, collagen IV and fibronectin was

described to localise strongly to the basement membrane with less expression in the substantia propria (section 4.6.4). Cell-extracellular matrix interactions are therefore of paramount importance for proliferation and differentiation.[185] In keeping with this, differential signalling patterns have been identified in conjunctival epithelia based upon interactions with specific isoforms of laminin.[187]

Results from this study comparing decellularised tissue from three donors with explant tissue from three further donors demonstrated variability in the potential of explants to develop on decellularised conjunctiva. The variability may be explained by differences in the donor age, post mortem retrieval time, and location from which the conjunctival explants originated. Studies on biopsy location in relation to the colony forming efficiency have been undertaken and it is of interest to note that increasing length of the post-mortem retrieval time and advancing donor age significantly lower both the clonogenic ability and expression of progenitor cell markers in culture.[19] Nevertheless, the majority of donors used within this study were elderly and given the small sample size, it is not possible to determine if these were major contributing factors. It was however of interest to note that the two of the later culture attempts in which fresh samples of decellularised tissue were used resulted in cultures with greater cell density, confluence and even became multi-layered constructs. A study investigated the effect of freezing prior to decellularisation of human umbilical cord and demonstrated that condensation of the extracellular matrix lead to greater residual DNA following decellularisation.[236] Reports on other tissue types in which tissue was frozen following decellularisation could not be found. It would be of interest in future work to determine whether freezing changes the ultrastructure and potentially influence culture potential.

Immunohistochemistry using one of the later multi-layered developed conjunctival constructs confirmed that the resulting stratified epithelium was of a conjunctival phenotype expressing CK19, CK7 and CK4 typical to conjunctival epithelium.[10, 127, 134]

CK7, regarded as goblet cell marker was found throughout the tissue sections suggesting the presence of goblet cells with the potential to produce mucin.[11, 134] Dartt and colleagues hypothesise that CK7+/UAE-1 negative cells may represent a population of immature goblet cells that may have proliferative capacity and potential to develop into mature goblet cells in their study of the migration patterns from conjunctival explant outgrowth and differentiation.[134] Unfortunately, UAE-1 lectin was not used as a marker in these immunohistochemistry studies in addition to CK7 and MUC5AC. MUC5AC is a gel forming mucin found exclusively in mature goblet cells.[11] Its expression was sparse but detectable, which may suggest the presence of immature goblet cells given the degree of CK7 staining.[133] To the best of our knowledge, this is the first conjunctival substrate-culture study in which CK7 positive conjunctival cells have been demonstrated. Furthermore, ex vivo cultivated human conjunctival epithelial grafts on amniotic membrane have not been shown to support mucin producing conjunctiva and therefore decellularised conjunctiva may be superior substrate than amniotic membrane for conjunctival expansion.[58, 68]

Markers of progenitor cells ΔNp63 and ABCG2 were also present in lesser frequency, with ABGC2 expression less abundant than ΔNp63. This would be in keeping with the quantitative analysis of conjunctival epithelial cell cultures on synthetic substrates described in section 5.2.2. Levels of PCNA expression appeared similar to that of ΔNp63. Caspase 3, a marker of apoptotic cells was also present and appeared to be expressed in apical rather than basal cells, in contrast to the other cell markers studied which appear to be more evenly distributed. This would be in keeping with the assumption that older cells that would be lost are more apical and would be replaced by basal cells, which may be at an earlier stage of differentiation. Indeed the distribution of these markers in healthy conjunctiva is poorly characterised in the literature. It would be of interest in future work therefore, to characterise the distribution of the markers investigated in this study in healthy conjunctiva and between different sites. Furthermore, a quantitative analysis of marker expression is

also warranted for both conjunctival tissues in addition to constructs expanded from explants. The evidence from this experiment, however, would suggest that the conjunctival construct had potential for self-renewal and supported a population of actively proliferating cells.

4.7.2 Limitations of the study

One of the problems associated with seeding primary conjunctival cells on decellularised tissue is the lack of cell number when cells are isolated from the tissues prior to culture and directly seeded. This was circumvented by the use of conjunctival explants in the present study. From the outset of the experiments, however, the cell numbers seeded or the growth potential of the explants (determined by factors such as the anatomical location of origin from the conjunctiva and donor age) were not controlled. This could be addressed in future work if a greater sample number is available.

A limitation of this study was that direct comparisons were not made between the phenotype of conjunctival cultures developed on decellularised conjunctiva and amniotic membrane. The potential benefits of amniotic membrane cannot be ignored. The young's modulus of amniotic membrane is higher than that of conjunctiva and there is greater consistency in the tissue architecture of amniotic membrane than that demonstrated between conjunctival samples. Given that conjunctiva would be derived from a cadaveric source, most donors will be elderly in whom the effects of tissue degeneration cannot be ignored. Human amniotic membrane is thought to promote cell adhesion and differentiation.[237] It is also recognised that the stromal matrix contains an abundance of foetal hyaluronic acid, which aids in the reduction of scarring via a TGF-ϒ pathway and also supresses pro-inflammatory cytokines.[237] It is yet to be determined how transplanted decellularised conjunctiva will compare in this regard.

Decellularisation may reduce the risk of disease transmission but may disrupt extracellular matrix components, the ultrastructure of the tissue and remove soluble proteins including growth factors.[65] The results from this study however do not suggest any alteration in the distribution of the major extracellular matrix proteins, glycosaminoglycan content by PAS staining or denaturation of collagen through a quantitative assay. Further analysis of other extracellular matrix components and tissue ultrastructure however is warranted.

4.8 Characterisation of patients with MMP and potential ocular surface reconstructions strategies

Mucous membrane pemphigoid can lead to painful loss of vision and in its most severe form can be life threatening. The onset of MMP is notoriously insidious, can be difficult to diagnose and often the presentation is delayed.[36] Treatment involving immunosuppression is crucial in active disease and to prevent or reduce the risk of disease progression. To this end it is important that objective and robust grading systems are developed and used to i) identify patients in need of treatment ii) monitor progression and treatment response. In this study, a novel pro forma was developed as a tool for use in corneal and external eye disease clinics to assess patients with mucous membrane pemphigoid.

4.8.1 Development of a pro forma to assess mucous membrane pemphigoid patients

A number of methods have been described for the grading of ocular mucous membrane pemphigoid without any consensus on the optimal method for use. To compare the scores of the grading systems, all well-known methods including that by Rowsey, Mondino and Foster, Tauber and the Tauber-Liverpool were included in the

pro forma.[46, 153-156] It should be noted that these methods grade cicatrisation and therefore the sequelae of disease without any assessment of the degree of inflammatory activity. To overcome this, Saw and colleagues developed a method for assessing disease activity based on the degree of conjunctival and limbal inflammation.[163, 164] This was therefore also included as part of the pro forma developed and used within St Pauls Eye Unit in consultation with the Corneal and External Eye Disease team. Also included, as part of the pro forma were photographs, fornix rule measurements, grading of lid deformities, presence/absence of trichiasis, presence/absence of lagophthalmos, and documentation of dryness according to The Oxford grading scheme. [158]

The adapted versions of existing grading schemes used for the assessment of lid deformities including grading of ectropion, entropion, the documentation of trichiasis and lagophthalmos as shown in the developed pro forma have not been validated for use as a measurement tools (Appendix). Furthermore, other components of the pro forma such as documentation with photographs in addition to anterior segment drawings also require formal validation studies. The aim of this process was to develop and pilot a pro forma that could be developed further for use in the clinic to identify patients that may benefit from ocular surface reconstruction and adjunctive therapies to reduce the risk of cicatrisation. To this end, it would be of interest to undertake validation studies in the future to assess the inter-rater and intra-rater reliability of the grading scales developed for use in this pro forma. In addition, it would be of interest to formally assess the time taken for completion of the pro forma and also the utility of anterior segment drawings in combination with photographic evidence for the documentation of disease activity and progression in MMP.

4.8.2 Characterisation of the patient examined using the novel pro forma

The patients examined as part of this pilot scheme were opportunistically sought from corneal and external eye disease clinics at St Paul's eye unit. All the patients were therefore under active follow up for ocular mucous membrane pemphigoid or were being monitored as they were receiving immunosuppression. None of the patients seen were treated for any cicatricial disease process other than ocular mucous membrane pemphigoid. This would be in keeping with the known incidence of conditions classed as cicatrising conjunctivitis in which mucous membrane pemphigoid affects the greatest proportion of patients.[36] Furthermore, many other conditions e.g. ocular burns undergo an active period of follow up following, which they may be discharged if stable, in contrast to ocular mucous membrane pemphigoid.

All the examined patients were graded as III (Tauber) in one or both eyes. All patients also had one or both eyes ≥60% vertical involvement and ≥50% horizontal involvement, and four out of five patients with a Rowsey score ≤50% of the total score. The grading scheme suggested none of the patients had significant corneal involvement and dryness (oxford grading scheme) was mild. Trichiasis was however a significant problem affecting eight of ten eyes examined. In terms of lid deformities, only one eye had a lower lid deformity. No upper lid deformities were recorded and this was in keeping with the pattern of cicatrisation in ocular mucous membrane pemphigoid. These data show that the group of patients examined had moderate to severe ocular mucous membrane involvement.

4.8.3 Pilot exercise to develop recommendations for a pro forma

Some of the problems with the pro forma became apparent during the pilot tests. The fornix rule was approximately 1mm thick. It became apparent therefore that it underestimated the true depth of the fornix. For example, in the patient photographed in Figure 97, the inferior fornix depth was measured as 0mm. The fornix ruler

measurements would however prove useful, particularly in the assessment of the superior fornices, which are otherwise difficult to assess and rarely documented.[157] Recommendations from this pilot are therefore to develop an alternative ruler that is sufficiently thin, long and curved to be inserted comfortably within fornices or use that designed by Williams and colleagues that has already undergone validation tests.[157]

The inflammatory score was easy to assess and was time efficient, taking on average around 2 minutes to complete. Some difficult was noted however in differentiating between 'minimal' and 'mild' inflammatory grades, however, advanced grades were easy to score. This grading system has been used in clinical trials however validation and further investigation into its inter-rater and intra-rater reliability may provide further opportunities for its improvement.[163, 164] My recommendation would be therefore to use the scoring system for disease activity following formal validation as there are no other available validated scoring systems. Furthermore, it is of paramount importance to include a tool for grading conjunctival inflammation, as it is the only available measurement of disease activity. In contrast, all other graded features measure disease sequelae. In end stage or near end stage ocular disease, however, it may be difficult to assess disease activity. This was demonstrated in the present study (patient 4, Figure 101). Although activity at alternative sites such as the oropharynx could be used, it is unclear whether this would mirror ocular activity. In the study by Reeves and colleagues, no correlation was found between the graded scores for the eyes and oropharynx. The score for the oropharynx, however, graded activity whereas the score for the ocular involvement measured cicatricial and therefore structural change. Future work to compare activity scores at multiple sites would therefore be warranted in patients who have extra-ocular manifestations of mucous membrane pemphigoid.

The presence or absence of trichiasis and lagophthalmos were included in the pro forma and could be assessed within minutes. Similarly, the Oxford grading scheme for

dryness, grading of lid deformity and corneal involvement were relatively quick to score. The ease of administration of the pro forma was determined by comparing the scoring tool with a tool designed to document a much greater level of detail designed by Rauz and colleagues, Birmingham and Midlands Eye Centre, Birmingham. The latter tool took approximately and hour to complete whereas the developed pro forma took approximately 20 minutes in total. Components of the information gathering process including eyelids, adnexa in addition to ocular dryness are important to note in the assessment of MMP patients as they may alert the clinician to initiate supportive interventions in a timely manner to prevent or delay the desiccation of ocular surface epithelia. The documentation of corneal signs provides an indication of the visual impairment and need for medical or surgical management. The treatment of a central corneal defect, for example, may be required, whereas peripheral corneal signs pathology such as limbitis or corneal vascularisation indicates a potential need for future limbal stem cell transplantation. This information is important when planning the sequence of ocular surface reconstruction.

There were insufficient numbers of patients examined as part of this pilot to comment on the correlation and agreement between the various methods of grading cicatrisation. It has been determined however that good levels of agreement exist between the Rowsey score and the Tauber-Liverpool.[156] Rowsey and colleagues have also demonstrated that their grading scheme is concordant with that of Tauber and Mondino and Brown. [46, 154, 155] During this pilot experiment, when using all the described grading schemes it became apparent that there was some overlap. Some grading systems prompt more detailed assessment of cicatricial features e.g. the Tauber scheme provides further subdivisions to that by Mondino and Brown, and the Liverpool scheme provides more accurate quantification that builds upon the existing Tauber scheme.[46, 154, 156] The Liverpool-Tauber scheme may detect more subtle structural progression than the Tauber grading scheme alone although the Tauber grading scheme is sensitive to tarsal conjunctival change. My recommendation based

on the pilot work therefore would be to grade cicatrisation as described on page 2 of the pro forma which includes the Tauber-Liverpool measurements together with the Rowsey scheme on the following page (Appendix 1). By doing so, there would be no need to also include the Foster and Mondino and Brown grading scheme as there is already overlap between these measurements.

4.9 Treatment of cicatrising eye disease and the potential use of the substrates developed in this study

There is no consensus on the degree of cicatrisation that would specifically warrant surgical ocular surface reconstruction. Some studies have suggested that 'pathogenic' symblephara may be defined by dry eye from interruption of spread of tears, blink related microtrauma from an irregular tarsal surface, cicatricial entropion, exposure due to lagophthalmos and restriction of ocular motility.[240] Furthermore, it is imperative that the disease process is controlled prior to any surgical intervention otherwise a marked inflammatory response in the post-operative period would compromise the success of reconstruction.

Of the patients studied, the right eye of patient 4 would warrant ocular surface reconstruction given the degree of symblepharon and almost complete obliteration of the inferior fornix in the right eye. The surgeon would need to be wary of the fact that signs of active disease were present in the fellow eye and delay treatment even though the activity score suggests disease quiescence in the right eye. Presuming that disease quiescence could be achieved through immunosuppression, surgical intervention could be undertaken. In the first instance the patient should undergo lash electrolysis to ensure permanent removal of misdirected lashes. As no other lid deformities were present, the next stage would involve lysis of symblephara and forniceal reconstruction. As described in earlier sections, amniotic membrane would be the

current available standard for forniceal construction but is prone to recurrent scarring and forniceal shortening.[54]

Such patients may be treated in the future with novel conjunctival grafts developed through the ex-vivo expansion of conjunctival epithelium on decellularised conjunctiva or ePTFE. A major problem to approach in this scenario is the autologous biopsy required to develop the construct. With this regard, the risk of scarring and inflammation is significant and therefore disease quiescence at the outset of treatment in addition to immunosuppression in the perioperative period would be of paramount importance. Culture methods and the substrates themselves need to be developed such that adequate conjunctival expansion could be achieved from small biopsies taken from the patient. Other research groups also advocate the use of intraoperative mitomycin C (MMC) or β-irradiation to prevent re-adhesion.[240, 241] It is unlikely that a construct developed from decellularised conjunctiva would afford any advantage over amniotic membrane for forniceal reconstruction as it may be equally prone to recurrent scarring given it will also degrade. I hypothesise that surface optimised ePTFE may be more suitable for forniceal reconstruction given that it is not biodegradable and may i) provide long-term forniceal support and ii) act as a substrate for the ex vivo expanded conjunctival epithelium. Ideally the developed epithelial culture would comprise a suitable proportion of mucin producing goblet cells that could improve the tear film of the eye and a subset of progenitor cells that would enable the epithelium to self renew.

Surgery has been described to involve cicatrix lysis via a circumlunar incision of the conjunctiva along the corneal limbus followed by relaxing incisions towards the fornix along the borders of the symblepharon with dissection of subconjunctival fibrovascular tissue. Following dissection, MMC exposure could be initiated via soaked sponges and the fornix extensively rinsed following their removal. This additional step may prevent the subsequent overgrowth of fibroblasts. The ex-vivo developed ePTFE conjunctival

construct could then be attached to bare sclera with fibrin glue and secured with sutures to the recessed conjunctiva on the bulbar and tarsal aspects as previously described.[240]

The decellularised conjunctival substrate is likely to be available in much smaller sections and therefore this will limit its use. It could be ideal, for example, in fornix reconstruction following an ocular burn once inflammation has settled, but this would depend on the size of decellularised tissue available for use. A decellularised conjunctival substrate may also suit indications such as that following the removal of pterygia, conjunctival tumours or even glaucoma surgery including following the placement of drainage valve implants.

5. Conclusions

This study determined the potential of both ammonia gas plasma modified ePTFE and decellularised conjunctiva as substrates for the ex-vivo expansion of conjunctival epithelium. These substrates may be used for a different range of indications and warrant consideration for use in tissue engineering applications to address the clinical need for conjunctival replacement. These therapies could lead to successful treatments for a range of sight threatening and painful ocular surface disorders.

Ammonia gas plasma treated ePTFE is an effective substrate for the expansion of conjunctival epithelium

- Ammonia gas plasma treatment of ePTFE increases its hydrophilicity and enables the culture of conjunctival epithelium on the treated surface. The cell density was further improved by treatment of the ePTFE membrane on both sides, an effect marked after 14 days in culture.

- A similar phenotype of conjunctival epithelial cultures was demonstrated on double side plasma treated ePTFE as PET membrane.

- The culture of primary cells on double side ammonia plasma treated ePTFE resulted in a decline in cell number after 14 days in culture in contrast to HCjE-Gi cells, which increased up to 28 days. Overall, the primary cell cultures were of a more differentiated phenotype with less proliferative potential demonstrated by greater CK4, CK7 and MUC5AC expression and lower PCNA, ΔNp63 and ABCG2 expression.

Decellularised human conjunctiva is an effective substrate for the ex vivo expansion of conjunctival epithelium

- Human conjunctival was successfully decellularised by optimising a previously developed protocol for the decellularisation of amniotic membrane.

- The decellularisation protocol was effective in the removal of DNA. The tissue did not exhibit cytotoxicity, there was no evidence of collagen denaturation and the histology demonstrated no significant change in the general tissue architecture, elastin or glycosaminoglycan distribution (basement membrane) demonstrated by H&E, Van Gieson's and PAS stains respectively.

- Decellularisation did not affect the distribution of extracellular matrix proteins laminin, collagen IV or fibronectin.

- There was greater variability in the architecture of the conjunctival tissue in comparison to amniotic membrane between donors.

- The development of stratified primary conjunctival epithelial culture on decellularised conjunctiva was demonstrated for the first time. Immunohistochemical staining also confirmed that the developed epithelium was of a conjunctival phenotype with a subpopulation of progenitor cells, proliferating cells and CK7 positive cells.

6. Future directions

There are opportunities in future research to influence the stem and goblet cell populations in cultures of conjunctival epithelium through the further investigation and optimisation of culture conditions. Important improvements in culture techniques have taken place such that serum-free media has been developed and the use of animal feeder layers has not been required in recent work. Further optimisation and investigation should lead to an improved understanding of media and culture requirements aiming to further reduce or eliminate animal products to reduce the risk of zoonotic infection. Indeed, a serum free system has been developed in an attempt to simulate the conjunctival stem cell niche by co-culture of conjunctival epithelium with subconjunctival fibroblasts.[238] It was found that that this allowed conjunctival cells with progenitor characteristics to develop and has been proposed as an ideal method to allow expansion of epithelial progenitor cells in vitro.[238] In addition, it has been demonstrated that a collagen gel containing human fibroblasts resulted in greater numbers of goblet cells, which were not observed on collagen gels seeded with Swiss 3T3 cells.[239]

Seeding explants from conjunctival sites known to be rich in stem cells and goblet cells and the development of methods to develop enriched cultures of progenitor/stem cells could result in optimised, self-renewing epithelial constructs.[19] Decellularised trachea, one of the most successful models of tissue engineering in which great success has been achieved in patients, crucially required an ex vivo epithelial culture rich in stem cells with the appropriate angiogenesis and differentiation promoting growth factors.[74] To this end, techniques to expand and support cultures rich in conjunctival stem cells are acutely warranted and currently lacking.

Examination of the proliferative capacity of conjunctival explants taken from several locations revealed that forniceal explants exhibit the greatest proliferative potential in

both rat and rabbit.[16, 133] In keeping with this, it has been suggested that the human fornices house conjunctival stem cells.[18] In particular, the inferior fornices and the medial canthus have been found to have the greatest density of cells expressing markers in keeping with conjunctival progenitor cells.[19] It has been also been proposed by Pellegrini and colleagues that goblet cells arise from a common bipotent cell from which conjunctival epithelial cells arise and that commitment to goblet cell differentiation can occur late in the differentiation pathway.[18] Pellegrini and colleagues found transiently amplifying cells at specific times in their life cycle prior to senescence and suggested that differentiation into a goblet cell lineage was influenced by a 'cell doubling clock'. [18] It follows therefore, that methods of explant culture using human conjunctiva should be optimised with respect to the biopsy location site and with an understanding of the factors that influence goblet cell differentiation.

Given that explants arising from the fornices and medial canthus have been shown to have the greatest growth potential, it may be possible in future work to develop a two-stage culture system if there is insufficient tissue for the direct seeding of explants from biopsies. Indeed, a two-stage procedure has been reported for other tissue engineering models e.g. endothelial cell seeding in vascular grafts to maximise the cell density of cells. Potential disadvantages are the potential for infection during this extended period of culture and also of potential alterations in the cell phenotype.[185] Alternative methods for greater efficiency of cell propagation include the use of fibroblast conditioned media and supplementation of media with human serum.[132]

Tsai and colleagues also demonstrated that conjunctival epithelial cell culture on collagen gels containing human fibroblasts resulted in epithelium stratified up to 8 cells thick in comparison to an acellular collagen matrix on which only a monolayer of epithelium was demonstrated.[239] Indeed, the epithelial cultures in the present study could be improved by a greater number of cell layers and stratification. This in turn may promote the differentiation of goblet cells. Alternatively, the differentiation of goblet

cells and stratification may be stimulated by a common factor such as the presence of fibroblasts. The role of subconjunctival fibroblasts warrants further study including the potential for initial culture within the substantia propria prior to seeding conjunctival epithelia on the basement membrane side. It would also be of interest to determine whether explant cultures develop successfully due to the presence of a stem cell 'niche' that potentially includes a small population of conjunctival fibroblasts.

Further optimisation of media constituents are warranted to promote conditions that support the maturation of goblet cells and mucin production. This could be achieved through a better understanding and use of the most appropriate growth factors and possibly a lengthened time in culture to upregulate MUC5AC expression.[17] Alternative methods to potentiate the culture of goblet cells could include the use of bronchial epithelial growth medium, epidermal growth factor mediated signalling or γ-secretase as studied by other research groups.[112, 131, 242]

The ePTFE is a promising substrate for cellular expansion that warrants further optimisation of surface chemistry to ensure that a favourable conjunctival phenotype can be developed on its surface. It may prove to be an ideal substrate for forniceal reconstruction and act as a long-term scaffold for conjunctiva whilst maintaining forniceal depth. Given the example of other tissue engineering applications of ePTFE use, it is unlikely that a vascular system would be required for the maintenance of conjunctival tissue given that is only a few cell layers deep.[185] Ultimately the number of cell layers may be limited by factors relating to the rate at which supply of nutrients and ability to remove waste occurs.[185] Following further optimisation of the surface chemistry on ePTFE, early animal studies are warranted to investigate it's potential for conjunctival growth and fornix reconstruction in vivo.

A soft, pliable graft derived from decellularised conjunctiva, with or without ex vivo expanded conjunctival epithelium, may suit a range of indications including glaucoma

surgery, conjunctival replacement following resection of conjunctival tumours and conjunctival chemical burns. The role of decellularised human conjunctiva may even be extended for other ocular cellular replacement therapies such as limbal stem cell transplantation. Indeed, xenogeneic conjunctival matrix has even been demonstrated as an effective scaffold for corneal epithelium in a rabbit model of limbal stem cell disease.[92] This therefore demonstrates the range of cellular replacement therapies in which decellularised matrices provide major advancements in the field of tissue engineering. Decellularised human conjunctiva warrants further investigation into its potential clinical applications in ocular surface disease.

7. Appendix

1. The Liverpool corneal and external eye disease clinic pro forma

(pages 224-228)

2. Ethical approval

(pages 229-231)

BCVA RE…….. LE……..

Affix patient label

Co-existing ophthalmic pathology (accounting for reduced VA)
……

Photograph taken Y N

Inflammation activity score (Grade 1-5)

RE LE

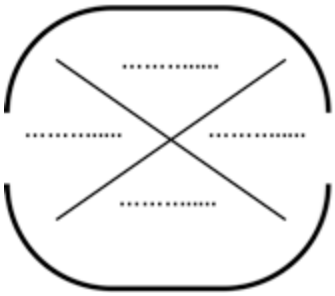

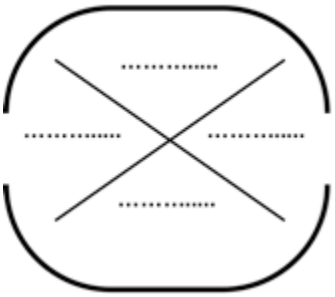

Total score …… Total score ……

Limbitis RE Y ……quadrants/score N
LE Y ……quadrants/score N

Anterior segment drawings

RE	**LE**

Cicatrisation grading (Tauber-Liverpool)

RE **LE**

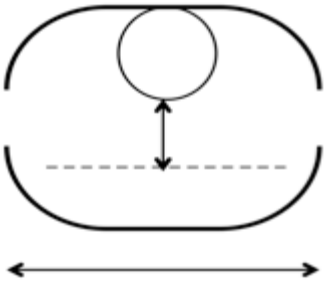

Horizontal width …….mm Symblephara …….mm	Horizontal width …….mm Symblephara …….mm
I Subconjunctival scarring and fibrosis **II** Fornix foreshortening a 0-25% b 25-50% c 50-75% d 75-100% Vertical grading = ……..%	**I** Subconjunctival scarring and fibrosis **II** Fornix foreshortening a 0-25% b 25-50% c 50-75% d 75-100% Vertical grading = ……..%
III Presence of symblepharon a 0-25% b 25-50% c 50-75% d 75-100% Horizontal grading = ……..%	**III** Presence of symblepharon a 0-25% b 25-50% c 50-75% d 75-100% Horizontal grading = ……..%
IV Ankyloblepharon/ frozen globe	**IV** Ankyloblepharon/ frozen globe

Cicatrisation by Foster grading scheme

RE	LE
I subconjunctival scarring and fibrosis	I subconjunctival scarring and fibrosis
II fornix foreshortening (any degree)	II fornix foreshortening (any degree)
III symblepharon (any degree)	III symblepharon (any degree)
IV ankyloblepharon/frozen globe	IV ankyloblepharon/frozen globe

Cicatrisation by Rowsey grading scheme

RE	LE
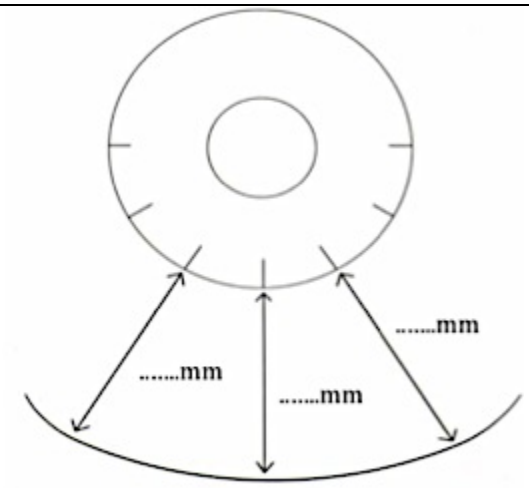	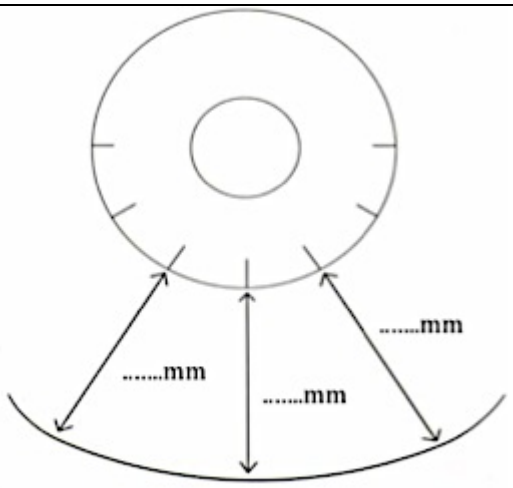
Score ……./45	**Score……/45**

Fornix measure

RE	Upper	mm	LE	Upper	mm
	Lower	mm		Lower	mm

Corneal involvement

		Grade 0	**Grade 1**	**Grade 2**	**Grade 3**
RE	Conjunctivalisation				
	Neovascularisation				
	Opacification-**peripheral**				
	Opacification-**central**				
LE	Conjunctivalisation				
	Neovascularisation				
	Opacification-**peripheral**				
	Opacification-**central**				

Ocular dryness score (oxford)

RE 0 1 2 3 4 5

LE 0 1 2 3 4 5

Eyelids

Lagophthalmos Y ……mm N ……mm

Lashes no trichiasis trichiasis acquired distichiasis

	RE		LE	
	Entropion/ Ectropion		Entropion/ Ectropion	
	Upper lid	Lower lid	Upper lid	Lower lid
Grade 0				
Grade 1				
Grade 2				
Grade 3				
Medial				
Lateral				
Lateral + Medial				

NHS
Health Research Authority

NRES Committee North West - Liverpool Central
3rd Floor
Barlow House
4 Minshull Street
Manchester
M1 3DZ

Telephone: 0161 625 7816
Facsimile: 0161 625 7299

16 March 2012

Professor S.B Kaye
Consultant Ophthalmologist
RLBUHT
St Paul's Eye Unit, Royal Liverpool University Hospital
Prescot Street
Liverpool
L7 8XP

Dear Professor Kaye

Study title:	**Isolation, characterisation and expansion of human ocular surface (corneal and conjunctival) stem cells.**
REC reference:	**11/NW/0766**
Protocol number:	**4182**

Thank you for your letter of 04 March 2012, responding to the Committee's request for further information on the above research and submitting revised documentation.

The further information has been considered on behalf of the Committee by the Chair and Dr Stephen Pennefather.

Confirmation of ethical opinion

On behalf of the Committee, I am pleased to confirm a favourable ethical opinion for the above research on the basis described in the application form, protocol and supporting documentation as revised, subject to the conditions specified below.

Ethical review of research sites

NHS sites

The favourable opinion applies to all NHS sites taking part in the study, subject to management permission being obtained from the NHS/HSC R&D office prior to the start of the study (see "Conditions of the favourable opinion" below).

Non-NHS sites

Conditions of the favourable opinion

The favourable opinion is subject to the following conditions being met prior to the start of the study.

Management permission or approval must be obtained from each host organisation prior to the start of the study at the site concerned.

Management permission ("R&D approval") should be sought from all NHS organisations involved in the study in accordance with NHS research governance arrangements.

Guidance on applying for NHS permission for research is available in the Integrated Research Application System or at http://www.rdforum.nhs.uk.

Where a NHS organisation's role in the study is limited to identifying and referring potential participants to research sites ("participant identification centre"), guidance should be sought from the R&D office on the information it requires to give permission for this activity.

For non-NHS sites, site management permission should be obtained in accordance with the procedures of the relevant host organisation.

Sponsors are not required to notify the Committee of approvals from host organisations

It is the responsibility of the sponsor to ensure that all the conditions are complied with before the start of the study or its initiation at a particular site (as applicable).

Approved documents

The final list of documents reviewed and approved by the Committee is as follows:

Document	*Version*	*Date*
Investigator CV	1	21 October 2011
Other: Data Collection Sheet	1	21 October 2011
Other: Supporting letter re-release of contact details of NOK		02 March 2012
Participant Consent Form	3	30 November 2011
Participant Information Sheet: Next of kin	2	30 November 2011
Protocol	2	21 February 2012
REC application	3.2	30 September 2011
Response to Request for Further Information		20 January 2012
Response to Request for Further Information		04 March 2012
Summary/Synopsis	Flowchart	

Statement of compliance

The Committee is constituted in accordance with the Governance Arrangements for Research Ethics Committees and complies fully with the Standard Operating Procedures for Research Ethics Committees in the UK.

After ethical review

Reporting requirements

The attached document *"After ethical review – guidance for researchers"* gives detailed guidance on reporting requirements for studies with a favourable opinion, including:

- Notifying substantial amendments
- Adding new sites and investigators
- Notification of serious breaches of the protocol
- Progress and safety reports
- Notifying the end of the study

The NRES website also provides guidance on these topics, which is updated in the light of changes in reporting requirements or procedures.

Feedback

You are invited to give your view of the service that you have received from the National Research Ethics Service and the application procedure. If you wish to make your views known please use the feedback form available on the website.

Further information is available at National Research Ethics Service website > After Review

11/NW/0766	**Please quote this number on all correspondence**

With the Committee's best wishes for the success of this project

Yours sincerely

Professor Sobhan Vinjamuri
Chair

Email: diane.catterall@northwest.nhs.uk

Enclosures: "After ethical review – guidance for researchers"

Copy to: *Dr Sharon Mason*
Heather Rogers, The Royal Liverpool & Broadgreen University Hospitals NHS Trust

8. References

1. Forrester J.V. DAD, McMenamin P.G., Roberts.F. Basic science in practice. 3rd ed. London: Saunders Elsevier; 2008.
2. Paulsen FP, Berry MS. Mucins and TFF peptides of the tear film and lacrimal apparatus. Progress in histochemistry and cytochemistry. 2006;41(1):1-53.
3. Schlotzer-Schrehardt U, Dietrich T, Saito K, Sorokin L, Sasaki T, Paulsson M, et al. Characterization of extracellular matrix components in the limbal epithelial stem cell compartment. Experimental eye research. 2007;85(6):845-60.
4. Lemp MA, Mathers WD. Corneal epithelial cell movement in humans. Eye. 1989;3 (Pt 4):438-45.
5. Dawson DG, Ubels, J.L. Cornea and Sclera. Edinburgh: Saunders; 2011.
6. Kuwabara T, Perkins DG, Cogan DG. Sliding of the epithelium in experimental corneal wounds. Investigative ophthalmology. 1976;15(1):4-14.
7. Gipson IK. Distribution of mucins at the ocular surface. Experimental eye research. 2004;78(3):379-88.
8. Budak MT, Alpdogan OS, Zhou M, Lavker RM, Akinci MA, Wolosin JM. Ocular surface epithelia contain ABCG2-dependent side population cells exhibiting features associated with stem cells. J Cell Sci. 2005;118(Pt 8):1715-24.
9. Kawasaki S, Tanioka H, Yamasaki K, Connon CJ, Kinoshita S. Expression and tissue distribution of p63 isoforms in human ocular surface epithelia. Experimental eye research. 2006;82(2):293-9.
10. Kasper M, Moll R, Stosiek P, Karsten U. Patterns of cytokeratin and vimentin expression in the human eye. Histochemistry. 1988;89(4):369-77.
11. Shatos MA, Rios JD, Horikawa Y, Hodges RR, Chang EL, Bernardino CR, et al. Isolation and characterization of cultured human conjunctival goblet cells. Investigative ophthalmology & visual science. 2003;44(6):2477-86.
12. Fukuda K, Chikama T, Nakamura M, Nishida T. Differential distribution of subchains of the basement membrane components type IV collagen and laminin among the amniotic membrane, cornea, and conjunctiva. Cornea. 1999;18(1):73-9.
13. Greiner JV, Henriquez AS, Covington HI, Weidman TA, Allansmith MR. Goblet cells of the human conjunctiva. Arch Ophthalmol. 1981;99(12):2190-7.
14. Dickinson AJ, Gausas RE. Orbital lymphatics: do they exist? Eye. 2006;20(10):1145-8.
15. Messmer EM, Valet VM, Kampik A. Differences in basement membrane zone components of normal conjunctiva, conjunctiva in glaucoma and normal skin. Acta Ophthalmol. 2012;90(6):e476-81.
16. Wei ZG, Wu RL, Lavker RM, Sun TT. In vitro growth and differentiation of rabbit bulbar, fornix, and palpebral conjunctival epithelia. Implications on conjunctival epithelial transdifferentiation and stem cells. Investigative ophthalmology & visual science. 1993;34(5):1814-28.
17. Dartt DA. Control of mucin production by ocular surface epithelial cells. Experimental eye research. 2004;78(2):173-85.
18. Pellegrini G, Golisano O, Paterna P, Lambiase A, Bonini S, Rama P, et al. Location and clonal analysis of stem cells and their differentiated progeny in the human ocular surface. J Cell Biol. 1999;145(4):769-82.

19. Stewart RM, Sheridan CM, Hiscott PS, Czanner G, Kaye SB. Human Conjunctival Stem Cells are Predominantly Located in the Medial Canthal and Inferior Forniceal Areas. Investigative ophthalmology & visual science. 2015;56(3):2021-30.
20. Butovich IA, Millar TJ, Ham BM. Understanding and analyzing meibomian lipids--a review. Curr Eye Res. 2008;33(5):405-20.
21. Selinger DS, Selinger RC, Reed WP. Resistance to infection of the external eye: the role of tears. Surv Ophthalmol. 1979;24(1):33-8.
22. Huang LC, Redfern RL, Narayanan S, Reins RY, McDermott AM. In vitro activity of human beta-defensin 2 against Pseudomonas aeruginosa in the presence of tear fluid. Antimicrob Agents Chemother. 2007;51(11):3853-60.
23. Aknin ML, Berry M, Dick AD, Khan-Lim D. Normal but not altered mucins activate neutrophils. Cell and tissue research. 2004;318(3):545-51.
24. Langer G, Jagla W, Behrens-Baumann W, Walter S, Hoffmann W. Secretory peptides TFF1 and TFF3 synthesized in human conjunctival goblet cells. Investigative ophthalmology & visual science. 1999;40(10):2220-4.
25. Tseng SC, Hirst LW, Maumenee AE, Kenyon KR, Sun TT, Green WR. Possible mechanisms for the loss of goblet cells in mucin-deficient disorders. Ophthalmology. 1984;91(6):545-52.
26. Gilbard JP, Rossi SR. Tear film and ocular surface changes in a rabbit model of neurotrophic keratitis. Ophthalmology. 1990;97(3):308-12.
27. Tanioka H, Kawasaki S, Sotozono C, Nakamura T, Inatomi T, Kinoshita S. The relationship between preoperative clinical scores and immunohistological evaluation of surgically resected tissues in chronic severe ocular surface diseases. Japanese journal of ophthalmology. 2010;54(1):66-73.
28. Argueso P, Gipson IK. Epithelial mucins of the ocular surface: structure, biosynthesis and function. Experimental eye research. 2001;73(3):281-9.
29. Ilari L, Daya SM. Long-term outcomes of keratolimbal allograft for the treatment of severe ocular surface disorders. Ophthalmology. 2002;109(7):1278-84.
30. Burton MJ, Mabey DC. The global burden of trachoma: a review. PLoS Negl Trop Dis. 2009;3(10):e460.
31. Ari AB. Eye injuries on the battlefields of Iraq and Afghanistan: public health implications. Optometry. 2006;77(7):329-39.
32. Kuckelkorn R, Schrage N, Keller G, Redbrake C. Emergency treatment of chemical and thermal eye burns. Acta Ophthalmol Scand. 2002;80(1):4-10.
33. Chan LS, Ahmed AR, Anhalt GJ, Bernauer W, Cooper KD, Elder MJ, et al. The first international consensus on mucous membrane pemphigoid: definition, diagnostic criteria, pathogenic factors, medical treatment, and prognostic indicators. Archives of dermatology. 2002;138(3):370-9.
34. Fritsch P. European Dermatology Forum: skin diseases in Europe. Skin diseases with a high public health impact: toxic epidermal necrolysis and Stevens-Johnson syndrome. Eur J Dermatol. 2008;18(2):216-7.
35. Patel TK, Barvaliya MJ, Sharma D, Tripathi C. A systematic review of the drug-induced Stevens-Johnson syndrome and toxic epidermal necrolysis in Indian population. Indian journal of dermatology, venereology and leprology. 2013;79(3):389-98.
36. Radford CF, Rauz S, Williams GP, Saw VP, Dart JK. Incidence, presenting features, and diagnosis of cicatrising conjunctivitis in the United Kingdom. Eye. 2012;26(9):1199-208.
37. Tseng SC. Staging of conjunctival squamous metaplasia by impression cytology. Ophthalmology. 1985;92(6):728-33.

38. Gipson IK, Hori Y, Argueso P. Character of ocular surface mucins and their alteration in dry eye disease. The ocular surface. 2004;2(2):131-48.
39. Saw VP, Dart JK. Ocular mucous membrane pemphigoid: diagnosis and management strategies. The ocular surface. 2008;6(3):128-42.
40. Schneck J, Fagot JP, Sekula P, Sassolas B, Roujeau JC, Mockenhaupt M. Effects of treatments on the mortality of Stevens-Johnson syndrome and toxic epidermal necrolysis: A retrospective study on patients included in the prospective EuroSCAR Study. Journal of the American Academy of Dermatology. 2008;58(1):33-40.
41. Power WJ, Saidman SL, Zhang DS, Vamvakas EC, Merayo-Lloves JM, Kaufman AH, et al. HLA typing in patients with ocular manifestations of Stevens-Johnson syndrome. Ophthalmology. 1996;103(9):1406-9.
42. Roujeau JC. Stevens-Johnson syndrome and toxic epidermal necrolysis are severity variants of the same disease which differs from erythema multiforme. The Journal of dermatology. 1997;24(11):726-9.
43. Sacher C, Rubbert A, Konig C, Scharffetter-Kochanek K, Krieg T, Hunzelmann N. Treatment of recalcitrant cicatricial pemphigoid with the tumor necrosis factor alpha antagonist etanercept. Journal of the American Academy of Dermatology. 2002;46(1):113-5.
44. Heffernan MP, Bentley DD. Successful treatment of mucous membrane pemphigoid with infliximab. Archives of dermatology. 2006;142(10):1268-70.
45. Taverna JA, Lerner A, Bhawan J, Demierre MF. Successful adjuvant treatment of recalcitrant mucous membrane pemphigoid with anti-CD20 antibody rituximab. Journal of drugs in dermatology : JDD. 2007;6(7):731-2.
46. Mondino BJ, Brown SI. Ocular cicatricial pemphigoid. Ophthalmology. 1981;88(2):95-100.
47. Thoft RA. Conjunctival transplantation. Arch Ophthalmol. 1977;95(8):1425-7.
48. Vastine DW, Stewart WB, Schwab IR. Reconstruction of the periocular mucous membrane by autologous conjunctival transplantation. Ophthalmology. 1982;89(9):1072-81.
49. Schrader S, Notara M, Beaconsfield M, Tuft S, Geerling G, Daniels JT. Conjunctival epithelial cells maintain stem cell properties after long-term culture and cryopreservation. Regen Med. 2009;4(5):677-87.
50. Hosni FA. Repair of trachomatous cicatricial entropion using mucous membrane graft. Arch Ophthalmol. 1974;91(1):49-51.
51. Shore JW, Foster CS, Westfall CT, Rubin PA. Results of buccal mucosal grafting for patients with medically controlled ocular cicatricial pemphigoid. Ophthalmology. 1992;99(3):383-95.
52. Kuckelkorn R, Schrage N, Redbrake C, Kottek A, Reim M. Autologous transplantation of nasal mucosa after severe chemical and thermal eye burns. Acta Ophthalmol Scand. 1996;74(5):442-8.
53. Wenkel H, Rummelt V, Naumann GO. Long term results after autologous nasal mucosal transplantation in severe mucus deficiency syndromes. The British journal of ophthalmology. 2000;84(3):279-84.
54. Schrader S, Notara M, Beaconsfield M, Tuft SJ, Daniels JT, Geerling G. Tissue engineering for conjunctival reconstruction: established methods and future outlooks. Curr Eye Res. 2009;34(11):913-24.
55. Fish R, Davidson RS. Management of ocular thermal and chemical injuries, including amniotic membrane therapy. Current opinion in ophthalmology. 2010;21(4):317-21.

56. Honavar SG, Bansal AK, Sangwan VS, Rao GN. Amniotic membrane transplantation for ocular surface reconstruction in Stevens-Johnson syndrome. Ophthalmology. 2000;107(5):975-9.
57. Barabino S, Rolando M. Amniotic membrane transplantation elicits goblet cell repopulation after conjunctival reconstruction in a case of severe ocular cicatricial pemphigoid. Acta Ophthalmol Scand. 2003;81(1):68-71.
58. Barabino S, Rolando M, Bentivoglio G, Mingari C, Zanardi S, Bellomo R, et al. Role of amniotic membrane transplantation for conjunctival reconstruction in ocular-cicatricial pemphigoid. Ophthalmology. 2003;110(3):474-80.
59. Tseng SC. Amniotic membrane transplantation for ocular surface reconstruction. Biosci Rep. 2001;21(4):481-9.
60. Akle C, McColl I, Dean M, Adinolfi M, Brown S, Fensom AH, et al. Transplantation of amniotic epithelial membranes in patients with mucopolysaccharidoses. Exp Clin Immunogenet. 1985;2(1):43-8.
61. Akle CA, Adinolfi M, Welsh KI, Leibowitz S, McColl I. Immunogenicity of human amniotic epithelial cells after transplantation into volunteers. Lancet. 1981;2(8254):1003-5.
62. Hao Y, Ma DH, Hwang DG, Kim WS, Zhang F. Identification of antiangiogenic and antiinflammatory proteins in human amniotic membrane. Cornea. 2000;19(3):348-52.
63. Tosi GM, Massaro-Giordano M, Caporossi A, Toti P. Amniotic membrane transplantation in ocular surface disorders. Journal of cellular physiology. 2005;202(3):849-51.
64. Fernandes M, Sridhar MS, Sangwan VS, Rao GN. Amniotic membrane transplantation for ocular surface reconstruction. Cornea. 2005;24(6):643-53.
65. Hernandez Galindo EE, Theiss C, Steuhl KP, Meller D. Expression of Delta Np63 in response to phorbol ester in human limbal epithelial cells expanded on intact human amniotic membrane. Investigative ophthalmology & visual science. 2003;44(7):2959-65.
66. Meller D, Dabul V, Tseng SC. Expansion of conjunctival epithelial progenitor cells on amniotic membrane. Experimental eye research. 2002;74(4):537-45.
67. Ang LP, Tan DT, Beuerman RW, Lavker RM. Development of a conjunctival epithelial equivalent with improved proliferative properties using a multistep serum-free culture system. Investigative ophthalmology & visual science. 2004;45(6):1789-95.
68. Ang LP, Tanioka H, Kawasaki S, Ang LP, Yamasaki K, Do TP, et al. Cultivated human conjunctival epithelial transplantation for total limbal stem cell deficiency. Investigative ophthalmology & visual science. 2010;51(2):758-64.
69. Ang LP, Tan DT. Autologous cultivated conjunctival transplantation for recurrent viral papillomata. Am J Ophthalmol. 2005;140(1):136-8.
70. Ang LP, Tan DT, Cajucom-Uy H, Beuerman RW. Autologous cultivated conjunctival transplantation for pterygium surgery. Am J Ophthalmol. 2005;139(4):611-9.
71. Solomon A, Espana EM, Tseng SC. Amniotic membrane transplantation for reconstruction of the conjunctival fornices. Ophthalmology. 2003;110(1):93-100.
72. International A. Materials and Coatings for Medical Devices: Cardiovascular Hardcover. USA: ASM International; 2009.
73. Bendavid R, Abrahamson, J., Arregui, E. Abdominal Wall Hernias: Principles and Management. 1 ed. New York: Springer-Verlag New York; 2001.
74. Elliott MJ, De Coppi P, Speggiorin S, Roebuck D, Butler CR, Samuel E, et al. Stem-cell-based, tissue engineered tracheal replacement in a child: a 2-year follow-up study. Lancet. 2012;380(9846):994-1000.

75. Bolland F, Korossis S, Wilshaw SP, Ingham E, Fisher J, Kearney JN, et al. Development and characterisation of a full-thickness acellular porcine bladder matrix for tissue engineering. Biomaterials. 2007;28(6):1061-70.
76. Mirsadraee S, Wilcox HE, Watterson KG, Kearney JN, Hunt J, Fisher J, et al. Biocompatibility of acellular human pericardium. J Surg Res. 2007;143(2):407-14.
77. Crapo PM, Gilbert TW, Badylak SF. An overview of tissue and whole organ decellularization processes. Biomaterials. 2011;32(12):3233-43.
78. Karabekmez FE, Duymaz, A., Moran, S.L. Early clinical outcomes with the use of decellularized
nerve allograft for repair of sensory defects within the hand. Hand. 2009;4(3):245–9.
79. Vorotnikova E, McIntosh D, Dewilde A, Zhang J, Reing JE, Zhang L, et al. Extracellular matrix-derived products modulate endothelial and progenitor cell migration and proliferation in vitro and stimulate regenerative healing in vivo. Matrix Biol. 2010;29(8):690-700.
80. Orlando G, Booth C, Wang Z, Totonelli G, Ross CL, Moran E, et al. Discarded human kidneys as a source of ECM scaffold for kidney regeneration technologies. Biomaterials. 2013;34(24):5915-25.
81. Allen RA, Seltz LM, Jiang H, Kasick RT, Sellaro TL, Badylak SF, et al. Adrenal extracellular matrix scaffolds support adrenocortical cell proliferation and function in vitro. Tissue Eng Part A. 2010;16(11):3363-74.
82. Cortiella J, Niles J, Cantu A, Brettler A, Pham A, Vargas G, et al. Influence of acellular natural lung matrix on murine embryonic stem cell differentiation and tissue formation. Tissue Eng Part A. 2010;16(8):2565-80.
83. Valentin JE, Turner NJ, Gilbert TW, Badylak SF. Functional skeletal muscle formation with a biologic scaffold. Biomaterials. 2010;31(29):7475-84.
84. Xu CC, Chan RW, Weinberger DG, Efune G, Pawlowski KS. A bovine acellular scaffold for vocal fold reconstruction in a rat model. J Biomed Mater Res A. 2010;92(1):18-32.
85. Waldrop FS, Puchtler H, Meloan SN, Younker TD. Histochemical investigations of different types of collagen. Acta Histochem Suppl. 1980;21:23-31.
86. Flynn LE. The use of decellularized adipose tissue to provide an inductive microenvironment for the adipogenic differentiation of human adipose-derived stem cells. Biomaterials. 2010;31(17):4715-24.
87. Wilshaw SP, Kearney J, Fisher J, Ingham E. Biocompatibility and potential of acellular human amniotic membrane to support the attachment and proliferation of allogeneic cells. Tissue Eng Part A. 2008;14(4):463-72.
88. Cox B, Emili A. Tissue subcellular fractionation and protein extraction for use in mass-spectrometry-based proteomics. Nat Protoc. 2006;1(4):1872-8.
89. Xu CC, Chan RW, Tirunagari N. A biodegradable, acellular xenogeneic scaffold for regeneration of the vocal fold lamina propria. Tissue Eng. 2007;13(3):551-66.
90. Petersen TH, Calle EA, Zhao L, Lee EJ, Gui L, Raredon MB, et al. Tissue-engineered lungs for in vivo implantation. Science. 2010;329(5991):538-41.
91. Zhang C, Nie X, Hu D, Liu Y, Deng Z, Dong R, et al. Survival and integration of tissue-engineered corneal stroma in a model of corneal ulcer. Cell and tissue research. 2007;329(2):249-57.
92. Zhao H, Qu M, Wang Y, Wang Z, Shi W. Xenogeneic acellular conjunctiva matrix as a scaffold of tissue-engineered corneal epithelium. PLoS One. 2014;9(11):e111846.
93. Hsu WC, Spilker MH, Yannas IV, Rubin PA. Inhibition of conjunctival scarring and contraction by a porous collagen-glycosaminoglycan implant. Investigative ophthalmology & visual science. 2000;41(9):2404-11.

94. Lee SY, Oh JH, Kim JC, Kim YH, Kim SH, Choi JW. In vivo conjunctival reconstruction using modified PLGA grafts for decreased scar formation and contraction. Biomaterials. 2003;24(27):5049-59.
95. Tsai RJ, Tseng SC. Substrate modulation of cultured rabbit conjunctival epithelial cell differentiation and morphology. Investigative ophthalmology & visual science. 1988;29(10):1565-76.
96. Drechsler CC, Kunze A, Kureshi A, Grobe G, Reichl S, Geerling G, et al. Development of a conjunctival tissue substitute on the basis of plastic compressed collagen. J Tissue Eng Regen Med. 2015.
97. Ang LP, Cheng ZY, Beuerman RW, Teoh SH, Zhu X, Tan DT. The development of a serum-free derived bioengineered conjunctival epithelial equivalent using an ultrathin poly(epsilon-caprolactone) membrane substrate. Investigative ophthalmology & visual science. 2006;47(1):105-12.
98. Wikol M, Hartman, B., Brendel, J.,. Filtration and Purification in the Biopharmaceutical Industry, Second Edition. Jornitz M, Meltzer, TH.,, editor. Florida: CRC Press; 2007.
99. Gallocher SL, Aguirre AF, Kasyanov V, Pinchuk L, Schoephoerster RT. A novel polymer for potential use in a trileaflet heart valve. J Biomed Mater Res B Appl Biomater. 2006;79(2):325-34.
100. Minale C, Nikol S, Hollweg G, Mittermayer C, Messmer BJ. Clinical experience with expanded polytetrafluoroethylene Gore-Tex surgical membrane for pericardial closure: a study of 110 cases. J Card Surg. 1988;3(3):193-201.
101. Leprince P, Rahmati M, Bonnet N, Bors V, Rama A, Leger P, et al. Expanded polytetrafluoroethylene membranes to wrap surfaces of circulatory support devices in patients undergoing bridge to heart transplantation. Eur J Cardiothorac Surg. 2001;19(3):302-6.
102. Lu S, Zhang P, Sun X, Gong F, Yang S, Shen L, et al. Synthetic ePTFE grafts coated with an anti-CD133 antibody-functionalized heparin/collagen multilayer with rapid in vivo endothelialization properties. ACS Appl Mater Interfaces. 2013;5(15):7360-9.
103. Sato Y, Murahara, M. Protein adsorption on PTFE surface modified by ArF excimer laser treatment. Journal of Adhesion Science and Technology 2004;18(13):1545-55.
104. Demirci H, Elner SG, Elner VM. Rigid nylon foil-anchored polytetrafluoroetyhlene (Gore-Tex) sheet stenting for conjunctival fornix reconstruction. Ophthalmology. 2010;117(9):1736-42.
105. Levin PS, Dutton JJ. Polytef (polytetrafluoroethylene) alloplastic grafting as a substitute for mucous membrane. Arch Ophthalmol. 1990;108(2):282-5.
106. Cillino S, Zeppa L, Di Pace F, Casuccio A, Morreale D, Bocchetta F, et al. E-PTFE (Gore-Tex) implant with or without low-dosage mitomycin-C as an adjuvant in penetrating glaucoma surgery: 2 year randomized clinical trial. Acta Ophthalmol. 2008;86(3):314-21.
107. Krishna Y, Sheridan C, Kent D, Kearns V, Grierson I, Williams R. Expanded polytetrafluoroethylene as a substrate for retinal pigment epithelial cell growth and transplantation in age-related macular degeneration. The British journal of ophthalmology. 2011;95(4):569-73.
108. Williams RL, Krishna Y, Dixon S, Haridas A, Grierson I, Sheridan C. Polyurethanes as potential substrates for sub-retinal retinal pigment epithelial cell transplantation. J Mater Sci Mater Med. 2005;16(12):1087-92.
109. Yuan Y, Lee,RT.,. Surface Science Techniques. Berlin: Springer-Verlag; 2013.
110. Freshney RI. Culture of Epithelial Cells. 2nd ed. Freshney RIF, M.G. , editor. New York: Wiley 2002. 461 p.

111. Ang LP, Do TP, Thein ZM, Reza HM, Tan XW, Yap C, et al. Ex vivo expansion of conjunctival and limbal epithelial cells using cord blood serum-supplemented culture medium. Investigative ophthalmology & visual science. 2011;52(9):6138-47.
112. Chung SH, Lee JH, Yoon JH, Lee HK, Seo KY. Multi-layered culture of primary human conjunctival epithelial cells producing MUC5AC. Experimental eye research. 2007;85(2):226-33.
113. Iversen E, Lykke A, Hensler M, Jorgensen LN. Abdominal wall hernia repair with a composite ePTFE/polypropylene mesh: clinical outcome and quality of life in 152 patients. Hernia. 2010;14(6):555-60.
114. Tan DT, Ang LP, Beuerman RW. Reconstruction of the ocular surface by transplantation of a serum-free derived cultivated conjunctival epithelial equivalent. Transplantation. 2004;77(11):1729-34.
115. Ang LP, Tan DT, Cajucom-Uy H, Phan TT, Beuerman RW, Lavker RM. Reconstruction of the ocular surface by transplantation of a serum free cultivated conjunctival tissue equivalent. Ann Acad Med Singapore. 2004;33(5 Suppl):S55-6.
116. Ang LP, Tan DT, Phan TT, Li J, Beuerman R, Lavker RM. The in vitro and in vivo proliferative capacity of serum-free cultivated human conjunctival epithelial cells. Curr Eye Res. 2004;28(5):307-17.
117. Ang LP, Tan DT, Seah CJ, Beuerman RW. The use of human serum in supporting the in vitro and in vivo proliferation of human conjunctival epithelial cells. The British journal of ophthalmology. 2005;89(6):748-52.
118. Spurr-Michaud SJ, Gipson IK. Methods for culture of human corneal and conjunctival epithelia. Methods Mol Biol. 2013;945:31-43.
119. Harun MH, Sepian SN, Chua KH, Ropilah AR, Abd Ghafar N, Che-Hamzah J, et al. Human forniceal region is the stem cell-rich zone of the conjunctival epithelium. Hum Cell. 2013;26(1):35-40.
120. Yang A, Schweitzer R, Sun D, Kaghad M, Walker N, Bronson RT, et al. p63 is essential for regenerative proliferation in limb, craniofacial and epithelial development. Nature. 1999;398(6729):714-8.
121. Truong AB, Kretz M, Ridky TW, Kimmel R, Khavari PA. p63 regulates proliferation and differentiation of developmentally mature keratinocytes. Genes Dev. 2006;20(22):3185-97.
122. Pellegrini G, Dellambra E, Golisano O, Martinelli E, Fantozzi I, Bondanza S, et al. p63 identifies keratinocyte stem cells. Proc Natl Acad Sci U S A. 2001;98(6):3156-61.
123. Vascotto SG, Griffith M. Localization of candidate stem and progenitor cell markers within the human cornea, limbus, and bulbar conjunctiva in vivo and in cell culture. The anatomical record Part A, Discoveries in molecular, cellular, and evolutionary biology. 2006;288(8):921-31.
124. Poli M, Burillon C, Auxenfans C, Rovere MR, Damour O. Immunocytochemical Diagnosis of Limbal Stem Cell Deficiency: Comparative Analysis of Current Corneal and Conjunctival Biomarkers. Cornea. 2015;34(7):817-23.
125. Krenzer KL, Freddo TF. Patterns of cytokeratin expression in impression cytology specimens from normal human conjunctival epithelium. Adv Exp Med Biol. 1994;350:289-92.
126. Ramirez-Miranda A, Nakatsu MN, Zarei-Ghanavati S, Nguyen CV, Deng SX. Keratin 13 is a more specific marker of conjunctival epithelium than keratin 19. Molecular vision. 2011;17:1652-61.
127. Moll R, Franke WW, Schiller DL, Geiger B, Krepler R. The catalog of human cytokeratins: patterns of expression in normal epithelia, tumors and cultured cells. Cell. 1982;31(1):11-24.

128. Barbaro V, Ferrari S, Fasolo A, Pedrotti E, Marchini G, Sbabo A, et al. Evaluation of ocular surface disorders: a new diagnostic tool based on impression cytology and confocal laser scanning microscopy. The British journal of ophthalmology. 2010;94(7):926-32.
129. Poli M, Janin H, Justin V, Auxenfans C, Burillon C, Damour O. Keratin 13 immunostaining in corneal impression cytology for the diagnosis of limbal stem cell deficiency. Investigative ophthalmology & visual science. 2011;52(13):9411-5.
130. Qi H, Zheng X, Yuan X, Pflugfelder SC, Li DQ. Potential localization of putative stem/progenitor cells in human bulbar conjunctival epithelium. Journal of cellular physiology. 2010;225(1):180-5.
131. Tian L, Qu M, Wang Y, Duan H, Di G, Xie L, et al. Inductive differentiation of conjunctival goblet cells by gamma-secretase inhibitor and construction of recombinant conjunctival epithelium. Experimental eye research. 2014;123:37-42.
132. Garcia-Posadas L, Arranz-Valsero I, Lopez-Garcia A, Soriano-Romani L, Diebold Y. A new human primary epithelial cell culture model to study conjunctival inflammation. Investigative ophthalmology & visual science. 2013;54(10):7143-52.
133. Eidet JR, Fostad IG, Shatos MA, Utheim TP, Utheim OA, Raeder S, et al. Effect of biopsy location and size on proliferative capacity of ex vivo expanded conjunctival tissue. Investigative ophthalmology & visual science. 2012;53(6):2897-903.
134. Fostad IG, Eidet JR, Shatos MA, Utheim TP, Utheim OA, Raeder S, et al. Biopsy harvesting site and distance from the explant affect conjunctival epithelial phenotype ex vivo. Experimental eye research. 2012;104:15-25.
135. Merjava S, Neuwirth A, Tanzerova M, Jirsova K. The spectrum of cytokeratins expressed in the adult human cornea, limbus and perilimbal conjunctiva. Histology and histopathology. 2011;26(3):323-31.
136. Shalini S, Dorstyn L, Dawar S, Kumar S. Old, new and emerging functions of caspases. Cell Death Differ. 2015;22(4):526-39.
137. Chen D, Texada DE, Duggan C, Deng Y, Redens TB, Langford MP. Caspase-3 and -7 mediate apoptosis of human Chang's conjunctival cells induced by enterovirus 70. Virology. 2006;347(2):307-22.
138. Liang K, Jiang Z, Ding BQ, Cheng P, Huang DK, Tao LM. Expression of cell proliferation and apoptosis biomarkers in pterygia and normal conjunctiva. Molecular vision. 2011;17:1687-93.
139. Eidet JR, Utheim OA, Raeder S, Dartt DA, Lyberg T, Carreras E, et al. Effects of serum-free storage on morphology, phenotype, and viability of ex vivo cultured human conjunctival epithelium. Experimental eye research. 2012;94(1):109-16.
140. Mailand N, Gibbs-Seymour I, Bekker-Jensen S. Regulation of PCNA-protein interactions for genome stability. Nat Rev Mol Cell Biol. 2013;14(5):269-82.
141. Moldovan GL, Pfander B, Jentsch S. PCNA, the maestro of the replication fork. Cell. 2007;129(4):665-79.
142. Rieseberg MK, C.; Reardon, KF.; Scheper, T. Flow cytometry in biotechnology. Appl Microbiol Biotechnol 2001;56(3):350-60.
143. Pisella PJ, Brignole F, Debbasch C, Lozato PA, Creuzot-Garcher C, Bara J, et al. Flow cytometric analysis of conjunctival epithelium in ocular rosacea and keratoconjunctivitis sicca. Ophthalmology. 2000;107(10):1841-9.
144. Brignole F, Pisella PJ, Goldschild M, De Saint Jean M, Goguel A, Baudouin C. Flow cytometric analysis of inflammatory markers in conjunctival epithelial cells of patients with dry eyes. Investigative ophthalmology & visual science. 2000;41(6):1356-63.

145. Contreras-Ruiz L, Ghosh-Mitra A, Shatos MA, Dartt DA, Masli S. Modulation of conjunctival goblet cell function by inflammatory cytokines. Mediators Inflamm. 2013;2013:636812.
146. Martinez-Osorio H, Calonge M, Corell A, Reinoso R, Lopez A, Fernandez I, et al. Characterization and short-term culture of cells recovered from human conjunctival epithelium by minimally invasive means. Molecular vision. 2009;15:2185-95.
147. Srikumaran D, Akpek EK. Mucous membrane pemphigoid: recent advances. Current opinion in ophthalmology. 2012;23(6):523-7.
148. Kumari S, Bhol KC, Simmons RK, Razzaque MS, Letko E, Foster CS, et al. Identification of ocular cicatricial pemphigoid antibody binding site(s) in human beta4 integrin. Investigative ophthalmology & visual science. 2001;42(2):379-85.
149. Lazarova Z, Hsu R, Yee C, Yancey KB. Antiepiligrin cicatricial pemphigoid represents an autoimmune response to subunits present in laminin 5 (alpha3beta3gamma2). The British journal of dermatology. 1998;139(5):791-7.
150. Zillikens D. BP180 as the common autoantigen in blistering diseases with different clinical phenotypes. The Keio journal of medicine. 2002;51(1):21-8.
151. Miserocchi E, Baltatzis S, Roque MR, Ahmed AR, Foster CS. The effect of treatment and its related side effects in patients with severe ocular cicatricial pemphigoid. Ophthalmology. 2002;109(1):111-8.
152. Rogers RS, 3rd, Seehafer JR, Perry HO. Treatment of cicatricial (benign mucous membrane) pemphigoid with dapsone. Journal of the American Academy of Dermatology. 1982;6(2):215-23.
153. Foster CS. Cicatricial pemphigoid. Trans Am Ophthalmol Soc. 1986;84:527-663.
154. Tauber J, Jabbur N, Foster CS. Improved detection of disease progression in ocular cicatricial pemphigoid. Cornea. 1992;11(5):446-51.
155. Rowsey JJ, Macias-Rodriguez Y, Cukrowski C. A new method for measuring progression in patients with ocular cicatricial pemphigoid. Arch Ophthalmol. 2004;122(2):179-84.
156. Reeves GM, Lloyd M, Rajlawat BP, Barker GL, Field EA, Kaye SB. Ocular and oral grading of mucous membrane pemphigoid. Graefe's archive for clinical and experimental ophthalmology = Albrecht von Graefes Archiv fur klinische und experimentelle Ophthalmologie. 2012;250(4):611-8.
157. Williams GP, Saw VP, Saeed T, Evans ST, Cottrell P, Curnow SJ, et al. Validation of a fornix depth measurer: a putative tool for the assessment of progressive cicatrising conjunctivitis. The British journal of ophthalmology. 2011;95(6):842-7.
158. Bron AJ, Evans VE, Smith JA. Grading of corneal and conjunctival staining in the context of other dry eye tests. Cornea. 2003;22(7):640-50.
159. Efron N. Clinical application of grading scales for contact lens complications. Optician. 1999;5604 (213):26–35.
160. IER. IER Grading Scales Sydney, Australia: Institute for Eye Research, 2007.
161. McMonnies CW C-DA. Assessment of conjunctival hyperaemia in contact lens wearers. Am J Optom Physiol Opt. 1987;64:246-50.
162. Elder MJ, Bernauer W. Monitoring of activity and progression in cicatrising conjunctivitis. Developments in ophthalmology. 1997;28:111-22.
163. Saw VP, Dart JK, Rauz S, Ramsay A, Bunce C, Xing W, et al. Immunosuppressive therapy for ocular mucous membrane pemphigoid strategies and outcomes. Ophthalmology. 2008;115(2):253-61 e1.
164. Saw VP. The role of inflammation and fibroblasts in conjunctival scarring in ocular mucous membrane pemphigoid: University College London; 2009.

165. Sotozono C, Ang LP, Koizumi N, Higashihara H, Ueta M, Inatomi T, et al. New grading system for the evaluation of chronic ocular manifestations in patients with Stevens-Johnson syndrome. Ophthalmology. 2007;114(7):1294-302.
166. Kemp EG, Collin JR. Surgical management of upper lid entropion. The British journal of ophthalmology. 1986;70(8):575-9.
167. Moe KS, Linder T. The lateral transorbital canthopexy for correction and prevention of ectropion: report of a procedure, grading system, and outcome study. Archives of facial plastic surgery. 2000;2(1):9-15.
168. Efron N, Pritchard N, Brandon K, Copeland J, Godfrey R, Hamlyn B, et al. A survey of the use of grading scales for contact lens complications in optometric practice. Clinical & experimental optometry. 2011;94(2):193-9.
169. O'Kell S HT, Farrow g, Aindow M, Jones C. Effects of low-power plasma treatment on polyethylene surfaces. Surf Interface Anal. 1995;23:319-3127.
170. Pringle S JV, Jones C. Ammonia plasma treatment of PTFE under known plasma conditions. Surf Interface Anal. 1996;24:821-9.
171. Markkula T, Hunt JA, Pu FR, Williams RL. Surface chemical derivatization of plasma-treated PET and PTFE. Surf Interface Anal. 2002;34:583-7.
172. Wilson DJ, Rhodes NP, Williams RL. Surface modification of a segmented polyetherurethane using a low-powered gas plasma and its influence on the activation of the coagulation system. Biomaterials. 2003;24(28):5069-81.
173. Hogg P, Rooney P, Ingham E, Kearney JN. Development of a decellularised dermis. Cell and tissue banking. 2013;14(3):465-74.
174. Pascali M, Corsi A, Brinci L, Corsi I, Cervelli V. The tarsal belt procedure for the correction of ectropion: description and outcome in 42 cases. The British journal of ophthalmology. 2014;98(12):1691-6.
175. Visakh PM ML. Poly(ethylene terephthalate) based blends composites and nanocomposites. Oxford, UK: Elsevier; 2015. 235 p.
176. Mole B. The use of Gore-Tex implants in aesthetic surgery of the face. Plastic and reconstructive surgery. 1992;90(2):200-6.
177. Pu FR, Williams RL, Markkula TK, Hunt JA. Effects of plasma treated PET and PTFE on expression of adhesion molecules by human endothelial cells in vitro. Biomaterials. 2002;23(11):2411-28.
178. Krishna Y. Use of artificial substrates for retinal pigment epithelial cell growth and transplantation. Liverpool: University of Liverpool; 2006.
179. Wilson DJW, R.L.; Pond, R.C. Plasma modification of PTFE surfaces. . Surf Interface Anal. 2001;31:385-408.
180. Pu FR, Williams RL, Markkula TK, Hunt JA. Expression of leukocyte-endothelial cell adhesion molecules on monocyte adhesion to human endothelial cells on plasma treated PET and PTFE in vitro. Biomaterials. 2002;23(24):4705-18.
181. Margel S, Vogler EA, Firment L, Watt T, Haynie S, Sogah DY. Peptide, protein, and cellular interactions with self-assembled monolayer model surfaces. J Biomed Mater Res. 1993;27(12):1463-76.
182. van Wachem PB, Vreriks CM, Beugeling T, Feijen J, Bantjes A, Detmers JP, et al. The influence of protein adsorption on interactions of cultured human endothelial cells with polymers. J Biomed Mater Res. 1987;21(6):701-18.
183. Cooke MJ, Phillips SR, Shah DS, Athey D, Lakey JH, Przyborski SA. Enhanced cell attachment using a novel cell culture surface presenting functional domains from extracellular matrix proteins. Cytotechnology. 2008;56(2):71-9.

184. Faia-Torres AB, Guimond-Lischer S, Rottmar M, Charnley M, Goren T, Maniura-Weber K, et al. Differential regulation of osteogenic differentiation of stem cells on surface roughness gradients. Biomaterials. 2014;35(33):9023-32.
185. Principles of Tissue Engineering. 4th ed: Elsevier; 2014. 1936 p.
186. Lin L, Kurpakus-Wheater M. Laminin alpha5 chain adhesion and signaling in conjunctival epithelial cells. Investigative ophthalmology & visual science. 2002;43(8):2615-21.
187. Lin L, Daneshvar C, Kurpakus-Wheater M. Evidence for differential signaling in human conjunctival epithelial cells adherent to laminin isoforms. Experimental eye research. 2000;70(4):537-46.
188. Ott MJ, Ballermann BJ. Shear stress-conditioned, endothelial cell-seeded vascular grafts: improved cell adherence in response to in vitro shear stress. Surgery. 1995;117(3):334-9.
189. Sheridan C, Williams R, Grierson I. Basement membranes and artificial substrates in cell transplantation. Graefe's archive for clinical and experimental ophthalmology = Albrecht von Graefes Archiv fur klinische und experimentelle Ophthalmologie. 2004;242(1):68-75.
190. Gipson IK, Spurr-Michaud S, Argueso P, Tisdale A, Ng TF, Russo CL. Mucin gene expression in immortalized human corneal-limbal and conjunctival epithelial cell lines. Investigative ophthalmology & visual science. 2003;44(6):2496-506.
191. Weinberg RA. Telomeres. Bumps on the road to immortality. Nature. 1998;396(6706):23-4.
192. Rosenman JE, Kempczinski RF, Pearce WH, Silberstein EB. Kinetics of endothelial cell seeding. J Vasc Surg. 1985;2(6):778-84.
193. Yassin MA, Leknes KN, Pedersen TO, Xing Z, Sun Y, Lie SA, et al. Cell seeding density is a critical determinant for copolymer scaffolds induced bone regeneration. J Biomed Mater Res A. 2015.
194. Wilson HK, Canfield SG, Hjortness MK, Palecek SP, Shusta EV. Exploring the effects of cell seeding density on the differentiation of human pluripotent stem cells to brain microvascular endothelial cells. Fluids Barriers CNS. 2015;12:13.
195. Nelson CM, Chen CS. Cell-cell signaling by direct contact increases cell proliferation via a PI3K-dependent signal. FEBS Lett. 2002;514(2-3):238-42.
196. Succu S, Pasciu V, Manca ME, Chelucci S, Torres-Rovira L, Leoni GG, et al. Dose-dependent effect of melatonin on postwarming development of vitrified ovine embryos. Theriogenology. 2014;81(8):1058-66.
197. Aoshima K, Baba A, Makino Y, Okada Y. Establishment of alternative culture method for spermatogonial stem cells using knockout serum replacement. PLoS One. 2013;8(10):e77715.
198. Kubota H, Brinster RL. Culture of rodent spermatogonial stem cells, male germline stem cells of the postnatal animal. Methods Cell Biol. 2008;86:59-84.
199. Kubota H, Avarbock MR, Brinster RL. Growth factors essential for self-renewal and expansion of mouse spermatogonial stem cells. Proc Natl Acad Sci U S A. 2004;101(47):16489-94.
200. Kanatsu-Shinohara M, Ogonuki N, Inoue K, Miki H, Ogura A, Toyokuni S, et al. Long-term proliferation in culture and germline transmission of mouse male germline stem cells. Biol Reprod. 2003;69(2):612-6.
201. Han XQ, Gong ZJ, Xu SQ, Li X, Wang LK, Wu SM, et al. Advanced glycation end products promote differentiation of CD4(+) T helper cells toward pro-inflammatory response. J Huazhong Univ Sci Technolog Med Sci. 2014;34(1):10-7.
202. Schiller JH, Bittner G. Loss of the tumorigenic phenotype with in vitro, but not in vivo, passaging of a novel series of human bronchial epithelial cell lines: possible role of an alpha 5/beta 1-integrin-fibronectin interaction. Cancer Res. 1995;55(24):6215-21.

203. Maqsood MI, Matin MM, Bahrami AR, Ghasroldasht MM. Immortality of cell lines: challenges and advantages of establishment. Cell Biol Int. 2013;37(10):1038-45.
204. Vaziri H, Benchimol S. Reconstitution of telomerase activity in normal human cells leads to elongation of telomeres and extended replicative life span. Curr Biol. 1998;8(5):279-82.
205. Bodnar AG, Ouellette M, Frolkis M, Holt SE, Chiu CP, Morin GB, et al. Extension of life-span by introduction of telomerase into normal human cells. Science. 1998;279(5349):349-52.
206. Devarajan E, Sahin AA, Chen JS, Krishnamurthy RR, Aggarwal N, Brun AM, et al. Down-regulation of caspase 3 in breast cancer: a possible mechanism for chemoresistance. Oncogene. 2002;21(57):8843-51.
207. Lavrik IN, Golks A, Krammer PH. Caspases: pharmacological manipulation of cell death. J Clin Invest. 2005;115(10):2665-72.
208. Nicholson DW, Ali A, Thornberry NA, Vaillancourt JP, Ding CK, Gallant M, et al. Identification and inhibition of the ICE/CED-3 protease necessary for mammalian apoptosis. Nature. 1995;376(6535):37-43.
209. Zoli W, Ulivi P, Tesei A, Fabbri F, Rosetti M, Maltoni R, et al. Addition of 5-fluorouracil to doxorubicin-paclitaxel sequence increases caspase-dependent apoptosis in breast cancer cell lines. Breast cancer research : BCR. 2005;7(5):R681-9.
210. Wan Y, Tu C, Yang J, Bei J, Wang S. Influences of ammonia plasma treatment on modifying depth and degradation of poly(L-lactide) scaffolds. Biomaterials. 2006;27(13):2699-704.
211. Haller-Schober EM, Schwantzer G, Berghold A, Fischl M, Theisl A, Horwath-Winter J. Evaluating an impression cytology grading system (IC score) in patients with dry eye syndrome. Eye. 2006;20(8):927-33.
212. Nelson JD, Havener VR, Cameron JD. Cellulose acetate impressions of the ocular surface. Dry eye states. Arch Ophthalmol. 1983;101(12):1869-72.
213. Tei M, Spurr-Michaud SJ, Tisdale AS, Gipson IK. Vitamin A deficiency alters the expression of mucin genes by the rat ocular surface epithelium. Investigative ophthalmology & visual science. 2000;41(1):82-8.
214. De Saint Jean M, Baudouin C, Di Nolfo M, Roman S, Lozato P, Warnet JM, et al. Comparison of morphological and functional characteristics of primary-cultured human conjunctival epithelium and of Wong-Kilbourne derivative of Chang conjunctival cell line. Experimental eye research. 2004;78(2):257-74.
215. Rosellini A, Papini S, Giannarini C, Nardi M, Revoltella RP. Human conjunctival epithelial precursor cells and their progeny in 3D organotypic culture. Int J Dev Biol. 2007;51(8):739-43.
216. Rajavelu P, Chen G, Xu Y, Kitzmiller JA, Korfhagen TR, Whitsett JA. Airway epithelial SPDEF integrates goblet cell differentiation and pulmonary Th2 inflammation. J Clin Invest. 2015;125(5):2021-31.
217. Gipson I, Alhatem, A., Chen,G., Whitsett,J., Clever,H., editor The role of transcription factor SPDEF in goblet cell differentiation in the conjunctiva. Association of Research in Vision and Ophthalmology; 2011; Ft. Lauderdale: IOVS.
218. Antonova OA, Loktionova SA, Romanov YA, Shustova ON, Khachikian MV, Mazurov AV. Activation and damage of endothelial cells upon hypoxia/reoxygenation. Effect of extracellular pH. Biochemistry Biokhimiia. 2009;74(6):605-12.
219. Luo JC, Li XQ, Yang ZM. [Preparation of human acellular amniotic membrane and its cytocompatibility and biocompatibility]. Zhongguo Xiu Fu Chong Jian Wai Ke Za Zhi. 2004;18(2):108-11.

220. Sakamoto T, Hirano K, Morishima Y, Masuyama K, Ishii Y, Nomura A, et al. Maintenance of the differentiated type II cell characteristics by culture on an acellular human amnion membrane. In Vitro Cell Dev Biol Anim. 2001;37(8):471-9.
221. Davis GE, Blaker SN, Engvall E, Varon S, Manthorpe M, Gage FH. Human amnion membrane serves as a substratum for growing axons in vitro and in vivo. Science. 1987;236(4805):1106-9.
222. Samandari MH, Yaghmaei M, Ejlali M, Moshref M, Saffar AS. Use of amnion as a graft material in vestibuloplasty: a preliminary report. Oral Surg Oral Med Oral Pathol Oral Radiol Endod. 2004;97(5):574-8.
223. Korossis SA, Booth C, Wilcox HE, Watterson KG, Kearney JN, Fisher J, et al. Tissue engineering of cardiac valve prostheses II: biomechanical characterization of decellularized porcine aortic heart valves. J Heart Valve Dis. 2002;11(4):463-71.
224. Courtman DW, Pereira CA, Kashef V, McComb D, Lee JM, Wilson GJ. Development of a pericardial acellular matrix biomaterial: biochemical and mechanical effects of cell extraction. J Biomed Mater Res. 1994;28(6):655-66.
225. Nagata S, Hanayama R, Kawane K. Autoimmunity and the clearance of dead cells. Cell. 2010;140(5):619-30.
226. Zheng MH, Chen J, Kirilak Y, Willers C, Xu J, Wood D. Porcine small intestine submucosa (SIS) is not an acellular collagenous matrix and contains porcine DNA: possible implications in human implantation. J Biomed Mater Res B Appl Biomater. 2005;73(1):61-7.
227. Wilshaw SP, Kearney JN, Fisher J, Ingham E. Production of an acellular amniotic membrane matrix for use in tissue engineering. Tissue Eng. 2006;12(8):2117-29.
228. Woods T, Gratzer PF. Effectiveness of three extraction techniques in the development of a decellularized bone-anterior cruciate ligament-bone graft. Biomaterials. 2005;26(35):7339-49.
229. Bank RA, Krikken M, Beekman B, Stoop R, Maroudas A, Lafeber FP, et al. A simplified measurement of degraded collagen in tissues: application in healthy, fibrillated and osteoarthritic cartilage. Matrix Biol. 1997;16(5):233-43.
230. Campbell EM, Cahill PA, Lally C. Investigation of a small-diameter decellularised artery as a potential scaffold for vascular tissue engineering; biomechanical evaluation and preliminary cell seeding. J Mech Behav Biomed Mater. 2012;14:130-42.
231. Stapleton TW, Ingram J, Katta J, Knight R, Korossis S, Fisher J, et al. Development and characterization of an acellular porcine medial meniscus for use in tissue engineering. Tissue Eng Part A. 2008;14(4):505-18.
232. Reproducibility and Accuracy of Mechanical Tests: A Symposium. 1977(626):136.
233. Petroll WM, Lakshman N. Fibroblastic Transformation of Corneal Keratocytes by Rac Inhibition is Modulated by Extracellular Matrix Structure and Stiffness. J Funct Biomater. 2015;6(2):222-40.
234. Yeung T, Georges PC, Flanagan LA, Marg B, Ortiz M, Funaki M, et al. Effects of substrate stiffness on cell morphology, cytoskeletal structure, and adhesion. Cell Motil Cytoskeleton. 2005;60(1):24-34.
235. Christopher RA, Kowalczyk AP, McKeown-Longo PJ. Localization of fibronectin matrix assembly sites on fibroblasts and endothelial cells. J Cell Sci. 1997;110 (Pt 5):569-81.
236. Tuan-Mu HY, Yu CH, Hu JJ. On the decellularization of fresh or frozen human umbilical arteries: implications for small-diameter tissue engineered vascular grafts. Ann Biomed Eng. 2014;42(6):1305-18.
237. Kwang W, J. International review of cell and molecular biology. USA: Academic Press, Elsevier; 2009.

238. Schrader S, Notara M, Tuft SJ, Beaconsfield M, Geerling G, Daniels JT. Simulation of an in vitro niche environment that preserves conjunctival progenitor cells. Regen Med. 2010;5(6):877-89.
239. Tsai RJ, Ho YS, Chen JK. The effects of fibroblasts on the growth and differentiation of human bulbar conjunctival epithelial cells in an in vitro conjunctival equivalent. Investigative ophthalmology & visual science. 1994;35(6):2865-75.
240. Kheirkhah A, Blanco G, Casas V, Hayashida Y, Raju VK, Tseng SC. Surgical strategies for fornix reconstruction based on symblepharon severity. Am J Ophthalmol. 2008;146(2):266-75.
241. Fein W. Repair of total and subtotal symblepharons. Ophthalmic Surg. 1979;10(6):44-7.
242. Hodges RR, Bair JA, Carozza RB, Li D, Shatos MA, Dartt DA. Signaling pathways used by EGF to stimulate conjunctival goblet cell secretion. Experimental eye research. 2012;103:99-113.